Synthesis and characterisation of new complexes with soft donor hybrid ligands

SYNTHESIS AND CHARACTERISATION OF NEW COMPLEXES WITH SOFT DONOR HYBRID LIGANDS

By

Paul M. Staniland

A Doctoral Thesis

Submitted in partial fulfillment of the requirements for the award of

Doctor of Philosophy of Loughborough University

Department of Chemistry

Loughborough University

Loughborough

Leicestershire

LE11 3TU

~*Abstract*~

Reliable, simple, substitution and one-pot radical reactions have enabled the preparation of a wide variety of novel bidentate and potentially tridentate ligands bearing combinations of P/S/Se/O and N donor atoms. The coordination chemistry of these ligands is investigated, and subsequent complexes have been tested for their potential catalytic activity in the Heck reaction. Furthermore, derivatives of these ligands have been prepared using oxidation reactions. The coordination chemistry of these subsequent ligands is also investigated.

Reaction of *o*-$C_6H_4Br(PPh_2)$ with thiophenol and phenylselenol in the presence of KOH gives the bidentate phosphine/chalcogenide ligands *o*-$C_6H_4(XPh)(PPh_2)$ (X = S/Se **2.1/2.17**). These have been characterised and reacted with transition metal precursors of the type MCl(X)(cod) (M = Pd/Pt X = Me/Cl) and also Ru/Rh chloro-bridged dimers. These formed complexes containing **2.1** and **2.17** chelated to the corresponding metal centre; complexes containing phosphine-selenide **2.17** characterised by X-ray crystallography are, to our knowledge, the first examples of complexes characterised by this method. One of the resulting chelate complexes, $PtCl_2$(**2.1**) **2.10** was subjected to further studies using additional equivalents of starting ligands. Simple radical reactions are used to prepare the bidentate ligands $(PhX)(CH_2)_2(PPh_2)$ (X = S/Se **2.21/2.22**), which are similarly characterised and their coordination chemistry probed. Using these techniques, a variety of functionalised thiols of the type *o/p*-$(HS)C_6H_4(X)$ (X = PPh_2/OMe/OH/NH_2) were used, along with Ph_2PCHCH_2 to prepare potentially tridentate ligands of the type {$Ph_2P(CH_2)_2S(C_6H_4)$*o/p*-(X)} (**2.32, 2.34-2.37**), containing both aromatic and alkyl backbones. Various transition metal complexes of these are formed and a number characterised by X-ray crystallography; The potential to force tridentate coordination by chloride abstraction, using salts such as $Ag[BF_4]$ is also analysed.

The chemistry of ligands and complexes containing bulky phospha-adamantane groups has also been analysed extensively. The ligands *o/m*-$C_6H_4(PAd)(X)$ (X = SPh/SePh/OMe/Br, PAd = 1,3,5,7,-tetramethyl-2,4,8-trioxa-6-

phospha-adamantane, (**3.1-3.5**) were prepared and characterised. Subsequently, Pd(II)/Pt(II) complexes of **3.1-3.5** were synthesised. Different coordination modes were observed for the various ligands; *o/m*-C_6H_4(PAd)Br (**3.1/3.2**) coordinated in a monodentate fashion and resulted in the formation of Pd(II) chloro-bridged dimers of the two ligands (**3.6/3.7**), whereas addition of one equivalent of ligands containing SPh/SePh/OMe moieties (**3.3-3.5**) coordinated in a bidentate fashion to give chelate complexes $PdCl_2${*o*-C_6H_4(X)(PAd)} **3.8-3.10**. A novel unsymmetrical diphosphine $PPh_2(CH_2)_2$PAd, **3.12** was also synthesised and characterised. Whilst reaction of **3.12** with Pd/Pt starting materials results in the expected chelate complexes $M(X)_2$(**3.12**) (X = Cl/Me, **3.13/3.14**), reaction with Ru/Rh/Ir chloro-bridged dimers enables the resulting complexes, coordinated in a monodentate fashion through the PPh_2 functionality, to be used as monodentate ligands themselves. Using this approach, novel heterobimetallic (Ru/Au) and heterotrimetallic (Ru_2Pt and Ru_2Pd) compounds have been prepared.

Derivatives of the phosphine-based ligands were prepared by oxidation using hydrogen peroxide, and amination of the phosphine/sulfide functionalities to give a number of new ionic monophosphazene/sulfimide compounds. The aminating agent *o*-mesitylenesulfonyl hydroxylamine (MSH) was used to prepare most of the latter types of compounds. Upon addition of the salt $NaBPh_4$ to the bis-aminated species {*o*-C_6H_4($S(NH_2)Ph$)($P(NH_2)Ph_2$)}{MSH} **2.1** and {$Ph_2P(NH_2)(CH_2)_2S(C_6H_4)$*o*-($P(NH_2)Ph_2$)}{MSH} **2.32**, large downfield shifts in the $^{31}P\{^1H\}$ NMR spectra were observed, theories for which are postulated.

Catalytic properties of the various Pd(II) complexes prepared have been analysed. Initial tests to establish their suitability to catalyse Heck reactions of iodobenzene and styrene were carried out. Initial results established that the complexes were effective as catalysts, and subsequent attempts to ascertain their efficiency by reducing catalyst loadings also proved to be successful.

~Acknowledgments~

I have so many people I would like to thank in this section, all of whom have contributed a great deal in the completion of this work. First of all, I would like to thank Loughborough University, and especially my supervisors Dr. Martin Smith and Dr. Paul Kelly. Your vast knowledge, guidance, support and patience have been invaluable; thank you again. I am also grateful to the EPSRC for half funding of this project.

I would like to thank all the academic staff in the Inorganic Section at Loughborough University, throughout my time at the University I have received excellent support and advice from all of the staff for which I am extremely grateful. I would especially like to thank Dr. Mark Elsegood for his help with crystal structure determinations, and Pauline King for her help with elemental analysis and putting up with my taste of music in the lab. I would also like to thank the EPSRC Mass Spectrometry service in Swansea.

In this mass thank you to everyone, I would like to move on to everyone in the lab who has helped me during my time here and generally made the department a good place to work – there are quite a few! Thanks to Duncan, Emma, Steve, Sophie and Katie (special thanks to these for help with the X-ray work!), Sarah J, Julia, Liam, Dennis, Gav, Andy, Rob S. P. King, Jo, Chris, Amy, Lee, Noelia, Leanne, Anna and Allen. I would also like to say a special thank you to Tom Cunningham.

A great big thank you must also go to a number of people in the department and from Lithers. I am really grateful to Jess (especially for reading through vast chunks of this!), Sean (who thankfully has been tolerant of my music/TV tastes over the past year!), Curley – when he is quiet!, Jaime, Toby, Gaz J, Mikel, Landon, Gav, Sharky, Ciaran, Paul Kent, Ben B., Big Tone, Si W., Van, Benoit and Cheech. All of you have made my time here brilliant.

Finally, but probably the most, I would like to thank my family. Throughout my life you have given me the chance and belief to be the best I can be. I am forever grateful to you for that. Thank you.

~Contents~

~*List of Figures*~

~*List of Equations*~

~*List of Schemes*~

~*List of Tables*~

~*Abbreviations and Glossary of Terms*~

Å	Angström unit, 10^{-10} m
AIBN	Azobisisobutyronitrile
Atm	atmospheres
Ar	aryl ring
B	broad
BINAP	Binaphthalene
Bu	butyl, $(CH_2)_3CH_3$
ca.	circa
$CHCl_3$	chloroform
CH_2Cl_2	dichloromethane, *see also* **DCM**
C H N	Carbon, Hydrogen, Nitrogen elemental analysis
cm^{-1}	wavenumber
cod	cycloocta-1,5-diene
Cp*	pentamethyl cyclopentadienyl, η^5-$C_5Me_5^-$
Cytop	1,3,5,7,-tetramethyl-2,4,8-trioxa-6-phospha-adamantane, *see also* **PAd**
d	days (in method)/doublet (in NMR data)
dd	doublet of doublets
DEPT	Distortionless Enhancement by Polarisation Transfer
DCM	dichloromethane, *see also* **CH_2Cl_2**
DMA	dimethylacetamide
DMSO	dimethylsulfoxide
DPPBT	2-diphenylphosphinobenzene thiolate
dppm	bis(diphenylphosphino)methane
***ee*s**	enantiomeric excesses
EI	Electron Impact
ES	Electrospray
Et	ethyl, CH_2CH_3
Et_2O	diethyl ether
EtOH	ethanol
FAB	Fast Atom Bombardment

Fc	Ferrocenyl, $(\eta^5\text{-}C_5H_5)_2Fe$
g	grams
h	hours
Hz	Hertz
IR	Infra red spectroscopy
LDA	Lithium diisopropylamide
med	medium
m	multiplet
***m*-CPBA**	*meta*-chloroperoxybenzoic acid
Me	methyl, CH_3
MeCN	acetonitrile
MeOH	methanol
min	minutes
MS	Mass Spectrometry
MSH	*o*-Mesitylenesulfonyl hydroxylamine
NMR	Nuclear Magnetic Resonance spectroscopy
OAc	acetate
p	para
PAd	1,3,5,7,-tetramethyl-2,4,8-trioxa-6-phospha-adamantane, *see also* **Cytop**
pet. ether	petroleum ether
ppm	parts per million
r.t.	room temperature
s	strong
sh	sharp
^{t}Bu	tertiary-butyl, $C(CH_3)_3$
THF	tetrahydrofuran
THT	tetrahydrothiophene
TMEDA	*N,N,N'*,N'-tetramethyl-1,2-ethanediamine
TON	Turnover Number (Number of moles of product/Number of moles of catalyst used)
TOF	Turnover Frequency (Turnover number/reaction time)
TTF	tetrathiafulvalene

w	weak
°	degrees
°C	degrees centigrade

Chapter One

~Introduction ~

This Chapter reviews the preparation of hybrid ligands containing a variety of phosphines and chalcogenide functionalities. Many examples are known of ligands and subsequent transition metal complexes containing PR_2 (R = alkyl or aryl groups) and S or Se-containing groups. In addition, the chemistry of derivatives of these ligands, namely sulfimides and phosphazenes will be reviewed. Finally, the vast amount of catalytic applications of phosphine-containing ligands will be examined.

1.1 CHEMISTRY OF PHOSPHORUS/SULFUR CONTAINING LIGANDS

The preparation, characterisation and use of phosphorus and sulfur based ligands has been the subject of a great deal of interest for many years. One of the main reasons for this is the diversity of catalytic applications enabled by such ligands and their subsequent complexes. Rates of hydroformylation and carbonylation reactions, for example, have been greatly increased using phosphorus/sulfide-based complexes, processes which are aided by the varying strengths of the metal-donor atom bonds. Preparation of the catalyst precursors is often extremely simple, due to the excellent coordinating ability of the phosphine functionality to heavy metals such as Pd and Pt.

The coordination of phosphines to metals consists of two main components (Figure 1.1). The first of these (**a**) is a σ bond, donation of a lone pair of electrons from a filled σ orbital of the phosphine to an empty orbital on the metal. The second component (**b**), reported by Orpen *et al.*[1] involves combination of the phosphorus 3d and σ* orbitals to form a hybridised phosphorus π acceptor orbital, followed by back donation from a filled d-orbital on the metal to an empty orbital on the phosphine.

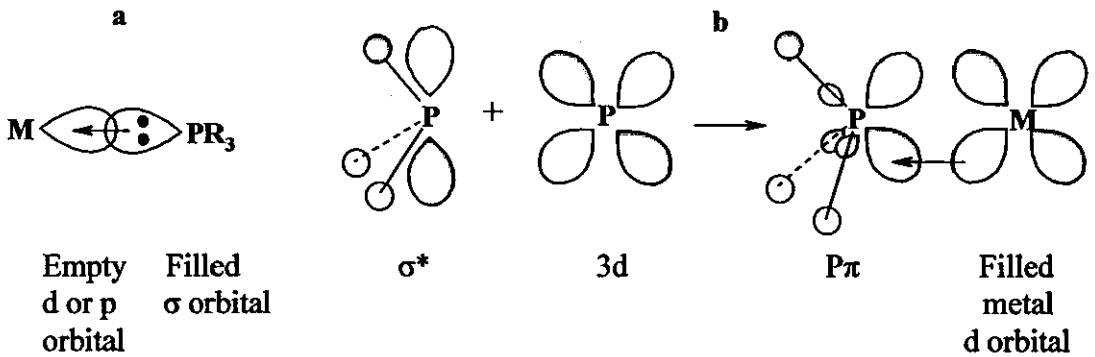

Figure 1.1 – Metal-phosphine bonding

Much of the early work on the preparation of ligands and complexes containing phosphine and chalcogenide functionalities was carried out in the 1960's. In particular, the work of Dyer and Meek in preparing ligands such as **1.1** (Figure 1.2), and Venanzi *et al.*[2] formed the basis for much more extensive research in this area. The work of the former group is returned to extensively in future sections in this review.

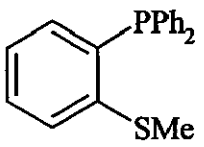

1.1

Figure 1.2 – *o*-$C_6H_4(PPh_2)(SMe)$

Many examples are known of phosphine/thiol/thioether containing ligands containing an alkyl backbone $R_2P(CH_2)_nSR$ (where n = 2 or 3).[3-6] Anderson *et al.*[7] prepared Pt(II) complexes containing such ligands, and these are shown in Figure 1.3. $Ph_2P(CH_2)_2SMe$ was prepared from $Cl(CH_2)_2SMe$ and $LiPPh_2$, and reacted with $PtX_2(cod)$ (X = I, Br, Cl, cod = cycloocta-1,5-diene) to give $PtX_2[Ph_2P(CH_2)_2SMe]$ **1.2-1.4**. Addition of an excess of $NaBF_4$ to **1.2-1.4** gave the ionic species **1.5** also shown in Figure 1.3. These reactions were similar to those carried out around the same time using $Ph_2P(CH_2)_2SPh$.[8]

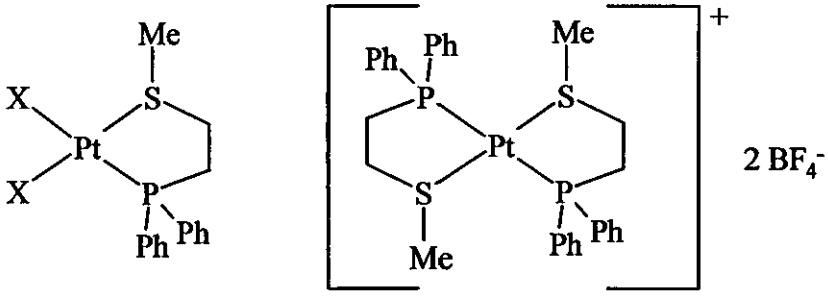

1.2 X = Cl
1.3 X = Br
1.4 X = I

1.5

Figure 1.3 – Pt alkyl P/S complexes

Kashiwabara *et al.* reported in 2003 the chemistry of analogous ligands to **1.2-1.4**.[9] Their work over the past fifteen years has centred on analysing the effects upon complexation of using $(Me)_2P(CH_2)_2SR$ (R = H/Me), changing the aryl phosphine substituents used in many examples for methyl groups.[10,11] Much of this work focused on transition metal centres such as Pd(II), Pt(II), and Ru(II). However, in 2003, these workers prepared Ti(IV) and Ti(III) complexes of $(Me)_2P(CH_2)_nS^-$ (n = 2/3). The complexes **1.7-1.9** (Scheme 1.1) were prepared by metathesis reactions using $(CH_3)_2P(CH_2)_2S^-Li^+$ **1.6** and different stoichiometries of Cp_2TiCl_2 (Cp = η^5-cyclopentadienide) (**1.7, 1.8**) and Cp^*TiCl_3 ($Cp^* = \eta^5$-$C_5Me_5^-$) (**1.9**).

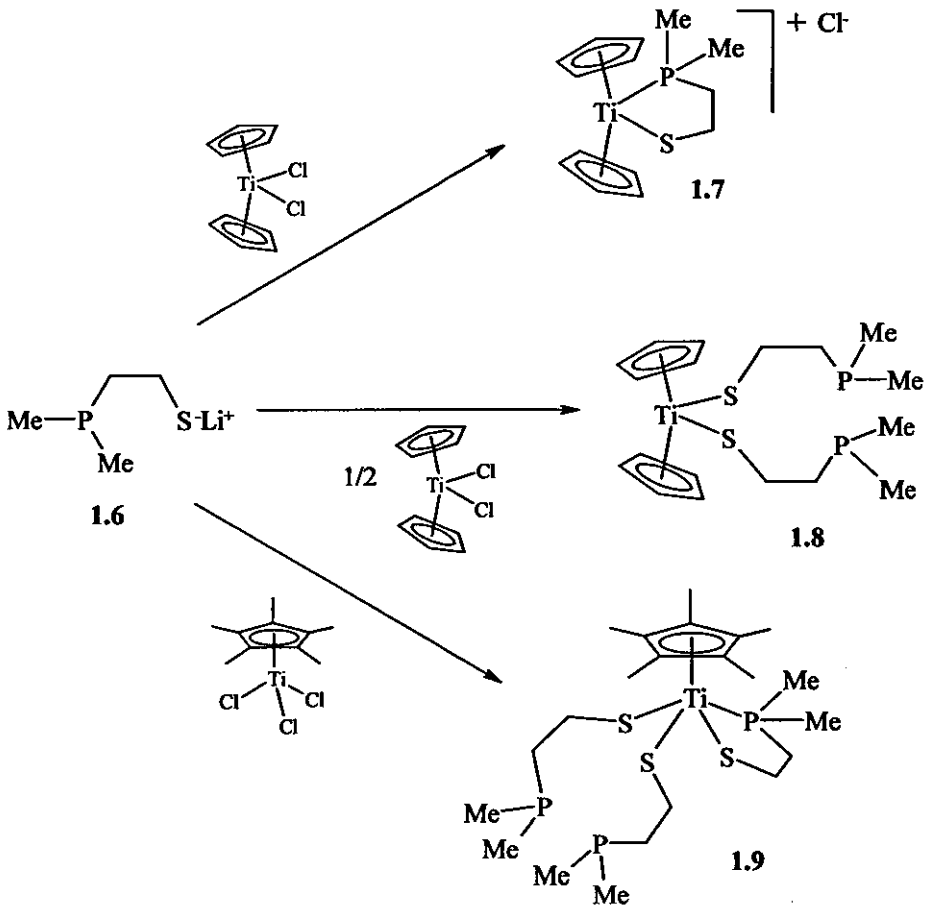

Scheme 1.1 – Ti P/S complexes

Many examples of P/S ligands incorporate simple alkyl or aryl backbones, though this is not always the case. Long *et al.*[12] recently prepared phosphine/thiolate substituted ferrocenediyl ligands, and subsequent Pd, Rh and Ni complexes. These ligands were prepared in a relatively simple manner compared to those reported

previously, in a two-step method beginning with 1,1'-dibromoferrocene. One equivalent of *n*-BuLi was added to give the monolithiated bromoferrocene, followed by addition of half an equivalent of sulfur dichloride in THF to form the S-S bridged dibromo-substituted diferrocene **1.10a**. Addition of $LiHBEt_3$ to cleave the S-S bridge, followed by $KPPh_2$ in THF yielded the target SH/PPh_2 substituted ferrocene **1.10b**.

Complexation reactions using **1.10** gave a mixture of monomeric and dimeric species. Reaction with *trans*-$Pd(PhCN)_2Cl_2$ or $\{Rh(CO)_2Cl\}_2$ gave $\{PdCl(C_5H_4S)Fe(C_5H_4PPh_2)\}_2$ **1.11** and $\{RhCO(C_5H_4S)Fe(C_5H_4PPh_2)\}_2$ **1.12** respectively. The thiolate groups in both dimers adopt a bridging mode, in a similar manner to previously reported compounds.[13]

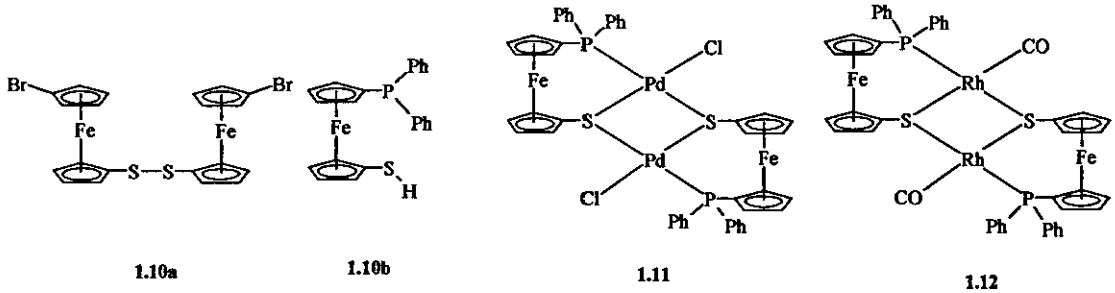

1.10a 1.10b 1.11 1.12

Figure 1.4 – M-ferrocene complexes

The properties of phosphine-sulfides can be enhanced by the incorporation of such functionalities onto other entities of interest, as shown by Pellon *et al.*[14] Here, a redox-active ligand **1.13** is formed by using trimethyltetrathiafulvalene as the core moiety (Scheme 1.2). The building block for the reaction was a cyanoethylthiolate analogue using a protected phosphino-borane as the starting material.

Varying modes of coordination were exhibited using *cis*-$Mo(CO)_4(piperidine)_2$ and *cis*-$W(CO)_4(piperidine)_2$ as starting materials. The molybdenum starting material allowed coordination of two phosphino ligands **1.13** through the phosphorus centre to give $Mo(CO)_4(\mathbf{1.13})_2$, whilst only one piperidine ligand was displaced using tungsten, affording $W(CO)_4(piperidine)(\mathbf{1.13})$, also through the phosphorus donor centre.

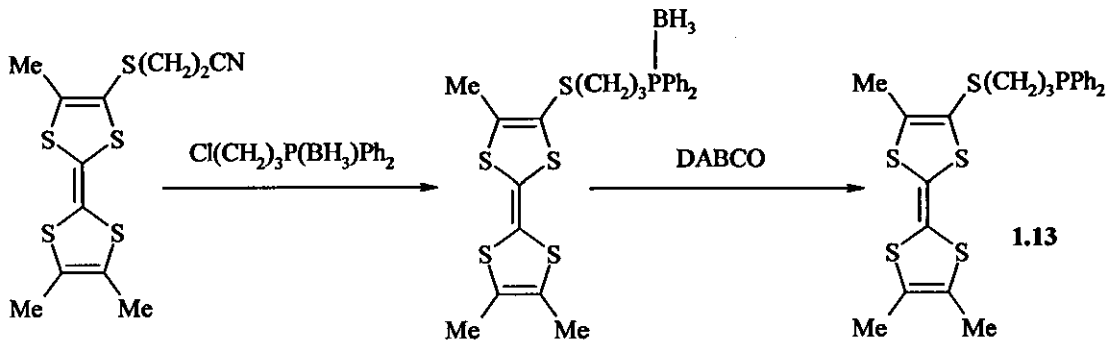

Scheme 1.2 – Mo complexes of trimethyltetrathiafulvalene

Recent work in the area of phosphine-sulfide ligands has included the synthesis of a number of mixed Rh/Ir/Sn complexes containing the phosphorus-sulfur proligand ($Ph_2PC_6H_4$-2-S^-), reported by Canseco-Gonzalez *et al.*[15] Organometallic Sn(IV) compounds were reacted with various Rh(I), Ir(I), Pd(II) and Pt(II) complexes. Previous reactions with Pd and Pt compounds resulted in the formation of the four-coordinate square planar complexes (Scheme 1.3). However, reaction of the tin compound with materials of type $M(Cl)(CO)(PPh_3)$ (M = Ir/Rh) resulted in the

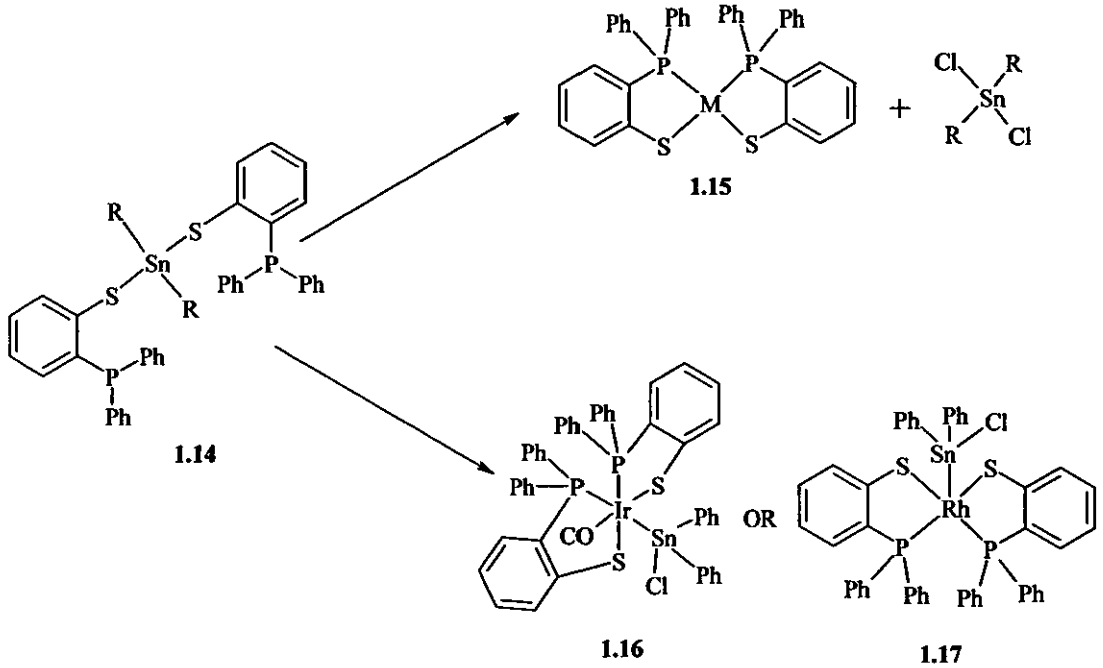

Scheme 1.3 – Rh/Ir/Sn complexes of P/S ligand

formation of the complexes $Ir(Cl)(CO)(Ph_2PC_6H_4\text{-}2\text{-}S)_2(SnClPh_2)$ **1.16** and $Rh(Ph_2PC_6H_4\text{-}2\text{-}S)_2(SnClPh_2)$ **1.17**. It was proposed that the resulting octahedral Rh(III) and Ir(III) complexes were formed by a transmetallation process.

An area of phosphine-sulfide chemistry which has received much attention is that of chiral ligands. Duran *et al.*[16] reported in 2003 the preparation of ((diphenylphosphino)methyl)-2-isopropyl-5-methylcyclohexanethiol and its Pd(II) and Pt(II) complexes. Two methods of complexation were attempted, the most successful of these was the addition of the phosphinothiol to $Pd(PPh_3)_4$ at room temperature. The product of this reaction, **1.18** is shown in Figure 1.15, with the two ligands *cis*- with respect to the P donor atoms. The Pd(II) complex, and a subsequent Pt(II) complex were characterised predominantly using $^{13}C\{^1H\}$ NMR, and also using $^{31}P\{^1H\}$ NMR (signals at 50.10 and 48.81 ppm respectively). In comparison, reaction of the phosphinothiol with $PdCl_2(PPh_3)_2$ was shown, to form a mixture of *cis*- and *trans*- products **1.19a** and **1.19b**.

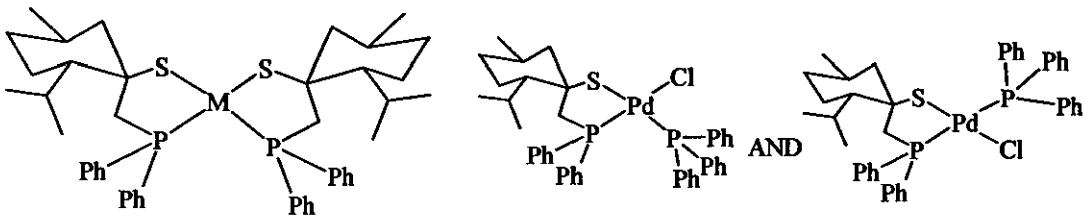

1.18 **1.19a** **1.19b**

Figure 1.5 – Chiral phosphines

In 2005 Grapperhaus *et al.*[17] extended the area of chiral phosphine-thioether complexes by investigating the oxygenation of a Ru(II) phosphino-thiolate complex, as shown in Scheme 1.4. Exposure of **1.20** to excess amounts of oxygen resulted in oxidation of the metal centre, followed by oxidation at sulfur to give **1.21**. Metal centred reduction was then carried out on **1.21** to give **1.22**.

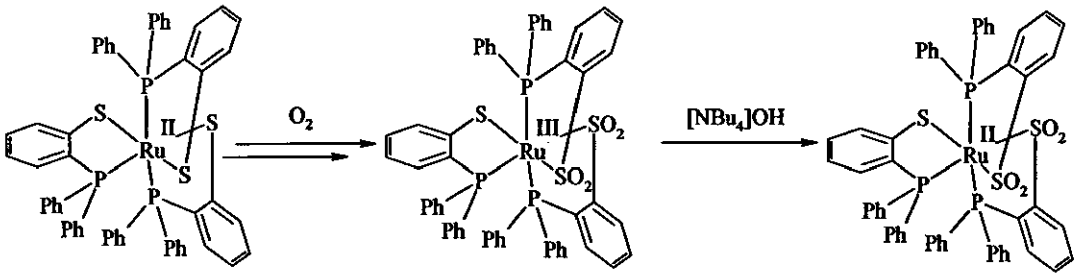

1.20 1.21 1.22

Scheme 1.4 – Ru chiral phosphine-thioether complexes

Recently, Malacea *et al.* prepared chiral phosphine-thioether ligands and subsequent Ir(I) complexes based on ferrocene starting materials.[18] Examples of this type of ligand have been prepared previously,[19-21] and their use in catalysis investigated. The complexes prepared by Malacea, (Equation 1.1) were formed by H_2 addition across the S-Ir-CO axis to give two diastereomeric products **1.25-1.28.**

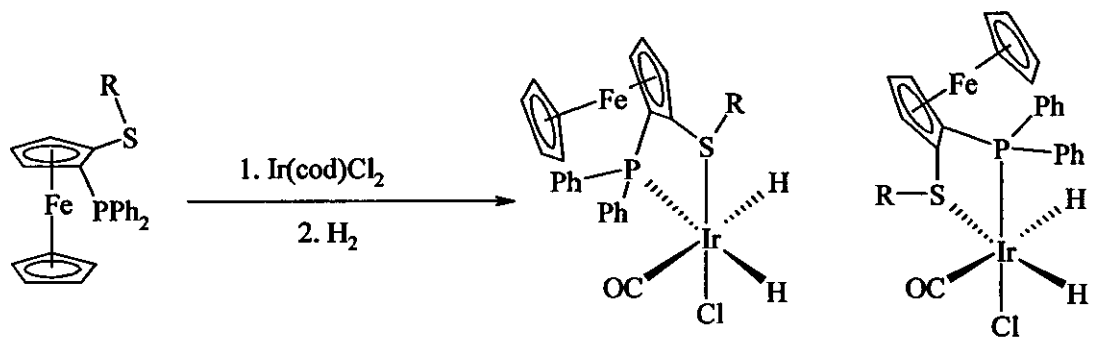

1.23 R = Ph
1.24 R = ^{t}Bu

1.25 R = Ph
1.26 R = ^{t}Bu

1.27 R = Ph
1.28 R = ^{t}Bu

Equation 1.1 – Ir chiral phosphine-thioether complexes

A number of phosphine/sulfide derivatives were prepared by Pérez-Lourido *et al,*[22] and these were incorporated in to a variety of lead(II) complexes **1.29-1.31** (Figure 1.6). The complexes were prepared by two methods; firstly electrochemical oxidation of lead anodes using the appropriate P=E/S ligands, and secondly by simple addition of the ligands to a solution of $Pb(OAc)_2$. The structure of $Pb\{2\text{-}(Ph_2P(O)CH_2)C_6H_4S\}_2$ **1.29** shows bidentate coordination of two ligands through the thiolate and oxygen of the phosphinyl groups. The structure of

$Pb\{2,6\text{-}(Ph_2P(S)CH_2)_2C_6H_3S\}_2$ **1.31** consists of two anionic sulfur atoms in equatorial positions.

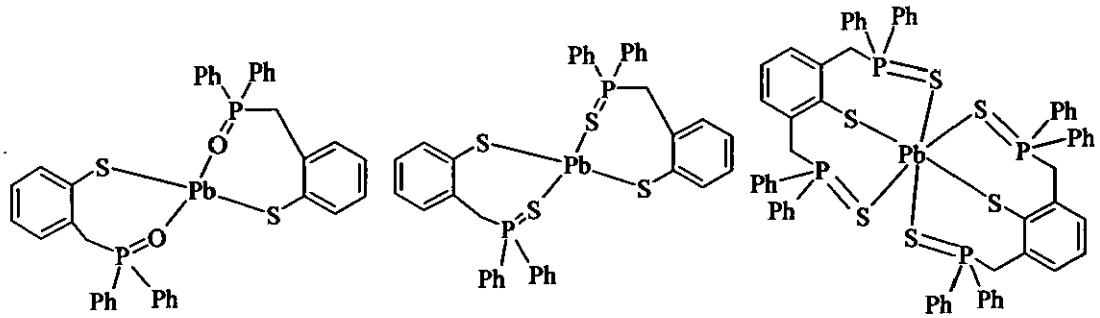

1.29 **1.30** **1.31**

Figure 1.6 – Pb complexes

1.2 CHEMISTRY OF PHOSPHORUS/SELENIUM CONTAINING LIGANDS

Whilst a wealth of research has been carried out towards the chemistry of phosphorus/sulfur ligands, very little work has been carried out on phosphorus/selenium ligands. This may have been for a number of reasons, such as the insolubility of selenium-based products, the difficulty of handling some selenium starting materials, or it may simply be an area that has been overlooked.

Similar ligands to those encountered in this project were prepared by Dyer and Meek in 1967 (**1.32, 1.33**),[23] and later by Hope *et al.* (**1.34**)[24] and Harbron *et al.* in 1987.[25] However, the compounds prepared by Hope and and Harbron are some of the very few examples of work on ligands containing phosphine and selenide groups in the last 20 years.

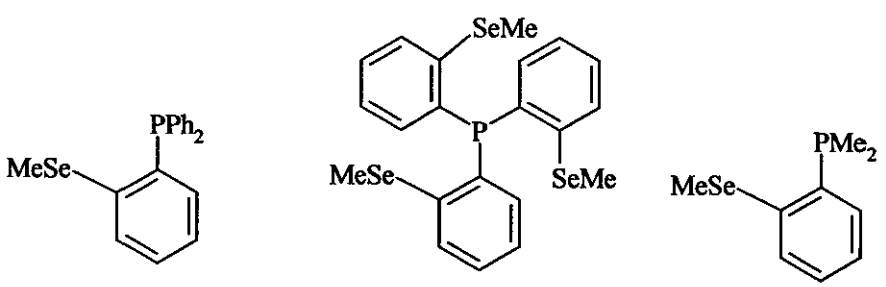

1.32 **1.33** **1.34**

Figure 1.7 – Early phosphine-selenide complexes prepared

Harbron *et al.*[25] prepared palladium and the first nickel complexes containing phosphine, sulfide and selenide groups, using the phosphine group and the rigid backbone of the *o*-C_6H_4 as a method of stabilising the M-X bond. As shown in Equation 1.2, palladium complexes **1.36a-d** containing the chelated phosphine-sulfide/selenide ligands **1.35a-d** were prepared easily using the starting material $Pd(MeCN)_2Cl_2$. The organic group on the phosphine dictated whether a chelate complex was formed; when alkyl phosphines such as PMe_2 were used the product was found to be $PdCl_2$(**1.34**). Here an equilibrium was formed between the two phosphine groups coordinating to the metal centre, and the sulfide/selenide and chloride groups competing for the two remaining coordination sites. Further Ni(II) complexes were prepared by Cauzzi *et al.* in 1999.[26] $Ph_2P(Se)(CH_2)PPh_2$ (dppmSe) and $NiCl_2.6H_2O$ were reacted together to form the complex $[Ni(dppmSe)_2]^{2+}$.

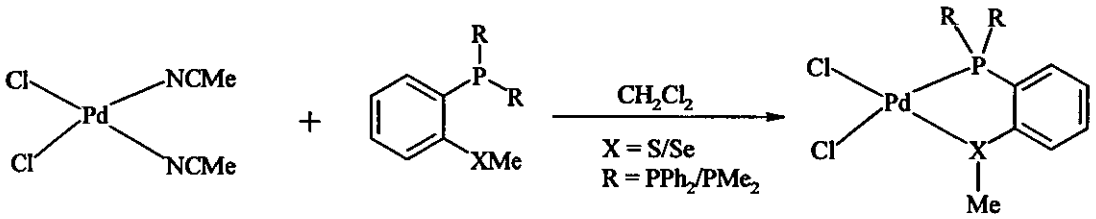

1.35a X = S, R = Ph
1.35b X = S, R = Me
1.35c X = Se, R = Ph
1.35d X = Se, R = Me

1.36a X = S, R = Ph
1.36b X = S, R = Me
1.36c X = Se, R = Ph
1.36d X = Se, R = Me

Equation 1.2 – First Ni(II) complexes containing P/S/Se groups

Woollins *et al.* reported the preparation of a series of P/Se-containing ligands prepared from $(PhP)_5$ and elemental selenium.[27, 28] An example of these, **1.37**, is shown in Figure 1.8. Now commonly known as 'Woollins reagent', **1.37** has been shown to have a number of uses, such as the conversion of carboxylic acid to selenocarboxylic acids.

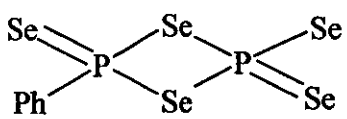

1.37

Figure 1.8 – 'Woollins reagent'

Recently, Aguado *et al.*[29] reported the reaction of both P/S and P/Se substituted ferrocene ligands with Group 11 metals (Figure 1.9). This work followed on from a previous attempt to prepare unsymmetrical ferrocenyl ligands by Liu *et al.*[30] After reaction of $FcLi_2$ with Cl_2PPh, LiPh and S_2Ph_2 or Se_2Ph_2, the ferrocenyl ligands **1.38** and **1.39** were formed. Reaction of **1.38** and **1.39** with various Au and Ag starting materials were used to prepare complexes such as **1.40** and **1.41**. Characterisation by $^{31}P\{^1H\}$ NMR showed the expected chemical shifts of around 45-55 ppm from -17.0 ppm to between 28 and 38 ppm. Whilst many of the silver reactions resulted in chelation of the ligands to the metal centre, gold complexes such as **1.40** and **1.41** contained free chalcogenide groups. These were subsequently reacted with Ag(I) or Pd(II) starting materials to form heterobimetallic complexes such as **1.42** (Figure 1.9). This approach was influential in some of the chemistry we attempted in our work on phospha-adamantane chemistry.

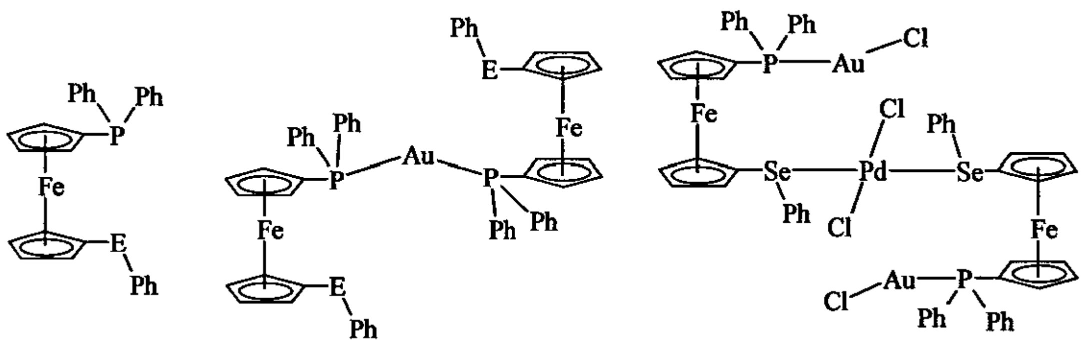

1.38 E = S
1.39 E = Se

1.40 E = S
1.41 E = Se

1.42

Figure 1.9 – Ferrocenyl phosphine-selenides

An example of a phosphorus/selenium complex, though where the P and Se were not part of the same ligand, was reported by Narayan *et al.*[31] This was based on the pyridine-2-selenolate ligand, *o*-C_5H_4NSe. Complexes of the type $MCl(NC_5H_4Se)(PR_3)$ **1.43** were prepared containing a variety of phosphine co-ligands such as PEt_3, PMe_2Ph, and PPr^n_3. The selenolate ligand proved to be more versatile than its sulfur analogue, and showed a tendency to form N,S bonded mononuclear chelate complexes with a number of Pd(II) and Pt(II) starting materials such as that shown in Equation 1.3. The fact that the pyridyl selenide ligands formed mononuclear complexes compared with the predominantly binuclear complexes formed with thiol analogues was attributed to the greater M-X bond length in the former. However, a

series of binuclear complexes were prepared on reaction of the chelate complexes with dimeric materials of the type $M_2Cl_2(\mu\text{-}Cl)_2(PR_3)_2$ **1.44**, as shown also in Equation 1.3. The metal centres were shown to be in distorted square planar environments, due to the fact that the pyridyl-selenide is chelated to only one of the two metal centres.

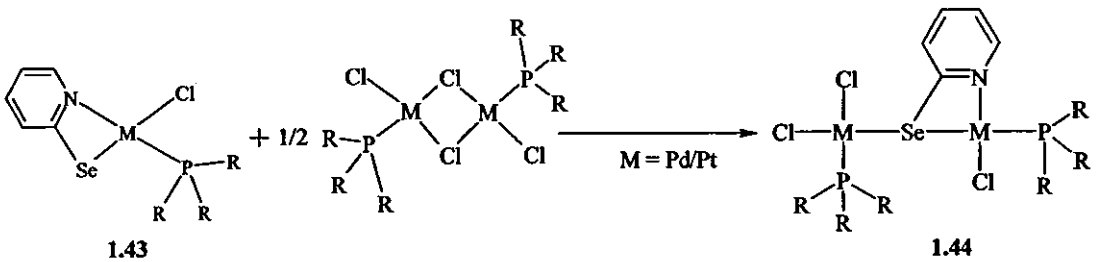

1.43 **1.44**

Equation 1.3 – Pd(II)/Pt(II) P/Se complexes

Jain *et al.*[32] prepared a number of Pt(II) complexes containing selenolato- and *bis*(diphenylphosphino)alkanes as separate ligands. The starting materials for this research were dichloroplatinum compounds $PtCl_2$(L-L) (where L-L is a chelating diphosphine ligand, for example dppe or dppp). These were reacted with various sulfides and selenides such as PhSH (using NEt_3) and NaSePh to yield *cis*-Pt complexes containing one or two *bis*-phosphines and one or two chalcogenide groups. One of these, $Pt(SePh)_2$(dppm) **1.46** (Equation 1.4), was characterised by X-ray crystallography. The metal centre was shown to be in a distorted square planar geometry, due to the small bite angle enforced by the nature of the diphosphine ligand; this has been shown in a number of previous complexes containing such a ligand.[33]

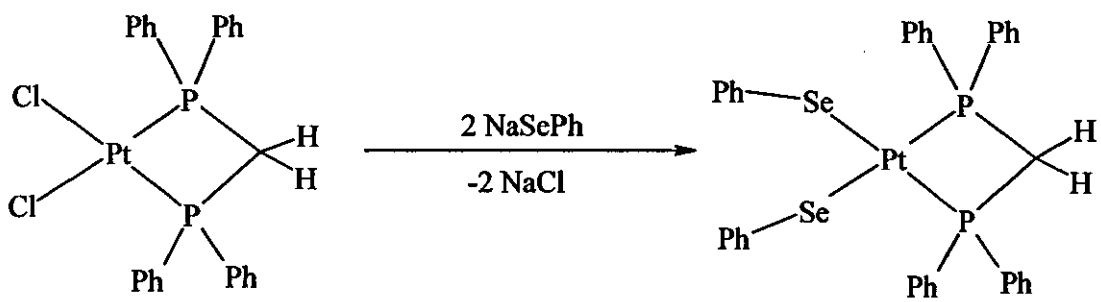

1.45 **1.46**

Equation 1.4 – Pt(II) complexes of phosphine-selenide ligands

Binuclear complexes were also prepared containing either thiolate or selenolate bridges, by treatment of the ionic species $[Pt(L\text{-}L)(MeOH)_2][BPh_4]_2$ with

the complexes such as **1.46**. The structures of these complexes were confirmed using $^{31}P\{^{1}H\}$ NMR spectroscopy, with the presence of ^{3}J(Pt-P) coupling (30 Hz) being indicative of a binuclear species.

Smith *et al.*[34] produced a series of phosphorus, nitrogen and selenium-containing ligands as shown in Figure 1.10. As can be seen, these contained P and N donor centres in the ideal positions to act as chelating ligands to metal centres such as Pd or Pt. The ligands **1.47** and **1.48** were prepared by reacting Ph_2PCH_2OH or (2-$Ph_2P)C_6H_4C(H)=O$ respectively with $H_2N(CH_2)_nSePh$ ($n = 2,3$). Reaction of **1.47** with $MCl_2(COD)$ (M=Pd/Pt) gave, as expected, the *P,P*-bound bidentate complexes displaying a *cis* configuration, leaving the alkyl selenide functionality uncoordinated. Reaction of $MCl_2(cod)$ with **1.48** allowed the iminophosphine to chelate to the metal centre through the P and N donor atoms to form **1.49**. The metal centres were shown to be in a slightly distorted square planar environment, with slightly different M-Cl bond lengths as a consequence of the groups *trans* to each Cl.

Using the P,N-bidentate complex **1.49** as a starting point, and reaction with one equivalent of $Ag[BF_4]$, it was then possible to displace one chloride and bring the pendant SePh arm round to coordinate the selenium atom to the metal centre. This formed the cationic complex **1.50**, characterised by X-ray crystallography, and this was one of the few examples of such a complex with a P/N/Se/Cl donor set.

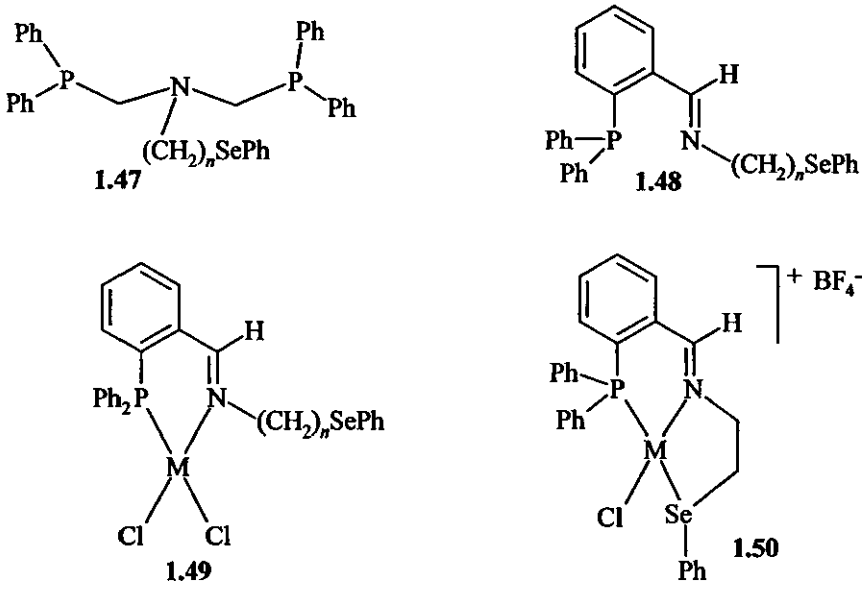

Figure 1.10 – P/Se/N ligands and complexes

The synthesis of ligands and subsequent complexes containing more than two potential donor atoms such as these has been a source of interest for a number of years. The potential for different coordination and subsequent catalytic properties due to the hemilabilty of the donor atoms involved, and hence the ability for the donor atoms to stably occupy three or more coordination sites around a metal centre, has been a major driving force behind this research.

1.3 CHEMISTRY OF MULTIFUNCTIONAL LIGANDS

A number of novel terdentate ligands containing different combinations of phosphorus, nitrogen and sulfur donor atoms were prepared by Vrieze *et al.*[35] These ligands, shown in Figure 1.11 (**1.51-1.53**), were coordinated to various methyl-, acetyl-, and allyl palladium(II) and platinum(II) centres to give complexes such as **1.54**. All of these complexes exhibited terdentate coordination, even **1.53**, which added to previous contrasting reports regarding the coordinating fashion of similar potentially terdentate ligands.[36,37]

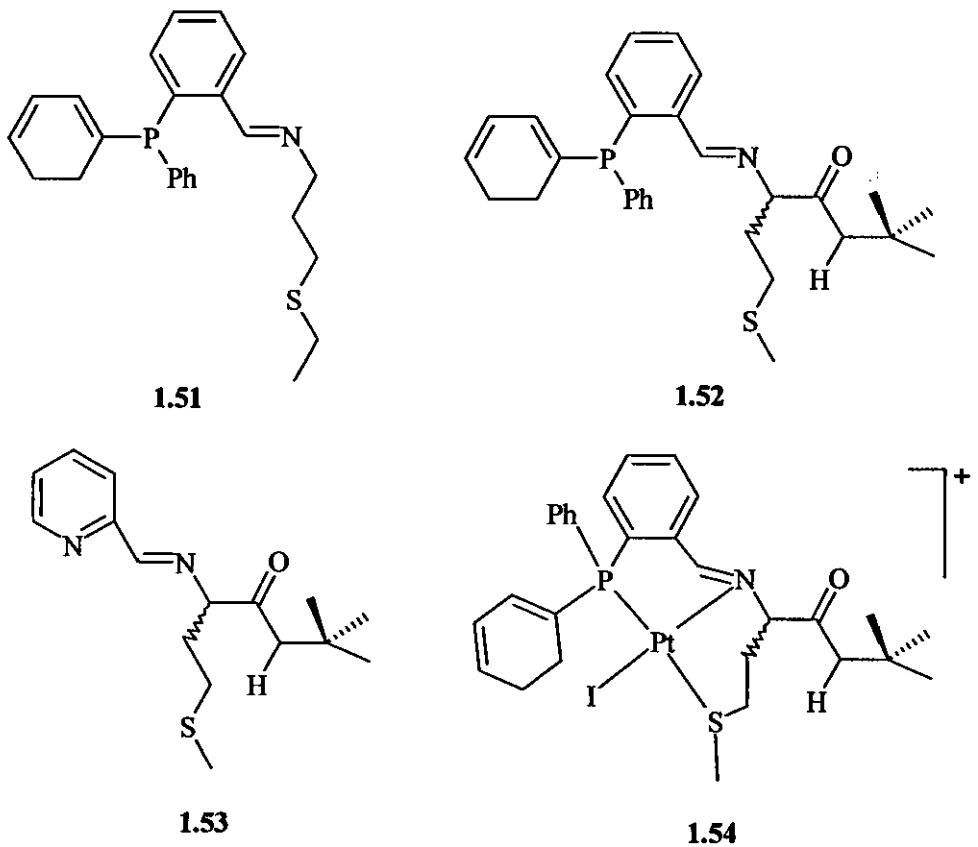

1.51 **1.52** **1.53** **1.54**

Figure 1.11 – Novel terdentate ligands

The research group of Meek have contributed heavily to the area of phosphine chemistry in general for a number of decades. Work on phosphine chalcogenide ligands and their complexes[23] was followed by an interest in the chemistry of multidentate phosphines. In particular, the synthesis of 'tripodal' tetradentate ligands featured heavily in their work, and many other research groups in the 1970s.[38-40] Many of the methods used for this, such as the use of alkyl metal phosphides, or radical addition of a P-H bond to vinyl substituents lead to impure products. In 1984, Waid and Meek[41] reported the synthesis of chelating triphosphine ligands on platinum metal centres. Some of these complexes, **1.57** and **1.58**, are shown in Equation 1.5. All of the complexes were prepared from the corresponding diphosphine complex (**1.55** or **1.56**) and diphenylvinylphosphine, in ethanol and in the presence of triethylamine catalyst.

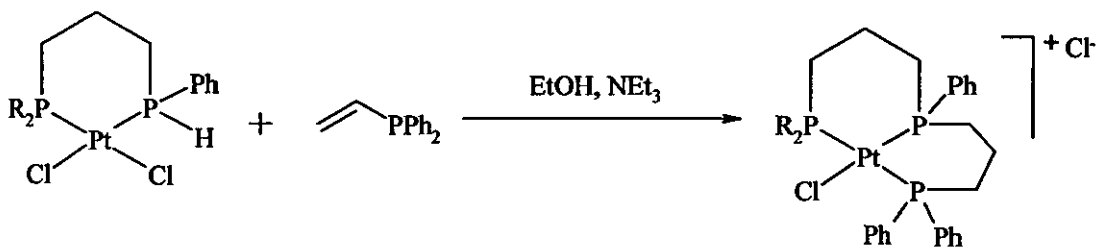

1.55 R = Ph
1.56 R = Cy

1.57 R = Ph
1.58 R = Cy

Equation 1.5 – Pt(II) complexes of chelating tridentate ligands

The chemistry of 'pincer' ligands has received an increased amount of attention in recent years. The interesting complexes formed with late transition metals gives extensive possibilities with regards to catalytic applications. A number of single-donor pincer ligands have been reported, such as the examples by van Koten ($[2,6\text{-}(Ph_2PCH_2)_2C_6H_3)]^-$),[42] and Milstein ($[2,6\text{-}C_6H_3(CH_2PBu_2)_2]^-$).[43] Even more recently, Laguna *et al.*[44] reported the preparation of $PPh(2\text{-}C_6H_4SH)_2$, **1.59** (Figure 1.12), and subsequent Ni(II) and Pd(II) complexes, such as **1.60**.

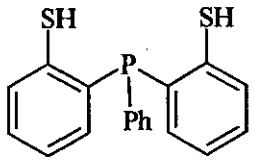

1.59

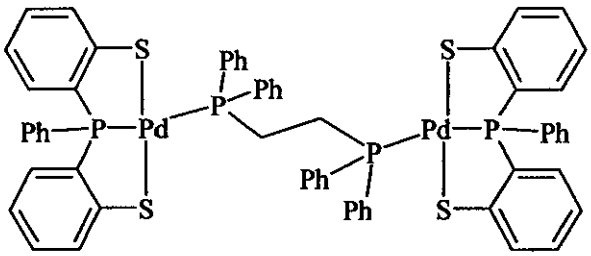

1.60

Figure 1.12 – S/P/S 'pincer' ligands

Similar P/S-ligands and complexes were synthesised by Reid *et al.*[45] The basic tetradentate ligand structure of **1.61** for example, shown in Figure 1.13, and could be derivatised to give the sulfur and selenium analogues **1.62** and **1.63**. Subsequent reaction of the ligands with $[Cu(MeCN)_4]PF_6$, and other Au(I) and Ag(I) starting materials gave a variety of tetracoordinate complexes such as $[Cu(\mathbf{1.61})]PF_6$.

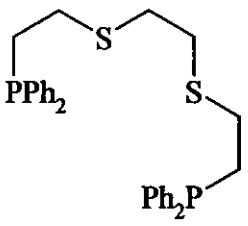

1.61

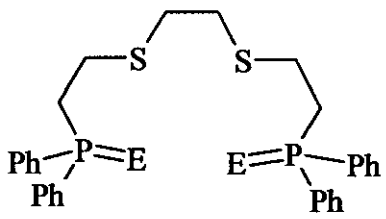

1.62 E = S
1.63 E = Se

Figure 1.13 – Tetradentate 2P/2S ligands

A number of metallamacrocycles containing two phosphinite functionalities and one sulfide group were prepared by Arena *et al.* in 2001.[46] The ligands **1.64-1.66**, shown in Figure 1.14, were also synthesised using a standard procedure for the preparation of phosphinites using Ph_2PCl and NEt_3 along with the parent phenol. Ligands with an isopropyl backbone were designed to induce a bridging coordination to the transition metal centres. The sulfide-containing ligand **1.64** gave the expected single signal in the $^{31}P\{^1H\}$ NMR at 117.1 ppm, along with two singlets at 1.26 and 1.31 ppm in the ^1H NMR spectrum due to the *tert*-butyl groups.

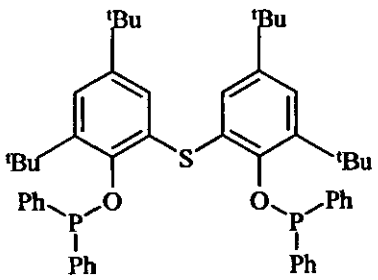

1.64

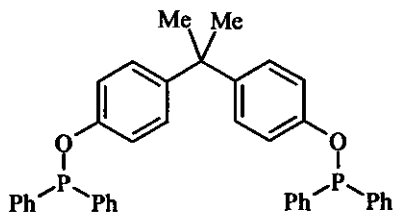

1.65

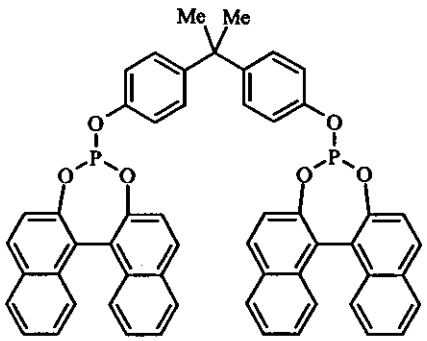

1.66

Figure 1.14 – Phosphine metallamacrocycles

A number of reactions were carried out using the ligands shown above with Pd(II) and Pt(II) starting materials. Ligands **1.65** and **1.66** were shown to form bridging metallamacrocycles and chain-like structures, especially with **1.65** as the starting ligand. The ligand more relevant to this section of the project, **1.64**, initially gave an unexpected product **1.67**, shown in Figure 1.15, containing one hydrolysed phosphinite group. The complex shown was formed as a mixture of two products, giving peaks in the $^{31}P\{^{1}H\}$ NMR spectrum at δ(P) 136 and 79 ppm. The resulting hydroxy-containing ligand, similar to target ligands in this project, was found to be

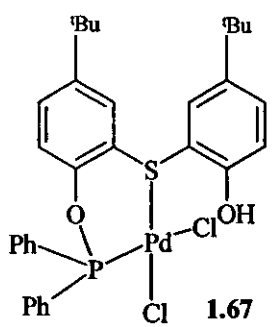

1.67

Figure 1.15 – Phosphine metallamacrocycles – $PdCl_2$ complex

chelated through just the phosphinite and sulfide groups, and this complex was separated as yellow crystals by fractional crystallisation and the structure determined crystallographically.

Andreasen *et al.*[47] reported a series of Pt(II) complexes containing a phosphine/sulfide/phosphine chelating ligand, bis(2-diphenylphosphinoethyl)sulfide, $(Ph_2PCH_2CH_2)_2S$ (**1.68**, Equation 1.6). Structural analysis of the complexes showed all three donor atoms to be coordinated to the platinum centre, with the coordination sphere of the metal completed with a variety of co-ligands e.g. (Cl^-, I^-, Br^-, SCN^-). The complexes were prepared using **1.68** and K_2PtCl_4 in a water/acetonitrile mixture, as shown in Equation 1.6. Once formed, a number of ligand substitution reactions were carried out using $LiClO_4$, KBr and NaI. Crystal structures of two of the Pt complexes, $[Pt(PSP)Cl]ClO_4$ and [Pt(PSP)I]I were elucidated. The structure of the former was as expected, with the P, S and second P atoms all coordinated to the Pt centre. Comparison of the Pt-P bond lengths [2.317(1) and 2.315(1)Å] with other mutually *trans*-diphosphines showed them to be similar. Distortion of the Pt geometry from square planar was shown, the P-Pt-P angle (161.14 (4)°) evidence of the strain being enforced on the tridentate ligand. On replacement of the Cl^- co-ligand with I^-, the steric demands of the iodide enforces even more distortion on the complex. The $^{31}P\{^1H\}$ NMR spectra exhibited singlets at either 38 or 45 ppm, along with the expected Pt satellites with ^1J(Pt-P) coupling around 2500 Hz.

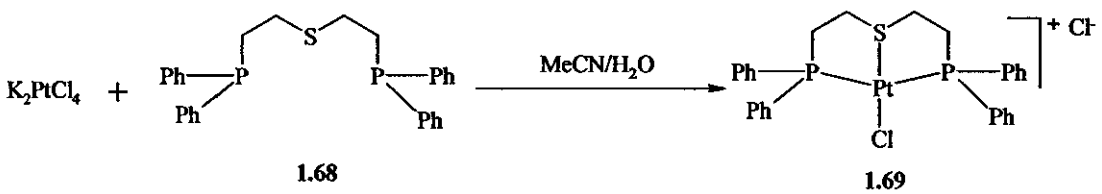

1.68 **1.69**

Equation 1.6 – Pt(II) complexes $(Ph_2PCH_2CH_2)_2S$

The chemistry of tetradentate macrocycles, containing combinations of P, S, O, and N donor centres and the Pt(II) complexes of one such example has been investigated extensively by Davis *et al.*[48] The synthesis of ligands **1.77-1.80** as shown in Scheme 1.5 was reported previously,[49,50] from lithiated diphosphines or disulfides and the corresponding linker. Initial attempts to form complexes of **1.77-1.80** gave

complexes of the type $(L)_2M$, where L = the mixed donor ligand and M = a variety of transition metals. However, incorporation of the thioether and phosphine into *cis*-positions in the macrocycle, followed by complexation using $PtCl_2(cod)$ and $Ag[PF_6]$ gave **1.81** (Scheme 1.5).

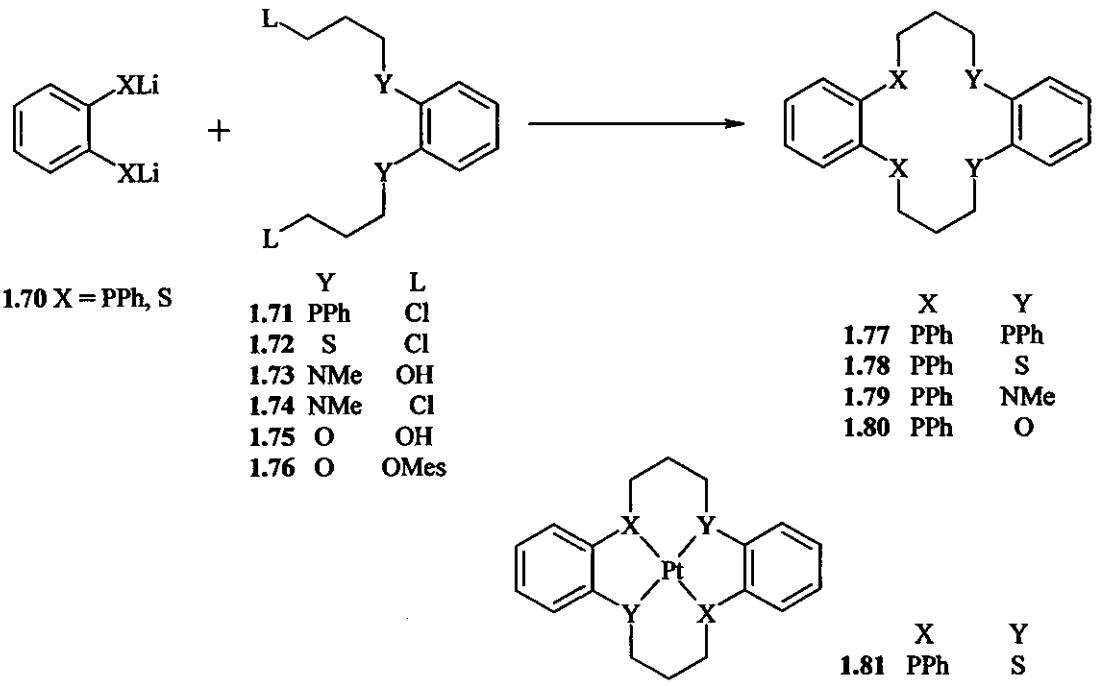

Scheme 1.5 – Chemistry of tetradentate macrocycles

1.3.1 Multifunctional Ligands Containing P/N/O Donor Atoms

Pyridylphosphines have received much interest, due to their ability to stabilise transition metal complexes, and their various catalytic applications.[51,52] Examples of multifunctional pyridylphosphines (P/Pyridyl/X, X = N/O) have been reported.[53,55]

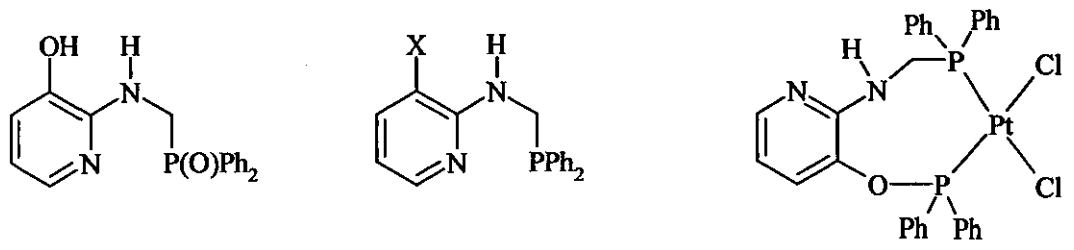

1.82

1.83 X = $OP(O)Ph_2$
1.84 X = $OP(O)(OPh)_2$
1.85 X = $OPPh_2$

1.86

Figure 1.16 – Multifunctional ligands – pyridyl phosphines

The Smith group reported the synthesis of functionalized pyridylphosphines derived from hydroxymethyldiphenylphosphine, Ph_2PCH_2OH.[56] The novel ligands (**1.82-1.85**, Figure 1.16) were prepared via an initial condensation reaction between 2-amino 3-hydroxypyridine and Ph_2PCH_2OH. Subsequent reaction using hydrogen peroxide (for **1.82**) and various halophosphines and halophosphites (for **1.83-1.85**) gave the desired ligands. These ligands were then reacted with various late transition-metal precursors to give complexes such as **1.86**.

The synthesis and use of aminophosphines has also received increased attention, especially in the last 10 years. These systems are of general formula R-N-X-PR'$_2$ [R and R' = any aryl or alkyl group, X = $(CH_2)_n$] and R-NH-PR'$_2$. Such compounds give new possibilities for coordination chemistry and utilisation of subsequent properties and have been prepared by Smith *et al.* recently.

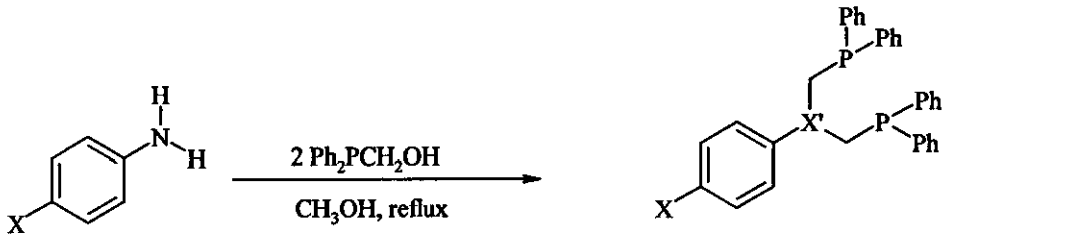

1.87. X = H/CO_2H/COMe/Br/I/OH/$CHCH_2$, X' = N
1.88. X = CO_2H, X' = CH_2N

Equation 1.7 – Aminophosphines prepared by Mannich-style reaction

Ligands of the type *p*-Ar-N$(CH_2PPh_2)_2$, **1.87** and **1.88**, were prepared [57] as shown in Equation 1.7. These used a Mannich-style condensation reaction, starting with hydroxymethyldiphenylphosphine, Ph_2PCH_2OH. Yields obtained were generally very good, for a variety of *p*-substitued functionalities, and all ligands prepared were characterised using $^{31}P\{^1H\}$ NMR spectroscopy.

More recently the Smith group has extended the idea of aminophosphine ligands containing additional functionalities to prepare a number of hexameric Pd(II) complexes.[58] The ligands, such as **1.89** (Equation 1.8), were again prepared from the corresponding amines and Ph_2PCH_2OH, and a solution of these mixed with a solution of Pd(Me)Cl(cod). The resulting complex, **1.90**, was shown by a variety of methods to contain the expected diphosphine six-membered chelate, and that the same metal

centre involved in this was coordinated to a carboxylic acid oxygen atom on a second molecule of **1.89**. The hydroxy group situated *para-* to the diphosphine gives rise to extensive hydrogen bonding motifs. A halide-substitution test attempt using NaI resulted in decomposition of the hexameric structure to give monomeric PdI_2(**1.89**).

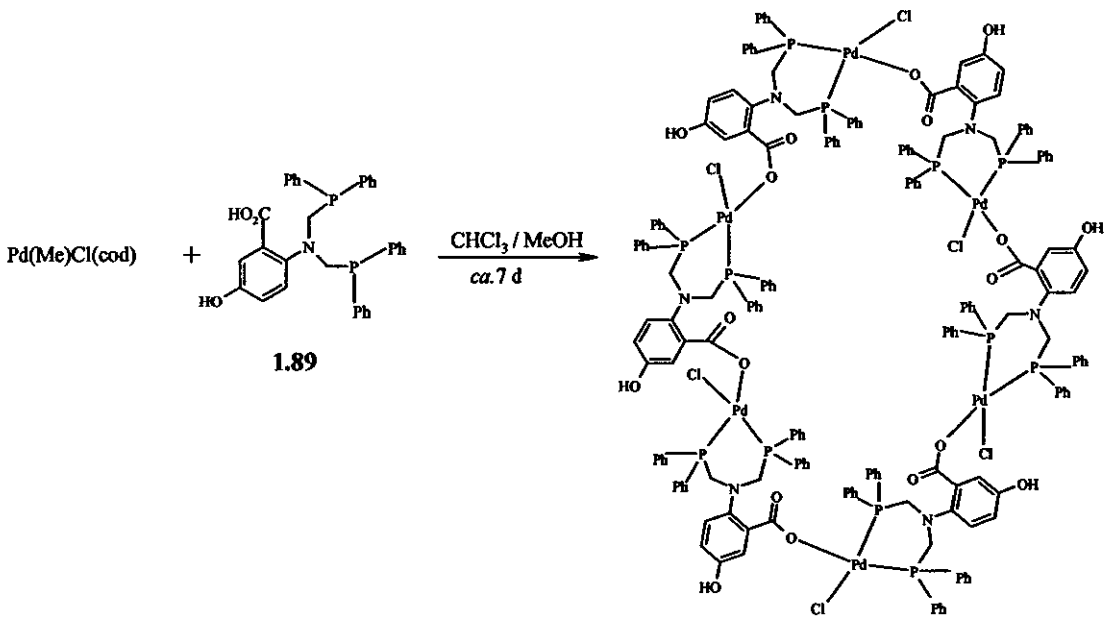

1.89 **1.90**

Equation 1.8 – Hexameric Pd(II) complexes

Previously,[59] ligands of the type *o*-Ar-NH(PPh_2) (where Ar = functionalised phenyl ring) were prepared from the corresponding functionalised amines and Ph_2PCl. These ligands were characterised using $^{31}P\{^1H\}$ NMR spectroscopy, giving signals around 25 ppm. Their coordination chemistry was demonstrated by the preparation of **1.91** and **1.92** (from $PtMe_2$(cod)) and $\{RhCl_2(Cp^*)\}_2$ respectively). These are shown in Scheme 1.6.

The platinum and rhodium complexes prepared both formed orthometalated complexes **1.93-1.95** upon heating in xylene for 24-48 h. This was shown by the large downfield shifts in the $^{31}P\{^1H\}$ NMR spectra, a trend previously seen in 5-membered metallacycles. Crystals of both cyclometallated products were grown and the X-ray structures elucidated.

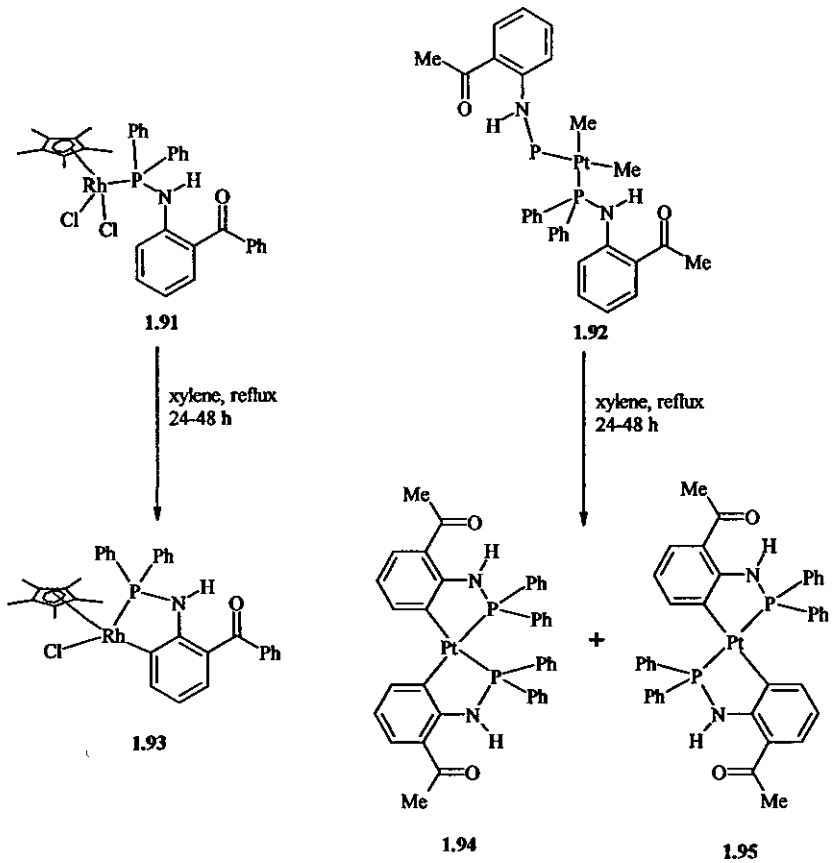

Scheme 1.6 – Pt/Rh complexes of aminophosphines

1.4 SULFIMIDE AND PHOSPHAZENE CHEMISTRY

1.4.1- The Chemistry of Sulfimides

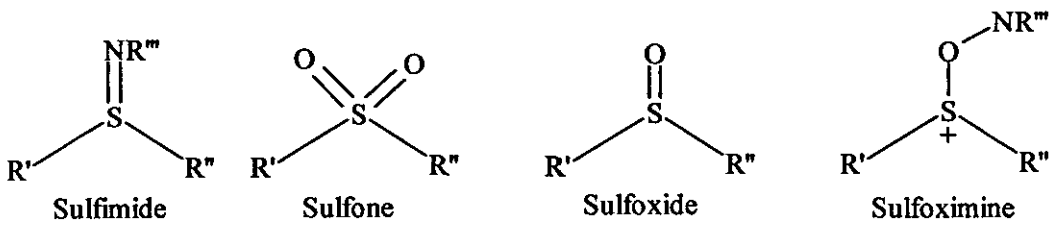

Figure 1.17 – Comparison of sulfimides, sulfones, sulfoxides and sulfoximines

Research into the chemistry of sulfimides (or sulfilimines) has increased steadily over a number of years. Of the general structure $R^1R^2S{=}NR^3$, they are closely related to sulfones, sulfoxides and sulfoximines, as shown in Figure 1.17. Examples are known for when R^1 and R^2 are both alkyl,[60,61] both aryl substituents[62] or a mixture,[63] though sulfimides are more temperature and air stable when the second combination of these substituents is used.

Sulfimides were discovered by Raper *et al.* in 1917,[64] when chloramine-T was reacted with mustard gas, and this method is still used widely today for the preparation of arylsulfonyl sulfimide derivatives. A variety of aryl- and alkyl- sulfides have been shown to react with *N*-halosulfonamides such as chloramine-T (**1.96**) to produce the corresponding sulfimides. The Mann-Pope reaction,[65] as shown in Scheme 1.7, involves the preparation of N-*p*-tosylsulfimides using chloramine-T. This is followed by neutralisation using H_2SO_4 and NaOH.

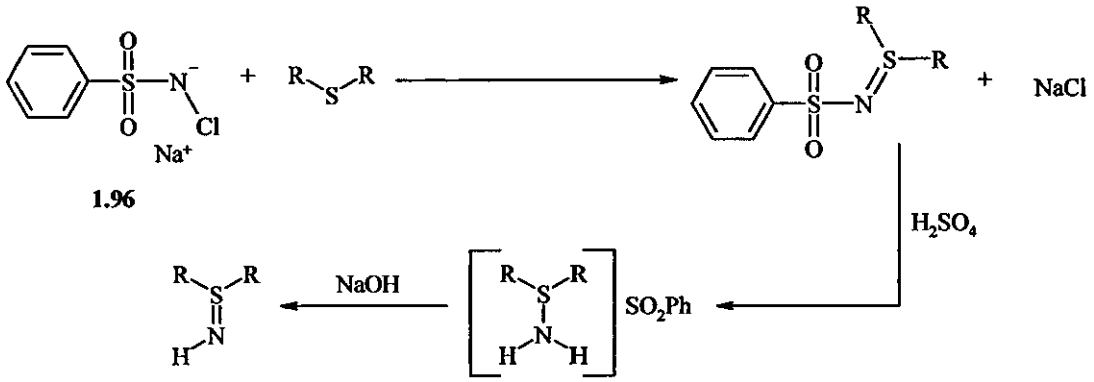

Scheme 1.7 – The Mann-Pope reaction

Many other methods for the preparation of sulfimides are known, and have been reviewed by Gilchrist *et al.* in 1977 (see Table 1.1 for summary).[66]

Type of Reaction	General Example	Reference Number
Reaction of sulfoxides with amines	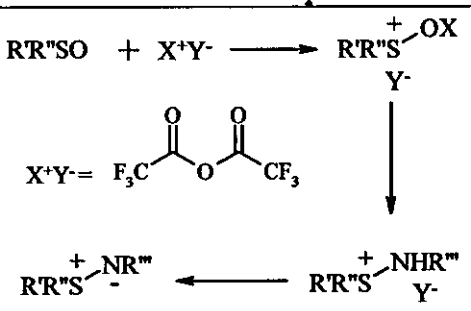	67
Reaction of dialkoxysulfuranes with amines and amides	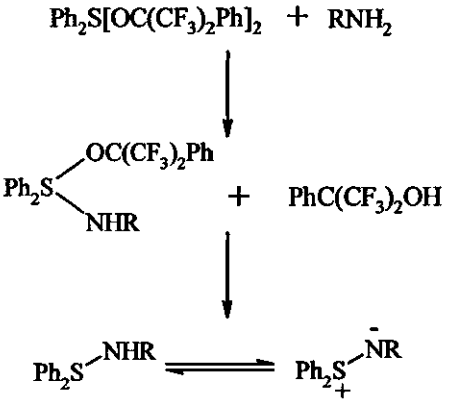	68
Reaction of sulfoxides with sulfur diimides	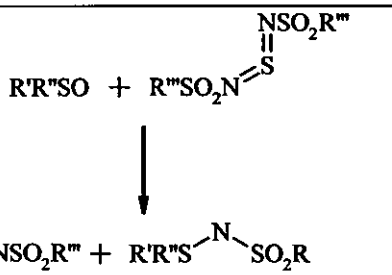	69
Use of azides	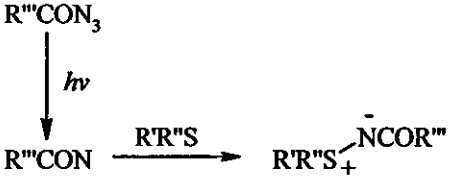	70
Reaction of sulfides with *o*-mesitylenesulfonyl hydroxylamine	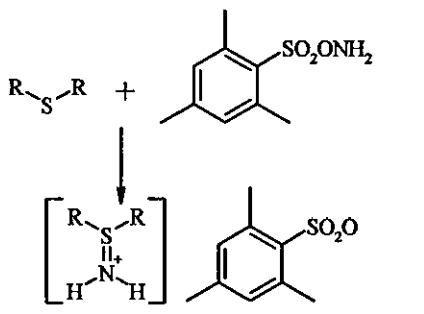	71,72

Table 1.1 – Methods of preparation for sulfimides

The last of these, reaction of sulfides with *o*-mesitylenesulfonyl hydroxylamine (MSH) is the method used for the majority of reactions to be discussed in this work.

Whilst the method of using chloramine-T has been known for a long time, Sharpless *et al.*[73] reported an improvement on the preparation of certain types of sulfimide. This improvement was based upon the use of pure acetonitrile for reactions involving chloramine-T and excluding the use of CuOTf reported previously. A series of thiabicyclononanes were reacted with an excess of various chloramine salts in acetonitrile at room temperature, generally giving excellent yields of the corresponding sulfimides ($\geq$ 86%). Also interesting were the high yields obtained when acyclic sulfides such as MeS(^{t}Bu) and EtS(CH_2CH_2OH) were used as starting materials. Previously yields of such sulfimides especially those with other functionalities on alkyl chains were low. Where reactions did not proceed sufficiently quickly (with some diarylsulfides), it was found that both use of a 20% excess of chloramine salt and refluxing reaction conditions could push the reaction through to completion.

A number of platinum and palladium complexes of sulfimides were prepared in 1989 by Davidson *et al.*,[74] incorporating heteroaromatic groups into the sulfimide ligands and analysing their coordination patterns. Upon addition of ligands such as Me_2SNR (R = 2-pyridyl, 2-pyrimidinyl) to the Pt(II) and Pd(II) materials $K_2[PtCl_4]$, $PtCl_2(PhCN)_2$ and $PdCl_2(PhCN)_2$, dimeric complexes such as **1.97** shown in Figure 1.18 were formed. The sulfimide ligand had two possible modes of coordination; through the sulfur ylid functionality or through the pyridyl nitrogen centre. In order to establish this, analogous reactions were carried out without the pyridyl group on the ligand. However, reactions of $PhNSMe_2$ with $PtCl_2(PhCN)_2$ and $PdCl_2(PhCN)_2$ in CH_2Cl_2 gave different products, $PtCl_2(Me_2SNPh)(PhCN)$ and $PdCl_2(Me_2NSPh)_2$ respectively.

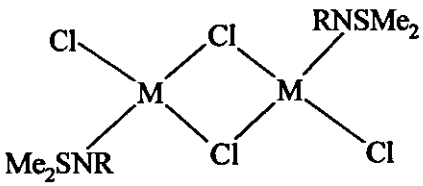

1.97

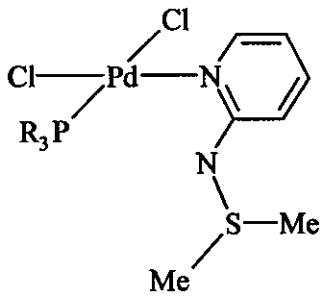

1.98

Figure 1.18 - Methylsulfimides

Halide bridge cleavage of the dimeric products formed by the pyridyl sulfimide ligands using a variety of phosphines, was carried out. One of these, $PdCl_2(PPh_3)(Me_2SNC_4H_3N_2)$ **1.98**, was characterised crystallographically and showed the expected *cis*-square planar structure and coordination of the ligand through the pyrimidine N donor. It is also interesting that halide bridge cleavage gave *cis*-structures when arylphosphines such as PPh_3 were used, whereas *trans*- products were obtained from reactions using alkylphosphines *e.g.* PEt_3.

Many of the more recent advances in sulfimide chemistry have been made by the Kelly group, in particular using diphenylsulfimide as starting material.[75] The idea behind the coordination chemistry of diphenylsulfimide has only recently been extended to bidentate sulfimide systems. Again, much of the work has been carried out by the Kelly group,[76] specifically highlighting systems containing both two sulfimide groups in various orientations, and also hybrid sulfide/sulfimide units.

Using MSH as aminating agent and 1,8-diazabicyclo[5.4.0]undec-7-ene (DBU) to deprotonate, $1,4\text{-}(PhS(NH))_2C_6H_4$ **1.99** (Figure 1.19) has been prepared by Kelly *et al.*, which is isolable in dehydrated or hydrated forms. This gives an interesting bridged species as expected due to the *para*- orientation of the functional groups, when $[PPh_4]_2[PdBr_6]$ was added in CH_2Cl_2. The complex was confirmed by shifts in the S=N and N-H stretches in the infrared spectrum compared to those of the free bis-sulfimide ligand, and also by X-ray crystallography. The latter reveals that the four sulfur atoms form an almost square-like orientation, and a lack of hydrogen bonding of the N-H unit, surprising in comparison with monosulfimide units previously mentioned.

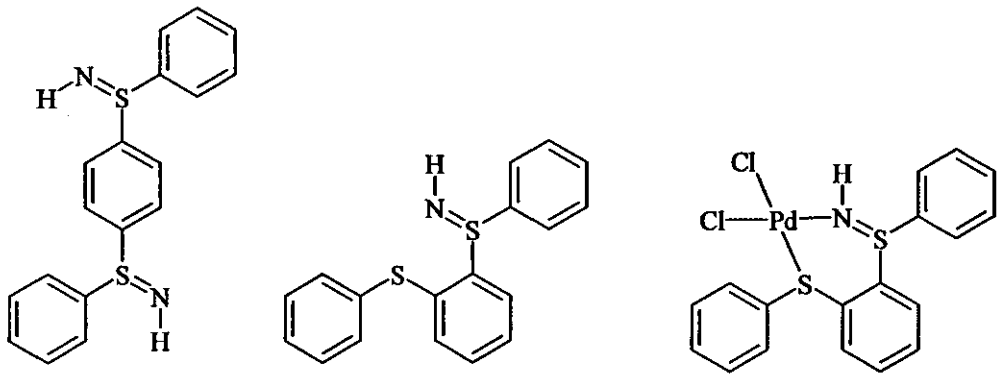

1.99 **1.100** **1.101**

Figure 1.19 – Hybrid sulfimides and complexes

Hybrid sulfide/sulfimide complexes using ligands such as *o*-C_6H_4{S(NH)Ph}(SPh) **1.100** have also been prepared upon reaction with Pd(II) starting materials.[77] When triphenylphosphine was added to the resulting chelate complexes such as **1.101**, the thioether-metal link was cleaved and the coordination site occupied by PPh_3.

Many other features of sulfimides have been discovered recently. For example, the structural diversity of cobalt[78] and copper[79,80] complexes of diphenylsulfimide has been investigated, the use of Ph_2SNBr as a nitrogen source to prepare the explosive nitride S_4N_4,[81] and a method of coupling sulfimides to thiacrowns and phosphines has been established.[82] Examples of the latter (**1.102** and **1.103**) are shown in Figure 1.20. Such work implies that the scope for further research in this area is ostensibly very wide.

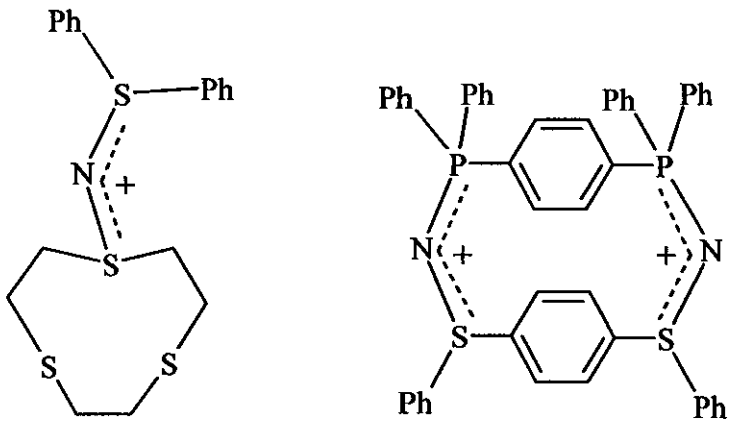

1.102 **1.103**

Figure 1.20 – Coupling of sulfimides to phosphines and thiacrowns

1.4.2 – The Chemistry of Phosphazenes

Phosphazenes are compounds which have been described as compounds that contain a phosphorus-nitrogen double bond i.e. derivatives of $H_3P{=}NH$ and $HP{=}NH$.[83] Phosphazenes are also types of ligands that have been studied extensively since the mid 1960's. Shown in Figure 1.21, monophosphazenes such as **1.104** are analogous to phosphorus ylids (**1.105**), and have a vast number of preparative routes. Possibly the most common method for preparing phosphazenes is the Staudinger reaction reported in 1919.[84] Whilst this is an extremely general reaction in terms of possibilities for organic R^1 groups, the method requires the preparation of organic azides of the type $R\text{-}N_3$, and is therefore also potentially extremely hazardous.

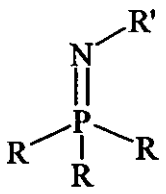

1.104

Monophosphazene

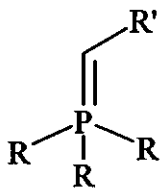

1.105

Phosphorus ylid

Figure 1.21 – Comparison of monophosphazenes and phosphorus ylides

A second common method is the Kirsanov reaction.[85] This uses a phosphorus dihalide starting material such as Ph_3PCl_2 and liberates two moles of the acid of the halide *i.e.* HCl in this case, upon reaction with an amine-bearing reagent such as aniline. A slight variation of this method has been used in this project.

Many complexes of phosphazenes have been reported in the literature. Imhoff *et al.*[86] reported a number of such examples containing rhodium centres and phosphazenes containing a number of aryl and alkyl substituents. As shown in Equation 1.9, when added to rhodium bridged dimers of the type $[RhLCl]_2$, phosphazenes were able to break the Rh-halide-Rh bridge, and coordinate through the nitrogen donor atom. A number of factors affect the position of the equilibrium between the reactants and the complex; firstly the nature of the co-ligand coordinated to the metal centre (when L=CO, the equilibrium lies entirely to the right), the temperature of the reaction, and finally the nature of the organic groups attached to

both P and N. The first of these can be explained by the higher π-backbonding capabilities of the CO ligand over the other co-ligand used, cod. The third point was shown to be especially important when L = cod, indeed these complexes were only isolable in a handful of cases. The nature of the N-R substituent is also of specific importance when considering steric restrictions to coordination, and this will be approached in work later.

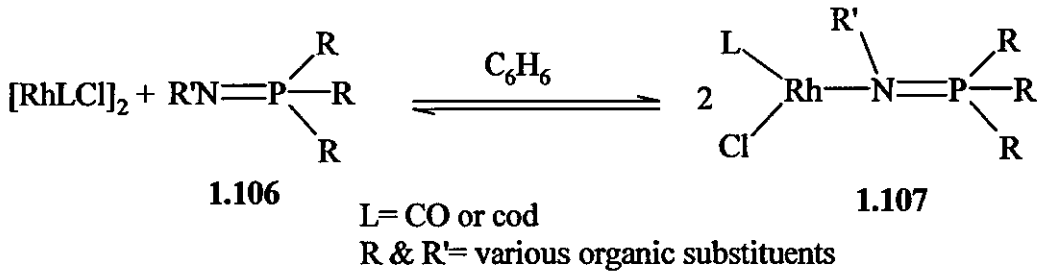

Equation 1.9 – Rh complexes of phosphazenes

Phosphazenes and their complexes have been shown to be important for use in catalysis. Bell *et al.*[87] reported the use of phosphazenes of general type $Cl_3P{=}NAr$ in carbodiimide metathesis reactions, based on the knowledge that such trichlorophosphazenes self-dimerize in solution. As shown in Scheme 1.8, when a carbodiimide such as $Pr^iN{=}C{=}NPr^i$ was added to the trichlorophosphazene, addition of the C-N bond across the P-N bond gave a mixed carbodiimide product. The diazaphosphetidene **1.108**, in equilibrium with the mixed carbodiimide **1.109**, was crystallographically characterised showing that in comparison with the structure shown in Scheme 1.8, the ring is unsymmetrical, explainable by the bond length differences. In an analogous fashion to this reaction, a metathesis reaction was also observed when $Pr^iN{=}C{=}NPr^i$ was heated with TolN=C=NTol. The same procedure was found not to occur when no phosphazene catalyst was added to the reaction.

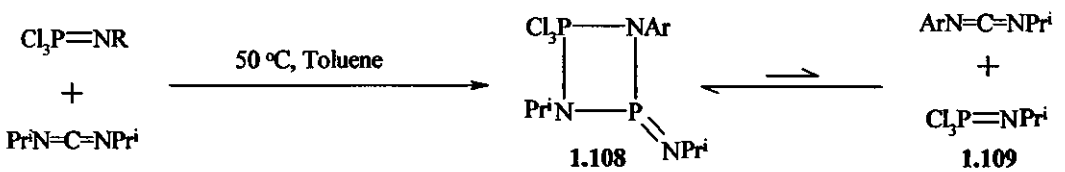

Scheme 1.8 – Use of $Cl_3P{=}Ar$ in carbodiimide metathesis reactions

1.5. CHEMISTRY OF PHOSPHA-ADAMANTANES

The study of phosphines bearing bulky organic groups has received increased interest in more recent years, due to their potential use in catalysis. The leaving group ability of phosphine-containing complexes often determines the rate of catalytic reactions, therefore bulkier phosphines are of great use in this subject area. Incorporation of ligands such as *tert*-tributylphosphine ($^tBu_3P$) and tricyclohexylphosphine (Cy_3P) into various complexes has been studied widely in the past.[88,89]

Stambuli *et al.* investigated the complexation reactions of such sterically hindered phosphine ligands.[90] The three-coordinate, 14-electron palladium complexes were prepared from $Pd(dba)_2$, phosphine ligands bearing both *t*-butyl and adamantane groups in the case of **1.110** (Figure 1.22) and just *t*-butyl groups for **1.111** and **1.112**, and the appropriate aryl halide. X-ray diffraction showed **1.111** to be a T-shaped monomer, unexpected due to previous examples of such complexes being dimeric.[91,92]

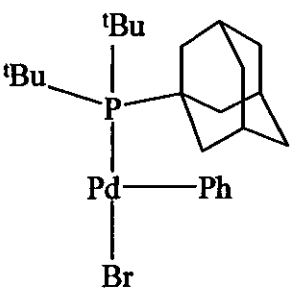

1.110

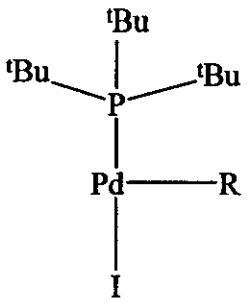

1.111 R = Ph
1.112 R = 2,4-xylyl

Figure 1.22 – Phosphine-adamantanes

The use of 'cage' phosphines such as 1,3,5,7,-tetramethyl-2,4,8-trioxa-6-phosphaadamantane (Cytop, **1.113**) has only just begun to receive wider attention. Discovered in 1961 by Epstein and Buckler,[93] **1.113** can be prepared by reaction of acetylacetone with phosphine (Equation 1.10). Use of secondary phosphines also yields different varieties of phospha-adamantane cage.

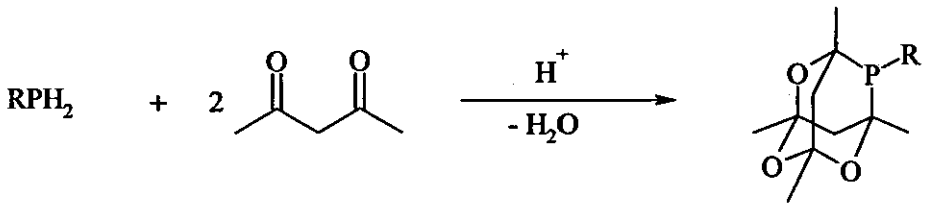

1.113 R = H, **1.114** R = Ph,
1.115 R = Cy, **1.116** R= i-butyl,
1.117 R = n-octyl

Equation 1.10–Preparation of 1,3,5,7-tetramethyl-2,4,8-trioxaphospha-adamantane

Pringle *et al.*[94] used this method to prepare a series of extremely bulky bis-phosphines, containing two phospha-adamantane groups on various alkyl chain length backbones. $PH_2(CH_2)_nPH_2$ (where n = 2 or 3) was reacted with acetylacetone or trifluoroacetylacetone in the presence of HCl to give the corresponding bis(phospha-adamantyl)alkanes **1.118-1.120**, as shown in Figure 1.23.

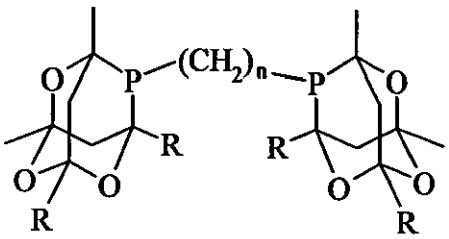

1.118 n = 3, R = CF_3
1.119 n = 2, R = Me
1.120 n = 2, R = CF_3

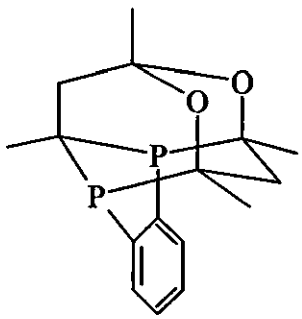

1.121

Figure 1.23 – Bis-phospha-adamantanes

The diastereomeric nature of the phospha-adamantane cages was shown by the shifts in the $^{31}P\{^1H\}$ NMR spectrum at –31.0 and –30.2 ppm. Dichloropalladium(II) chelates of **1.118-1.120** were prepared and characterised, exhibiting the characteristic large cone angles (*ca.* 173°) shown by phospha-adamantane containing complexes.[95] The use of some of these complexes as methoxycarbonylation catalysts has also been reported separately.[96] Compound **1.121** was also prepared using a similar condensation method.

Titanium complexes containing derivatives of **1.114** and **1.115** were prepared by Carraz *et al.*.[97] The phosphorus(V) derivatives were prepared by reacting **1.114** and **1.115** with Me_3SiN_3 to give the corresponding (trimethylsilyl)phosphinimines **1.122** and **1.123**, shown in Figure 1.24.

Reaction of phosphazenes **1.122** and **1.123** with $CpTiCl_2$ in benzene afforded the subsequent titanium complexes $CpTiCl_2\{NPR(C_6H_4O_3Me_4)\}$ **1.124** and $CpTiCl_2\{NPR(C_6H_4O_3Me_4)\}$ **1.125**, confirmed by NMR data. Reaction of these with MeMgBr resulted in substitution of the chloride groups for methyl groups, and these were screened for potential catalytic activity in olefin polymerization. Low activities (<10 g of poly(ethylene)/mmol/h) were observed and it was postulated that this was due to 'rupturing' of the phospha-adamantane cage during the polymerization process.

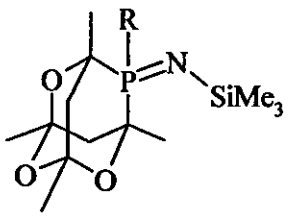

1.122 R = Ph
1.123 R = Cy

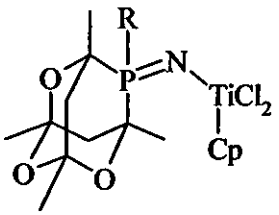

1.124 R = Ph
1.125 R = Cy

Figure 1.24 – Derivatives of phospha-adamantanes

Ferrocenylphosphines have been widely studied due to the ease with which they can be used as ligands,[98] and the catalytic properties of subsequent transition metal complexes.[99] Butler *et al.*[100] prepared phosphaadamantyl derivatives of ferrocene **1.126** and **1.127** (Figure 1.25). These were synthesised by reaction of ortho lithiated 1-(dimethylaminomethyl)ferrocene with ICH_2NMe_2, and subsequent reaction

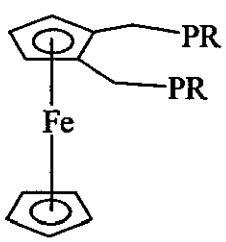

1.126 - 2R = 1-adamantyl
1.127 - R = 1,3,5,7-tetramethyl-2,4,8-trioxa-6-phosphaadamantane

Figure 1.25 – Ferrocenyl phospha-adamantanes

of the bis(dimethylamino) product with di-1-adamantyl phosphine (to give **1.126**) or 1,3,5,7-tetramethyl-2,4,8-trioxa-6-phosphaadamantane (**1.127**).

1.6 USES OF PHOSPHINES IN CATALYSIS

Interest in the industrial and academic uses of complexes containing phosphine based ligands has been well documented for many years. Catalysis is one such area which has benefited from the use of phosphine based ligands. Many organic transformations have seen a dramatic improvement in yield and efficiency with the use of these systems. Turnover numbers (TON, Number moles product/Number moles of catalyst used) obtained have also seen large improvements using certain complexes. Chemical reactions using such complexes include Heck[101,102] and Suzuki[103] C-C bond formations, hydroformylation reactions[104] and alkene copolymerisations.[105,106] Ligands containing phosphine and sulfide functionalities have also been shown to be extremely useful in catalytic carbonylation.[107] General reaction schemes for three of these are shown in Scheme 1.9.

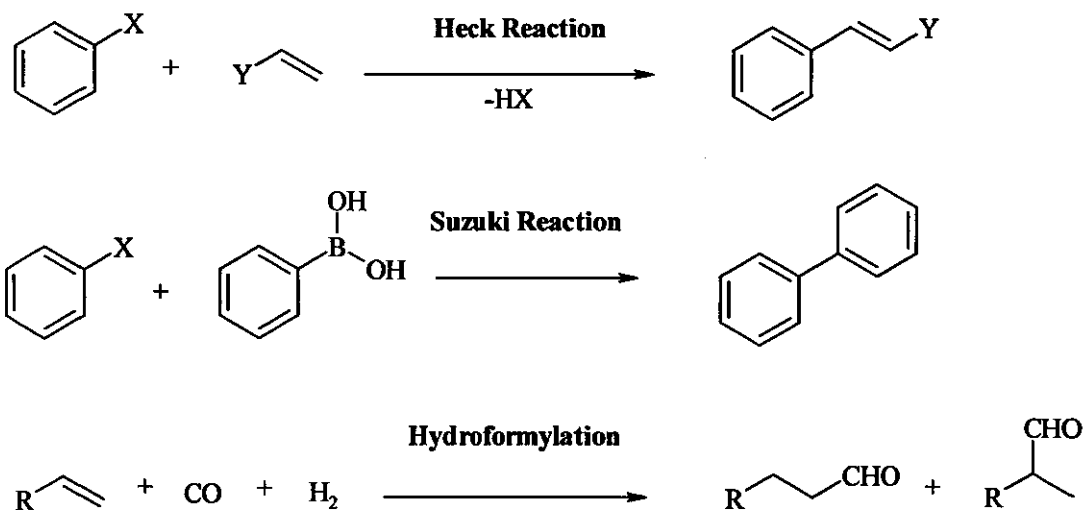

Scheme 1.9 – Heck, Suzuki and Hydroformylation reactions

The Heck reaction was discovered in the late 1960's,[108] and involves the formation of new C-C bonds from alkyl or aryl halides and alkenes. The mechanism for this reaction is shown in Scheme 1.10. The acidic side product is removed from

the reaction by the addition of bases such as tributylamine, and the catalyst reformed by loss of the product to give the starting intermediate.

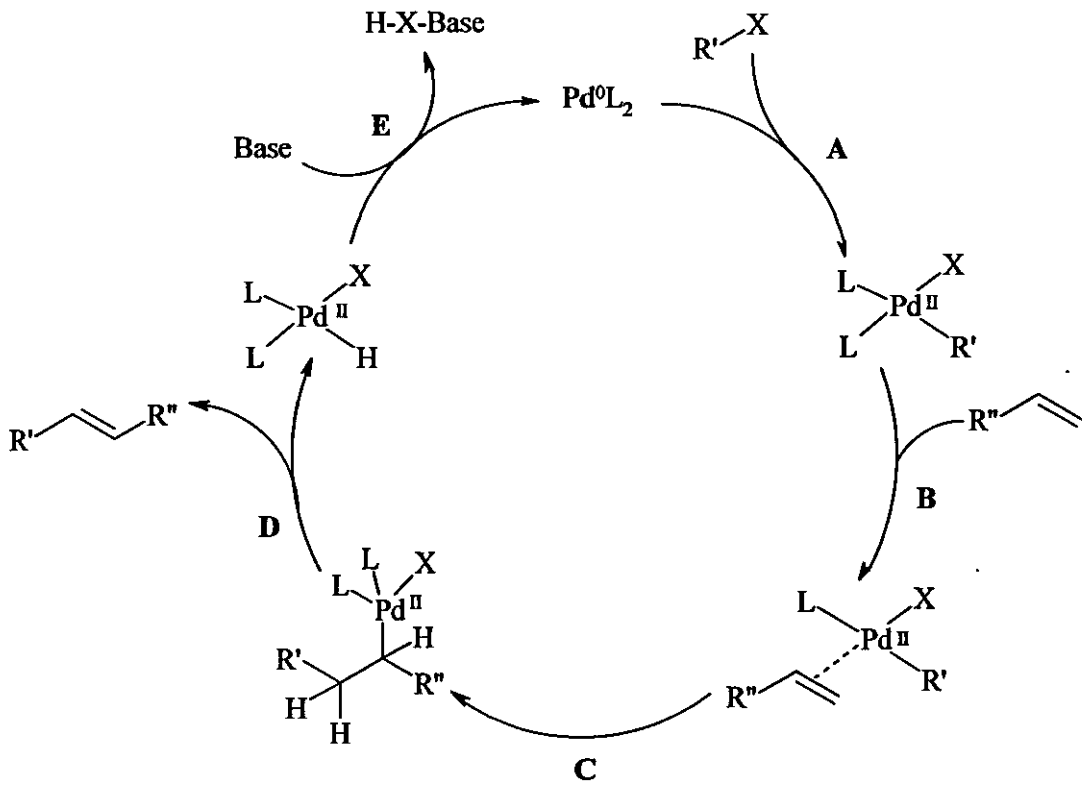

A - Oxidative addition reaction, palladium inserts across R'-X bond
B - Formation of a pi complex upon addition of alkene
C - Alkene inserts across Pd-C bond
D - Beta hydride elimination to give alkene product
E - Reductive elimination reaction using base to regenerate Pd^0 catalyst

Scheme 1.10 – The Heck reaction mechanism

Pd(II) diphosphine complexes have proven to be especially good Heck reaction catalysts. Shaw and Perera[109] showed this using a variety of aryl halides and

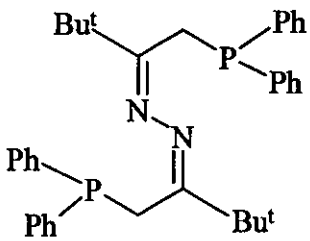

1.128

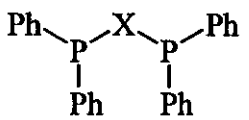

$X = (CH_2)_n = 1,2,3,4$

1.129

Figure 1.26 – Pd(II) diphosphine complexes in catalysis

dichloropalladium(II) complexes with different chelating diphosphines. Previous to this, it had been reported that chelating diphosphines would not produce good catalysts;[110] this was later agreed by Cabri *et al.*[111] However, exceptionally high TON's were obtained and good rates observed using phosphines **1.128** and **1.129** shown in Figure 1.26.

Whilst four membered palladium(II) chelates formed by dppm converted styrene to stilbene in the presence of iodobenzene with a TON of 76300 in 87% yield, larger chelate rings gave much higher TON's. The six-membered palladium chelate ring complex, containing dppp (diphenylphosphino propane), gave a TON of 224700, whilst $PdCl_2$(dppb) (with a seven-membered chelate ring) gave stilbene and a TON of 170300.

The Suzuki reaction is another organic transformation which has used phosphorus containing ligands and complexes extensively to decrease reaction times.[112,113] The Suzuki cross-coupling reaction requires aryl/alkyl boron reagents that can be prepared from aryl halides, these boronic acids are coupled with aryl halides or triflates in the presence of a basic reagent to form various biaryl products. The general mechanism for the Suzuki reaction is similar to other Pd catalysed organic reactions involving oxidative addition and reductive elimination steps. With the variety of substrates that can be used, a trend has been observed with their relative reactivity. For example, as might be expected, the relative reactivity of leaving groups is I > OTf > Br > Cl. Also, the rate of elimination is affected by the two substrates being used, *i.e.* two aryl compounds have a faster rate of reductive elimination than one aryl and

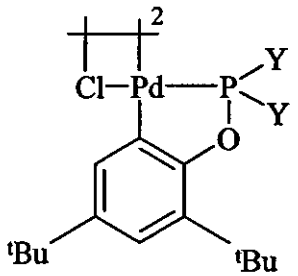

1.130

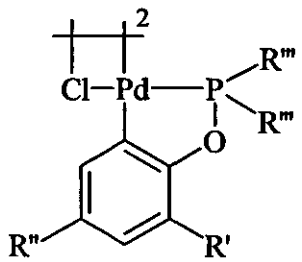

1.131

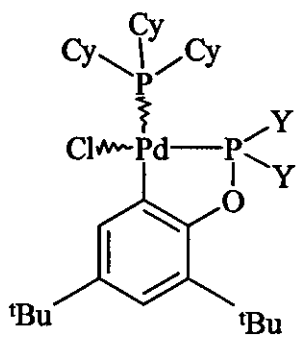

1.132

Figure 1.27 – Suzuki catalysis using phosphinite ligands

one alkyl, which in turn have a faster rate than two alkyl substrates in the order propyl > ethyl > methyl.

Bedford *et al.* reported[114] that palladium complexes containing phosphinite ligands were high-activity catalysts for the Suzuki reaction. Pd(II) complexes of a range of phosphinites (**1.130-1.132**) were prepared as shown in Figure 1.27, the ligands being prepared by reaction of the functionalised phenol with a variety of chlorophosphines and triethylamine. $^{31}P\{^{1}H\}$ NMR data for the ligands ranged from δ(P) 108-151 ppm, this range being shifted upfield from $Ph_2P(OAr)$ analogues due to the presence of bulky alkyl groups in the *ortho* position.

It was shown that these types of ligands are able to catalyse reactions involving aryl chlorides, which had previously shown little or no activity due to the high C-Cl bond strength. This was particularly interesting due to the relative low cost of aryl chlorides compared to bromides or iodides. 4-Bromoanisole was used as a test substrate as it is able to show optimum catalyst performance over other more electronically activated substrates. Preformed complexes of the type $PdCl_2(L)_2$ were shown to give much lower TON's than those which were formed *in situ* from $Pd(dba)_2$ (dba = dibenzylideneacetone). Likewise, the activity of both of these types was much lower than the activities observed for the orthopalladated phosphinite ligands. TONs between 1 and 9 million were observed for the reaction using dimeric complexes of the type shown in Figure 1.28; these were increased to around 475 million when a catalyst loading of 1×10^{-7} mol% was used along with BrC_6H_4(*p*-COOMe) as substrate.

Dilworth *et al.*[115] showed how rhodium(I) complexes can be used to catalyse the carbonylation of methanol. The preparation of such monomeric and dimeric complexes as **1.133** (Figure 1.27) was driven by the failure of previous attempts to improve the known carbonylation catalyst, $[RhI_2(CO)_2]^-$, to withstand the harsh reaction conditions of 150-200 °C and 25-45 atm.

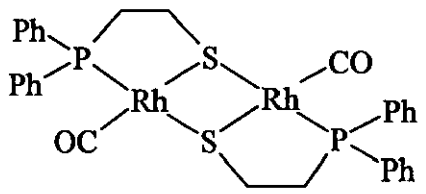

1.133

Figure 1.28 – Rh complex used for carbonylation of MeOH

The complexes were prepared by reaction of $C_6H_4(PPh_2)(SH)$ or $(Ph_2P)CH_2CH_2SH$ with $[RhCl(CO)_2]_2$ dimer, the structure of the complexes being confirmed by the presence of just one doublet resonance in the $^{31}P\{^1H\}$ NMR spectrum, and by a crystal structure determination. It was shown that the maximum rate of reaction was four times that when $[RhI_2(CO)_2]^-$, was used. The mechanism put forward for the reaction was a little surprising at the time, as, despite being similar to the known mechanism using $[RhI_2(CO)_2]^-$, all intermediates were believed to be neutral. Previously, the first reaction of the mechanism with MeI was believed to be driven by the anionic charge on the catalyst.

Gladiali *et al.*[116] have shown how phosphine sulfides can be used as catalysts for asymmetric hydrogenation reactions. The functionalities were part of a BINAP bridged heterobidentate ligand, and these were coordinated to Rh(I) centres to form catalytically active centres. Whilst the metal-sulfur bond strength is different to that of a phosphine, the incorporation of a sulfide group brings the softness of both to a similar level. Complexes of the type $[Rh(L)(NBD)][BF_4]$ **1.135** (L = $\{C_{10}H_6(PPh_2)C_{10}H_6(SR)\}$, NBD = 1,4-norbornadiene) were prepared, and then used to catalyse the hydrogenation of α,β-unsaturated acids and esters (Equation 1.11). The catalytic activity was dependent not only on the nature of the BINAP ligand, but also on the types of R and X groups on the acid/ester substrate. One improvement, however, was often at the expense of another as shown by the hydrogenation of dimethyl itaconate (R = CH_3, X = CH_2CO_2Me). Here, high conversion was observed (93%), but *ee*'s were extremely low. Conversely, when R = CH_3, X = NHCOMe, some of the highest *ee*'s using Rh-P/S ligands were observed (60%), however percentage conversion was relatively very low (13%).

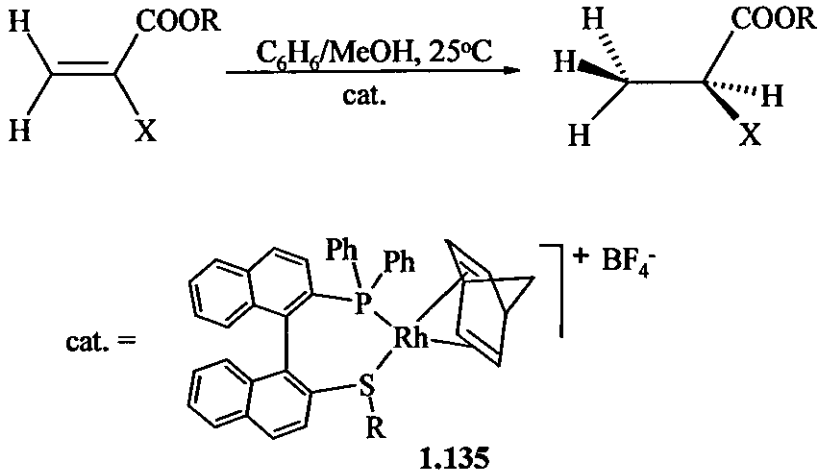

1.135

Equation 1.11 – BINAP bridged P/S ligands

Amer *et al.*[117] reported how phosphine oxides could be used in hydroformylation reactions. It was found that rhodium complexes such as **1.136** containing phosphine oxides of the type $R_2N(CH_2)_nP(O)R'_2$ (n = 2,3), were much better than their phosphine analogues at catalysing the hydroformylation of olefins (Equation 1.12).

Changing various parts of the ligand structure dramatically alters both the yield and the rate of reaction. For example, both varying the nature of the N-R group (*i.e.* yield varies as R = Me > Et > Ph), and the value of n dramatically affected the yield and rate. It was found that replacement of the P=O group in the ligands with a P=S group reduced the yield of the carbonyl product to zero. Replacement of the amino group with a second phosphorus-containing group, *e.g.* PPh_2, meant that

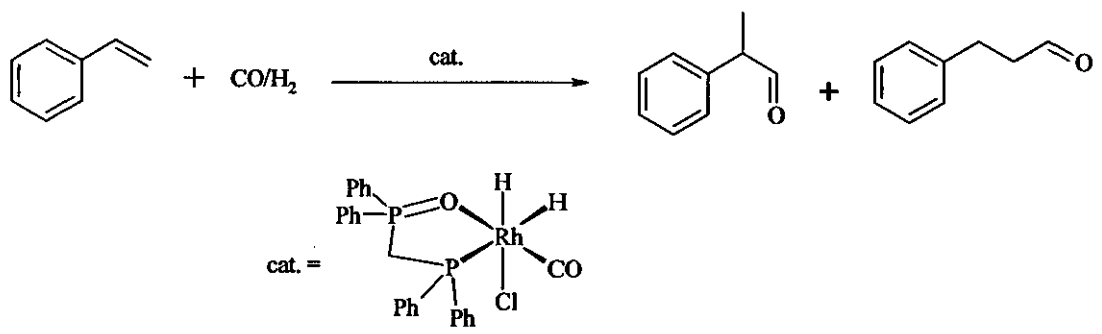

1.136

Equation 1.12 – Phosphine oxides in hydroformylation reactions

addition of an external base such as NEt_3 was needed to reduce the stability of the chelated intermediate.

Reactions involving carbonyl compounds as starting materials are catalysed by phosphorus based complexes in a number of cases. Ru-phosphine 'pincer' complexes were used by Dani *et al.*[118] for hydrogen transfer reactions between ketones and alcohols. Various ketones were converted to the corresponding alcohols using bis(amino)aryl and bis(phosphine)aryl pincer complexes **1.137-1.140** (Figure 1.29).

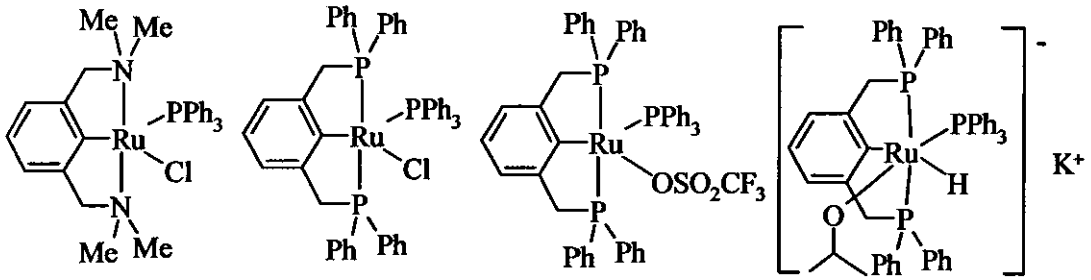

1.137 **1.138** **1.139** **1.140**

Figure 1.29 – Ru-phosphine 'pincer' ligand complexes

These reactions used *i*-PrOH as a hydrogen source and potassium hydroxide as a promoter, the general scheme also being shown in Figure 1.29. TOF's [TOF = Turnover Frequency, TON/Time (h)] obtained and conversions were extremely high; these were especially high (around 90-98% conversion and 10000-27000 TOF's) for the PCP pincer complexes. A number of essential reaction conditions were observed for example, reactions work better at higher temperatures and best under reflux, and that the presence of air gave no reaction. It was also assumed that the active species in this reaction was a $Ru^{(II)}$-hydrido complex (**1.140**, Figure 1.29). This was observed when a PCP complex was heated to reflux in *i*-PrOH/KOH without a ketone.

1.6.1 - Catalytic uses of phospha-adamantane containing compounds

Phospha-adamantane cages have multiple uses within the area of catalysis. As stated previously, the steric bulk of such ligands results in large 'bite angles' in subsequent transition metal complexes, one of the main advantages of any ligand with respect to efficient catalytic activity.[119,120] Many catalytic processes have benefited from the use of phospha-adamantanes. The main advantage of using phospha-adamantane containing compounds for catalysis and other purposes comes with the handling. Whilst other bulky phosphines such as $P(^tBu)_3$ require special handling due to rapid oxidation, the phospha-adamantanes mentioned in this section and chapter 1.5 are air stable, and mainly crystalline materials.

Pringle *et al.*[121] reported the effectiveness of ligands such as **1.119** (Figure 1.23) in the selective methoxycarbonylation of internal alkenes to linear esters. This followed a previous communication by the same group[122] reporting the effectiveness of similar diphosphines for carbonylation reactions. A number of different ligand system/reaction condition combinations were attempted, including the use of the C_3 analogue of **1.119**, **1.141** (Figure 1.30). Interesting catalytic results were obtained from experiments involving tetradecene and its various analogues. The complex obtained by reaction of **1.141** with $Pd(OAc)_2$ showed extremely high rates of isomerisation/carbonylation of tetradecene, especially in comparison with an analogous complex containing di-*tert*-butyl propylphosphine, which showed almost none. The activity of the catalysts was shown to differ even between the diastereomeric versions of **1.141**, with a factor of two difference resulting from catalytic experiments involving the *rac*- and *meso*- isomers in some cases.

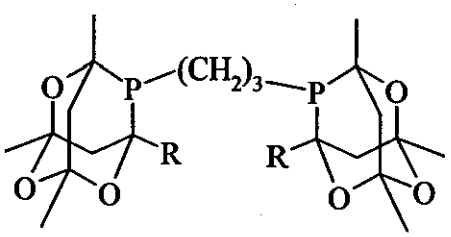

1.141

Figure 1.30 – Bis-phospha-adamantanes

Gerristma *et al.*[123] showed that a wide variety of aryl halides could be aminated effectively using $Pd_2dba_3.CHCl_3$ and 1,3,5,7-tetramethyl-2,4,8-trioxa-6-phenyl-6-phospha-adamantane, **1.114** (Equation 1.13). Using higher temperatures in the order chloro > bromo > iodo halides, and more vigorous conditions for aryl anilines, it was shown that excellent yields of tertiary amines (>90%) could be obtained for all reactions involving secondary amines. However, GC/MS analysis showed that yields were distinctly lower when using primary aliphatic amines.

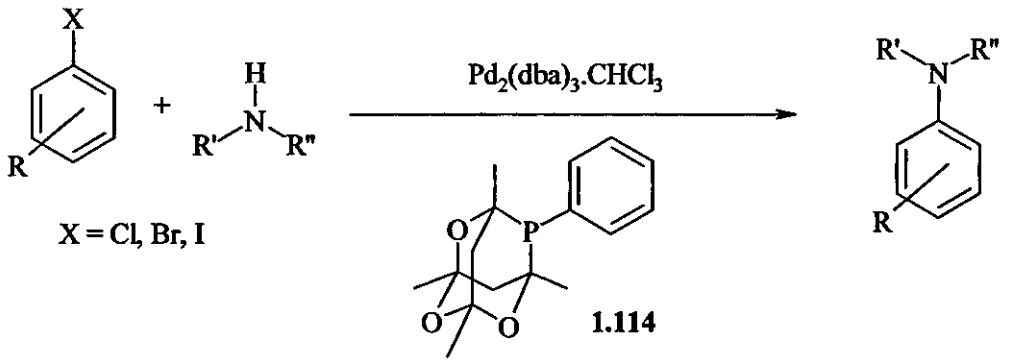

Equation 1.13 – Amination reactions using phospha-adamantanes

The use of phospha-adamantane frameworks such as **1.114** for Suzuki coupling reactions of aryl halides was reported by Adjabeng *et al.*[124] A variety of tertiary phosphines were prepared, alkyl or aryl bromides and Pd(II) or Ni(II) catalysts, and used to catalyse reactions between aryl iodides, bromides and activated chlorides with aryl boronic acids under mild conditions. Using **1.114**, excellent yields were obtained for the reaction shown in Equation 1.14. Reactions involving substituted iodobenzenes were completed in high yield within one hour at room temperature, whilst those involving substituted bromo- and chlorobenzenes took between 3 and 24 h, with sterically demanding chlorides such as 2-methyl chlorobenzene requiring mild heating to react.

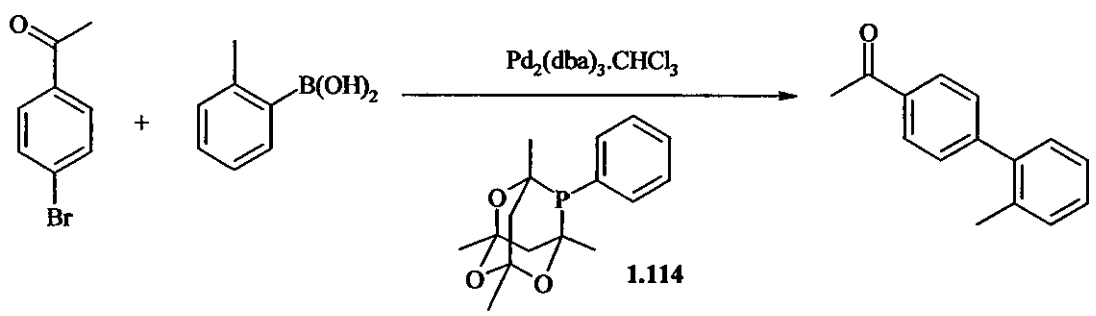

Equation 1.14 – Suzuki coupling reactions using phospha-adamantanes

Substituted derivatives of **1.114** have been utilized by Brenstrum *et al.*[125] Previous attempts to use **1.113** and **1.114** for coupling of alkyl halides containing β-hydrogens with alkylboranes had been unsuccessful. Use of alkyl and nitrogen-substituted aryl phospha-adamantanes for the coupling of alkyl bromides with phenyl boronic acid resulted in low yields of the desired product, 1-dodecylbenzene. However, use of methoxy containing phospha-adamantanes **1.142-1.144** (Figure 1.31) resulted in very good yields of the coupled reaction product.

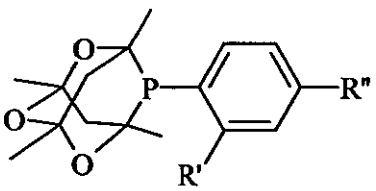

1.142 R' = OMe, R" = H
1.143 R' = H, R" = OMe
1.144 R' = OMe

Figure 1.31 – Methoxy phospha-adamantanes

1.7 – AIMS OF THIS RESEARCH

There were a number of aims of this research, based on the sections of this introduction. These often changed in the duration of the work, adapting as to which parts succeeded and which did not. The first aim was to establish a reproducible, reliable method for producing ligands based on phosphine and chalcogenide groups, and to exhibit the complexation behaviour of these ligands. Whilst some of these ligands were known, this was used as a basis for the second aim, that of preparing potentially multidentate ligands, based on various combinations of P/S/N and O donor atoms.

We then moved to establishing the chemistry of 1,3,5,7-tetramethyl-2,4,8,-6-phospha-adamantane, an area which has received limited yet increasing attention recently. We hoped the adamantane group could be combined with various functionalities containing group 15 and 16 donor atoms, and subsequently reacted with a number of metal centres to form a variety of complexes. A fourth aim of this research was to see how all of the ligands prepared could be modified by preparation of phosphazenes and sulfimides.

The final aim of this research was to assess the ability of the complexes formed from the phosphine-based ligands to act as catalysts for a number of organic transformations. The main process to be analysed was the Heck reaction. Successful initial investigations would enable optimisation of the reaction conditions to establish the extent to which the complexes can act as catalysts.

Chapter Two

~Chemistry of Phosphine/ Chalcogenide-Containing Ligands ~

2.1 – AIMS OF THE CHAPTER

The first aim of the work in this Chapter was to obtain a reliable and simple method for synthesising *o*-$C_6H_4(PPh_2)(SPh)$ **2.1**. Having done this, and applied it to the selenium analogue **2.17**, the coordinating ability of the ligands was investigated using a number of transition metal centres. We also aimed to make comparisons with the alkyl $(CH_2)_2$ phosphine/chalcogenide analogues and their complexes. We hoped both of the methods for synthesising the above ligands could be used to make novel, potentially tridentate ligands, which could then be used to investigate their modes of coordination.

2.1.1 – Preparation and Characterisation of *o*-$C_6H_4(SPh)(PPh_2)$ 2.1

Initial attempts at preparing **2.1** using the method shown in Scheme 2.1 were successful. This firstly involved preparation of the sulfide intermediate *o*-$C_6H_4Br(SPh)$ using *o*-dibromobenzene and benzenethiol. However, this required a vacuum distillation which was time consuming and did not always give a clean product. The second step involved reaction of chlorodiphenylphosphine and it was this step that proved most difficult. The final crystallisation of the product, using degassed ethanol was unreliable, and on certain occasions failed to give any solid material at all.

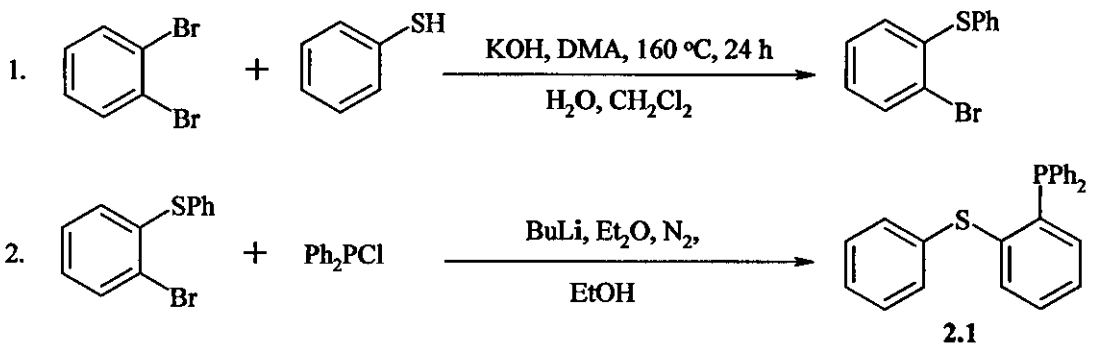

Scheme 2.1 – Preparation of *o*-$C_6H_4(PPh_2)(SPh)$, **2.1**

It was decided to address this problem slightly differently, preparing first the phosphine intermediate *o*-$C_6H_4Br(PPh_2)$ **2.2** using a method reported by Stelzer *et al.*[126] (Scheme 2.2). By using 1-bromo-2-iodobenzene, it was anticipated that the

reaction would be slightly more selective for the desired product, the problem of which was observed in the previous preparation of *o*-$C_6H_4Br(SPh)$, and was rectifiable only by distillation. The second step was reaction with benzenethiol using KOH as base. Initial problems with optimising time, and isolation of a suitable solid from a waxy crude material were addressed and overcome. The method proved to be an extremely reliable and reproducible preparation in comparison to the first method tried, even when attempted on larger scales using around 10 g of *o*-$C_6H_4Br(PPh_2)$. This reproducibility is obviously an advantage when considering carrying out the reaction on even larger scales.

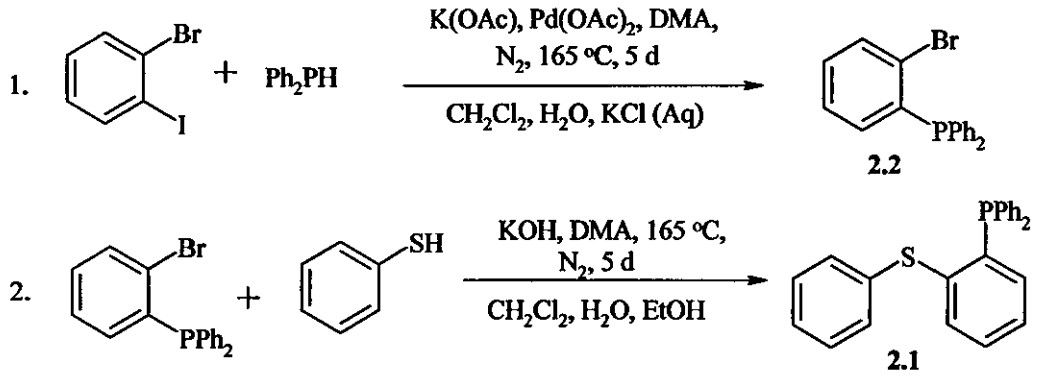

Scheme 2.2 – Preparation of **2.1** – Method 2

Compound **2.1** was isolated as a slightly off-white solid, similar to triphenylphosphine, and was characterised using a number of methods. Firstly $^{31}P\{^1H\}$ NMR showed an expected single resonance at δ(P) –12 ppm. Any signs of starting material **2.2** (at –4 ppm) from *in-situ* analysis were separated during work-up. ^1H NMR spectroscopy also showed the expected phenyl group as a multiplet around 7-8 ppm.

2.1.2 – Preparation and Complexation of $C_6H_4\{P(O)Ph_2\}(SPh)$ 2.3

On the basis of the wide-ranging applicability of phosphine oxides as reported in Chapter one, **2.1** was reacted with an excess of hydrogen peroxide in THF to form the oxidised species $C_6H_4\{P(O)Ph_2\}(SPh)$ **2.3**. This was characterised primarily by $^{31}P\{^1H\}$ NMR, with a downfield shift of *ca.* 41 ppm, from δ(P) –12 ppm to 29 ppm being indicative of the formation of a pentavalent phosphorus atom. The infra-red

spectrum of **2.3** also showed a strong P=O at 1252 cm^{-1}, along with the previously observed peaks at 1112 and 1023 cm^{-1} for the C-S and C-P bonds respectively.

As shown in Scheme 2.3, two complexation reactions were carried out using phosphine oxide **2.3**. These were prepared by reaction of **2.3** in CH_2Cl_2, initially at r.t. However, a further 5 h reflux was needed for any significant change to be observed in the $^{31}P\{^1H\}$ NMR spectrum. Initial analysis using this method showed a single peak at δ(P) 29 ppm, corresponding to the free ligand **2.3**. However, after heating, the singlet peaks in both the Rh and Ru-containing reactions had shifted to *ca.* 34 ppm. This suggests that the ligand may have coordinated, though whether this is through

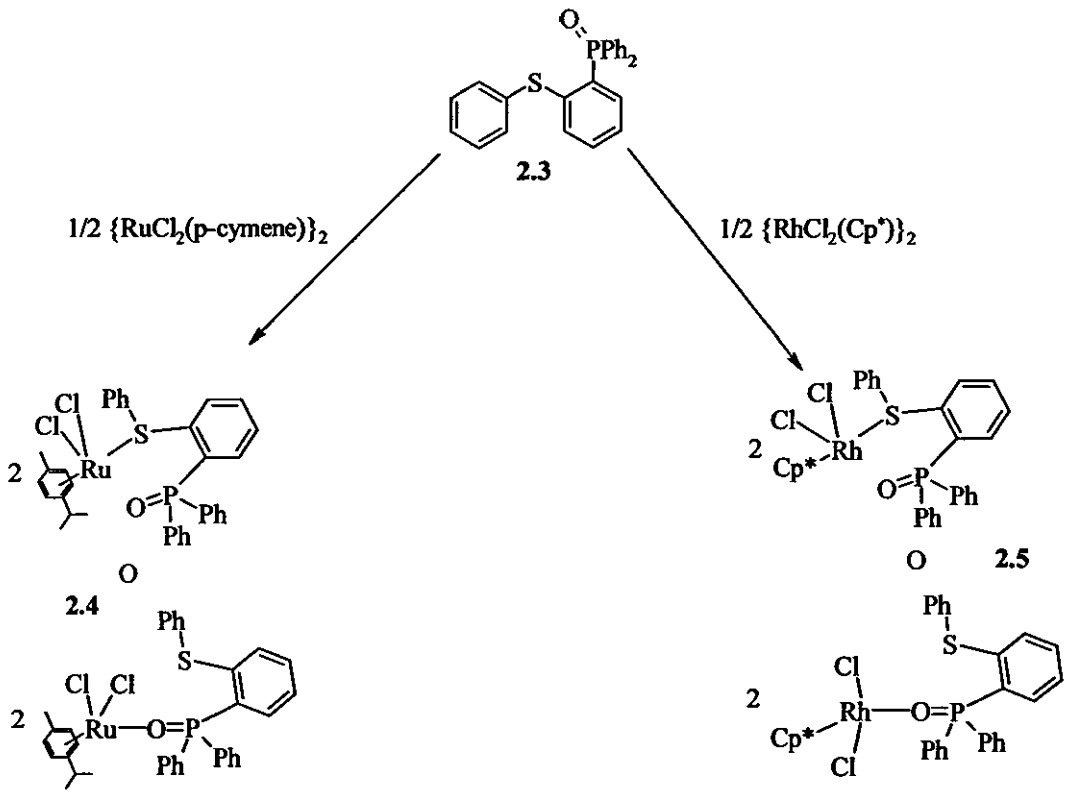

Scheme 2.3 – Preparation of Ru and Rh complexes of *o*-$C_6H_4(P(O)PPh_2(SPh)$, **2.4** and **2.5**

the sulphide or phosphine oxide group as shown in Scheme 2.3 is unknown. The slight shift of the P=O peak in the infra-red spectrum from 1251 to 1260 cm^{-1} also suggests that coordination to form complexes **2.4** and **2.5** occurred. Elemental analysis results also show concordance with those expected; these can be seen in the experimental section. Repeated experiments to obtain X-ray quality crystals of **2.4** and **2.5** were unsuccessful.

2.1.3 – Reactions of (camphorsulfonyl) oxaziridene with 2.1

Oxaziridenes have been widely reported to have good selectivity for the oxidation of sulfides to sulfoxides.[127,128] Therefore, in a slight variation to the hydrogen peroxide experiment, a reaction of **2.1** with one such oxaziridene, **2.7** was attempted. It was hoped that oxidation would show selectivity towards the sulfur donor instead of the phosphorus, as reported elsewhere. Reaction of **2.6** with *m*–CPBA in CH_2Cl_2 gave oxaziridene **2.7** in almost quantitative yield (Scheme 2.4). Reaction of **2.7** with $C_6H_4(PPh_2)(SPh)$ **2.1**, however, did not give the desired sulfoxide product, instead yielding the phosphine oxide **2.3**. Having carried out the reaction under anaerobic conditions, it can be concluded that selectivity for the phosphorus centre rather than the sulfur is greatly preferred. A possible route to forming the sulfoxide in molecules such as **2.1** would be to protect the phosphine using a borane, for example, then deprotect it once the sulfoxide has been formed.

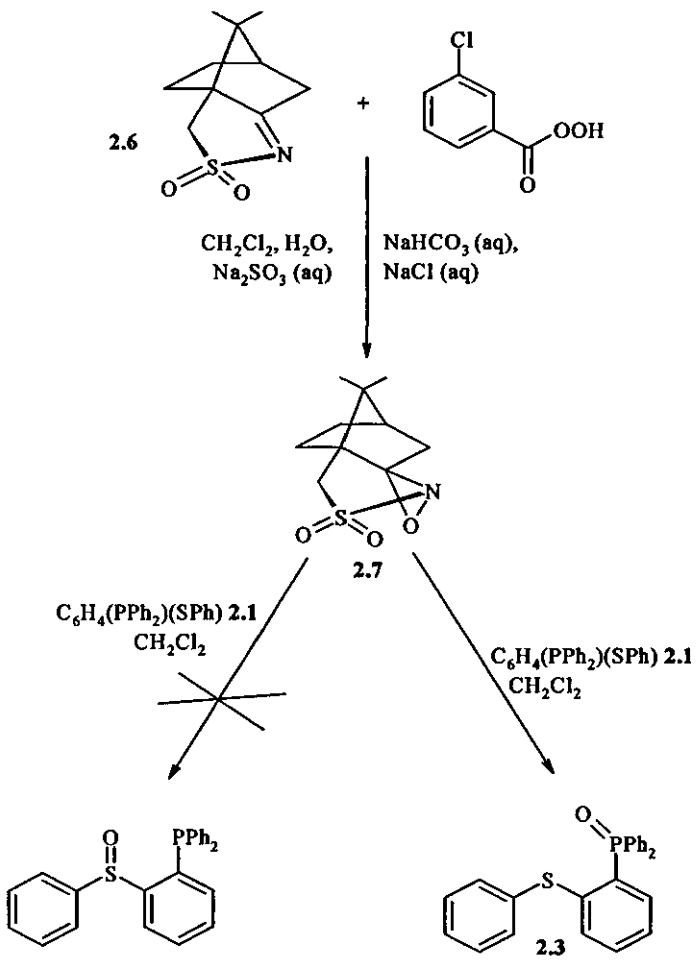

Scheme 2.4 - Reaction of **2.1** with oxaziridene **2.7**

The structure of product **2.3** (from the reaction described in Scheme 2.4) was confirmed by X-ray crystallography, with crystals grown from a $CDCl_3$ solution and petroleum ether (60-80 °C). The structure is shown in Figure 2.1, and is as expected; the P=O bond length of 1.4909(11) Å is very similar to that reported for triphenylphosphine oxide [1.494 Å].[129] The C(1), C(7) and C(13)-P-O bond angles of 113.12(7), 113.97(7) and 111.08(6)° respectively are also similar to the values reported for triphenylphosphine oxide of 113.6, 111.9 and 111.6°. This is all to be expected, as only one P-R group is different to that with $O{=}PPh_3$.

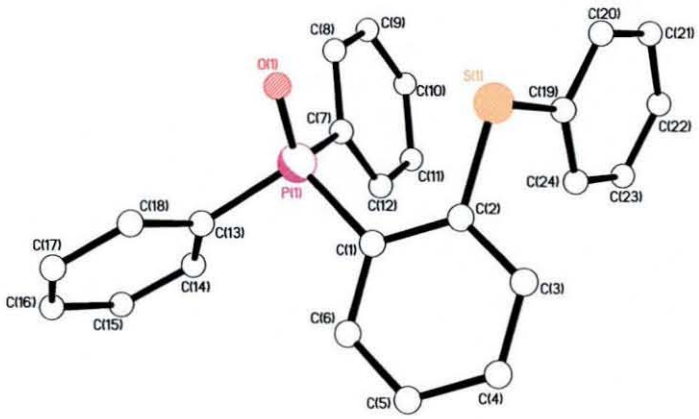

Figure 2.1 – X-ray structure of **2.3**

Bond Lengths (Å)		Bond Angles (°)	
O(1)-P(1)	1.4909(11)	O(1)-P(1)-C(7)	113.97(7)
P(1)-C(1)	1.8186 (15)	O(1)-P(1)-C(1)	113.12(7)
S(1)-C(2)	1.7866(16)	O(1)-P(1)-C(13)	111.08(6)

Table 2.1 – Selected bond lengths and angles for **2.3**

2.1.4 – Coordination Chemistry of 2.1

A number of complexes were prepared using **2.1**, using a variety of starting materials as shown in Scheme 2.5. These were prepared using a general method of reaction in CH_2Cl_2 for 2 h followed by reduction in volume of the reaction mixture and crystallisation using Et_2O and petroleum ether (60-80 °C).

Firstly, compound **2.1** was reacted with $PdCl_2$(cod) (cod = cycloocta-1,5-diene) to form the complex $PdCl_2$(**2.1**), **2.8**. The shift in the $^{31}P\{^1H\}$ NMR spectrum at δ(P) 58 ppm was concordant with shifts for 5-membered chelate complexes prepared previously, and can be seen in a summary of $^{31}P\{^1H\}$ NMR data for compounds **2.1** – **2.20** (Table 2.2). Whilst the peaks due to aromatic hydrogen atoms in the ^1H NMR spectrum were fairly inconclusive, peaks due to the ligand could be seen in the infra-red spectrum at 1435, 1099 and 509 cm^{-1}, along with two Pd-Cl stretches [296 and 335 cm^{-1}]. Elemental analysis results can be seen in the experimental section. Reaction of **2.1** with Pd(Me)Cl(cod) displaced the cod ligand to afford Pd(Me)Cl(**2.1**) **2.9**. The $^{31}P\{^1H\}$ NMR spectrum showed a single peak at δ(P) 50 ppm, slightly higher than seen in other complexes prepared. This is more than likely to be due the presence of a methyl group *trans*- to the coordinated phosphorus.

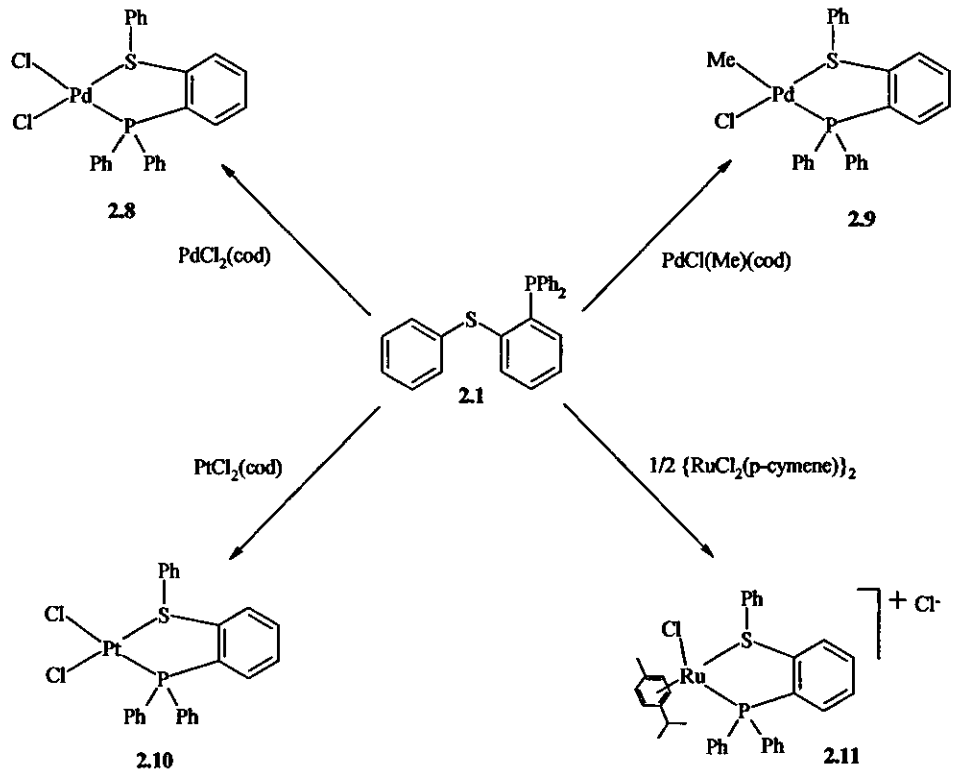

Scheme 2.5 – Preparation of complexes **2.8-2.11**

The crystal structure of **2.9** is shown in Figure 2.2a. Crystals were grown by vapour diffusion of diethyl ether into a $CDCl_3$ solution of **2.9**. There are two molecules within the unit cell with only one shown in Figure 2.2a. Both molecules show the Pd centre to be in a slightly distorted square planar environment, with angles shown in Table 2.3 only deviating slightly from the values expected for a perfect

square planar geometry. For example, the P(1)–Pd(1)–S(1) angle of 88.29(2)° is just over 1.5° away from the theoretical angle of 90°. In both molecules, the four atoms in the coordination sphere of the Pd centre also form an almost planar structure, shown by the values that the metal lies above or below the P(1)/S(1)/Cl(1)/Cl(2) plane [0.0109 and 0.0059 Å for Pd(1) and Pd(2) respectively, shown by 'a' in Figure 2.2b]. The angle between the metal centre, the phosphorus or sulfur atom and the aromatic backbone (the 'hinge angle', indicated by 'b' in Figure 2.2b) can also be used to define the deviation from a perfectly planar five-membered chelate ring. This is also very small for both molecules (0.7 and 3.1° respectively), and therefore shows that the hinge angle for this type of molecule is very shallow.

Compound	$^{31}P\{^{1}H\}$ NMR δ (ppm)
2.1	–12
2.2	–5
2.3	30
2.4	34
2.5	34
2.8	58
2.9	51
2.10	36
2.11	57
2.12	17 (Pt-PPh_3, ^{1}J(PtP) 3281 Hz) 39 (d, Pt-P-S, ^{1}J(PtP) 3510 Hz)
2.13	18 (Pt-P(Br), ^{1}J(PtP) 3391 Hz), 37 (d, Pt-P-S, ^{1}J(PtP) 3550 Hz)
2.14	25 ($PtCl_2$(P-S)$_2$, ^{1}J(PtP) 3508 Hz)
2.15	42
2.16	33
2.17	–9
2.18	54
2.19	37
2.20	50 and 51 (d, chelated ligand), 63 and 65 (d, monodentate ligand)

Table 2.2 – Summary of $^{31}P\{^{1}H\}$ NMR data for compounds **2.1 - 2.20**

Likewise, reaction of **2.1** with $PtCl_2$(cod) gave $PtCl_2\{(C_6H_4(PPh_2)(SPh)\}$, **2.10**. The structure was confirmed by $^{31}P\{^{1}H\}$ NMR spectrocopy, which showed a signal at δ(P) 36 ppm flanked by two Pt satellites [^{1}J(Pt-P) 3420 Hz]. Microanalysis also indicated that the structure was the one postulated (see Experimental Section).

Crystals of **2.10** were grown from a $CDCl_3$ solution and diethyl ether; the crystal structure is also shown in Figure 2.2a. The Pt centre is shown to be in a square planar

environment, surrounded, as expected by the phosphorus and sulfur donors of **2.1** coordinated in a bidentate fashion, and two chloride co-ligands. Like **2.9**, the structure of **2.10** contains two molecules in the unit cell, and angles observed are very similar to those observed for **2.9**.

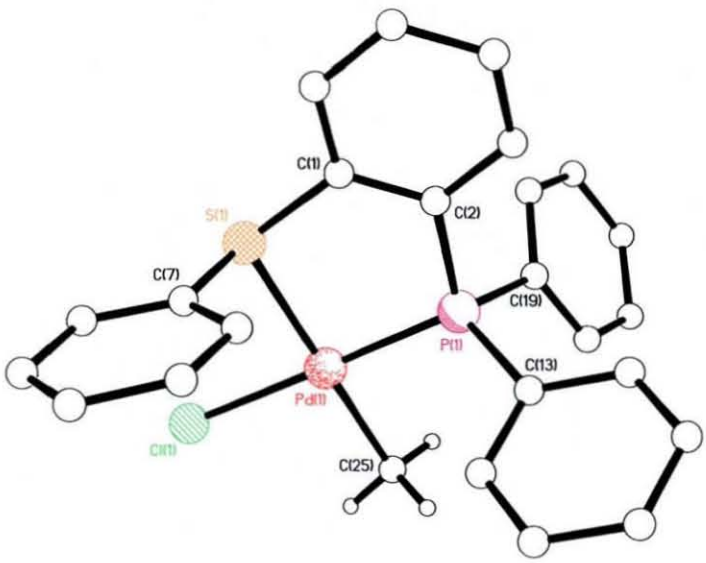

Figure 2.2a - Above: X-ray structure of **2.9**; below: X-ray structure of **2.10**.

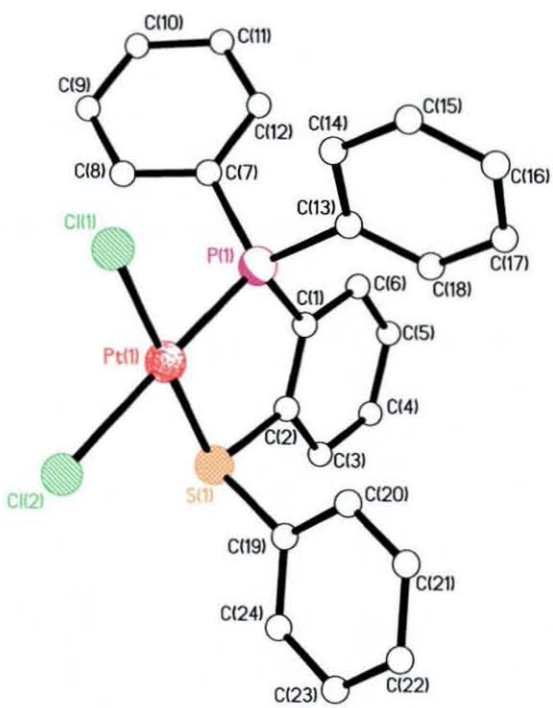

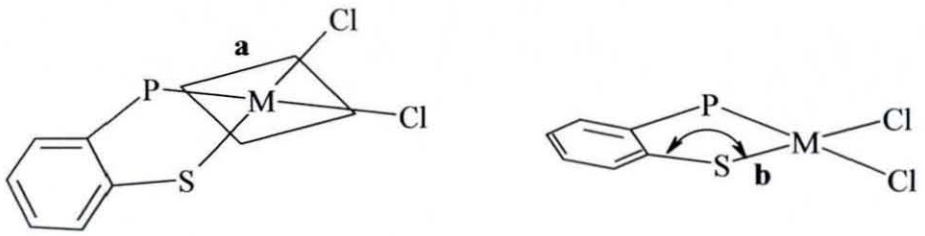

Figure 2.2b – General diagram of transition metal phosphine-sulfide complexes.

	2.9	**2.10**
M	Pd	Pt
X	C(25)	Cl(2)
M(1)-P(1)	2.2054(5) [a][2.2020(5)]	2.2122(10) [2.1986(10)]
M(1)-S(1)	2.3945(6) [2.3910(6)]	2.2497(10) [2.2586(10)]
M(1)-Cl(1)	2.3603(5) [2.3656(5)]	2.3015(9) [2.3103(10)]
M(1)-X(1)	2.061(2) [2.0570(2)]	2.3607(10) [2.3536(10)]
Cl(1)-M(1)-P(1)	179.07(2) [179.33(2)]	90.29(4) [89.97(4)]
X-M(1)-P(1)	89.84(6) [88.97(6)]	177.11(4) [178.54(4)]
P(1)-M(1)-S(1)	88.29(2) [88.64(2)]	90.29(4) [89.60(4)]
Cl(1)-M(1)-X	90.49(6) [90.72(6)]	92.32(4) [91.45(4)]
Cl(1)-M(1)-S(1)	91.42(2) [91.68(2)]	178.22(3) [177.54(4)]
X-M(1)-S(1)	177.22(7) [177.24(7)]	87.13(4) [89.00(4)]

[a] Values in square brackets are for equivalent atoms in the second molecule

Table 2.3 – Selected bond lengths and angles for **2.9** and **2.10**.

Reaction of **2.1** with the ruthenium starting material $\{RuCl_2(p\text{-cymene})\}_2$ required a number of attempts, as initial efforts resulted in oxidation of the phosphine. Presumably this was because of the extra time required to break the Ru-Cl-Ru dimer bridge. Eventually RuCl(*p*-cymene)(**2.1**) **2.11** formed (Scheme 2.5), and this was characterised using $^{31}P\{^1H\}$ and ^1H NMR spectroscopy. Both of these showed quite extensive peak broadening, so much so that *p*-cymene resonances in the latter could only just be made out. One broad peak was exhibited at δ(P) 57.4 ppm in the $^{31}P\{^1H\}$ NMR spectrum. The peak broadening suggests that fluxional processes are occurring in **2.11**; indeed this was seemingly confirmed by a test reaction of $\{RuCl_2(p\text{-cymene})\}_2$ with triphenylphosphine. As can be seen in Figure 2.13, if the ligand was chelated to the metal centre as suggested, the *p*-cymene proton signals in the ^1H spectrum would be inequivalent, and any fluxionality down the Ru-*p*-cymene bond would result in peak broadening in both spectra.

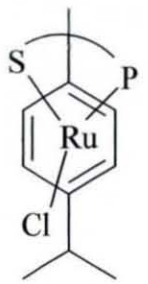

Figure 2.3 - RuCl(p-cymene)(**2.1**), **2.13**

2.1.5 – Small-scale bond strength tests using 2.10

A number of ring-opening tests were carried out on **2.10** to establish the strength of the Pt-S bond. Firstly, **2.10** was reacted with one equivalent of triphenylphosphine. The resulting $^{31}P\{^{1}H\}$ NMR spectrum showed that the Pt-S bond had indeed been cleaved to give a structure consistent with **2.12** (Scheme 2.6). The main Pt-P/S peak shifted by 3 ppm to 39 ppm, maintaining the same $^{1}J(PtP_A)$ coupling of around 3400 Hz. A second main peak, corresponding to the Pt-PPh_3 bond, is of equal intensity to the first, and also exhibits Pt satellites with a slightly smaller $^{1}J(PtP_X)$ coupling of around 3220 Hz. A third peak at –4.9 ppm showed some unreacted triphenylphosphine.

Secondly, **2.10** was reacted with one equivalent of *o*-$C_6H_4Br(PPh_2)$ **2.2**. The pattern shown was similar to that exhibited when triphenylphosphine was used, though the reaction took slightly longer than the previous example. Initially a complicated $^{31}P\{^{1}H\}$ NMR spectrum was observed, containing the chelate complex (δ(P) 36 ppm), *o*-$C_6H_4Br(PPh_2)$ starting material **2.2** (–4 ppm), small signs of a 2 ligand monodentate complex (18 ppm) and various other unknown peaks. After 6 d, despite still containing many unknown peaks, the peak at 18 ppm had grown substantially, had formed the expected doublet for such a complex as **2.13** (Scheme 2.6), and had Pt satellites with $^{1}J(PtP)$ coupling of 3500 Hz. Signs of Pt-S bond cleavage were shown by the shift of the initial main peak to δ(P) 38 ppm.

Finally, one equivalent of **2.1** was added to the platinum complex **2.10**, in an attempt to give a complex containing two phosphine-sulfide ligands binding in a P-

monodentate fashion (**2.14**). This would be anticipated to give a single peak in the $^{31}P\{^{1}H\}$ NMR spectrum, as, with two of the same co-ligand (Cl) being present, the phosphorus environments would be identical. Indeed, after 2 d this was the case, though there was starting material present. The peak at δ(P) 25 ppm flanked by two Pt satellites suggests this; the broadness of the peaks may be due to fluxionality within the molecule.

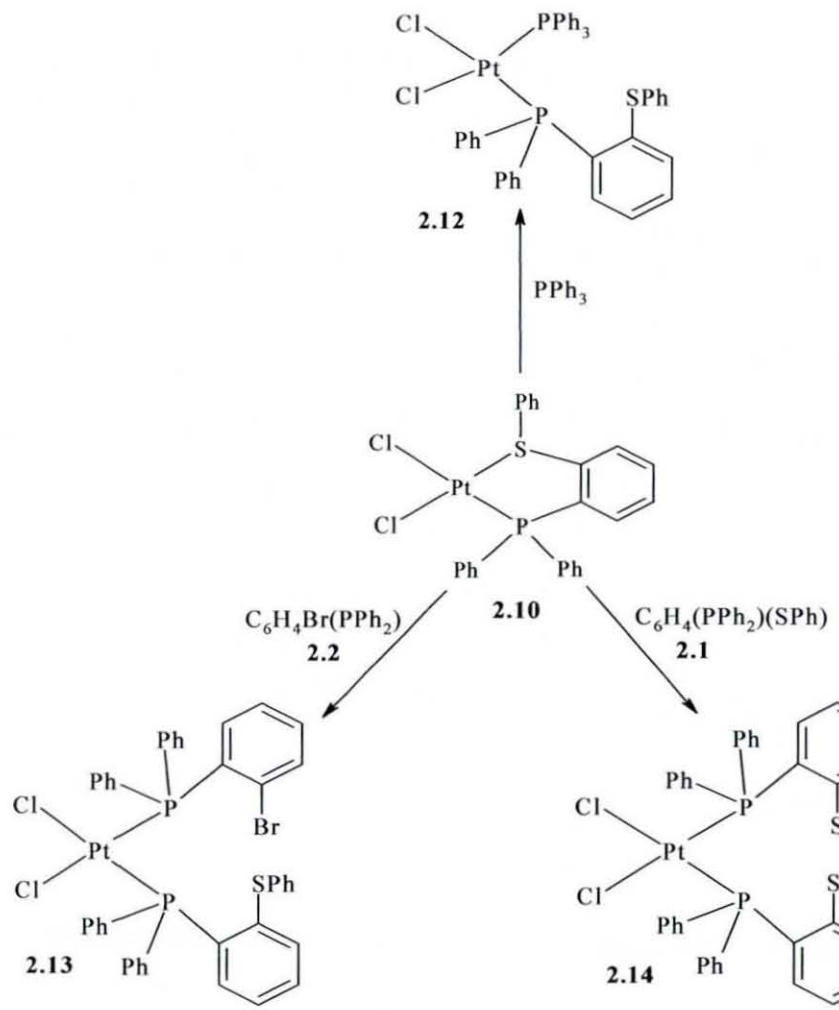

Scheme 2.6 - Small scale bond strength experiments using $PtCl_2$(**2.1**), **2.10**

In conclusion, initial Pt-S bond cleavage in the phosphine sulfide complex is facile, breaking upon addition of a number of P-based ligands. However, some of these ligand addition reactions take longer than others. This is to be expected, the time taken varying with the size and nature of the incoming ligand. Using **2.14**, attempts

were made to re-coordinate two sulfide groups to the Pt centre by adding two equivalents of $Ag[BF_4]$, hence prompting loss of AgCl. Microanalysis of the yellow solid formed seems to suggest the reaction may have occurred, (see Experimental Section). The downfield shift of *ca.* δ(P) 3 ppm (compared to complex **2.10**) and 13 ppm (compared to **2.14**) to 38 ppm in the $^{31}P\{^{1}H\}$ spectrum also indicates that the reaction was successful.

2.1.6 – Further derivatives of 2.1

Further derivatives of phosphine sulfide **2.1** were also prepared in an attempt to assess the effects of having different basicities of donor atoms available for complexation. Firstly, **2.1** was reacted with S_8 in THF to form $C_6H_4\{P(S)Ph_2\}(SPh)$, **2.15.** The ^{31}P NMR spectrum of **2.15** shows a significant downfield shift to 42 ppm, and the IR spectrum exhibits peaks at 637 and 689 cm^{-1}, corresponding to the P=S stretch. Secondly, in an analogous reaction, **2.1** was reacted with selenium powder to give an off-white solid, $C_6H_4\{P(Se)Ph_2\}(SPh)$ **2.16**. This was characterised using the same methods, the $^{31}P\{^{1}H\}$ NMR spectrum showing a peak at δ(P) 33 ppm. Elemental analysis for both products showed that the desired products had been synthesised; results for this are shown in the Experimental Section.

Despite repeated attempts to form complexes of **2.15** and **2.16**, these were unsuccessful. Firstly, a change was made to the choice of starting material containing monodentate leaving groups such as PhCN. Further ionic starting materials were tried, including $Na_2[PdCl_4]$, but this, like the previous attempts failed.

2.1.7 – Preparation of *o*-C_6H_4(SePh)(PPh_2) 2.17

A slight variation on the sulfur-phosphine chemistry described in sections 2.1.1-2.1.6 was the preparation of chelating ligands containing selenides. Whilst it was known that certain similarities between the two types of ligands would be apparent, as mentioned previously, very little work except that carried out by Levason *et al.*[130] has been carried out on phosphine-selenide compounds, and as such it was believed that the area should be looked at in some detail.

In section 2.2.1 it was established that the best method for preparation of the basic *o*-C_6H_4(PPh_2)(SPh) ligand was to start with the preparation of *o*-$C_6H_4Br(PPh_2)$. In a similar fashion **2.2** was reacted with phenylselenol and potassium hydroxide to form *o*-C_6H_4(PPh_2)(SePh) **2.17**. This was characterised firstly using $^{31}P\{^1H\}$ NMR, the chemical shift of –9 ppm being similar to that exhibited by **2.1** (–12 ppm). This spectrum also exhibited ^3J(PSe) coupling of 59 Hz. ^{77}Se NMR spectroscopy showed a single peak at δ(Se) 205 ppm. The multiplet around 7–8 ppm in the ^1H NMR spectrum, whilst confirming the presence of phenyl groups, again is not particularly diagnostic. However, the lack of any selenol proton in the same spectrum (at δH 4.1 ppm) is indicative of the purity of the product.

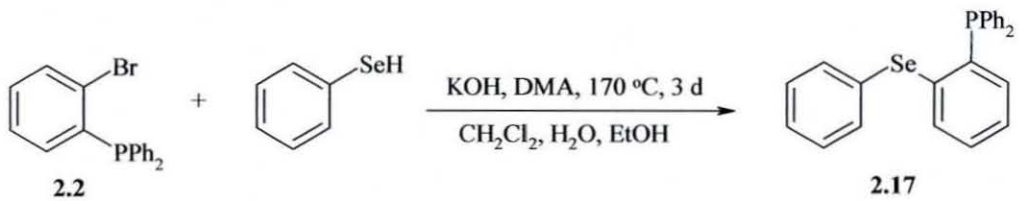

2.2 **2.17**

Equation 2.1 - Preparation of o-C_6H_4(PPh_2)(SePh), **2.17**

Upon repetition of the reaction in Equation 2.1, it was noted that different reaction times were required. It seems that a slight variation in the reaction temperature affects the reaction time significantly. The first attempt, carried out at *ca.* 150 °C, took 13 d to proceed to completion, whereas when the temperature was raised to a constant 170 °C, the reaction took only 3 d to complete.

2.1.8 – Complexation of *o*-$C_6H_4(SePh)(PPh_2)$ 2.17

A number of complexes were prepared using **2.17**. $PdCl_2\{C_6H_4(PPh_2)(SePh)\}$, **2.18**, was formed when Pd(Me)Cl(cod) was reacted with **2.17**; the fact that the reaction was carried out in $CDCl_3$ (hence trace amounts of HCl present) resulted in protonolysis of the CH_3 group as methane and coordination of a second chloride ligand. Compound **2.18** gave a $^{31}P\{^1H\}$ NMR shift of δ(P) 54 ppm, which, by analogy with the sulfur containing examples, is within the region expected for this type of complex. The $^{31}P\{^1H\}$ NMR spectrum also showed ^2J(PSe) coupling of 61 Hz, which is similar to the value obtained for **2.17**. Mass spectrometry showed the correct molecular ion peak, and elemental analysis gave concordant results with those expected; both of these can be seen in the Experimental Section.

The X-ray crystal structure of **2.18**, obtained from a crystal grown from a $CDCl_3$ solution and petroleum ether (60-80 °C), is shown in Figure 2.4. This shows the Pd centre to be in a square planar environment, with two of the phenyl rings (one P-Ph and one Se-Ph) sitting above the plane to avoid excessive steric interactions. The angles containing Cl(2) are fairly significantly distorted from 90/180°C; indeed the distortion of the angles containing the co-ligand *trans* to the P atom is a feature found in both complexes solved crystallographically in this Chapter.

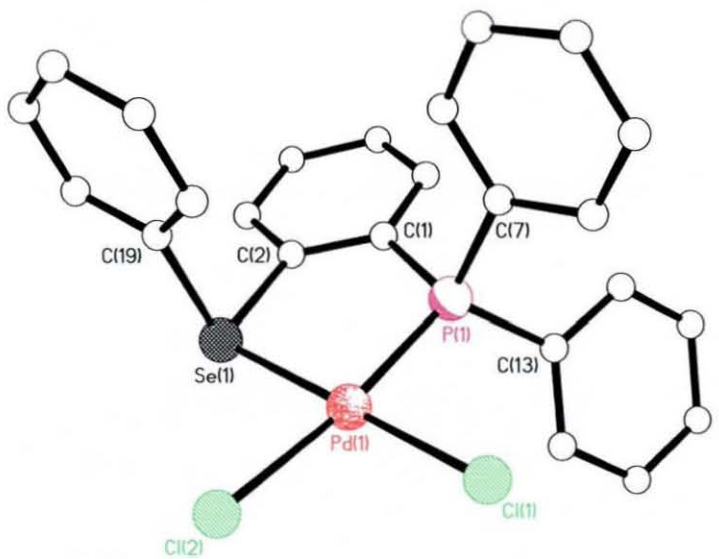

Figure 2.4 – X-ray structure of compound **2.18**

Ligand **2.17** was also reacted with one equivalent of $PtCl_2(cod)$ to form the analogous complex to **2.10**, $PtCl_2\{C_6H_4(PPh_2)(SePh)\}$ **2.19**. This was again characterised by $^{31}P\{^1H\}$ NMR, with a signal at δ(P) 36.7 ppm (almost identical to the sulfur analogue **2.10**) and Pt satellites showing a ^1J(PtP) coupling of 3548 Hz. The latter value is slightly different to that quoted for **2.10**, 3420 Hz. The ^3J(PSe) coupling shown in the $^{31}P\{^1H\}$ NMR spectrum was slightly larger than for the parent ligand, at 68 Hz.

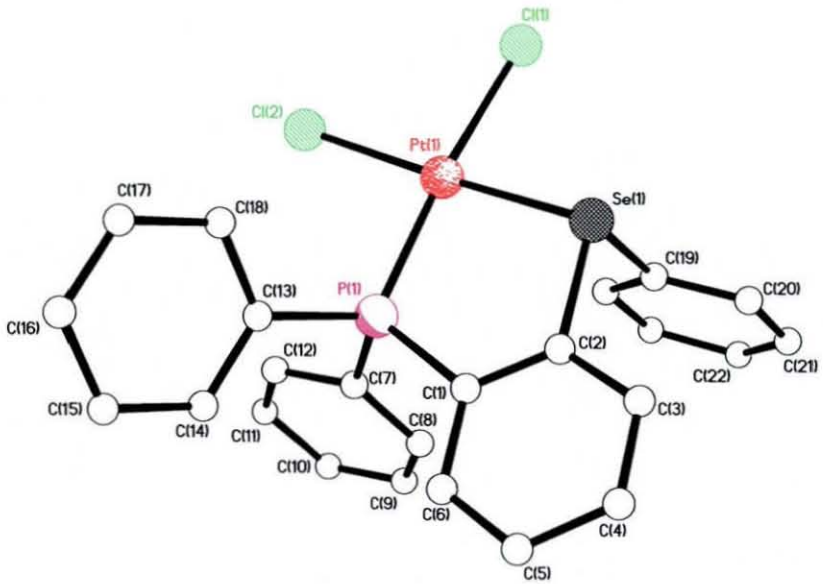

Figure 2.5 – X-ray structure of **2.19**.

	2.18	**2.19**
M	Pd	Pt
M(1)–P(1)	2.2210(6)	2.2093(11)
M(1)–Se(1)	2.3885(4)	2.3560(5)
M(1)–Cl(1)	2.3075(8)	2.3143(12)
M(1)–Cl(2)	2.3743(7)	2.3668(11)
Cl(1)–M(1)–P(1)	90.06(3)	173.95(4)
Cl(2)–M(1)–P(1)	172.95(2)	91.90(4)
P(1)–M(1)–Se(1)	89.78(19)	90.28(3)
Cl(1)–M(1)–Cl(2)	94.67(3)	92.03(5)
Cl(1)–M(1)–Se(1)	178.95(2)	85.94(3)
Cl(2)–M(1)–Se(1)	85.58(2)	177.14(3)

Table 2.4 – Selected bond lengths and angles for **2.18** and **2.19**.

By analogy with other examples studied, it was assumed that **2.19** contained a chelating ligand and this was confirmed by X-ray crystallography, using a crystal grown from a $CDCl_3$/DMSO solution and Et_2O. This can be seen in Figure 2.5. As can be seen from the values in Table 2.4, the Pt centre is in a slightly distorted square planar environment. Both bond lengths and angles are slightly different from those in the sulfur analogue **2.10**; certainly, whilst one of the Cl(1)–Pt(1)–P(1) and P(1)–Pt(1)–Se(1) bond angles [91.90(4) and 90.28(3)^o respectively] is similar to **2.10**, (where they are both 90.29(4)^o) both are not the same. As might be expected for different donor centres, the Pt-Se distance (2.3560(5)) is also slightly different compared to 2.2497(10) (for **2.10**). The platinum centre is only 0.0265 Å below the plane of the four coordinating groups (P(1), Se(1), Cl(1) and Cl(2)), indicating a great deal of planarity within the coordination environment of the metal. The chelate ring is also shown to be fairly planar, with the angle between the Pt, donor atoms (P and S) and aromatic backbone being 4.9^o. Whilst a larger value than for **2.10**, this apparently almost planar structure might be expected with the rigidity of the C_6H_4 backbone, and the lack of groups within the molecule which might distort the structure, such as bulky co-substituents.

Reaction of **2.17** with the rhodium dimer $\{RhCl_2(Cp^*)\}_2$ over 24 h gave a mixture of products, as shown by $^{31}P\{^1H\}$ NMR spectroscopy. The spectrum

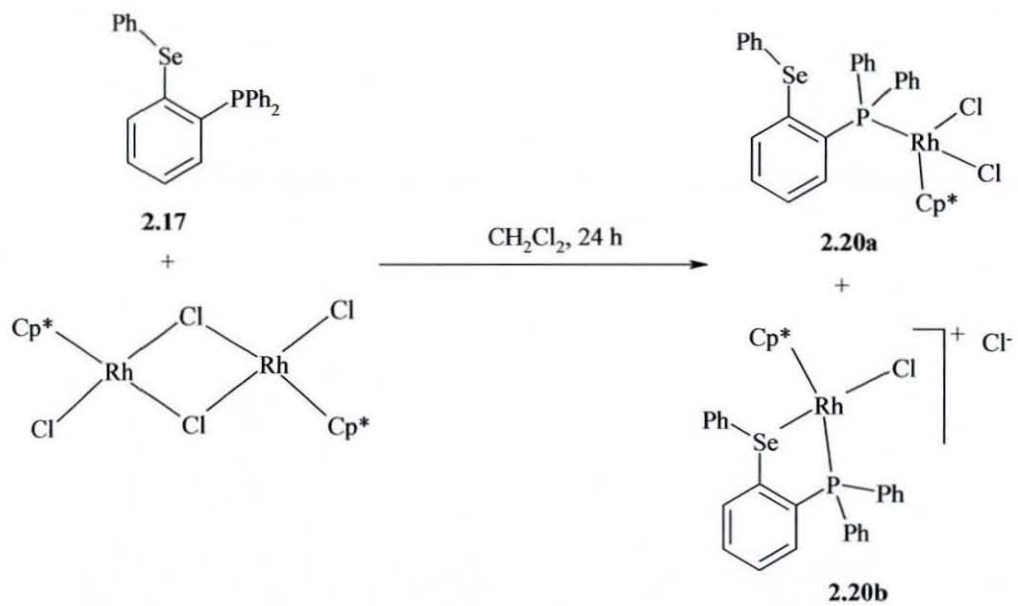

Equation 2.2 - Preparation of $RhCl_2(Cp^*)$(**2.17**), compounds **2.20a** and **2.20b**

observed on the crude product showed two major doublets (due to ^{103}Rh coupling) at 50 ppm and 64 ppm, the former being the major species. An assumption could be made that these correspond to the monodentate and chelated species as shown in Equation 2.2. The reaction was continued under reflux for a further 24 h, and the solution re-analysed. However, this produced very little change, with only a small increase in the intensity of the signal at 50 ppm. The identity of each of these signals could be further proved by use of X-ray crystallography; however numerous attempts to obtain suitable crystals for analysis proved unsuccessful.

2.2 – PREPARATION OF ALKYL-BASED LIGANDS

2.2.1 - Preparation and characterisation of 2.21 – 2.24

In an attempt to follow up some of the work carried out using aryl-based phosphine-chalcogenides, the preparation of a number of alkyl-based analogues of **2.1** and **2.17** were attempted.

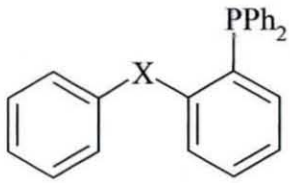

X = S = **2.1**
X = Se = **2.17**

Figure 2.6 – Compounds **2.1** and **2.17**

Both **2.1** and **2.17** contain aryl-backbones between the P and S donor centres. It was thought the properties of similar ligands, containing alkyl backbones, would

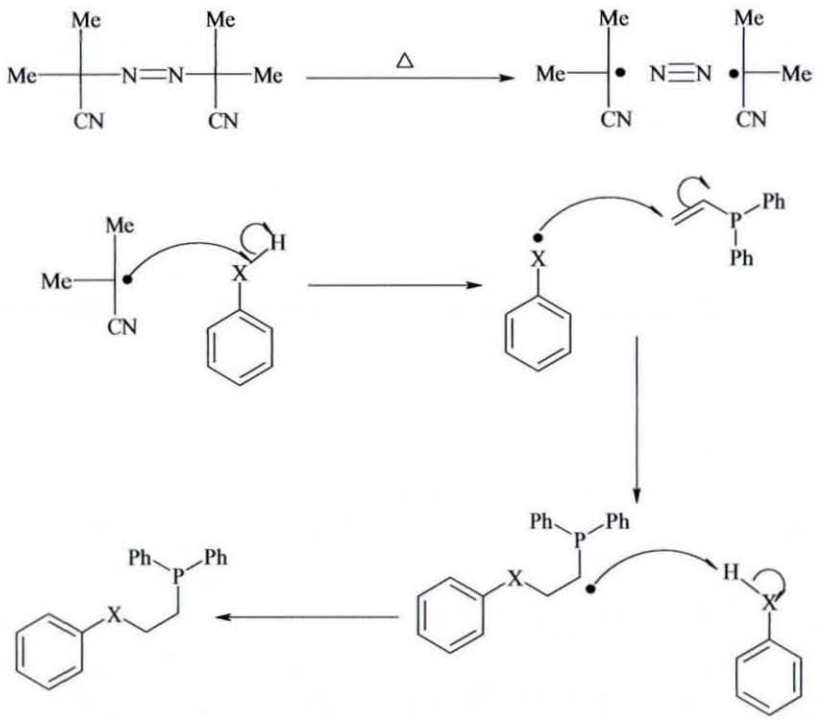

Scheme 2.7 - Radical mechanism for preparation of o-$C_6H_4(PPh_2)(SePh)$, compound **2.17**

present different coordination chemistry, for example by influencing metal-ligand ring conformations and possibly as a result, different catalytic properties. Therefore, the known ligand $PhSCH_2CH_2PPh_2$ **2.21**, and also the unknown $PhSeCH_2CH_2PPh_2$, **2.22** were prepared. These were synthesized similarly to a known method[131] using vinyldiphenylphosphine. This was reacted with the corresponding thiol or selenol in a simple, solvent-free radical reaction, using the initiator azobisisobutyronitrile, AIBN. Both were obtained as solid materials upon cooling under vacuum. The mechanism for the radical initiation and subsequent reaction is shown in Scheme 2.7.

Compounds **2.21** and **2.22** were characterised using a number of methods. Firstly, the $^{31}P\{^1H\}$ NMR spectra show both materials to be reasonably clean with respect to phosphorus-containing material, with peaks at δ(P) –15 ppm (**2.21**) and –14 ppm (**2.22**). Very small amounts of vinyldiphenylphosphine (–10 ppm) and $Ph_2P(O)CH_2CH_2XPh$ (*ca.* 31 ppm) were observed as the only impurities. The ^3J(PSe) coupling shown in the $^{31}P\{^1H\}$ NMR spectrum is considerably larger for **2.22** than for **2.17**, at 174 Hz. The ^{77}Se NMR spectrum showed a single peak at δ(Se) 350 ppm. In the ^1H NMR spectra, the multiplet due to the PPh_2 aromatic protons are seen around

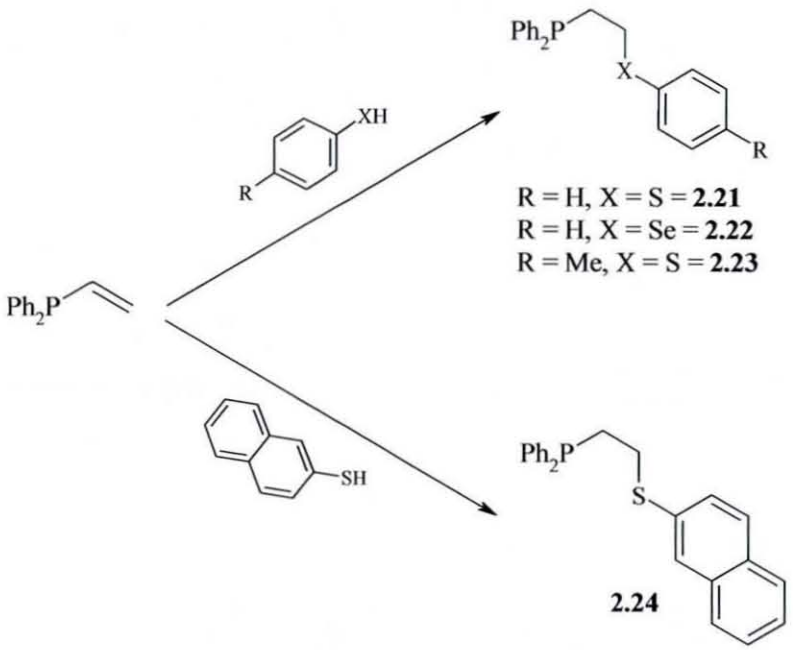

Scheme 2.8 – Preparation of compounds **2.21** – **2.24**

7.2 ppm, whilst the only other signals were those due to the CH_2 backbone, which are seen in the range 2.4–3.0 ppm. The corresponding vinyl protons in the starting material are seen between 5.6 and 6.0 ppm, their absence indicating that C-C bond formation, and hence synthesis of **2.21** and **2.22** occurred.

In the same way, two other similar phosphine-sulfides were produced. Firstly, to assess the effect of adding an alkyl group to the sulfide functionality, vinyldiphenylphosphine was reacted with *p*-thiocresol (4-methylbenzenethiol) to form the ligand $PPh_2(CH_2CH_2)S(p\text{-}C_6H_4CH_3)$, **2.23**. This had many of the same characteristics as **2.21** and **2.22**; the $^{31}P\{^1H\}$ NMR spectrum gave a peak at δ(P) –17 ppm, and the CH_3 peak could be seen at 2.2 ppm in the ^1H NMR spectrum. A small amount of vinylphosphine impurity (*ca.* 3%) corresponds with the similar size thiol peak at δ(P) 3.8 ppm in the proton spectrum.

Finally, 2-thionaphthol was reacted with vinyldiphenylphosphine to form $PPh_2(CH_2CH_2)S(C_{10}H_7)$, **2.24**. This, it was hoped, would give an indication as to the effects of having the sulfide, once bonded to the metal centre, connected to a different aryl-group. A $^{31}P\{^1H\}$ NMR spectrum was obtained, showing the expected single peak at δ(P) –16 ppm. All of the phosphine sulfides prepared are shown in Scheme 2.8.

2.2.2 – Complexation of alkyl-based phosphine chalcogenide ligands

A number of complexes of ligands **2.21** and **2.22** were prepared, as for **2.1** and **2.16**. These reactions are shown in Scheme 2.9. Both **2.21** and **2.22** were reacted with $PdCl_2(cod)$ to form $PdCl_2\{PPh_2(CH_2)_2XPh\}$, (X = S = **2.25**, X = Se = **2.26**), both of which have potential as catalysts for C-C bond coupling reactions. These were isolated as bright yellow solids having crystallised out of solution during the reaction, and once isolated were insoluble in a number of solvents. The $^{31}P\{^1H\}$ NMR spectrum taken in d^6 DMSO showed single sharp peaks at δ(P) 67 (**2.25**) and 63 ppm

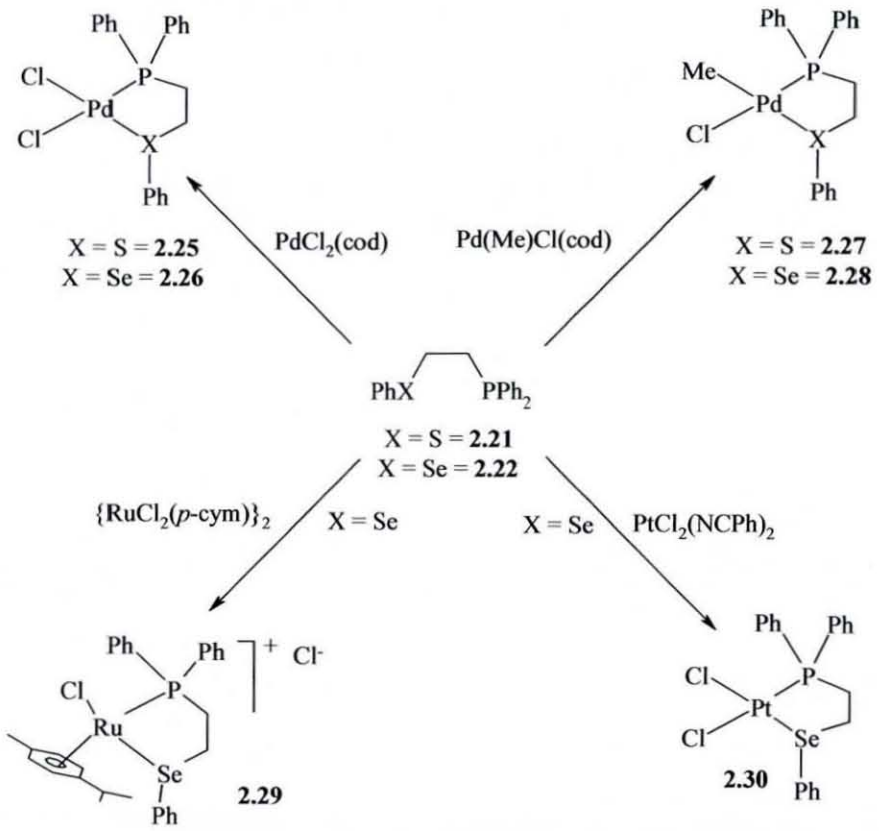

Scheme 2.9 – Preparation of complexes **2.25** – **2.30**

(**2.26**), and both sets of elemental analysis results showed good concordance with those expected. The infra-red spectra of both **2.25** and **2.26** showed two Pd-Cl bands at *ca.* 290 and 320 cm^{-1}, indicating that, as expected, the chelating phosphine chalcogenide ligand is coordinated in a *cis* conformation.

Compound	$^{31}P\{^{1}H\}$ NMR δ (ppm)
2.21	−15
2.22	−15
2.23	−17
2.24	−17
2.25	66
2.26	63
2.27	60
2.28	55
2.29	23
2.30	40
2.31	58
2.32	−16 ($CH_2CH_2PPh_2$), −13 ($C_6H_4PPh_2$)
2.33	−12
2.34	−17
2.35	−17
2.36	−17
2.37	−17
2.38	−13 ($NCH_2\mathbf{P}Ph_2$), −17 ($SCH_2CH_2\mathbf{P}Ph_2$)
2.39	−13 ($NCH_2\mathbf{P}Ph_2$), −17 ($SCH_2CH_2\mathbf{P}Ph_2$)
2.40	10
2.41	40 ($CH_2CH_2\mathbf{P}Ph_2$) and 47 ($C_6H_4\mathbf{P}Ph_2$)
2.42	71
2.43	65
2.44	70
2.45	71
2.46	46
2.47	59

Table 2.5 – Summary of $^{31}P\{^{1}H\}$ NMR data for compounds **2.21** – **2.48**

Compounds **2.21** and **2.22** were also reacted with Pd(Me)Cl(cod) to form the complexes Pd(Me)Cl{$PPh_2(CH_2)_2XPh$}, (X = S = **2.27**, X = Se = **2.28**). These were formed in good yield [88% (**2.27**) and 65% (**2.28**)], as yellow solids. The $^{31}P\{^{1}H\}$ NMR spectroscopy data of **2.28** showed a single peak at δ(P) 55 ppm, and the microanalysis data obtained are in agreement with that calculated (see experimental section). Complex **2.28** was characterised by X-ray crystallography. The structure, shown in Figure 2.7, is as expected, with the coordination sphere of the Pd(II) metal centre consisting of the P and Se donor atoms, one Cl^- ligand and a further carbon atom of a methyl group. The Pd centre lies beneath the plane of the four surrounding substituents by 0.0272 Å, a similar distance to the Pt(II)-Se-based analogue, **2.19**. The

mean deviation from the plane of the 5-membered chelate ring is surprisingly similar (4.7° compared to 4.9° in **2.19**), with the P and Se donor atoms now part of an alkyl-backbone. As with a number of these types of complexes, the geometry around the Pd centre is distorted square planar, with the angles containing atoms opposite to each other (P–Pd–Cl and Se–Pd–C) deviating from 180° by around 7–8°. The P atom is situated *cis*- to the methyl co-ligand, and, as shown in Table 2.6, the Pd-P and Pd-Se bond lengths are as expected, with the larger Se resulting in a slightly longer bond length [2.5167(3) Å].

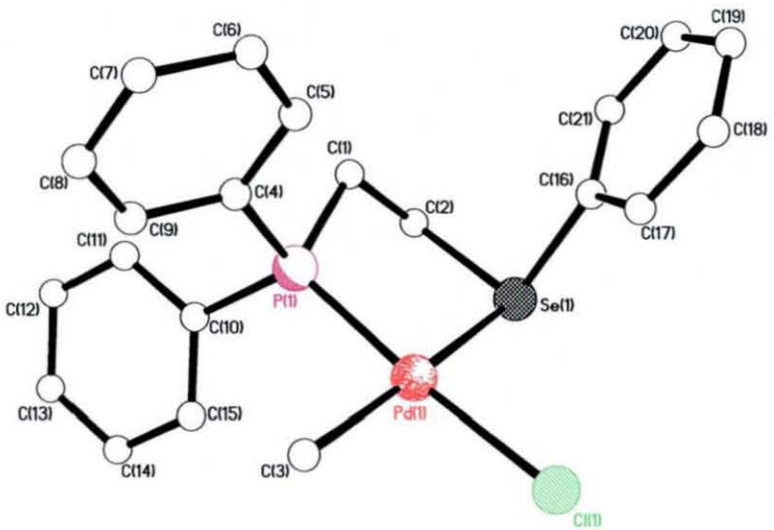

Figure 2.7 – X-ray structure of **2.28**.

Bond Lengths (Å)		Bond Angles (°)	
Pd(1)-P(1)	2.2012(5)	P(1)-Pd(1)-Se(1)	88.64(15)
Pd(1)-Se(1)	2.5167(3)	P(1)-Pd(1)-Cl(1)	172.11(19)
Pd(1)-Cl(1)	2.3966(5)	Se(1)-Pd(1)-C(3)	173.42(5)
Pd(1)-C(3)	2.1123(18)	Se(1)-Pd(1)-Cl(1)	93.13(15)

Table 2.6 - Selected bonds lengths and angles for **2.28**.

Compound **2.2** was also reacted with $\{RuCl(\mu\text{-}Cl)(p\text{-cymene})\}_2$ and $PtCl_2(cod)$ to give complexes **2.29** and **2.30**. Like many of the complexes before, both were characterised by $^{31}P\{^1H\}$ NMR spectroscopy, giving characteristic shifts [δ(P) 23 (**2.29**) and 40 (**2.30**)] for these types of phosphine complexes as shown by previous

complexes prepared, whilst the ^{1}H NMR spectrum, especially for **2.29**, showed the expected peaks for the ligand and *p*-cymene groups. The infra-red spectrum for **2.30** showed two peaks corresponding to Pt-Cl stretches at 280 and 325 cm^{-1}. Further IR data and elemental analysis data can be seen in the Experimental Section.

$PdCl_2$(cod) was also reacted with ligand **2.24** in CH_2Cl_2 to form $PdCl_2\{\{PPh_2(CH_2CH_2)S(C_{10}H_7)\}$, **2.31**. **2.24** was also characterised by $^{31}P\{^{1}H\}$ NMR spectroscopy, a peak at δ(P) 58 ppm indicated that the P and S centres had indeed chelated to the metal centre. The infra-red spectrum showed both two Pd-Cl stretches [329 and 287 cm^{-1}] and peaks due to naphthyl aromatic groups around 680 cm^{-1}.

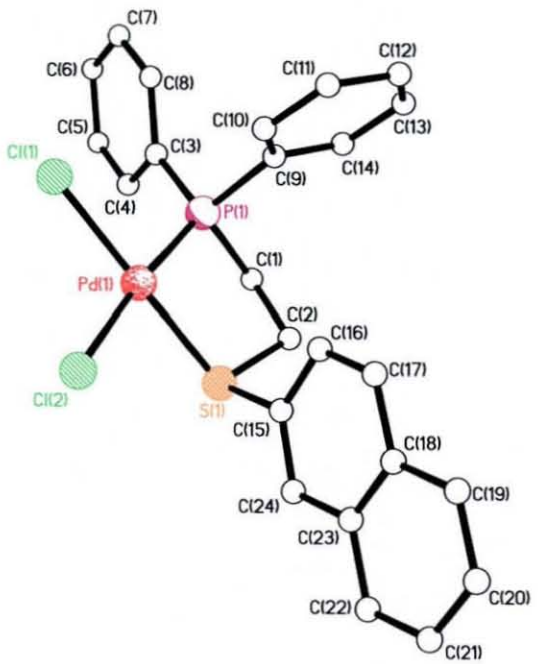

Figure 2.8 – X-ray structure of **2.31**.

Bond Lengths (Å)		Bond Angles (°)	
Pd(1)–P(1)	2.2248(6)	P(1)–Pd(1)–S(1)	87.48(2)
Pd(1)–S(1)	2.2809(6)	P(2)–Pd(2)–S(2)	88.28(2)
Pd(2)–P(2)	2.2288(6)	S(1)–Pd(1)–Cl(1)	175.51(2)
Pd(2)–S(2)	2.2848(6)	S(2)–Pd(2)–Cl(4)	87.33(15)

Table 2.7 - Selected bonds lengths and angles for **2.31**.

Compound **2.31** was also characterised using X-ray crystallography. Crystals were grown by vapour diffusion of Et_2O into a $CDCl_3$/MeCN solution. The structure is shown in Figure 2.8. The Pd metal centre is in a square planar environment,

surrounded by the expected groups; one phosphine, one sulfide and two chloride ions. Two molecules of **2.31** make up the asymmetric unit, and in both of these, the bond lengths/angles are extremely similar. These can be seen in Table 2.7.

2.2.3 – Preparation of mixed P/S/O/N–containing ligands

After preparation of the chelating phosphine chalcogenide ligands, this opened up possibilities for new ligands. It was believed that the addition of a third substituent onto the phenyl ring connected to the sulfide may give different coordination chemistry and therefore catalytic properties to those experienced already. Using the techniques acquired in previous sections, a range of ligands containing a variety of new functionalities were prepared.

Firstly, in an attempt to observe similar properties to chelating diphosphine ligands, the ligand $PPh_2(CH_2)_2S(C_6H_4)o\text{-}PPh_2$, **2.32** was prepared. This would give different phosphine properties due to the alkyl- and aryl- based phosphine groups within the ligand. Subsequently, the different M-P bond strengths could enable interesting catalytic properties to be observed. **2.32** was synthesised in a similar way to the method used for **2.21** and **2.22**. As shown in Scheme 2.10, $o\text{-}C_6H_4(SH)(PPh_2)$ **2.33**, was prepared from thiophenol, n-BuLi and TMEDA,[132] and this was reacted with vinyldiphenylphosphine in the presence of AIBN to form **2.32**. The reaction was carried out at 110 °C, and was again solvent-free, taking 16 h to complete. The work-up procedure involved simple evaporation of any volatile components under vacuum at 80 °C.

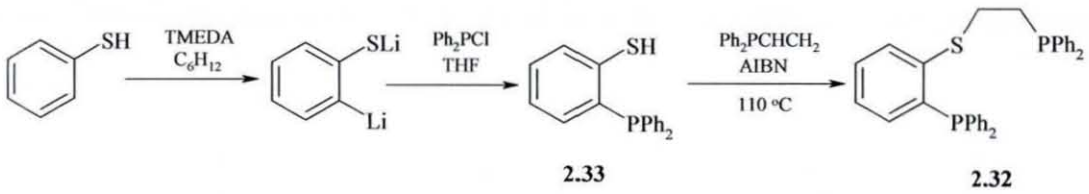

2.33 **2.32**

Scheme 2.10 – Preparation of compounds **2.32** and **2.33**

Compound **2.32** was characterised using a variety of methods. The $^{31}P\{^1H\}$ NMR spectrum showed the expected two peaks at δ(P) –13 ppm and –17 ppm, these corresponding to the aryl and alkyl based phosphine components respectively, based on knowledge gained from the chemical shift values of **2.1** and **2.21**. The ^1H NMR of

2.32 showed two broad triplets around 2.3 and 3.0 ppm due to the two CH_2 groups of the alkyl backbone. The broadness suggests that there may be some degree of fluxionality about the ethyl backbone. The aromatic protons in the molecule are also visible as a multiplet between 7.0 and 7.5 ppm, as is a very small peak at 4.1 ppm, due to the SH proton from a residual amount of PhSH. Mass spectrometry showed the molecular ion peak at 507, along with fragments at 321 [due to $Ph_2P(CH_2)_2S(C_6H_4)^+$], 293 [$C_6H_4(SH)(PPh_2)^+$] and 133 (PPh_2^+).

Using a similar method to this, further ligands were prepared, containing O– and N–based substituents. Both 2– and 4–methoxythiophenol were used separately to form the corresponding ligands $PPh_2(CH_2)_2S(C_6H_4)$*o*-OMe **2.34** and $PPh_2(CH_2)_2S(C_6H_4)$*p*-OMe, **2.35**. In preparing **2.34** and **2.35**, the consequences of the addition of the OMe substituent could be analysed, also observing whether its proximity to the sulfide group would alter the coordination chemistry of the ligand. Both ligands gave characteristic signals in the $^{31}P\{^1H\}$ NMR spectra, at 16.3 and 16.8 ppm (the values of these giving further evidence for the assignments of the chemical shifts of **2.32**). The ^1H NMR spectrum of **2.35** was shown to be reasonably clean, with the Me singlet at 3.82 ppm and the two CH_2 signals in the range 2.31–2.98 ppm. The PPh_2 aromatic protons were seen as a multiplet around 7.2 ppm. The mass spectra of both **2.34** and **2.35** showed molecular ion peaks at *m/z* 353, and molecular fragments at 138/139 ($OMeC_6H_4S^+$), 107 ($C_6H_4OMe^+$) and 166/167 & 185 [$OMeC_6H_4S(CH_2)_2^+$ and PPh_2^+ respectively].

In much the same way as for **2.33–2.35**, various other thiols were used to form potentially tridentate ligands. These are shown, along with the previously mentioned ligands, in Scheme 2.11. 2–hydroxythiophenol was used to form $Ph_2P(CH_2)_2S(C_6H_4)$*o*-OH, **2.36**. This was formed in good yield, as a clear oil which solidified upon freezing. The expected $^{31}P\{^1H\}$ NMR spectroscopy peak was seen at δ(P) –17 ppm, though a small impurity at –12 ppm, constituting around 6% of the overall product, was also observed. This is possibly due to a small amount of the hydroxy-group reacting before the thiol-group, hence producing the ether-thiol product, $PPh_2(CH_2)_2O(C_6H_4)SH$ (shown in Scheme 2.11 in brackets). The ^1H NMR spectrum contains the expected two triplets in the region of 2-2.5 ppm due to coupling

of the two CH_2 groups with the adjacent carbon atoms. The multiplet around 7 ppm, due to the aromatic protons in the molecule, is also present.

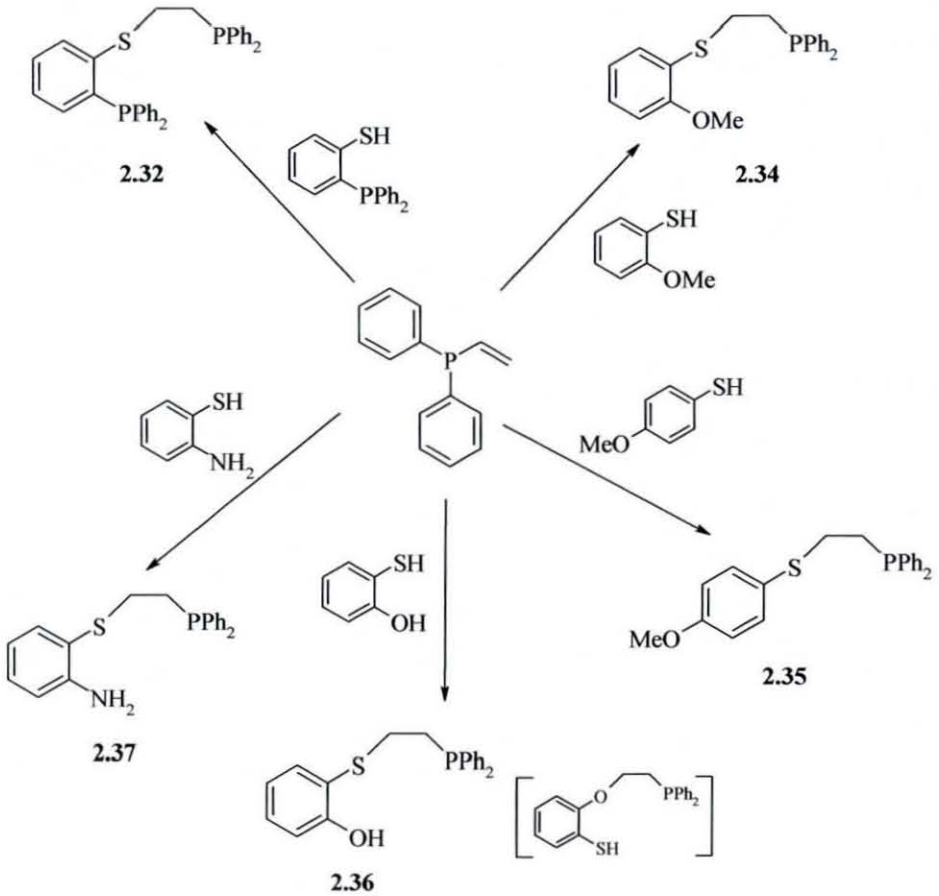

Scheme 2.11 – Preparation of compounds **2.32** – **2.37**

Vinyldiphenylphosphine was also reacted with 2-aminothiophenol to give $Ph_2P(CH_2)_2S(C_6H_4)o\text{-}NH_2$, **2.37**. This, like the hydroxy- analogue **2.36** before, would hopefully give opportunities for further reaction once formed, due to the additional reactive functionalities. For example, as reported in Chapter One, the amine group is reactive with hydroxy-alkyl phosphines. Compound **2.37** was formed as a yellow waxy solid, and gave a characteristic $^{31}P\{^1H\}$ NMR spectroscopy signal at $\delta(P)$ –17 ppm. The phosphine produced seemed to be air stable relative to the parent phosphine, Ph_2PCHCH_2, shown by further $^{31}P\{^1H\}$ NMR spectra recorded 2-3 h after the initial spectrum was run. However, **2.37** and the other examples detailed were stored under nitrogen at 0 °C as an extra precaution.

Compound **2.37** was subsequently reacted with one (and two) equivalents of Ph_2PCH_2OH, in an attempt to form $PPh_2(CH_2)_2S(C_6H_4)o\text{-}N(CH_2)PPh_2$, **2.38** and $PPh_2(CH_2)_2S(C_6H_4)o\text{-}N\{(CH_2)PPh_2\}_2$, **2.39**. In adding an extra functionality to the ligand, it was assumed that new catalytic properties might be observed. The ligands were prepared by addition of Ph_2PCH_2OH, dissolved in MeOH, to a solution of **2.37** in the same solvent. After stirring for *ca.* 3 h, the solution was reduced to dryness to yield an oily product. Both products would be expected to give two signals in the $^{31}P\{^1H\}$ NMR spectrum; indeed this is the case with peaks at δ(P) –13 & –17 ppm for both. These are in the correct ratios [1:1 (**2.38**), and 2:1 (**2.39**)] for the respective products. Further data for these compounds was not obtained however, and more tests are required to confirm these compounds as **2.38** and **2.39**.

The pyridyl-containing ligand $PPh_2(C_6H_4)S(C_5H_4N)$ **2.40** was prepared in a similar fashion to **2.1** and **2.17**. However, instead of using $o\text{-}C_6H_4Br(PPh_2)$ **2.2**, bromopyridine was added to the previously prepared phosphine-thiol $o\text{-}C_6H_4(SH)(PPh_2)$, as shown in Equation 2.3. Previous attempts to prepare compound **2.40** using mercaptopyridine resulted in extremely low conversion, presumably due to tautomerism of the SH & N functionalities. The product was isolated as a grey solid, though the yield (33%) was appreciably lower than similar preparations of **2.1** and **2.17**. The $^{31}P\{^1H\}$ NMR spectrum showed the ligand to be free of phosphorus-containing starting material, with a single peak at –10 ppm, though a small amount of oxidation of the product had occurred, as shown by a peak at 26.6 ppm. The ^1H NMR spectroscopy data shows five peaks in the aromatic region of the spectrum, with four doublets (6.7, 6.9 7.6 and 8.3 ppm) due to the aromatic ring containing both the sulfide and phosphine functionalities. The final, much larger multiplet in this region is due to the remaining (pyridyl and phenyl) aromatic protons.

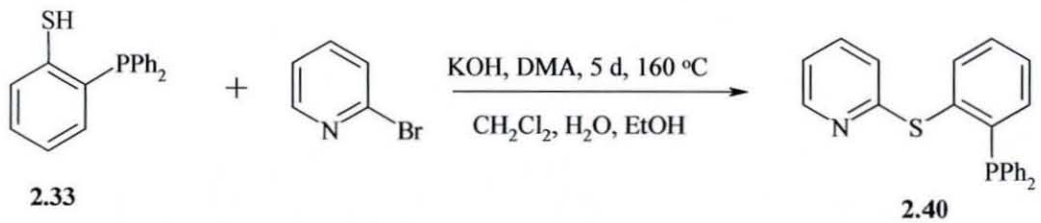

2.33 **2.40**

Equation 2.3 – Preparation of C_6H_4(S-Pyridine)(PPh_2)

2.2.4 – Pd and Pt Complexes of mixed P/S/O/N-containing ligands

Having prepared ligands **2.32-2.40**, a number of complexes were synthesised, mainly towards compounds which could subsequently be used for catalytic experiments. These can be seen in Equation 2.4.

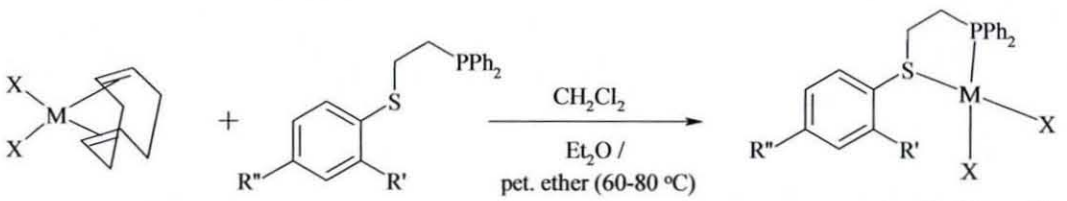

	R'	R"
2.32	PPh_2	H
2.34	OMe	H
2.35	H	OMe
2.36	OH	H
2.37	NH_2	H

	M	X	R'	R"
2.41	Pd	Cl	PPh_2	H
2.42	Pd	Cl	OMe	H
2.43	Pd	Cl	H	OMe
2.44	Pd	Cl	NH_2	H
2.45	Pd	Cl	OH	H
2.46	Pt	Me	NH_2	H

Equation 2.4 – Pd and Pt complexes of mixed P/S/O/N-containing ligands

Firstly, the Pd(II) complex of **2.32**, $PdCl_2$(**2.32**) **2.41** was prepared using $PdCl_2$(cod) and **2.32**. This was isolated as a yellow solid in reasonable yield (59%), and characterised using a number of methods. The mass spectrum showed a molecular ion peak at 649, corresponding to the complex containing just one M-Cl bond. This suggests that the ligand may be bound through the P, S and the second P donor atom, hence the loss of one Cl^- group. It must be noted, however, that a number of M-Cl complexes prepared in this work and beyond exhibit molecular ion peaks minus a chloride ion. Other peaks were seen at 185, due to PPh_2^+, and at 507, due to the free ligand. The $^{31}P\{^1H\}$ NMR spectrum showed a number of unusual peaks. The first two main phosphine peaks were seen at δ(P) 40 and 47 ppm, with two further smaller peaks at δ(P) 36 and 52 ppm. The latter two peaks may be due to coupling of the two phosphorus atoms if both are coordinated to the Pd centre. This would be the case even if the phosphorus atoms adopted a '*trans*-spanning' arrangement, with the sulfide group bridging the metal centre. This gives ^2J(PP) coupling of around 400 Hz, not dissimilar to values given for other reported *trans*-spanning ligands.[133] Other peaks are also seen in the spectrum, at 14, 19 and 58 ppm. It is likely that these can be assigned to both other methods of coordination of the ligand, *i.e.* with the $CH_2CH_2PPh_2$ group uncoordinated, and also to the coordination of the small number

of impurities which were seen in the $^{31}P\{^{1}H\}$ NMR spectrum of **2.32**. The infra-red spectrum gave those of the parent ligand, along with two Pd-Cl peaks [280 and 324 cm^{-1}], inferring that the ligand is only coordinated either *via* one of the phosphine and sulfide moieties, or as suggested before by bridging of **2.32** over the metal centre. Repeated attempts to obtain X-ray quality crystals of **2.41** were unsuccessful.

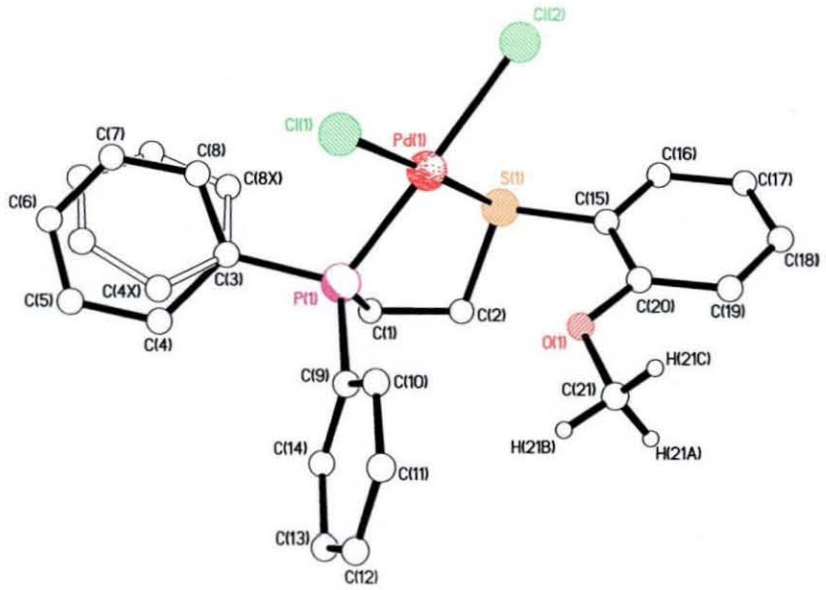

Figure 2.9 – X-ray structure of **2.42** (solid lines – main component, white lines – disordered component

Secondly the complexes $PdCl_2\{PPh_2(CH_2)_2S(C_6H_4)o\text{-}OMe\}$ **2.42**, and $PdCl_2\{PPh_2(CH_2)_2S(C_6H_4)p\text{-}OMe\}$ **2.43** were prepared from $PdCl_2(cod)$, along with **2.34** and **2.35** respectively. Both were isolated in good yield as yellow and orange solids. The $^{31}P\{^{1}H\}$ NMR spectra both indicated that single species were present with signals at δ(P) 70 and 65 ppm respectively. These peaks are shifted upfield from bidentate ligands previously prepared in this section, possibly a factor of the slightly more electron donating OMe group on the ligand.

The X-ray structures of **2.42** and **2.43** were elucidated. Crystals of **2.42** were grown by vapour diffusion of Et_2O into a CH_2Cl_2/MeOH solution; the structure is shown in Figure 2.9. The coordination sites are taken up by both the phosphine and sulfide groups forming a 5-membered ring, and two further Cl^- groups; hence the ligand is not bound in a tridentate fashion. The Pd centre is shown to be in a slightly

distorted square planar environment. Some of the angles, such as the P–Pd–Cl angle [172.58(5)°] (Table 2.8) are shown to be quite distorted from a normal square planar geometry. This may be due to disorder in one of the phenyl rings in the structure, the quaternary carbon [C(3)] of this disordered phenyl ring being the only carbon common to both possible aryl groups. The disorder component ratio for main:disordered components for the structure is 64:36. The angles involving the quaternary carbon atoms bonded to the phosphine, and the alkyl backbone of the ligand [C(9)–P(1)–C(1) = 107.5(2) & C(3)–P(1)–C(1) = 105.8(2)] are such that any steric interactions between the aryl groups in the structure are minimised. The Pd centre is 0.0493 Å above the plane of the four groups which surround it, which is similar to values obtained previously; however as was the case with almost all the complexes containing three donor atoms, the 'hinge angle' between the metal and the alkyl backbone is slightly larger [5.6°] than previous angles. The distance between

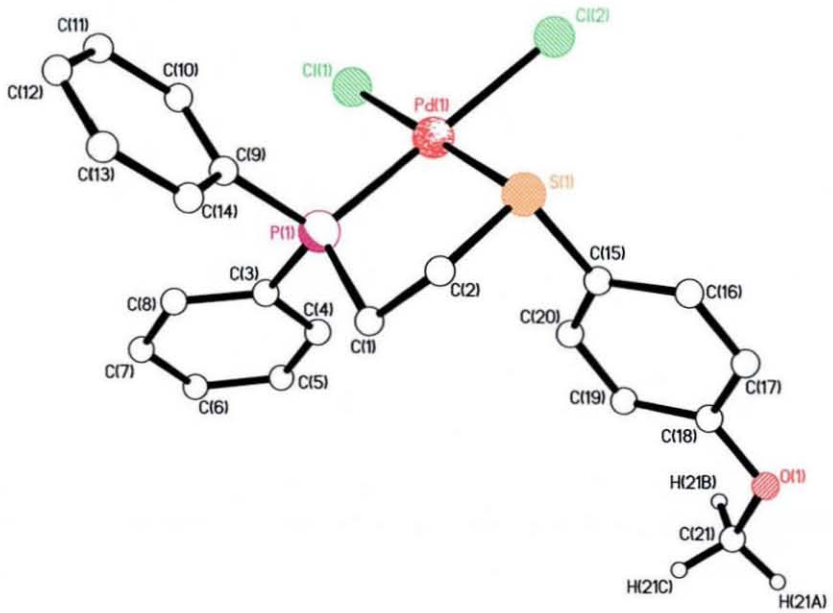

Figure 2.10 – X-ray structure of **2.43**

Bond Lengths (Å)			Bond Angles (°)		
	2.42	**2.43**		**2.42**	**2.43**
Pd(1)-P(1)	2.2178(15)	2.2345(5)	P(1)-Pd(1)-S(1)	87.80(5)	88.58(19)
Pd(1)-S(1)	2.2836(13)	2.2711(5)	P(1)-Pd(1)-Cl(1)	90.01(5)	91.35(19)
Pd(1)-Cl(1)	2.3242(12)	2.3101(5)	S(1)-Pd(1)-Cl(2)	87.38(5)	86.25(2)
Pd(1)-Cl(2)	2.3720(15)	2.3681(5)	S(1)-Pd(1)-Cl(1)	177.68(5)	179.38(2)

Table 2.8 - Selected bonds lengths and angles for **2.42** and **2.43**

Pd(1) and O(1) is 3.308 Å. As a result of this it was anticipated that the OMe group could quite easily be brought into coordination with the Pd centre if the Cl^- ligand was removed using $Ag[BF_4]$, for example.

The crystal structure of $PdCl_2\{Ph_2P(CH_2CH_2)S(C_6H_4)p\text{-}OMe\}$, **2.43** was also solved; this is shown in Figure 2.10. As expected, **2.43** is structurally similar to its *ortho-* OMe analogue **2.42**, with the Pd(II) centre again in a slightly distorted square planar environment. The four atoms coordinated to the metal centre are the same as for **2.42**, (P,S, and 2 x Cl), with, as shown in Table 2.8, one of the bonds (Pd-P) being slightly longer than the same bond in **2.42**. The other three Pd bonds are slightly shorter in this complex than for the previous example.

Using $\{PPh_2(CH_2)_2S(C_6H_4)NH_2\}$ **2.37** and $PdCl_2(cod)$, the corresponding Pd(II) complex, **2.44**, was prepared. The $^{31}P\{^1H\}$ NMR spectrum using DMSO as solvent, gave a single peak at δ(P) 71 ppm, with no phosphorus-based impurities. The infra-red spectrum exhibits two Pd-Cl bands at 286 and 313 cm^{-1}, expected for bidentate coordination of the ligand, along with NH_2 stretches at 1250, 1614 and 3393 cm^{-1}. The ^1H NMR does show a NH_2 peak at 5.90 ppm, though this spectrum does show some sign of solvent impurities. Upon addition of deuterium oxide, the peak at 5.90 ppm disappeared, thus confirming the assignment of the NH_2 peak. In a similar way to **2.44**, using 2–hydroxythiophenol, $PdCl_2\{Ph_2P(CH_2CH_2)S(C_6H_4)o\text{–}OH\}$, **2.45**, was also prepared. This, like the other complexes in this section, gave a $^{31}P\{^1H\}$ NMR shift further downfield than the bidentate analogues, at 70 ppm, and was formed in excellent yield (80%).

By adding **2.37** dropwise to a solution of $PtMe_2(cod)$, the corresponding complex, $PtMe_2\{Ph_2P(CH_2CH_2)S(C_6H_4)o\text{-}NH_2\}$, **2.46** was prepared. This gave a similar shift in the $^{31}P\{^1H\}$ NMR spectrum to those prepared previously (46 ppm), so it was assumed that the complex probably consisted of a pendant NH_2 group, with the P and S donor atoms coordinated to the metal centre. Elemental analysis results gave excellent concordance with those expected (see Experimental Section). The X-ray structure of **2.46** was also solved, and can be seen in Figure 2.11a and b. Two molecules of **2.46** make up the asymmetric unit, with both complexes containing

ligands coordinated through both the phosphorus and sulfur donor atoms. The coordination sphere of the Pt centre is completed by two C atoms of Me groups, the various angles of which with the P and S groups giving a distorted square planar geometry. As shown in Table 2.9, metal-donor distances are larger than for **2.42** and **2.43**, though this is expected with both an increase in metal size and co-ligands situated opposite. The free amine groups in both molecules interact with the metal centres in an intra- and intermolecular fashion. In both cases, one N-H bond faces the Pt centre in the same molecule, whilst another N-H bond faces the Pt centre in the next molecule along. The through-space NH-Pt distances for four of these interactions can be seen in Table 2.9, these are fairly short; 2.47-2.48 for the intramolecular cases, and 2.76–2.79 for the intermolecular interactions.

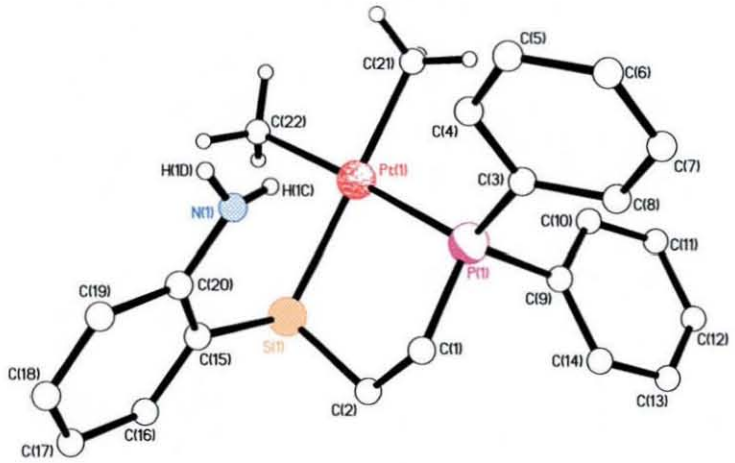

Figure 2.11b – X-ray structure of **2.46**

Bond Lengths (Å)		Bond Angles (°)	
Pt(1)–P(1)	2.2847(10)	P(1)–Pt(1)–S(1)	87.27(3)
Pt(1)–S(1)	2.3601(10)	P(1)–Pt(1)–C(21)	96.17(11)
Pt(2)–P(2)	2.2837(10)	S(1)–Pt(1)–C(21)	175.32(12)
Pt(2)–S(2)	2.3566(10)	S(1)–Pt(1)–C(22)	89.96(11)
Pt(1)–H(1C)	2.48(2)	P(2)–Pt(2)–S(2)	87.00(4)
Pt(1)–H(2D')	2.76(3)	S(2)–Pt(2)–C(43)	176.57(12)
Pt(2)–H(2C)	2.47(2)	S(2)–Pt(2)–H(2C)	71.3(10)
Pt(2)–H(1D)	2.79(3)	S(2)–Pt(2)–H(1D)	75.9(8)

Table 2.9 – Selected bond lengths and angles for **2.46**

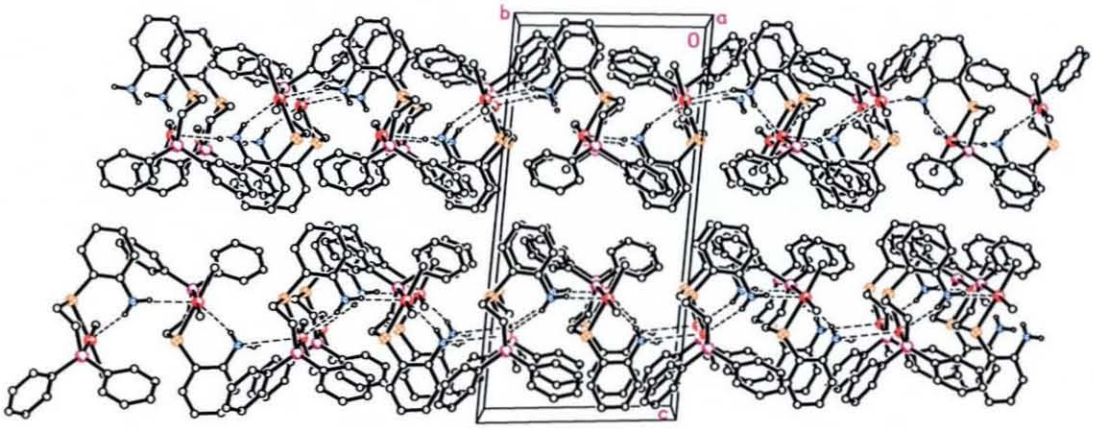

Figure 2.11b – Packing plot showing interactions in **2.49**

The packing plot shown in Figure 2.11b shows intra- and intermolecular interactions in the structure of **2.49**. The short distances between the NH_2 functional groups and Pt centres results in the formation of 'chains' of **2.49**. In each molecule, one hydrogen of the NH_2 group interacts with the Pt centre from the same molecule, whilst the other interacts in an intermolecular fashion. The chains of molecules formed are arranged in layers, such that each corresponding atoms are arranged on top of each other.

$PdCl_2(cod)$ was also reacted with one equivalent of *o*–$PPh_2(C_6H_4)S(C_5H_5N)$ **2.38**, to give $PdCl_2\{Ph_2P(C_6H_4)S(C_5H_5N)\}$, **2.47**. This was carried out in anticipation of coordination of the pyridyl–N atom. The crystal structure of $PdCl_2\{Ph_2P(C_6H_4)S(C_5H_5N)\}$ **2.47** is shown in Figure 2.12. Characterisation of **2.47** was carried out with the methods used previously. The $^{31}P\{^1H\}$ NMR spectrum gave a single peak at 61 ppm. By analogy with other examples studied, and comparison with the chemical shift for the parent ligand **2.38** (10 ppm), this was fairly good evidence as to the nature of the product. Whilst the ^1H NMR spectroscopy data proved fairly inconclusive due to the presence of many aromatic resonances, the elemental analysis data proved to be within the range expected (See Experimental Section).

Crystals of **2.47** were grown by layering a $CHCl_3$ solution with petroleum ether (60–80 °C). The asymmetric unit is shown to contain one molecule of chloroform from this solvent layering. The N donor atom on the ligand is uncoordinated, this therefore leaves the coordination sphere to be made up from the two Cl^- ligands, and the P and S donor atoms in a square planar environment around the Pd centre. The metal-ligand bond lengths and angles, shown in Table 2.10, are, as expected, similar to those for complexes reported previously in the Chapter. The Pd metal centre is sat only a small distance out of the plane of the four donor atoms surrounding it (0.0075 Å), thus suggesting that the structure as a whole is almost planar. The 'hinge angle' also suggests this, with the angle between the metal centre, S/P atoms and the aryl backbone shown to be only 0.8°. The shallowness of the five membered chelate rings in this structure, as shown throughout, is an extremely common characteristic of all of the phosphine/chalcogenide based ligands prepared in this section.

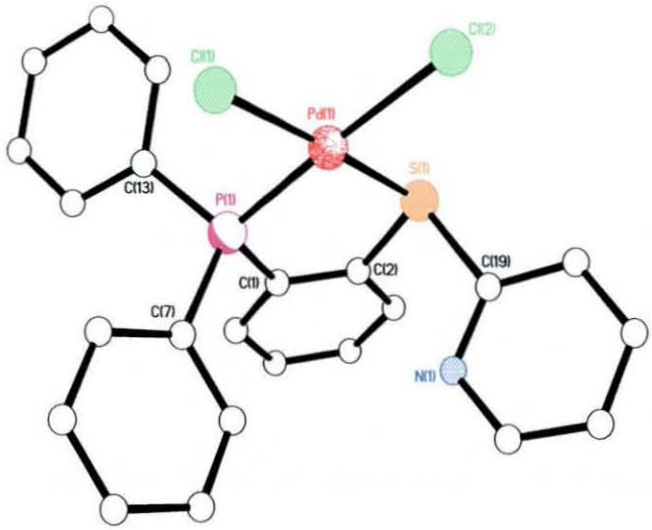

Figure 2.12 – X-ray structure of compound **2.47**

Bond Lengths (Å)		Bond Angles (°)	
Pd(1)-P(1)	2.2129(10)	P(1)-Pd(1)-S(1)	88.82(4)
Pd(1)-S(1)	2.2809(11)	P(1)-Pd(1)-Cl(1)	87.42(4)
Pd(1)-Cl(1)	2.3161(11)	S(1)-Pd(1)-Cl(2)	88.76(4)
Pd(1)-Cl(2)	2.3643(10)	S(1)-Pd(1)-Cl(1)	176.01(4)

Table 2.10 – Selected bond lengths and angles for **2.47**

2.2.5 – Coordination experiments using 2.42/2.43

As seen in section 2.2.4, none of the potentially tridentate ligands had coordinated to the Pd/Pt metal centres in such a fashion, instead binding only *via* the phosphine and sulfide groups. However, it was believed these could be coordinated to the metal centres, prompted by addition of reagents to cleave Pd-Cl bonds. Distances from the 'free' functional group to the nearest metal centre can be seen in Table 2.11. The distances for the three ligands containing *ortho-* groups are fairly similar, the smallest of these being for PtMe(**2.37**) **2.46**. The largest value was, as expected, for the complex containing *para-* substituted **2.35**.

With the realisation that $PdCl_2\{Ph_2P(CH_2CH_2)S(C_6H_4)o\text{-}OMe$, **2.42** was bound in a bidentate fashion, a reaction was carried out to cleave the Pd–Cl bond *trans*– to the phosphine, and replace the vacant coordination site with the OMe group. $Ag[BF_4]$ was reacted with one equivalent of **2.42** to give **2.48**, as shown in Equation 2.5. The reaction was carried out in nitromethane, to eliminate the possibility of

Compound Number	Distance (Å)
2.42	3.308
2.43	5.887
2.46	3.285
2.47	3.664

Table 2.11 – Distances of 'free' functionality to nearest metal centre for complexes containing multifunctional ligands

solvent coordination, and to allow both reactants to be added as solutions. The $^{31}P\{^1H\}$ NMR spectrum of **2.48** shows there to be one very broad peak which shifted further upfield from the known **2.42** to δ(P) 78 ppm. The broadness suggests that any tridentate coordination of the ligand may be fluxional. This would be understandable due to the relative weakness of a Pd-O bond compared to, for example, a Pd–P bond in the previous complex **2.31**.

In much the same way, we assumed that if a Pd–Cl bond could be cleaved in the *para-* OMe complex **2.43**, a second molecule may be able to coordinate to the vacant site to produce a chain-like structure. This reaction was attempted using one

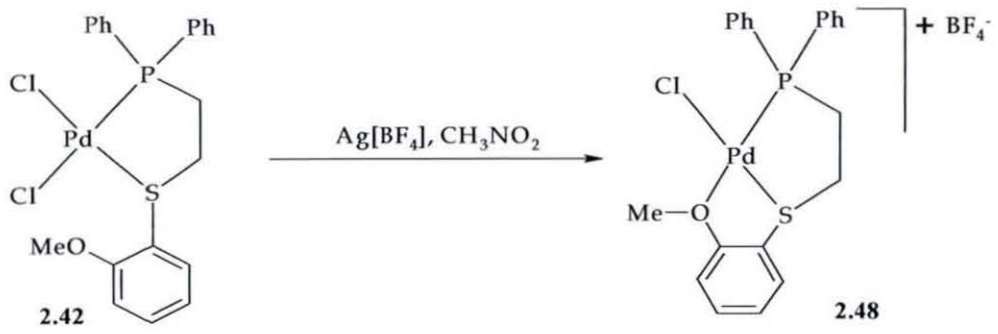

Equation 2.5 – $Ag[BF]_4$ reaction using compound **2.42**

equivalent of $Ag[BF_4]$ (based on starting materials), to avoid any loss of a second chloride ligand. This was added *in-situ*, after the assumed formation of **2.43**. The $^{31}P\{^1H\}$ NMR spectrum showed a mixture of peaks. The largest of these was at δ(P) 62 ppm, with two other peaks at 69 and 44 ppm. In comparing these to **2.43** (65 ppm), all of these peaks may be assigned. One may be the correct product, with the OMe group coordinated. A second may be a small amount of the previously mentioned product with no Cl^- ligands left, *i.e.* P–S–O coordinated, with the coordination sphere completed by a P donor atom from a further ligand, giving a dicationic species. Another possibility could be that when both chloride ligands are displaced, the rate of OMe coordination is slower than the rate of chelation of another P/S ligand, hence a dicationic species with two BF_4^- anions is present. The latter two are only possible if excess $Ag[BF_4]$ is present. Numerous attempts to obtain crystals suitable for X-ray analysis to elucidate the structure of one or more of these species proved unsuccessful.

Table 2.12 - Comparison of Bond Lengths and Bond Angles for Transition Metal Complexes Prepared in Chapter Two				
Compound[a]	**Bond lengths (Å)**			
	M–P [b]	**M–S/Se** [b,c]	**M–X** [b,c]	**M–X'** [b,c]
2.9 (Pd)	2.2054(5) [2.2020(5)]	(S) 2.3945(6) [2.3910(6)]	(CH_3) 2.0610(2) [2.057(2)]	(Cl) 2.3603(5) [2.3656(5)]
2.10 (Pt)	2.2122(10) [2.1986(10)]	(S) 2.2497(10) [2.2586(10)]	(Cl) 2.3015(9) [2.3103(10)]	(Cl) 2.3607(10) [2.3536(10)]
2.18 (Pd)	2.2210(6)	(Se) 2.3885(4)	(Cl) 2.3075(8)	(Cl) 2.3743(7)
2.19 (Pt)	2.2093(11)	(Se) 2.3560(5)	(Cl) 2.3143(12)	(Cl) 2.3668(11)
2.28 (Pd) [d]	2.2012(5)	(Se) 2.5167(3)	(CH_3) 2.1123(18)	(Cl) 2.3966(5)
2.31 (Pd) [d]	2.2248(6)	(S) 2.2809(6)	(Cl) 2.2288(6)	(Cl) 2.2848(6)
2.42 (Pd) [d]	2.2178(15)	(S) 2.2836(13)	(Cl) 2.3242(12)	(Cl) 2.3720(15)
2.43 (Pd) [d]	2.2345(5)	(S) 2.2711(5)	(Cl) 2.3101(5)	(Cl) 2.3681(5)
2.46 (Pt) [d]	2.2847(10)	(S) 2.3601(10)	(CH_3) 2.066(4)	(CH_3) 2.092(4)
2.47 (Pd)	2.2129(10)	(S) 2.2809(11)	(Cl) 2.3161(11)	(Cl) 2.3643(10)

	Bond Angles (°)					
	P–M–S/Se	**P–M–X**	**P–M–X'**	**S/Se–M–X**	**S/Se–M–X'**	**X–M–X'**
2.9 (Pd)	88.29(2) [88.64(2)]	89.84(6) [88.97(6)]	179.07(2) [179.33(2)]	177.22(7) [177.24(7)]	91.42(2) [91.68(2)]	90.49(6) [90.72(6)]
2.10 (Pt)	90.29(4) [89.60(4)]	90.29(4) [89.97(4)]	177.11(4) [178.54(4)]	178.22(3) [177.54(4)]	87.13(4) [89.00(4)]	92.32(4) [91.45(4)]
2.18 (Pd)	89.78(19)	90.06(3)	172.95(2)	178.95(2)	85.58(2)	94.67(3)
2.19 (Pt)	90.28(3)	91.90(4)	173.95(4)	177.14(3)	85.94(3)	92.03(5)
2.28 (Pd)	88.64(15)	87.55(5)	172.11(19)	173.42(5)	93.13(15)	91.37(5)
2.31 (Pd)	87.48(2) [88.28(2)]	89.08(2) [90.13(2)]	173.60(2) [174.39(2)]	175.51(2) [178.20(2)]	87.98(2) [87.33(15)]	95.67(2) [94.20(2)]
2.42 (Pd)	87.80(5)	90.01(5)	172.58(5)	177.68(5)	87.38(5)	94.87(4)
2.43 (Pd)	88.58(19)	91.35(19)	172.99(2)	179.38(2)	86.25(2)	93.87(2)
2.46 (Pt)	87.27(3)	96.17(11)	177.23(11)	175.32(12)	89.96(11)	86.58(16)
2.47 (Pd)	88.82(4)	87.42(4)	177.51(4)	176.01(4)	88.76(4)	95.01(4)

[a] Metal type in brackets. [b] Values in square brackets for equivalent atoms in second molecule. [c] Coordinating group in first brackets.
[d] Phosphine/chalcogenide groups on alkyl backbone.

2.3 – CONCLUSIONS

In summary, a wide range of novel ligands have been prepared using highly reproducible methods. These ligands are based on both aromatic and alkyl backbones, thus enabling different modes of coordination to be observed when added to various transition metal starting materials. The methods used for preparation of the bidentate phosphine chalcogenide ligands, and the theories used for their characterisation assignments have helped in the synthesis of a number of potentially tridentate ligands containing combinations of P/S/O and N donor atoms. We can conclude that these ligands, whilst not coordinating through all three donor atoms initially, have shown the potential to do so when further reagents such as $Ag[BF]_4$ are added, and this is an area which could be investigated further.

Chapter Three

~Chemistry of Phosphaadamantane-Containing Ligands ~

3.1 – AIMS OF THE CHAPTER

As reported in Chapter One, the benefits of using phosphines containing bulky organic groups for catalytic processes is well known. The use of the phospha-adamantane group 'Cytop' (abbreviated to 'PAd') (**1.113**) is rather less well documented, though some examples are known.

3.1.1 – Preparation of ligands with aromatic backbones

A number of ligands containing Cytop (**3.1-3.3**) were produced using synthetic procedures similar to those used for the preparation of **2.1** and **2.16**. These are shown in Scheme 3.1. *o*-C_6H_4Br(PAd) **3.1**, was prepared by reacting 1-bromo-2-iodobenzene with **1.113** in dimethylacetamide. In comparison to the same reaction using

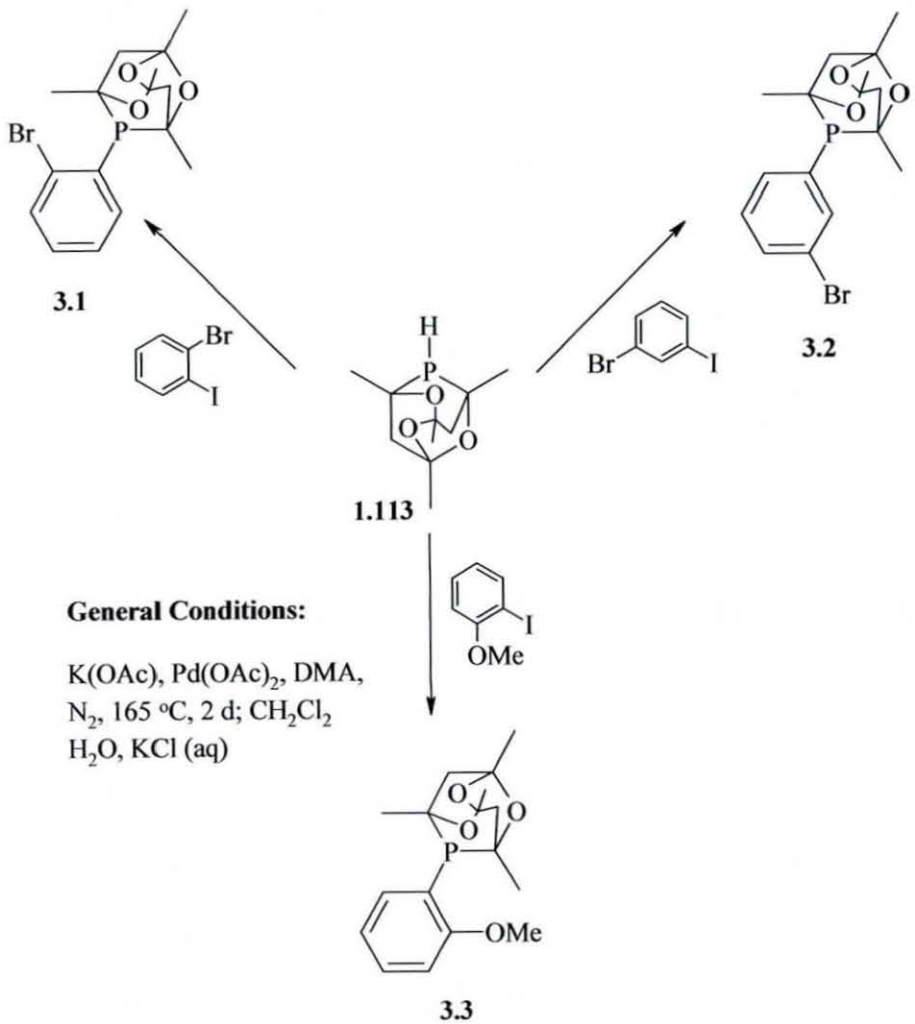

Scheme 3.1 - Preparation of *o*-C_6H_4Br(PAd), *o*-C_6H_4Br(PAd) and *o*-$C_6H_4(OMe)$(PAd), compounds **3.1** - **3.3**

diphenylphosphine (Scheme 2.2, Chapter Two), which consistently took 5 d to proceed to completion, this reaction took only 2 d. Due to the only difference being the use of the secondary dialkyl phosphine **1.113** rather than diphenylphosphine, it was assumed that electronic effects are the major reason for the difference in reaction time. Compound **3.1** was isolated as a white crystalline solid. As can be seen in Table 3.1, one peak at δ(P) -29.0 ppm was observed in the $^{31}P\{^{1}H\}$ NMR spectrum. The ^{1}H NMR spectrum showed the expected multiplet of peaks between δ(H) 1.2 and 2.1 ppm, whilst the four aromatic protons in **3.1** give two doublets and two triplets between δ(H) 7.1 and 8.2 ppm, corresponding to two protons *ortho-* and *meta-* to the phospha-adamantane substituent, and the remaining two protons respectively. The molecular ion of **3.1** is observed at *m/z* 371, though the largest peak in the mass spectrum is seen at 272, due to fragmentation of **3.1**, to the phospha-adamantane ion.

	δ(P) / -PAd (ppm)
3.1	–29.0
3.2	–25.0
3.3	–42.0
3.4	–37.7
3.5	–34.7
3.6	1.3, 2.8
3.7	7.2, 7.3
3.8	48.0
3.9	46.0
3.10	13.7, 14.2
3.11	–4.0

Table 3.1 – Selected $^{31}P\{^{1}H\}$ NMR data for compounds **3.1-3.11**

The structure of **3.1** was confirmed by X-ray crystallography, this is shown in Figure 3.1. Crystals of **3.1** suitable for X-ray crystallography were grown by slow evaporation of an Et_2O solution. The structure derived from the crystallographic data obtained showed the bond lengths from the aromatic backbone to the two substituents to be as expected. One slightly smaller C–C(2)–Br angle, however [117.02(15) for C(3)–C(2)–Br(1) compared to 120.50(14) for C(1)–C(2)–Br(1)], suggests there is slight repulsion of the bromide group away from the bulky phosphine substituent. This is confirmed by the large distance between P(1) and Br(1) [3.273 Å].

The X-ray structure also allowed the 'intracage' angle [the angle between C(7)–P(1)–C(10)] to be calculated for **3.1**. This is shown, along with the corresponding angle for ligands and complexes further in Chapter Three in Table 3.3. The intracage angle is smaller for **3.1** [93.10(8)], and in general for all ligands than angles for the complexes, which suggests that strain is placed on the adamantane cage around the phosphorus donor atom upon complexation.

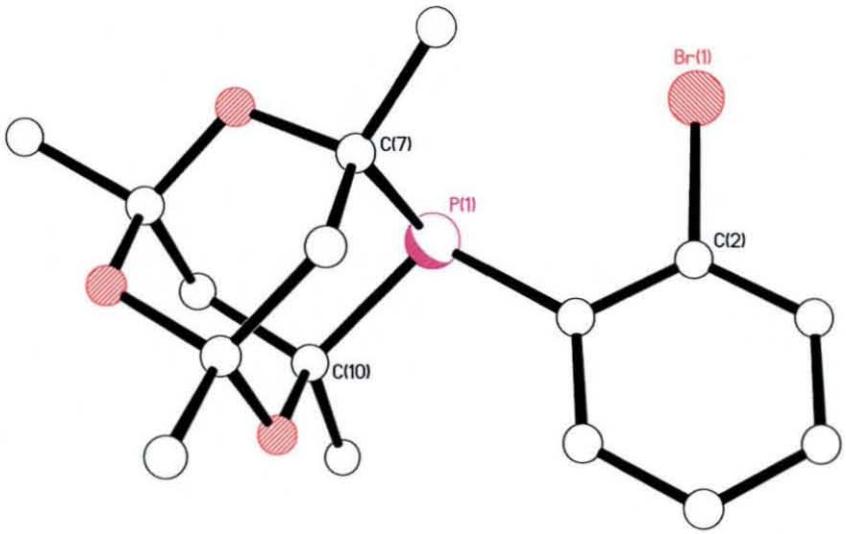

Figure 3.1 – X-ray structure of **3.1**

Bond Lengths (Å)		**Bond Angles (°)**	
C(1)–P(1)	1.839(2)	C(1)–P(1)–C(7)	104.49(8)
C(2)–Br(1)	1.910(2)	C(1)–P(1)–C(10)	106.23(8)
		C(7)–P(1)–C(10)	93.10(8)
		C(1)–C(2)–Br(1)	120.50(14)
		C(3)–C(2)–Br(1)	117.02(15)

Table 3.2 - Selected bonds lengths and angles for **3.1**

Compound Number	C–P–C Intracage angle (°)
3.1	93.1(8)
3.5	92.4(14)
3.6	93.9(2)
3.8	94.9(16)
3.9	94.1(8)
3.11	94.7(3)
3.14	93.6(3)
3.17	92.2(14)
3.18	95.2(3)
3.19	94.2(3)
3.22	93.0(5)

Table 3.3 – Intracage bond angles in phospha-adamantane containing ligands and complexes.

In a similar manner, reactions to prepare *m*-BrC_6H_4(PAd) **3.2** and *o*-(OMe)C_6H_4(PAd) **3.3** were attempted using *m*-bromoiodobenzene and *o*-iodoanisole respectively. Compound **3.2** was isolated as a slightly green crystalline solid, which was a relatively unusual colour compared to the consistently white/off white colour of all the other crystalline phosphines prepared. A singlet at δ(P) –25 ppm was observed in the $^{31}P\{^1H\}$ NMR spectrum of **3.2**, with a small singlet at δ(P) 17 ppm, presumably due to a minimal amount of the oxidised compound. The ^1H NMR spectrum showed the multiplet expected for the phospha-adamantane fragment, and also four distinct peaks for the aromatic protons. Shown in Figure 3.2, proton H_A is seen as a doublet at 8.00, whilst the other three protons, H_B, H_C, and H_D are seen as six peaks at 7.98, 7.52 and 7.26 respectively due to coupling with the other two inequivalent proton nuclei. The mass spectrum of **3.2** gave a peak at *m/z* 372, corresponding to the parent ion.

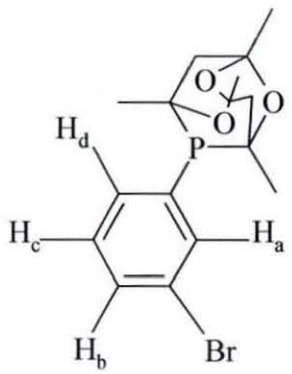

3.2

Figure 3.2 – *m*-C_6H_4Br(PAd)

Compound **3.3** was also characterised using $^{31}P\{^{1}H\}$ NMR spectroscopy, showing a singlet at δ(P) –42 ppm, corresponding to the single phosphorus atom of the phospha-adamantane fragment. An extremely small peak was seen at δ(P) 20 ppm, presumably due to a small amount of phosphine oxide. In the ^{1}H NMR spectrum, the methyl resonance of the OMe group could be seen as a singlet at δ(H) 3.85 ppm. The four protons on the aromatic backbone can be seen as doublets of doublets between 6.87 and 8.10 ppm, presumably due to both coupling and the two different enantiomeric products. The phospha-adamantane fragment remains as a rather complicated multiplet between δ(H) 1.41 and 2.13 ppm. Elemental analysis also gave further evidence for the nature of **3.3**, the results of which can be seen in the experimental section.

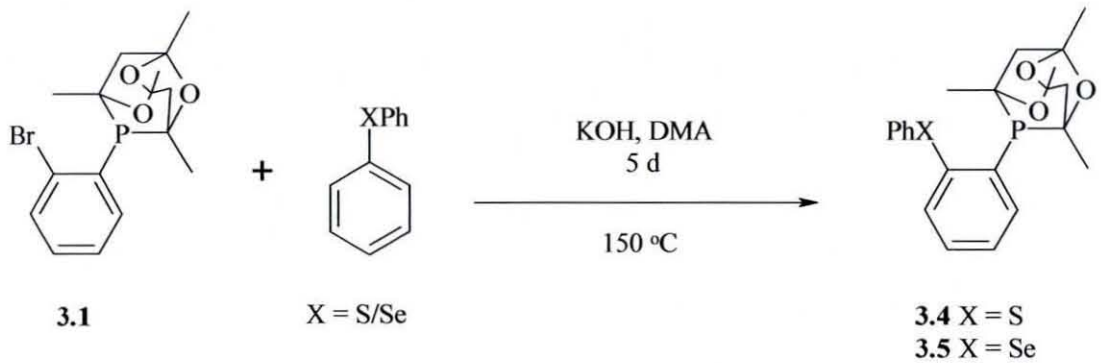

3.1 X = S/Se **3.4** X = S **3.5** X = Se

Equation 3.1 - Preparation of *o*-C_6H_4(SPh)(PAd) and *o*-C_6H_4(SePh)(PAd), compounds **3.4** - **3.5**

As for **2.1** and **2.16**, **3.1** was reacted with thiophenol and phenylselenol in dimethylacetamide to give **3.4** and **3.5** as a white solid in reasonable yield (56 and 40% respectively) (Equation 3.1). To our knowledge, these are the first examples of ligands to contain both chalcogenide and phospha-adamantane moieties. Both products were characterised by $^{31}P\{^{1}H\}$ NMR spectroscopy. Compound **3.4** gave a single peak at δ(P) –37.7 ppm, whilst **3.5** gave a similar signal at δ(P) –34.7 ppm. These are significantly different to **2.1** and **2.16**, both based on aromatic phosphines, which gave peaks at δ(P) –12 and –9 ppm respectively.

Crystals of compound **3.5** suitable for X-ray crystallography were grown by vapour diffusion of Et_2O into a $CDCl_3$ solution. The results confirmed the identity of **3.5** and are shown in Figure 3.3 and Table 3.4. As can be seen in Figure 3.3, the bulky phospha-adamantane group points in the opposite direction to the selenide, though separation of P(1) and Se(1) [3.230 Å] is extremely similar to that observed for **3.1**. Once again, the intracage angle about the phosphorus atom in the phospha-adamantane group is smaller than that for complex containing **3.5** [92.43(14)].

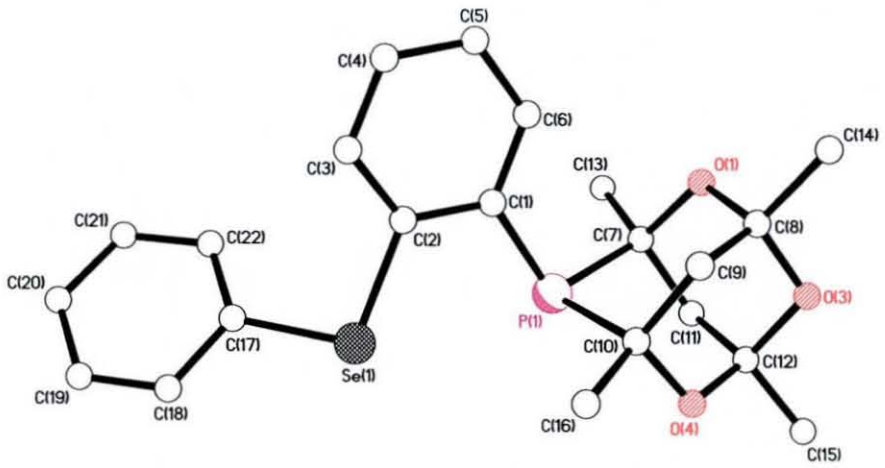

Figure 3.3 – X-ray structure of **3.5**

Bond Lengths (Å)		**Bond Angles (°)**	
C(1)–P(1)	1.845(3)	C(1)–P(1)–C(7)	106.71(14)
C(2)–Se(1)	1.925(3)	C(1)–P(1)–C(10)	103.35(14)
Se(1)–C(17)	1.931(3)	C(7)–P(1)–C(10)	92.43(14)
		C(1)–C(2)–Se(1)	119.6(2)
		C(3)–C(2)–Se(1)	119.7(2)

Table 3.4 - Selected bonds lengths and angles for **3.5**

3.1.2 – Complexes of ligands 3.1-3.5

Complexes containing the cytop-based ligands **3.1–3.5** were prepared readily using standard transition metal precursors. Initially, when using $PdCl_2(cod)$ as with ligands described in Chapter One, no coordination was observed, presumably as a result of a combination of the rate of dissociation of the cycloocta–1,5–diene group being too

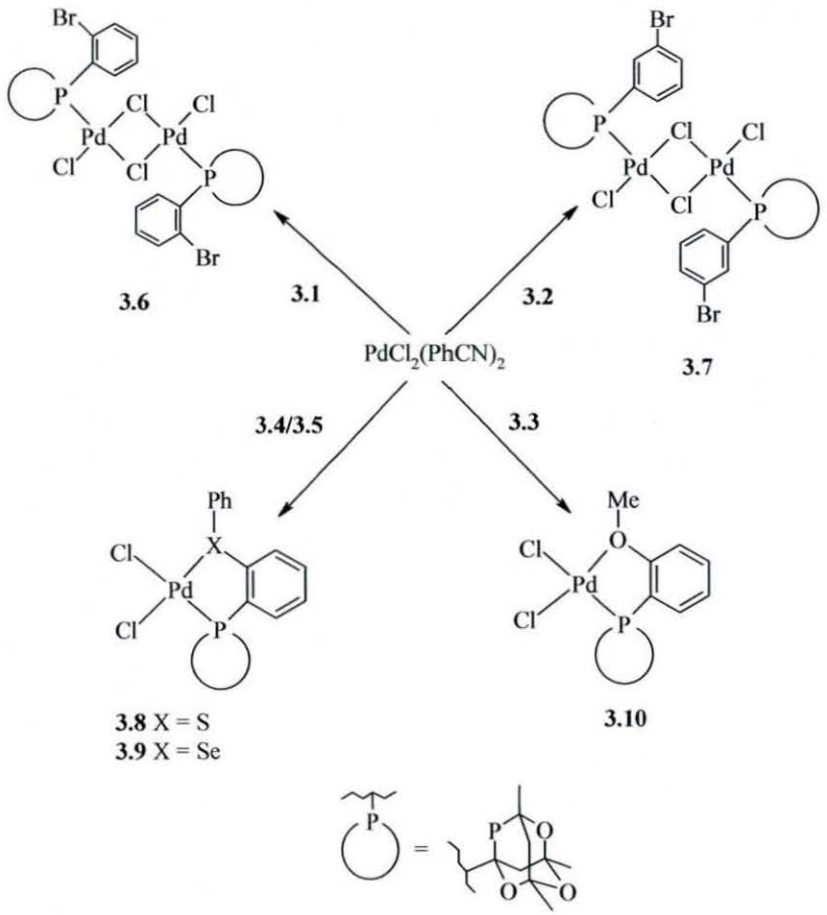

Scheme 3.2 – Preparation of complexes **3.6 – 3.10**

slow, and the steric bulk of the ligand. As a result, the more labile $PdCl_2(PhCN)_2$ was used as the palladium based metal starting material, thereby increasing the possibility of coordination of the ligand. The reactions attempted are shown in Scheme 3.2.

Firstly, *o*-C_6H_4Br(Cytop) **3.1** was reacted with $PdCl_2(PhCN)_2$ with both compounds in CH_2Cl_2 as with previous complexation reactions. After stirring for 4 h, a bright yellow solid was obtained, which gave a slightly different $^{31}P\{^1H\}$ NMR spectrum to that expected. The two peaks at δ(P) 1.3 & 2.8 ppm gave three possibilities; either a dimer had formed, the peaks being two singlets due to the two

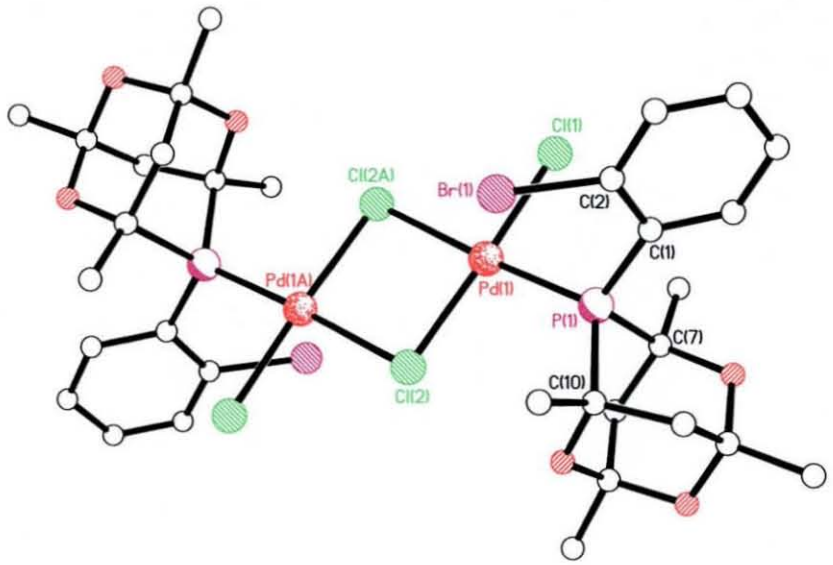

Figure 3.4 – X-ray structure of **3.6**

Bond Lengths (Å)		Angles (°)	
Pd(1)–P(1)	2.2423(12)	P(1)–Pd(1)–Cl(1)	87.24(5)
Pd(1)–Cl(1)	2.2863(12)	P(1)–Pd(1)–Cl(2)	97.71(4)
Pd(1)–Cl(2)	2.3401(12)	P(1)–Pd(1)–Cl(2A)	176.70(4)
Pd(1)–Cl(2A)	2.4226(12)	Cl(1)–Pd(1)–Cl(2)	174.04(4)
C(2)–Br(1)	1.898(5)	Cl(1)–Pd(1)–Cl(2A)	90.09(4)
		Cl(2)–Pd(1)–Cl(2A)	85.06(4)
		Pd(1)–Cl(2)–Pd(1A)	94.94(4)
		C(7)–P(1)–C(10)	93.90(2)

Table 3.5 - Selected bonds lengths and angles for **3.6**

possible stereoisomers of the cytop fragment, or the possible anti- and syn-arrangements of the ligand in the dimer. A third possibility was that two ligands had coordinated to the metal centre, forming *trans*-$PdCl_2\{C_6H_4Br(Cytop)\}_2$. The latter of these was quickly ruled out due to the stoichiometries of starting materials used. Also, the infra-red spectrum of the product contained two Pd–Cl stretches at 248 and 265 cm^{-1} which would be a single stretch if the product were *trans*-

$PdCl_2\{C_6H_4Br(Cytop)\}_2$, and the NMR peak would be a doublet. Crystals suitable for X-ray analysis were grown from CH_2Cl_2/Et_2O vapour diffusion and this confirmed the structure to be the dimer $[PdCl_2\{1,2\text{–}C_6H_4Br(Cytop)\}]_2$ **3.6**, shown in Figure 3.4. The coordination sphere of Pd(1) consists of three chloride groups, two of which bridge to a second Pd(II) centre, and the phosphorus donor atom of the adamantane group. One of the bridging chloride groups is part of half of the molecule shown by symmetry generation. As seen in Table 3.5, Pd(1)–Cl(2A) (*trans*– to the coordinated phospha–adamantane) is over 0.8 Å longer than Pd(1)–Cl(2); this is in contrast to other known complexes containing Pd(II)/Pt(II), phospha-adamantanes and chloride co-ligands.[134] The distance between P(1) and Br(1) stays almost exactly the same as for **3.1** despite the ligand being part of a complex [3.342 Å]. Also the Pd-Br separation calculated [3.353 Å] indicates that there is little chance of any significant interactions between the metal centre and halide.

$PdCl_2\{C_6H_4(SPh)(Cytop)\}$ was prepared using **3.8** and $PdCl_2(PhCN)_2$, both dissolved in CH_2Cl_2. The product was isolated as a yellow solid, and gave the characteristic change in chemical shift for a coordinated phosphine in the $^{31}P\{^1H\}$ NMR spectrum, moving from δ(P) –12 ppm to 48 ppm. This downfield shift is in accordance with five-membered chelate ring formation. The ^1H NMR spectrum showed the expected multiplets in the aromatic and adamantane regions (7.3–8.4 ppm and 1.2–2.2 ppm respectively), whilst FAB^+ mass spectrometry carried out on **3.8** showed peaks at *m/z* 543 (M^+ –Cl) and a fragmentation pattern containing ligand **3.3** at *m/z* 404. Elemental analysis results showed excellent concordance with those expected, and can be seen in the experimental section.

Compound **3.9** exhibited many of the same chemical properties as **3.8**. The $^{31}P\{^1H\}$ spectrum showed a peak at δ(P) 46 ppm, though this was a doublet. A number of the complexes prepared containing phospha-adamantane groups gave doublets in the $^{31}P\{^1H\}$ NMR spectrum; whilst **3.8** showed a rather broader peak, a small amount of splitting could be seen at the top of the peak which would give a doublet. As with **3.8**, **3.9** gave multiplets for the adamantane and aromatic groups.

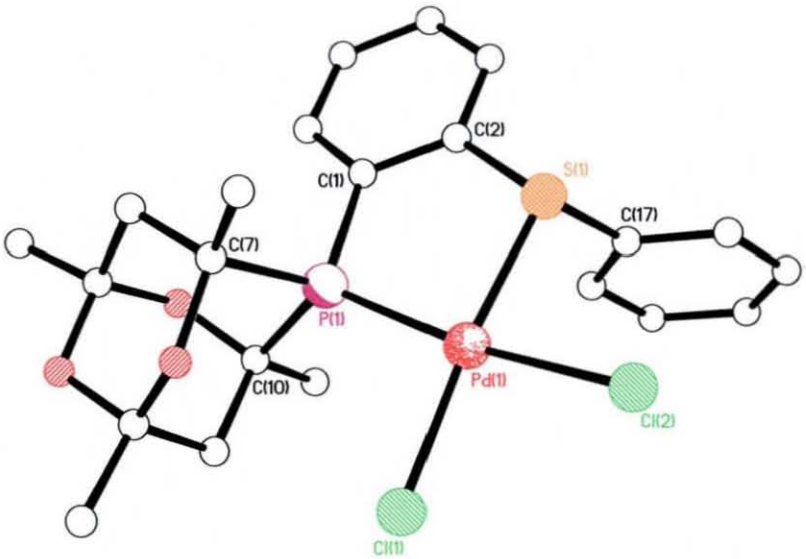

Figure 3.5 - X-ray structure of **3.8**; All hydrogen atoms and solvent molecules have been removed for clarity

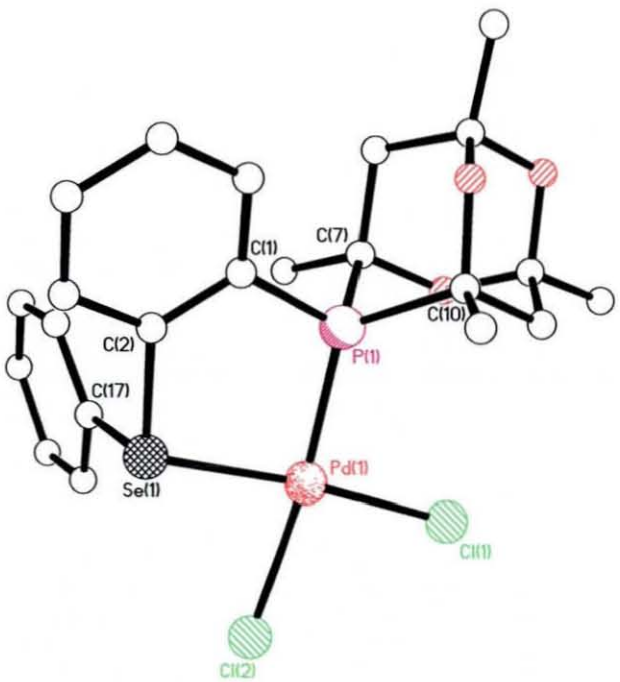

Figure 3.6 – X-ray structure of **3.9**; All hydrogen atoms and solvent molecules have been removed for clarity

	3.8 X = S	**3.9** X = Se
Pd(1)–P(1)	2.2556(8)	2.2615(4)
Pd(1)–X(1)	2.2590(9)	2.3656(2)
Pd(1)–Cl(1)	2.2990(9)	2.3180(5)
Pd(1)–Cl(2)	2.3631(8)	2.3506(4)
Cl(1)–Pd(1)–P(1)	97.04(3)	98.800(17)
Cl(2)–Pd(1)–P(1)	171.73(3)	172.479(17)
P(1)–Pd(1)–X(1)	88.39(3)	87.902(12)
Cl(1)–Pd(1)–Cl(2)	90.25(3)	88.709(18)
Cl(1)–Pd(1)–X(1)	174.00(4)	172.533(14)
Cl(2)–Pd(1)–X(1)	84.51(3)	84.577(14)

Table 3.6 - Selected bonds lengths (Å) and angles (°) for **3.8** and **3.9**

Crystals of **3.8** and **3.9** suitable for X-ray analysis were grown by vapour diffusion of diethyl ether into CH_2Cl_2 solutions of the complexes. The results are shown in Figures 3.5 and 3.6, and selected bond lengths and angles shown in Table 3.6. Both of these x-ray analyses confirm the phosphine-chalcogenide ligands to have chelated to the Pd metal centre in a similar fashion. As expected, the Pd-X (where X = S/Se) distance is slightly larger for **3.9** (2.366(2) Å compared to 2.259(9) Å for **3.8**). Other bond lengths are extremely similar, generally within 0.1 Å. Angles for both **3.8** and **3.9** show the Pd(II) centre to be in a distorted square planar environment. However, in comparison to complexes containing less bulky phosphine groups, the angles involving P(1) are heavily distorted away from ideal angles for square planar geometry. For example, the angle involving the phosphorus atom and the corresponding *trans*- group is markedly different for **3.8** and **3.9** (171.73(3) and 172.479(17) respectively) to the comparable angles for **8** and **9** in Chapter One (179.07(2) and 177.11(4) respectively). This is to be expected, as the strain enforced on the chelate ring for **3.8** and **3.9** due to the presence of the adamantane group is substantial compared to that for the smaller aromatic phosphines investigated previously. Angles involving Cl(1) are generally more distorted from the ideal for **3.9** than **3.8**, showing that the combined effects of the larger phosphine and chalcogenide groups greatly distorts angles all around the coordination sphere of the Pd(II) centre.

$PdCl_2(PhCN)_2$ was also reacted with a stoichiometric amount of the potentially bidentate ligand *o*–$(OMe)C_6H_4$(cytop) **3.3** to see if this would P,O-chelate, as for the

chalcogenide containing ligands **3.4** and **3.5** or form a dimer, as observed when using **3.1** and **3.2**. Two singlets were observed in the $^{31}P\{^{1}H\}$ NMR spectrum, at δ(P) 13.7 and 14.2 ppm, slightly further downfield from signals when the bromo-adamantanes **3.1** and **3.2** were used. This suggested that **3.3** had chelated to the metal centre, backed up by the observation that the OMe signal in the ^{1}H NMR spectrum shifted slightly further downfield to δ(H) 4.4 ppm. Elemental analysis also suggested that compound **3.10** (Scheme 3.2) was formed. Numerous attempts were made to prepare crystals suitable for X-ray analysis, however these proved unsuccessful.

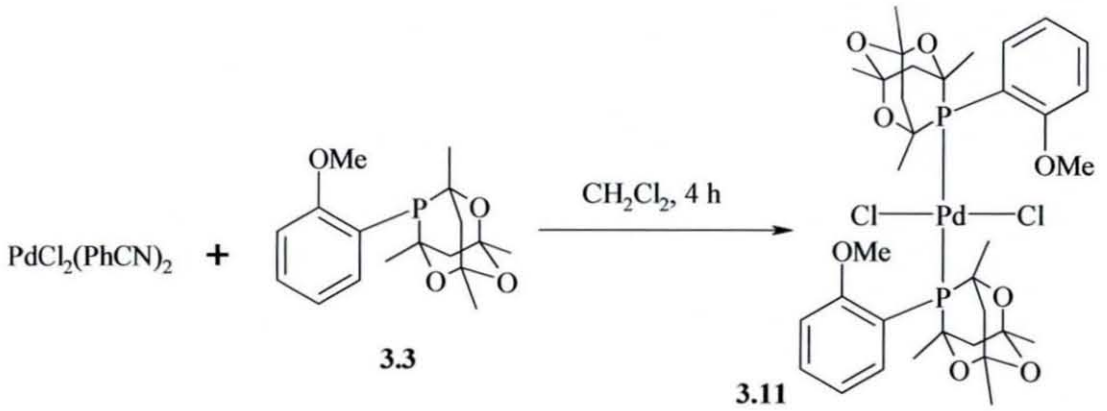

Equation 3.2 - Preparation of $PdCl_2\{o\text{-}C_6H_4(OMe)(PAd)\}_2$, **3.11**

Using an identical method as for **3.10**, two equivalents of **3.3** were added to a CH_2Cl_2 solution of $PdCl_2(PhCN)_2$, to establish if the bis-phosphine product **3.11** could be prepared, as shown in Equation 3.2. The bright yellow solid was isolated in good yield (75%) and characterised via methods used previously. The $^{31}P\{^{1}H\}$ NMR gave a very similar peak pattern to that observed for **3.10**. However these signals came further upfield at δ(P) –4 ppm, in the same region for dimers **3.6** and **3.7** which contain non-chelating phosphine ligands. ^{1}H NMR results are concordant with those expected; in comparison to **3.10**, the OMe signal stays at around δ(H) 3.9 ppm, much closer to the value for the free ligand, where the methoxy group is also unchelated. Elemental analysis results also match those expected when calculated for the presence of one molecule of CH_2Cl_2, as this solvent can be seen in the ^{1}H NMR spectrum as well.

Crystals of **3.11** suitable for X-ray diffraction were grown by layering of pet. ether (60-80°C) onto a CH_2Cl_2 solution of the complex. The structure of **3.11** is shown in Figure 3.7 and selected bond lengths and angles in Table 3.7. The full molecule of **3.11** is made by symmetry generation of the PdCl(**3.3**) fragment. The coordination sphere of **3.11** consists of two coordinated phosphorus atoms situated *trans*- to each other, and two chloride groups. The two Pd–P bond lengths shown in Table 3.5 [2.3382(18) Å] are larger than those observed for all complexes prepared in Chapter Two and in this chapter by around 0.1 Å, but are very close to those observed for *trans*-bisphosphine complexes prepared previously.[135]

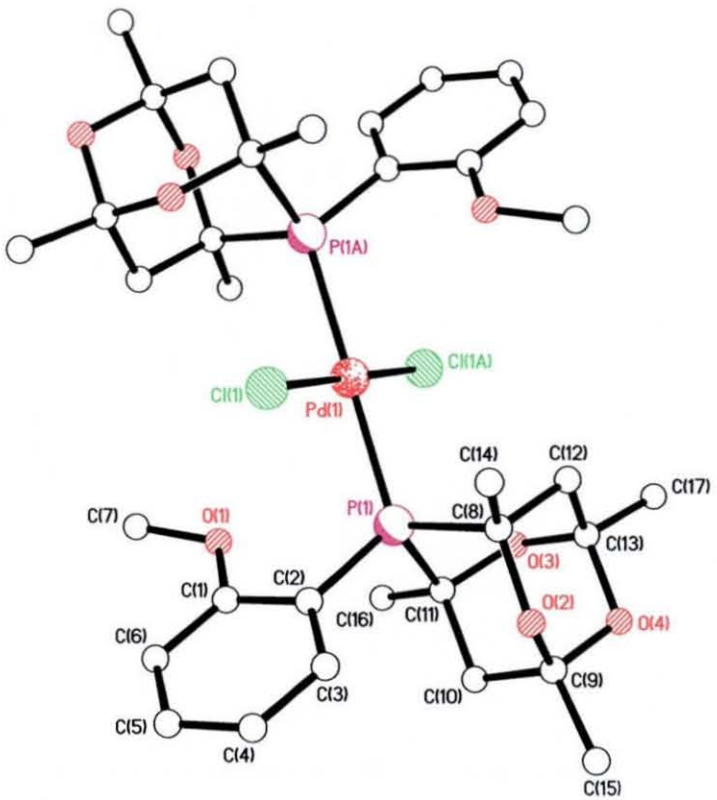

Figure 3.7 – X-ray structure of **3.11**

Bond Lengths (Å)		**Angles (°)**	
Pd(1)–P(1)	2.3382(18)	Cl(1)–Pd(1)–P(1)	92.90(7)
Pd(1)–Cl(1)	2.3013(19)	Cl(1)–Pd(1)–P(1')	87.10(7)
C(1)–O(1)	1.359(10)	Cl(1')–Pd(1)–P(1)	92.90(7)

Table 3.7 - Selected bonds lengths and angles for **3.11**

3.2 – CHEMISTRY OF $Ph_2P(CH_2)_2PAd$, 3.12

3.2.1 – Preparation of 3.12

The ligand $Ph_2P(CH_2)_2$Cytop **3.12** was prepared using a similar radical reaction to that employed for the alkyl-based ligands prepared in Chapter Two. In this example a secondary phosphine radical was formed by reaction of **1.113** with AIBN instead of the thiol analogue. After removal of volatile residues from the solvent-free reaction, **3.12** (shown in Equation 3.3) was formed reproducibly in good yield (82%) as a transparent colourless wax, and the purity of **3.12** shown by $^{31}P\{^1H\}$ NMR was also very high each time the ligand was reproduced. The $^{31}P\{^1H\}$ NMR pattern showed two doublets, at δ(P) –24 ppm (corresponding to the cytop phosphorus centre) and δ(P) –12 ppm (due to PPh_2), split due to coupling between the two inequivalent phosphorus centres. These data, along with $^{31}P\{^1H\}$ NMR spectroscopy data for other ligands prepared is summarised in Table 3.6. **3.12** also proved to be extremely air stable, even in solution. The $^{31}P\{^1H\}$ NMR spectrum was carried out after 24 h using the same $CDCl_3$ solution, showing no evidence of further oxidation, and even after 2 weeks very little oxidation was observed.

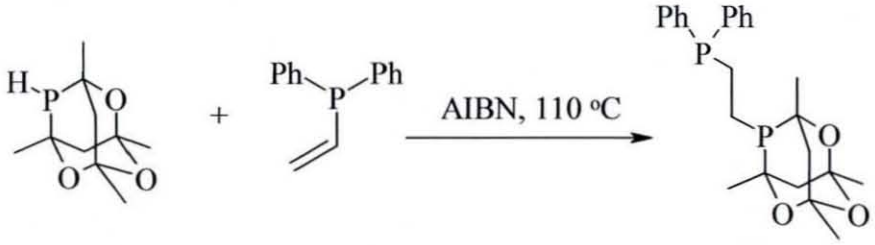

1.113 **3.12**

Equation 3.3 - Preparation of $Ph_2P(CH_2)_2PAd$, **3.12**

The ^1H NMR spectrum also gave evidence that the diphosphine had been formed. Not only did the phospha-adamantane give the characteristic four singlets and a doublet, and the aromatic fragment give the expected multiplet in the range δ(H) 7.25-7.45 ppm, but also only an extremely small trace of vinyldiphenylphosphine is noticeable between δ(H) 5.5-6.0 ppm. As the method does not require any major work-up procedure, it is likely that any significant amounts of unused vinyldiphenylphosphine would stay in the reaction vessel and therefore would be observed in the ^1H NMR spectrum.

$^{13}C\{^{1}H\}$ NMR spectroscopy gave further evidence that **3.12** had been formed. As can be seen in Figure 3.8, coupling of carbon atoms to the two phosphorus centres, along with magnetic interactions within the molecule give the spectrum observed. For example, the methyl carbon atoms labelled C_d give two doublets around δ(C) 26 and 28 ppm, due to their close proximity to the phosphorus atom. The two quaternary

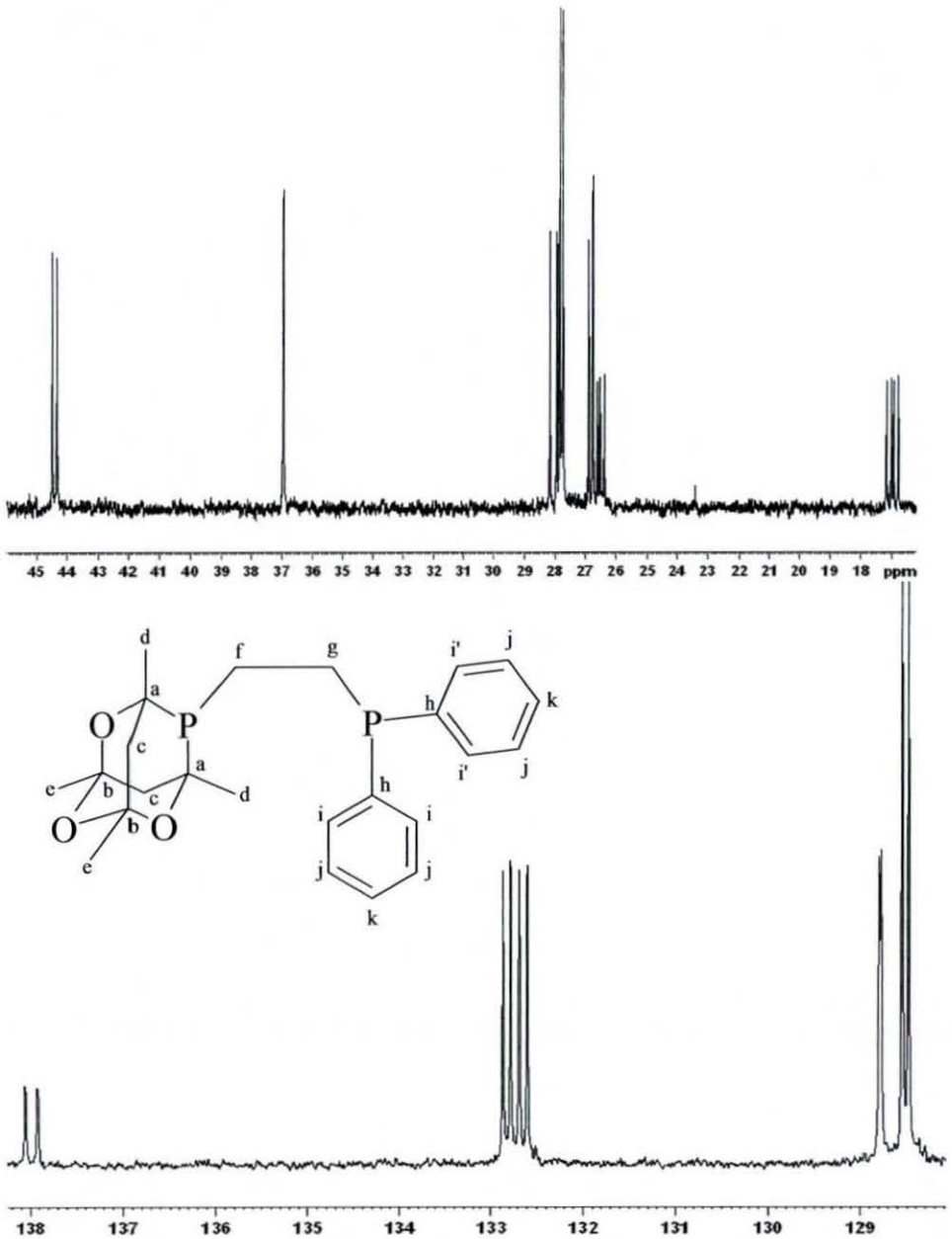

Figure 3.8 – ^{13}C NMR spectra of $Ph_2P(CH_2)_2PAd$, **3.12**

carbon atoms labelled C_a are observed as a doublet at δ(C) 96 ppm [J(CP) 142 Hz], whilst the doublet due to the other two quaternary carbon atoms C_b are further upfield (δ(C) 72 ppm), and show a much smaller coupling with the phosphorus atom [*J*(CP) 35 Hz]. The aromatic region of the $^{13}C\{^{1}H\}$ NMR spectrum shows coupling between

the phosphorus centre and the various aromatic carbon atoms. The quaternary carbon atoms denoted C_h are observed as a doublet [*J*(CP) 20.9 Hz] due to coupling with the phosphorus centre, shifted slightly further downfield than the rest of the peaks between δ(C) 137.9 and 138.1 ppm. The carbon atoms given the symbol C_i in Figure 3.8, however, give a doublet of doublets between 132.6 and 132.9 ppm [*J*(CP) 12.9 Hz]. The two carbon atoms denoted C_k give a very poorly resolved doublet at 128.8 ppm [*J*(CP) 3.22], the small value being due to the four bond distance between the two atoms. The four carbon atoms C_j give a much larger doublet at around 128.5 ppm [*J*(CP) 11.3 Hz]. Rapid rotation around the C_g-P bond may help explain the splitting of C_i into two doublets. This facile movement means that the carbon atoms of each different aromatic ring are different distances from the phosphaadamantane cage. The atoms with symbol C_i, being at the top of the phenyl ring, are brought in closer contact with the adamantane cage. This effect is less pronounced for atoms labelled C_j, as they are further down the phenyl ring. The four carbon atoms are in the same environment, hence only coupling with the phosphorus centre gives the doublet observed. This magnetic effect is even less pronounced for C_k. Splitting of the peak is hardly visible and any splitting is solely due to minimal interactions with the PPh_2 phosphorus atom. Elemental analysis data gave further evidence that the assignment of the product as **3.12** was correct, and can be seen in the experimental section.

Table 3.8 – Selected $^{31}P\{^1H\}$ NMR spectroscopy data for compounds **3.12-3.22**[a]

	δ(P) / -PPh_2	δ(P) / -PAd	^3J(PP)	^2J(PP)	J(PtPPh_2)	J(PtPAd)
3.12	-12.0	–24.0				
3.13	66.0	61.0		8		
3.14	51.5	40.2		10	1663	1687
3.15	45.4				1794	
3.16	-40.4				1434	
3.17	25.0	–26.0	36			
3.18	30.5	22.3	47			
3.19	24.0, 25.0	9.5, 16.0	71, 62			
3.20	23.6, 24.0	2.5, 3.1				1694
3.21a	30.5	–25.0				
3.21b	48.2[b], 56.8	62.5[b], 63.9		16, 24[b]		
3.22	-1.5	–25	42			

[a] Chemical shifts in ppm, coupling constants in Hz. [b] Values for minor species in mixture of chelate complexes

3.2.2 – Transition metal complexes of 3.12

3.2.2.1 – Pd(II) and Pt(II) complexes of 3.12

A number of complexes were prepared with **3.12**. This was carried out to establish whether the binding modes of the diphosphine would be affected by the size of the phospha-adamantane group, such as whether chelation to metal centres would occur, or whether the formation of complexes carrying pendant phospha-adamantane groups could lead to the preparation of homo- and heterobimetallic complexes.

Stirring a stoichiometric amount of compound **3.12** with $PdCl_2(PhCN)_2$ in CH_2Cl_2, followed by work-up using Et_2O gave complex **3.13** in good yield (76%) as a bright yellow solid. Two doublets were observed in the $^{31}P\{^1H\}$ NMR spectrum due to the two inequivalent nuclei. As expected, these shifted much further downfield compared to **3.12** due to five-membered chelation of **3.12** to the metal centre, to δ(P) 61 and 66 ppm. The infra red spectrum of **3.13** showed all of the expected peaks, though the region where metal-chloride stretches may be expected to be seen was

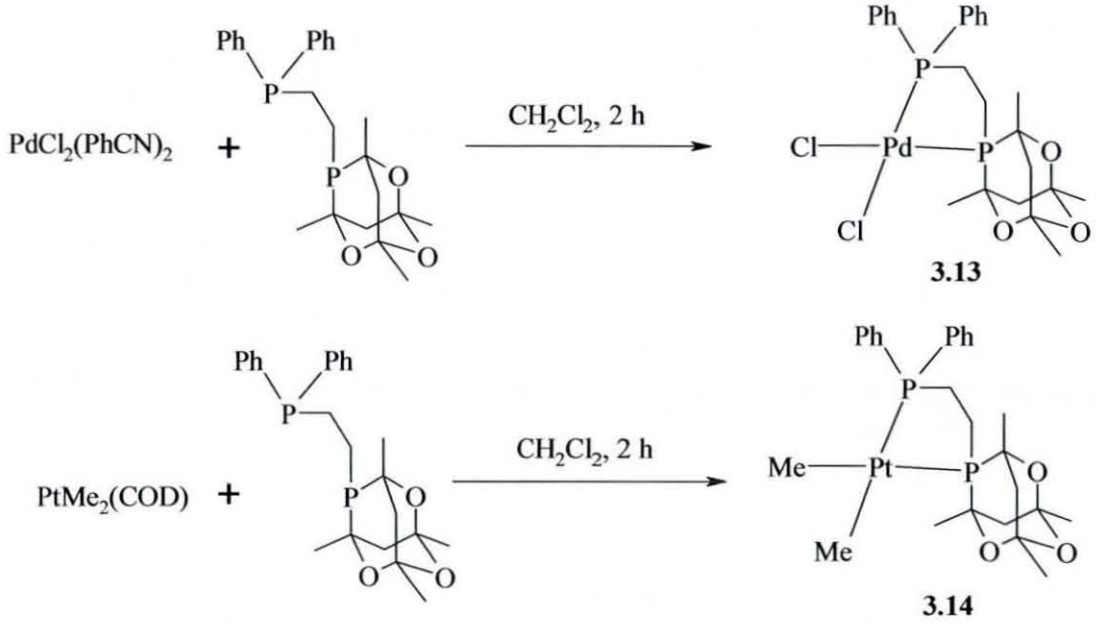

Scheme 3.3 – Preparation of complexes **3.13** and **3.14**

rather complicated. Peaks due to C-O groups in the cytop fragment (at 1212 and 1135 cm^{-1}), C-P (1435 and 1377 cm^{-1}) and CH_3 groups (3040 cm^{-1}) could be observed, however.

Compound **3.12** was also reacted with $PtMe_2(cod)$ to give $PtMe_2$(**3.12**), **3.14**. Purification of **3.14** involved taking the volume of the initial suspension to *ca.* 2-3 cm^3 and addition of petroleum ether (60-80 °C, 50 cm^3), to leave the cyclooctadiene in solution. Two signals were observed in the $^{31}P\{^1H\}$ NMR spectrum of **3.14** at δ(P) 40.2 and 51.5 ppm, these corresponding to the diphenylphosphine and phosphaadamantane groups respectively. As expected, ^{195}Pt satellites were also distinguishable, with ^1J(Pt–P) couplings of 1663 Hz and 1687 Hz respectively. These values are in agreement with those for platinum complexes containing diphosphine ligands *trans*– to methyl groups prepared previously.[136]

Crystals of **3.14** suitable for X-ray diffraction were grown by layering a $CHCl_3$ solution with pet. ether (60-80 °C). One molecule of $CHCl_3$ is contained in the asymmetric unit. The X-ray structure of **3.14** is shown in Figure 3.9 and the important data given in Table 3.9. The coordination sphere of the Pt(II) centre contains two phosphorus donor atoms in a *cis*-configuration, and is completed with two chloride ligands. As can be seen from Table 3.9, these four donor atoms are arranged in a heavily distorted square planar environment, with the four angles expected to be to 90° ranging between 83.9(3)° and 97.25(18)°. This is due to a combination of the size of the phospha-adamantane fragment, the large size of the Pt(II) centre and the strain put on the molecule by the ethane backbone. The corresponding range of bond lengths and angles reported for $PtMe_2\{(Ph_2P)_2CH_2CH_2\}$ **3.15** (also shown in Table 3.6) and $PtMe_2\{(Me_2P)_2CH_2CH_2\}$ **3.16**[137] are considerably different to those for **3.14**. The extremely small C–Pt–C angle [83.9(3)°] in **3.14** is presumably due to the strain put on the molecule by the phospha-adamantane group, and means that when comparing **3.14** and **3.15**, the remaining angles are markedly different. The two Pt(1)–P distances in **3.14** are extremely similar, and are slightly longer than those reported for **3.15** [2.246(2) and 2.254(2) Å].

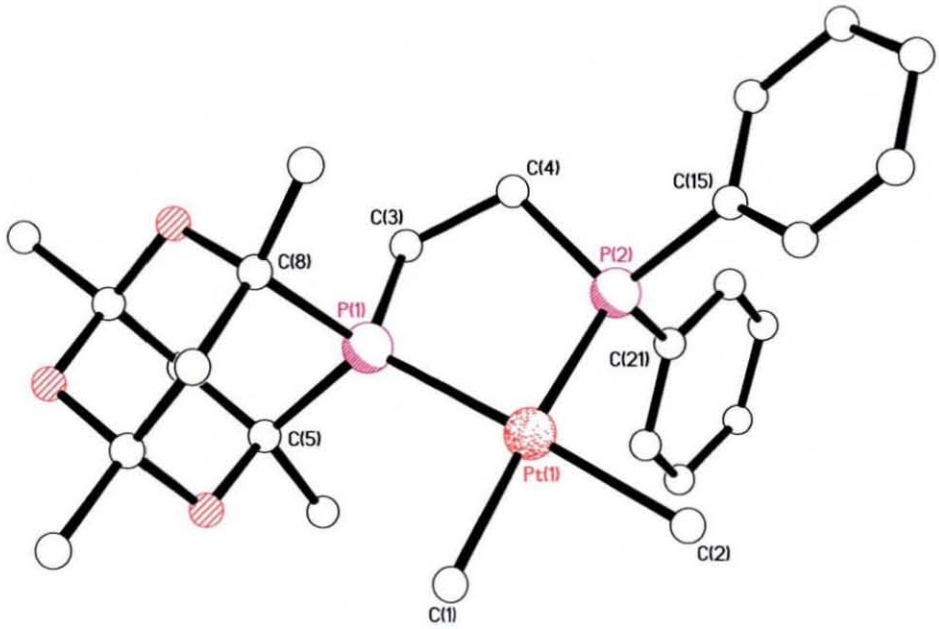

Figure 3.9 – X-ray structure of **3.14**. All hydrogen atoms and solvent molecules omitted for clarity.

Bond Lengths (Å)			**Bond Angles (°)**		
	3.14	**3.15**		**3.14**	**3.15**
Pt(1)–P(1)	2.271(19)	2.246(2)	P(1)–Pt(1)–P(2)	85.73(7)	86.01(7)
Pt(1)–P(2)	2.277(17)	2.254(2)	C(3)–Pt(1)–P(1)	92.90(2)	94.30(2)
Pt(1)–C(3)	2.109(7)	2.108(7)	C(4)–Pt(1)–P(2)	97.25(18)	93.20(2)
Pt(1)–C(4)	2.136(6)	2.112(6)	C(3)–Pt(1)–C(4)	83.90(3)	86.60(3)
			C(4)–Pt(1)–P(1)	176.42(18)	177.50(2)
			C(3)–Pt(1)–P(2)	172.40(3)	176.60(2)

Table 3.9 - Selected bonds lengths and angles for **3.14** and $PtMe_2\{(Ph_2P)_2CH_2CH_2\}$[137] (**3.15**)

The effect of the steric bulk of the phospha-adamantane fragment is shown by the 'twisting' of the ethylene backbone to accommodate both phosphorus donor atoms around the metal centre. This is shown in Figure 3.10. The plane of the donor atoms coordinated to the metal centre can be seen, with the *ipso* carbons of the phenyl rings on the furthest visible phosphorus atom. The 'crossing' of the P(1)–C(3)/P(2)–C(4) bonds in Figure 3.10 give a visible indication of distortion of the ethylene backbone. The mean deviation of the ethylene backbone from the P(1)–Pt(1)–P(2) plane in **3.14**

[0.185 Å] confirms that there is significant distortion; this is larger than the values for the 5–membered chelate complexes **3.8** and **3.9** [0.001 and 0.011 Å respectively].

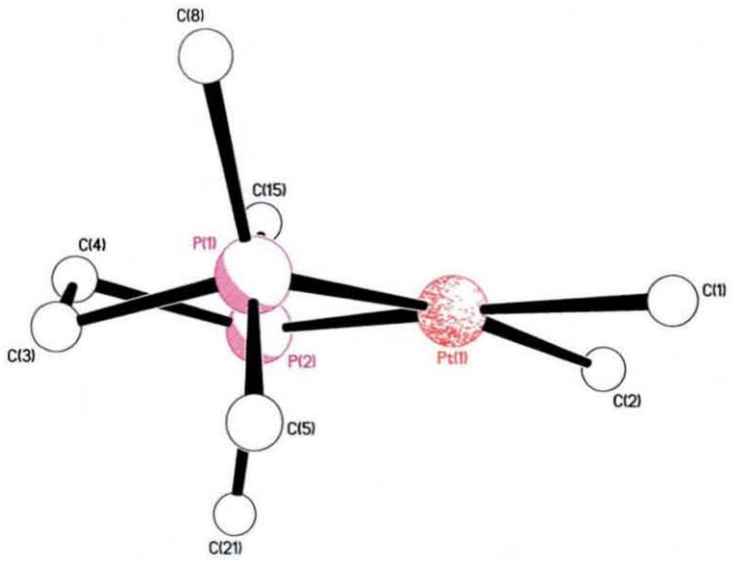

Figure 3.10 – 'Twisting' of the 5–membered chelate ring in **3.14;** adamantane group and phenyl rings simplified for clarity

3.2.2.2 – Ru complexes containing $Ph_2P(CH_2)_2PAd$ 3.12

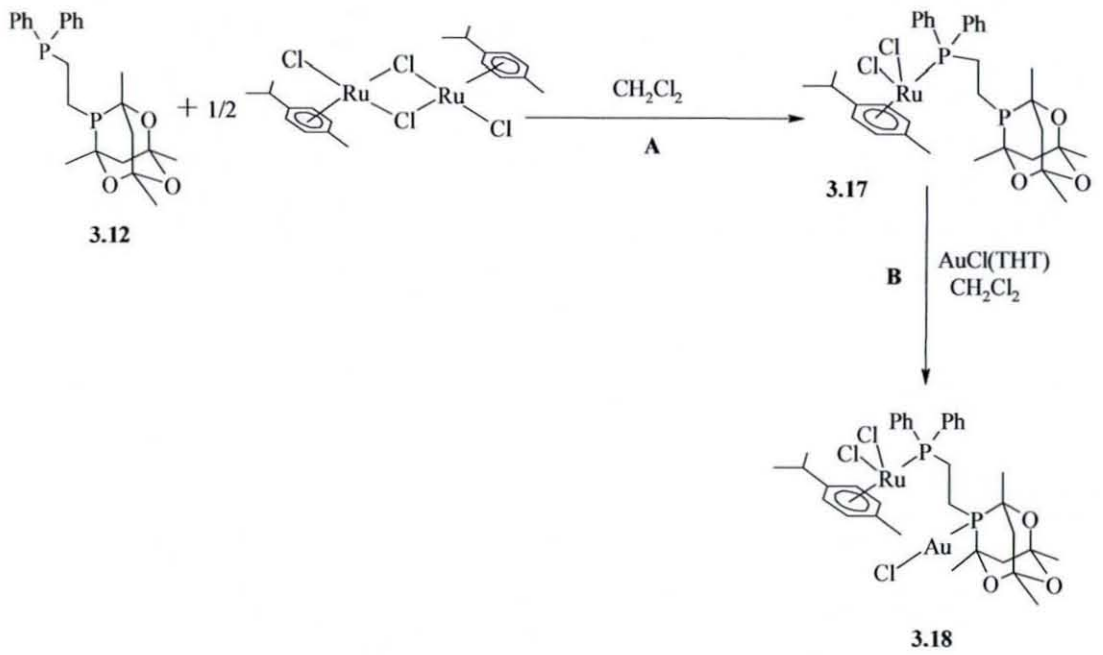

Scheme 3.4 – Preparation of complexes **3.17** and **3.18**

The capacity of **3.12** to form complexes with slightly harder transition metals was tested by reaction with some Group VIII and IX metals. The preparation of compounds containing Ru–P bonds, formed by cleavage of Ru–Cl–Ru dimers has been widely reported,[138,139] indeed the formation of complexes containing Ru(II) centres and diphosphine ligands with pendant phosphine arms has very recently been observed by Dyson *et al.*[140] Two equivalents of diphosphine **3.12** were reacted with $\{RuCl_2(p\text{-cymene})\}_2$ to see if one or both of the phosphorus donor atoms would coordinate to the metal centre, as indicated in Scheme 3.4. The resulting complex was $\{RuCl_2(p\text{-cymene})(\mathbf{3.12})\}$ **3.17**. As seen in Figure 3.11, the $^{31}P\{^1H\}$ NMR of the bright orange solid **3.17** showed one doublet at δ(P) –26 ppm, corresponding to an uncoordinated phospha-adamantane fragment, and one doublet at δ(P) 25 ppm, thus corresponding to the PPh_2 group coordinated to the metal centre. This was expected, as breaking of the Ru–Cl–Ru bridge, leaving one obvious coordination site would most probably lead to coordination of the PPh_2 group over the more bulky phospha-adamantane fragment. A small amount (around 6%) of a further species was present in the NMR spectrum as two doublets at δ(P) 16 and 31 ppm, possibly due to the cleavage of a further Ru–Cl bond and formation of an ionic chelated P–Ru–P species,

containing one coordinated chloride group and one chloride group as an anion. Further heating of **3.17** to attempt to give just the ionic species proved unsuccessful, suggesting that the energy needed to coordinate the bulky cytop group is too large.

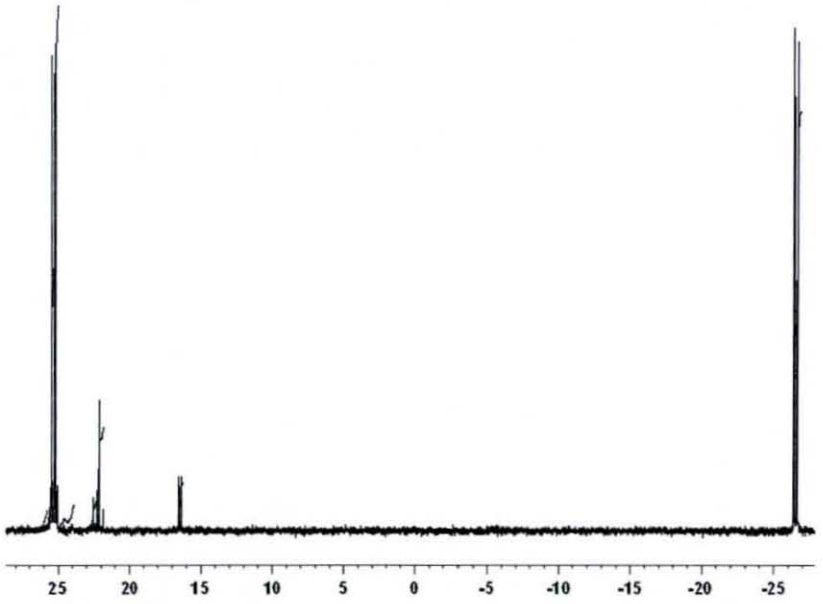

Figure 3.11 - $^{31}P\{^{1}H\}$ NMR spectrum of $RuCl_2$(*p*-cymene)(**3.12**), **3.17**

Crystals of **3.17** suitable for X-ray analysis were grown by slow diffusion of hexanes into a CH_2Cl_2/MeOH solution. The structure of **3.17** and data from the X-ray experiment can be seen in Figure 3.12 and Table 3.10. The phospha-adamantane fragment, is left uncoordinated to the metal centre while the diphenylphosphine end of **3.12** is coordinated to the ruthenium. The coordintation sphere of the ruthenium, completed by two chloride groups and the η^6-*p*-cymene group, adopts a distorted 'piano stool' geometry. The Cl–Ru–Cl and P–Ru–Cl angles are all slightly less than 90°, whilst the 'intracage angle' formed between phospha-adamantane phosphorus atom and the two cage carbon atoms directly attached [92.2°(14)] is as small as that observed for ligands previously prepared in Section 3.1.1.

Due to the free phospha-adamantane fragment in **3.17**, it was realised this had potential to act as a ligand in further reactions. **3.17** was reacted with AuCl(THT) (THT = tetrahydrothiophene) in CH_2Cl_2 for 4 h as shown in reaction **B**, Scheme 3.4. The reaction gave {$RuCl_2(\eta^6$-*p*-cymene)(**3.17**)(AuCl)} **3.18** in good yield (72%), which is an extremely rare example of a heterobimetallic complex of a phospha-adamantane-containing ligand.[134] The $^{31}P\{^{1}H\}$ NMR spectrum of **3.18** contains two

doublets at δ(P) 22.3 and 30.5 ppm, with very few residual peaks from starting materials or side products. Elemental analysis confirmed the assignment of **3.18**, the results of which can be seen in the experimental section.

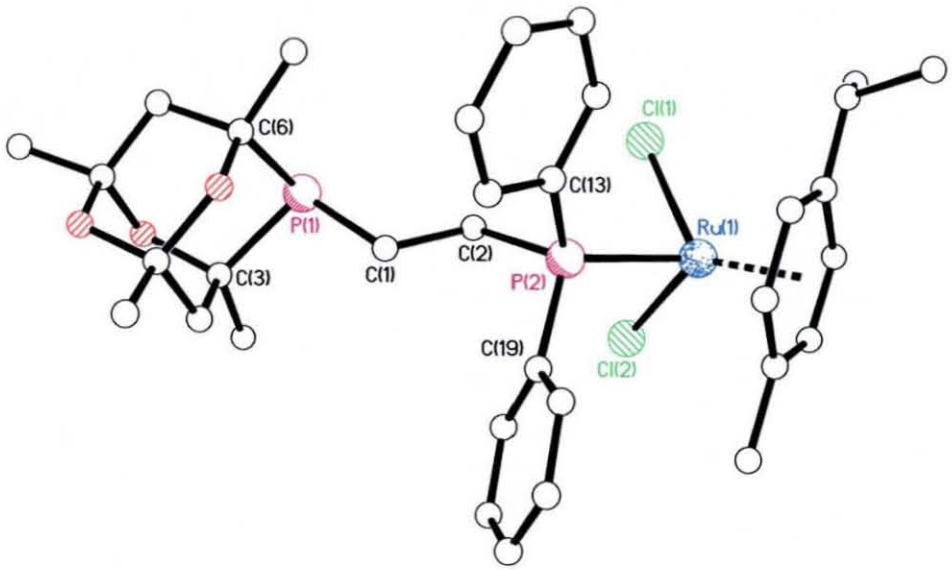

Figure 3.12 – X-ray structure of **3.17**

Bond Lengths (Å)		Bond Angles (°)	
Ru(1)–P(2)	2.3347(6)	Cl(2)–Ru(1)–P(2)	85.48(2)
Ru(1)–Cl(2)	2.4085(6)	Cl(1)–Ru(1)–P(2)	86.42(2)
Ru(1)–Cl(1)	2.4110(6)	Cl(1)–Ru(1)–Cl(2)	85.54(2)
		Ru(1)–P(2)–C(2)	116.18(8)
		C(3)–P(1)–C(6)	92.23(14)

Table 3.10 - Selected bonds lengths and angles for **3.17**

Crystals of **3.18** suitable for X-ray diffraction were grown from a CH_2Cl_2 solution with Et_2O and pet. ether (60-80 °C). The structure of **3.18** and data derived from the X-ray experiment are shown in Figure 3.13 and Table 3.11. The Ru(II) centre, as expected, is coordinated to the less bulky diphenylphosphine fragment of **3.18**, with the coordination sphere completed by two chloride groups and an η^6-*p*-cymene group. The Ru(II) centre is in an typical 'piano-stool' geometry, with the Ru-arene distance comparable with previously reported η^6 Ru-arene complexes. The Ru–P bond length [2.3545(17) Å] is also extremely close to values reported for

$[RuCl_2(PMe_3)(\eta^6C_6Et_6)]$[138] and $[RuCl_2(PPh_3)(\eta^6$*p*-cymene)],[139] whilst the angles around the ruthenium centre [87.86(6), 86.84(6) and 86.15(6)°] are slightly smaller than those observed in the former example [87.09(19), 90.27(2) and 88.41(2)°].[5] The Au(I) metal centre is in a slightly distorted linear geometry, indicated by the P–Au–Cl angle of 177.09(10)°. The coordination sphere is made up of the bulky phospha-adamantane group and a chloride co-ligand. The angle about the Au(I) centre previously mentioned, and the bond lengths around the metal are very close to those observed previously for Au(I) phosphine complexes mentioned in Chapter One.[29] The

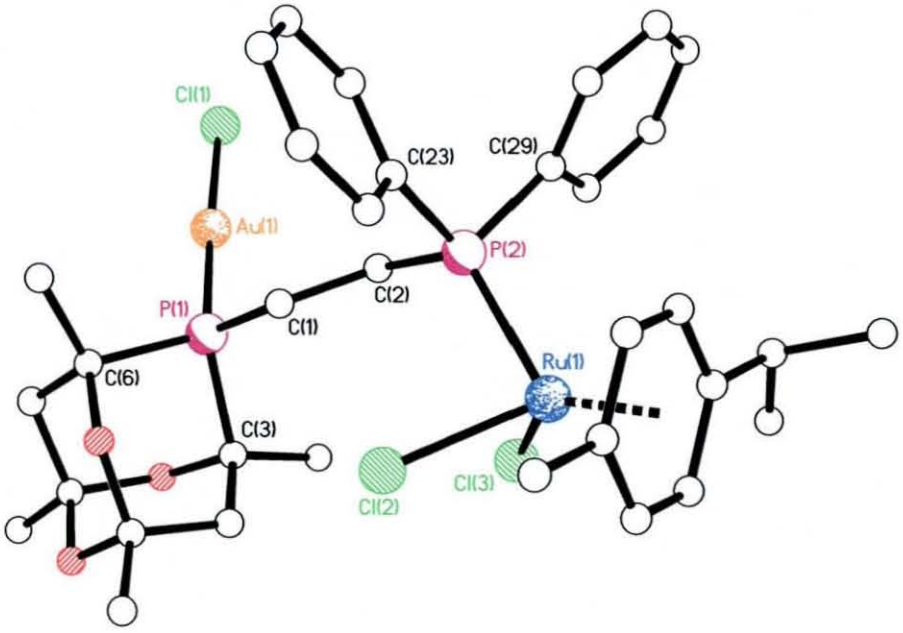

Figure 3.13 – X-ray structure of **3.18**

Bond Lengths (Å)		Bond Angles (°)	
Ru(1)–P(2)	2.3545(2)	Cl(2)–Ru(1)–P(2)	87.86(6)
Ru(1)–Cl(2)	2.4068(2)	Cl(1)–Ru(1)–P(2)	86.84(6)
Ru(1)–Cl(1)	2.4059(2)	Cl(1)–Ru(1)–Cl(2)	86.15(6)
Au(1)–P(1)	2.2317(2)	Ru(1)–P(1)–C(2)	110.8(2)
Au(1)–Cl(1)	2.280(2)	Cl(1)–Au(1)–P(1)	177.09(10)
		C(3)–P(1)–C(6)	95.2(3)

Table 3.11 - Selected bonds lengths and angles for **3.18**

P–P and Ru–Au intramolecular separations [4.487 Å and 7.162 Å respectively], whilst being large are smaller than those reported for similar unsymmetrical heterobimetallic complexes [5.238 and 8.304 Å][140], though this is presumably due to the longer backbone on the diphosphine ligand in the documented example. The intermolecular Au-Au separation [5.595 Å] is too large to enable any significant aurophilic interactions between neighbouring P–Au–Cl units. The intracage angle, shown in Table 3.3, is significantly larger (*ca.* 3 Å) than in the previous Ru(II) complex **3.17**, due to the coordination of the phospha-adamantane fragment to the metal centre in **3.18.**

With the capability of **3.17** to act as a ligand itself established, two equivalents of **3.17** were reacted with $PdCl_2(PhCN)_2$, to give the trinuclear complex *trans*-$PdCl_2$(**3.17**)$_2$, **3.19** (Equation 3.4). To our knowledge, this is the first example of a trimetallic complex using a phospha-adamantane containing ligand. The $^{31}P\{^1H\}$ NMR spectrum of the orange/red product (Figure 3.14) shows four main sets of peaks. The first of these two is what, upon initial inspection, appears to be a set of 'virtual triplets' around δ(P) 9.5 ppm. A second similar pattern of peaks is observed around δ(P) 24 ppm. The splitting between the sets of 'virtual triplets' within each of these regions of peaks is slightly different (62 Hz and 71 Hz respectively), giving the possibility that two different species are present. On closer inspection, it seems that each 'virtual triplet' is in fact two doublets, with the middle two peaks in each two doublets coincident. This would fit in with the assignment for compound **3.19**. Whilst it is almost impossible to tell which set of peaks corresponds to **3.19**, it can be

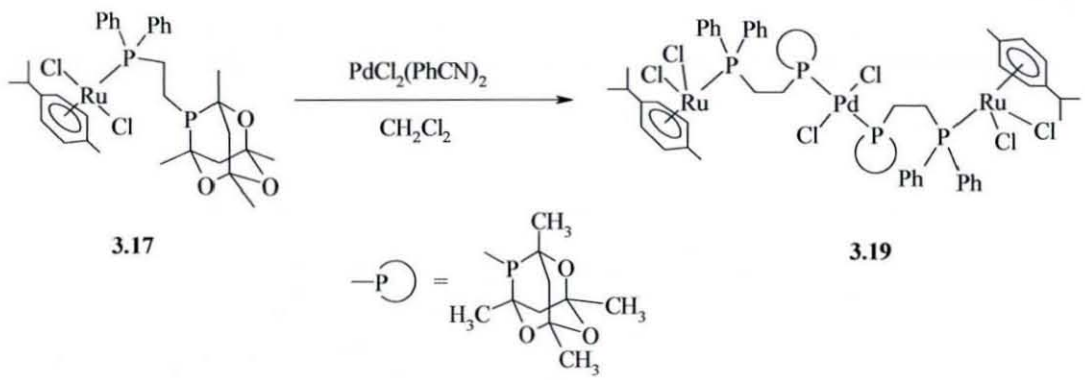

3.17 3.19

Equation 3.4 - Preparation of $PdCl_2[RuCl_2(p\text{-cymene})\{\mathbf{3.12}\}]_2$, compound **3.19**

confidently assumed that one of these sets of peaks is due to the target compound. Assignment of the second species formed is more difficult. One possibility would be that the other peaks are *cis*- $PdCl_2$(**3.17**)$_2$, though the likelihood of **3.17** coordinating to the Pd(II) centre to give this is extremely unlikely due to the bulkiness of the phopsphaadamantane group. Another possibility is that a dimer is formed, in a similar fashion to **3.6**. Certainly, the peaks at *ca.* 9 ppm are in a similar region to those for **3.6**, though the stoichiometries of the two reactants used experimentally is different to that required to form the dimer. The identity of the second set of peaks is more likely to be due to the diastereomeric nature of the phospha-adamantane cage. The presence of two phospha-adamantane cages in the same compound induces differences in the

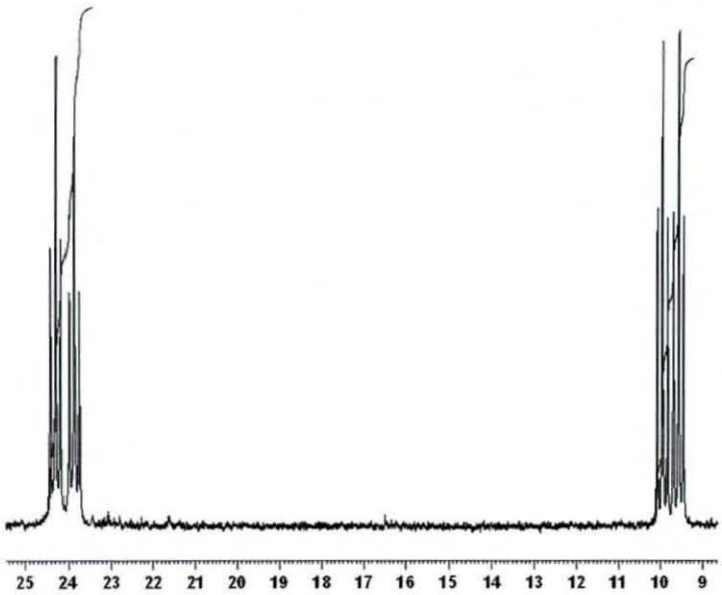

Figure 3.14 - $^{31}P\{^1H\}$ NMR spectrum of compound $PdCl_2$(**3.17**)$_2$, **3.19**

conformation of each ligand, hence the difference in the $^{31}P\{^1H\}$ NMR spectrum is observed.

The signals and isotope patterns observed in the mass spectrum of **3.19** suggest that the desired complex was formed. The signal at 1645, along with the peak at 1610 (M^+-Cl) indicate that the product is present, although these signals are not the most intense in the spectrum. Signals at 876 (showing loss of **3.17** and Cl^-) and 699 [showing loss of $PdCl_2$(**3.17**) and Cl^-] indicate that fragments of **3.19** are also present.

Crystals of **3.19** suitable for X-ray diffraction were grown by diffusion of diethyl ether into a CH_2Cl_2 solution. The structure obtained from these data confirmed

the identity of the **3.19**, as shown in Figure 3.15. The asymmetric unit of **3.19** is made up of one molecule of **3.17** coordinated to one Pd(II) centre and the two chloride co-ligands.

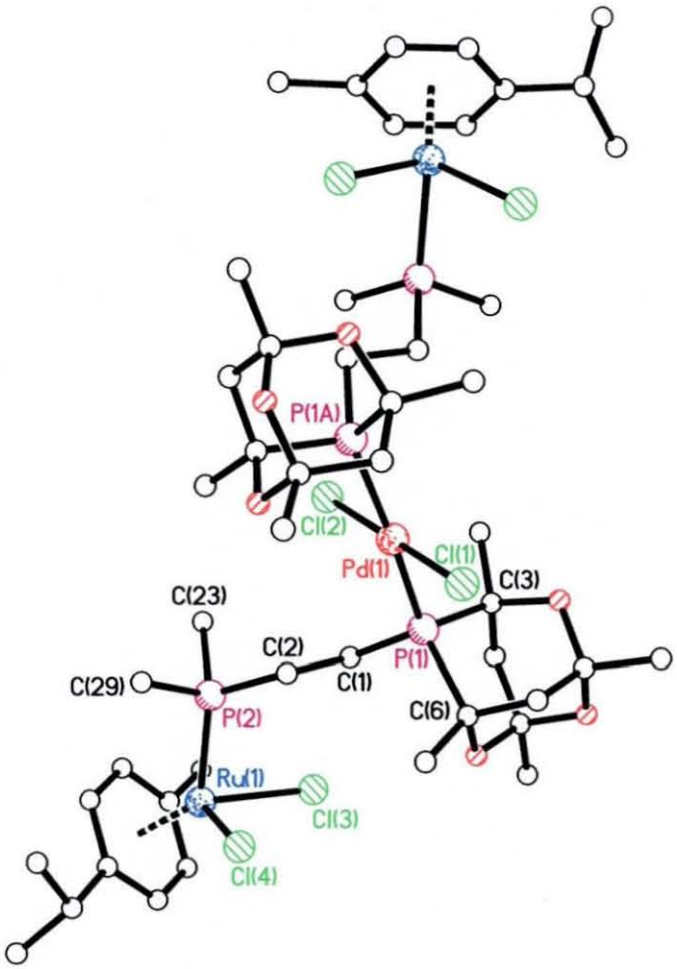

Figure 3.15 – X-ray structure of **3.19**

Bond Lengths (Å)		Angles (°)	
Pd(1)–P(1)	2.3406(15)	P(1A)–Pd(1)–P(1)	172.18(7)
Pd(1)–Cl(2)	2.304(2)	Cl(2)–Pd(1)–P(1)	86.09(4)
Pd(1)–Cl(1)	2.282(2)	Cl(1)–Pd(1)–P(1)	93.91(4)
Ru(1)–P(2)	2.3570(14)	Cl(3)–Ru(1)–Cl(4)	89.61(6)
Ru(1)–Cl(4)	2.4147(16)	P(2)–Ru(1)–Cl(4)	82.46(5)
Ru(1)–Cl(3)	2.4162(16)	P(2)–Ru(1)–Cl(3)	88.92(5)
		C(3)–P(1)–C(6)	94.2(3)

Table 3.12 - Selected bonds lengths and angles for **3.19**

The full molecule of **3.19**, as shown in Figure 3.12 is formed by symmetry generation, reflection along the Cl-Pd-Cl bonds. The coordination sphere of the palladium contains two molecules of **3.17**, coordinated *trans-* to each other via the phospha-adamantane fragment. The geometry of the Pd(II) centre is distorted from square planar, with the bond [P(2A)–Pd(1)–P(2) (172.18(7)°)] slightly different from the 180° expected. The extra flexibility of the ethylene backbone, in comparison to complexes formed in Chapter 3.1, allows the Ru/PPh_2 ends of the molecule to point both away from each other and away from the bulky cytop fragments, thereby minimising steric interactions. The Ru(II) centre itself is distorted from a tetrahedral geometry, again in a 'piano stool' configuration, with one particular angle [P(1)–Ru(1)–Cl(1) (82.46(5)°)] deviating significantly away from 90°. The deviation of one angle so markedly away from 90° has been seen previously,[137] though many other examples of analogous complexes have angles much closer to 90°.[139]

Compound **3.20** was prepared in much the same way as **3.19**, using $PtCl_2(PhCN)_2$. Isolated as an off-white solid in good yield (72%), the same two regions of peaks were seen in the $^{31}P\{^1H\}$ NMR spectrum as for **3.19**. One set of two 'double doublets' is observed between δ(P) 23.5 and 24.1 ppm, whilst the other is between δ(P) 2.3 and 3.2 ppm. As for **3.19**, this is due to the presence of two

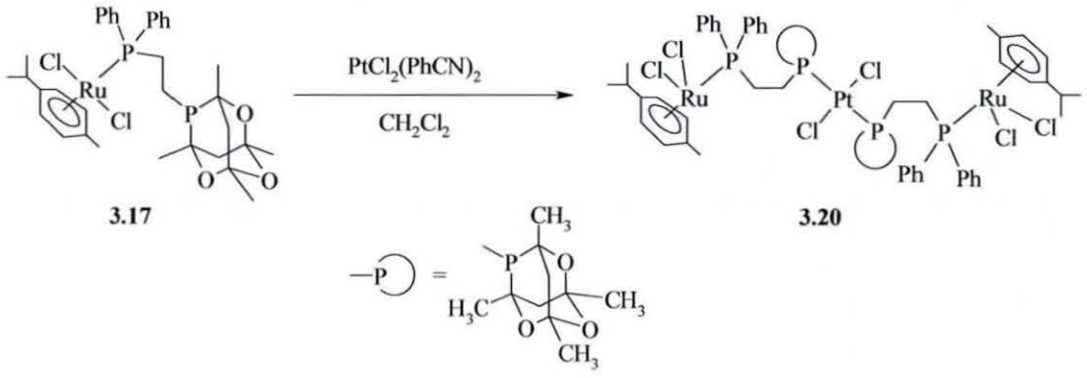

Equation 3.5 - Preparation of $PtCl_2[RuCl_2(p\text{-cymene})\{\mathbf{3.12}\}]_2$, compound **3.19**

diastereomeric phospha-adamantane groups in the molecule. Confirmation of the latter set of peaks as the phospha-adamantane group is given not only by the 6 ppm upfield shift of the peaks around 3 ppm in comparison to **3.19**, but mainly by the presence of ^{195}Pt satellites for this set of peaks. The ^1J(Pt–P) coupling observed for

3.20 (1694 Hz) is similar to the chelated unsymmetrical phospha-adamantane complex mentioned earlier in this Chapter, **3.14** (Table 3.8). Unfortunately, the proximity of the middle two peaks in each set of doublets makes calculation of the P-P coupling impossible. The assignment of the phosphorus peaks as two compounds, slightly conformationally different due to diastereoisomerism is consolidated by the splitting of almost all sets of peaks in the ^{1}H NMR spectrum. Whilst many of the peaks due to the phospha-adamantane fragment are part of a largely indistinguishable multiplet, at least three of the peaks, intended to be singlets are in fact doublets. Elemental analysis carried out on a sample of **3.20** shows excellent concordance with results, and can be seen in the Experimental Section.

3.2.2.3 – Rh and Ir complexes of 3.17

In an attempt to see if the pattern with **3.17** could be repeated with other metal centres, **3.17** was reacted with both $\{RhCl(\mu\text{-}Cl)(\eta^5C_5(CH_3)_5)\}_2$ and $\{IrCl(\mu\text{-}Cl)(\eta^5C_5(CH_3)_5)\}_2$ to give **3.21** and **3.22** respectively (Scheme 3.5). Both were isolated in fairly low yield (29% and 23%), as orange and yellow solids respectively. The $^{31}P\{^1H\}$ NMR spectra of these products proved to be slightly more complicated than for other complexes previously prepared. For **3.21**, one doublet at δ(P) –25, and a doublet of doublets at δ(P) 49.5 ppm were observed (Figure 3.16), corresponding to the free phosphaadamantane and the coordinated diphenylphosphine fragment in **3.21a** respectively. Addition of a small amount of methanol to the NMR sample of **3.21a** resulted in the appearance of eight doublets around δ(P) 48, 57 and 63 and 64 ppm, along with the peaks from **3.21a**. These correspond to a mixture of both chelated diphosphine complex **3.21b** (split due to P-P and P-Rh coupling, and the diastereomeric nature of the phospha-adamantane), and mono-coordinated complex **3.21a**.

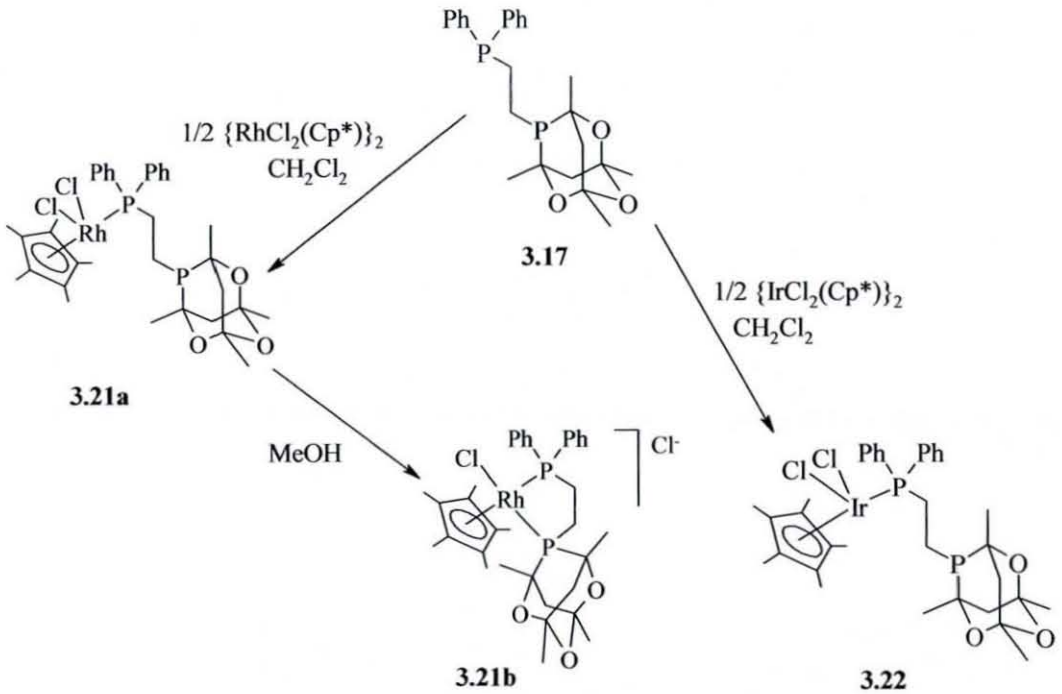

Scheme 3.5 – Preparation of compounds **3.21a**, **3.21b** and **3.22**

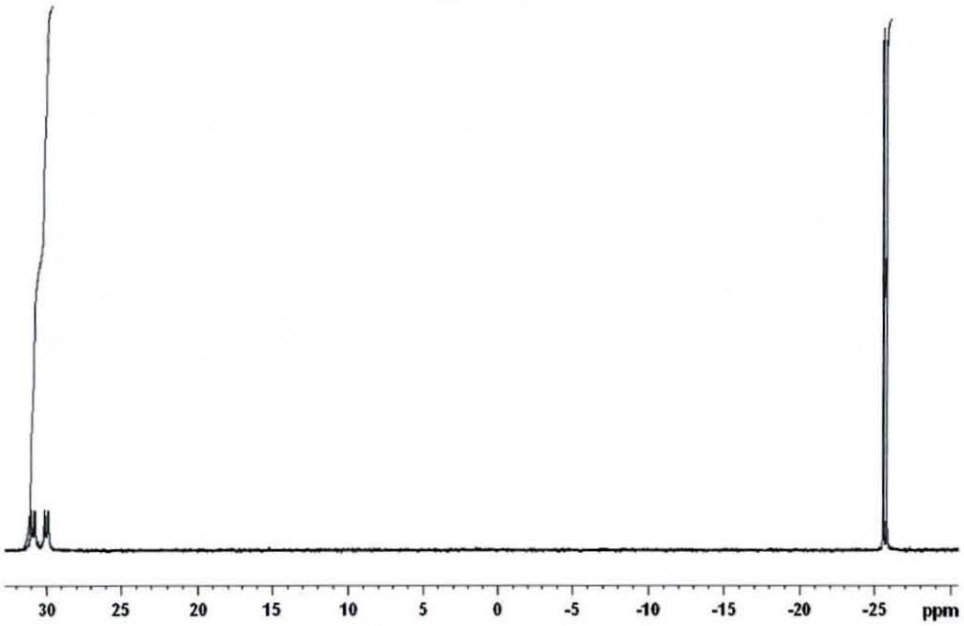

Figure 3.16 – $^{31}P\{^{1}H\}$ NMR spectrum of **3.21a**

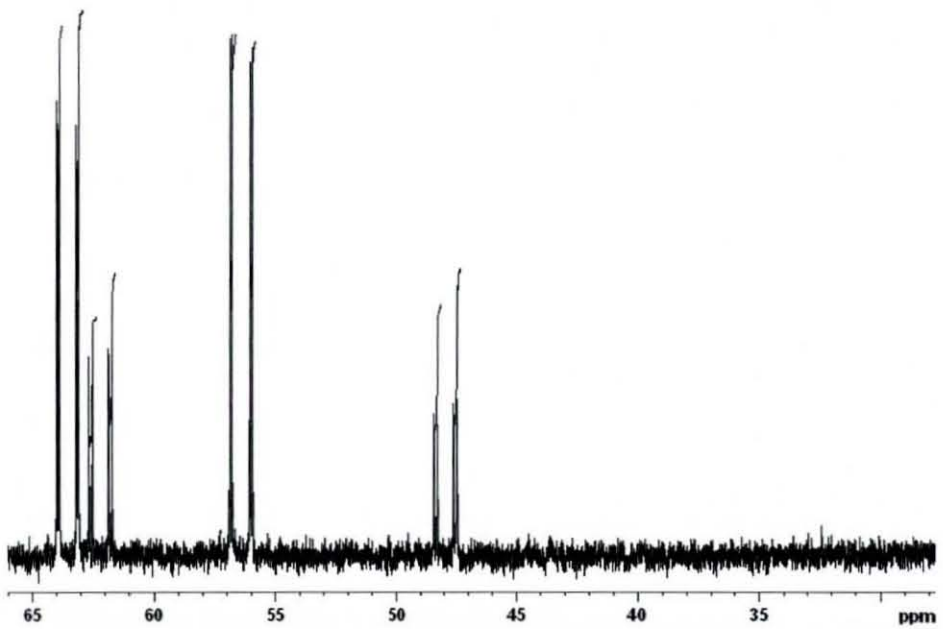

Figure 3.17 – $^{31}P\{^{1}H\}$ NMR spectrum of **3.21b**

Upon re-running of the $^{31}P\{^{1}H\}$ NMR 6 h later, only the peaks due to **3.21b** remained, and hence only the chelated ionic diphosphine complex was present. As can be seen in Figure 3.17, two species are observed due to the two diasteroisomers, roughly in a 2:1 ratio. Elemental analysis results show excellent concordance with those expected, corresponding to the mono-coordinated rhodium complex **3.21a**. The results can be seen in the Experimental Section.

In a similar manner, two equivalents of **3.17** were added to the iridium(III) dimer $\{IrCl(\mu\text{-}Cl)(\eta^5C_5(CH_3)_5)\}_2$ in CH_2Cl_2, as shown in Scheme 3.7. Cleavage of the metal-chloride bond as for the ruthenium and rhodium examples resulted in the formation of $IrCl_2(Cp^*)$(**3.17**), **3.22**. The $^{31}P\{^1H\}$ NMR spectrum of **3.22** showed the presence of two doublets of equal intensity at δ(P) –25.3 ppm and δ(P) –1.5 ppm. Once again these correspond to the free pendant phospha-adamantane group and the PPh_2 group coordinated to the iridium centre, though this has shifted significantly in comparison with the coordinated fragment in **3.22**. The presence of very few other residual peaks in the $^{31}P\{^1H\}$ NMR spectrum indicated that the purity of **3.22** is excellent. The observation of a signal in the mass spectrum of **3.22** at *m/z* 791 is indicative of the presence of the molecular ion (*m/z* 826) minus a chloride group, and fragment can be seen at 756, presumably where two chloride groups have been lost. When calculated for $IrCl_2(\eta^5C_5(CH_3)_5)$(**3.17**).$CHCl_3$, as shown in the crystal structure, elemental analysis of the crystals grown of **3.22** show concordance with the expected results, and can be found in the experimental section.

Crystals of **3.22** suitable for X-ray analysis were grown by diffusion of Et_2O into a $CDCl_3$ solution. The structure of **3.22** is shown in Figure 3.18 and selected bond lengths and angles given in Table 3.13. The coordination sphere of the iridium centre is made up of two chloride groups, an η^5-coordinated pentamethyl cyclopentadienyl group, and the coordinated phosphorus from the PPh_2 group. A molecule of chloroform is present in the unit cell of the structure. The iridium centre, like the metal centre in **3.17**, is in a 'piano-stool' pseudo tetrahedral geometry. The three chloride-containing angles are reasonably similar to those for around the ruthenium centre in **3.18**, with the exception of one Cl–Ir–P angle [91.13(8)°]. This is around 4° away from the value in **3.18**. However this may be due to the presence of a second metal centre [Au(I)] in **3.18,** hence the ability of the free phospha–admantane fragment in **3.22** to move away from the coordinated end of the molecule and increase the Cl–Ir–P angle. The P-P distance for all of the transition metal diphosphine complexes is shown in Table 3.14, and shows this point. As expected, that the P-P distance for the chelated diphosphine in **3.14** is the smallest by 1.5 Å [3.093 Å]. The monometallic and bimetallic systems prepared in contrast, have much larger values due to the flexibility about the ethylene backbone and the bulkiness of the co-ligand

on the transition metal centre. **3.22** exhibits the largest P-P distance, though this value is only slightly larger than the other monometallic and bimetallic systems prepared.

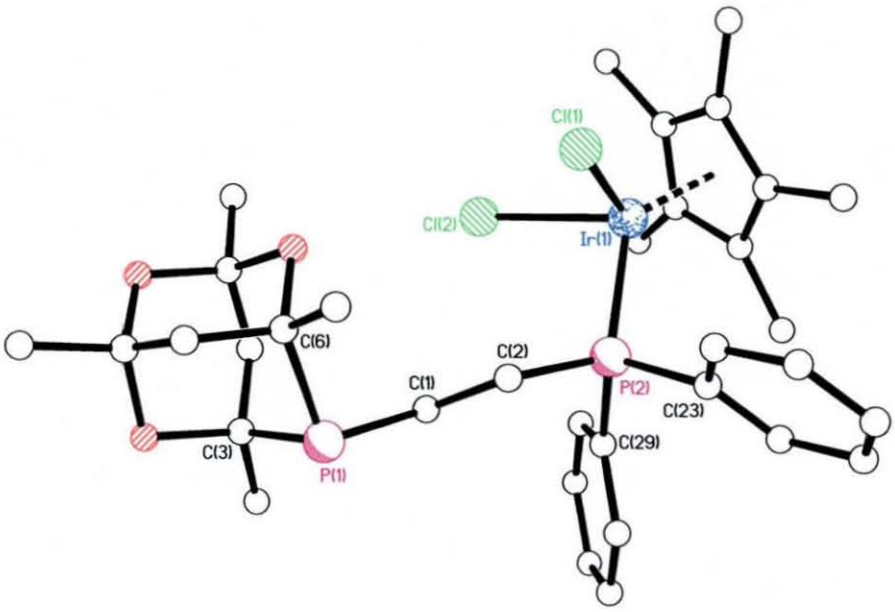

Figure 3.18 – X-ray structure of **3.22**

Bond Lengths (Å)		Angles (°)	
Ir(1)–P(2)	2.303(2)	P(2)–Ir(1)–Cl(2)	91.13(8)
Ir(1)–Cl(2)	2.412(2)	P(2)–Ir(1)–Cl(1)	87.55(8)
Ir(1)–Cl(1)	2.407(3)	Cl(2)–Ir(1)–Cl(1)	87.46(9)
		C(29)–P(1)–Ir(1)	116.1(3)
		C(3)–P(1)–C(6)	93.0(5)

Table 3.13 - Selected bonds lengths and angles for **3.22**, all hydrogen atoms and solvent molecules removed for clarity

Compound Number	P....P Distance (Å)
3.14	3.093
3.17	4.514
3.18	4.487
3.19	4.516
3.22	4.545

Table 3.14 – P…P distances for all complexes prepared using **3.12** and characterised by X-ray crystallography

3.3 – CONCLUSIONS

A variety of methods have been used to prepare unsymmetrical ligands containing bulky phospha-adamantane. Many of these ligands are new; the ligand containing the chalcogenide functionalities are the first known ligands of this type. Likewise, almost all of the complexes prepared and characterised from these ligands are novel. Indeed the heterobimetallic and trimetallic complexes synthesised from the unsymmetrical phosphine ligand **3.12** are one of very few of these types known in the literature. A large number of these complexes have been characterised by X-ray crystallography, uncovering a large number of interesting coordination patterns and possibilities for future research.

Chapter Four

~Phosphazenes and Sulfimides ~

4.1 – AIMS OF THE CHAPTER

This section looks at the preparation of both sulfimide and phosphazene derivatives of previously prepared phosphine sulfide ligands. Like a number of previously prepared sulfimides, *o*-mesitylenesulfonylhydroxylamine, MSH is used to aminate both the phosphorus and sulfur atoms, and the products formed are characterised using a variety of methods. Brief coordination studies have also been attempted using both sulfimides and phosphazenes prepared, along with amination reactions using complexes synthesised in previous chapters.

4.1.1 – Reaction of *o*-$C_6H_4(PPh_2)(SPh)$ 2.1 with Chloramine-T

As reported in Chapter One, the most commonly used method of preparing phosphazenes and sulfimides is the use of chloramine-T **4.1**. Whilst preparation of many sulfimide systems seems to be feasible,[141] contact with these unsymmetrical derivatives seems to result in reaction with the phosphine functionality. Numerous attempts were made to prepare **4.2** as shown in Equation 4.1, only to find that the phosphine had been almost completely oxidised (shown by $^{31}P\{^1H\}$ NMR spectroscopy resonance at δ(P) 30 ppm). This is surprising, as it has been reported that such reactions do not produce oxidised phosphines when simple arylphosphines of the type PR_3 (where R = Ph, etc.) are used.[142]

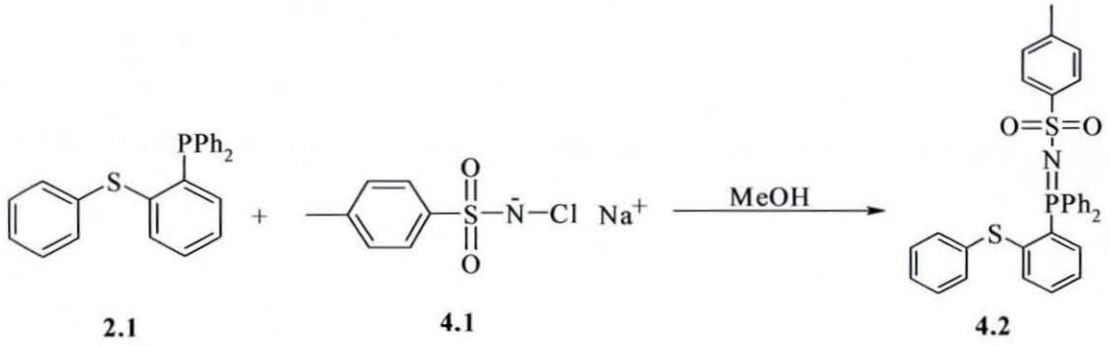

2.1 **4.1** **4.2**

Equation 4.1 - Reaction of o-$C_6H_4(PPh_2)(SPh)$, **2.1** with Chloramine-T to give **4.2**

4.1.2 – Amination reactions using MSH

Preparation of MSH **4.3** was carried out in two stages in a similar fashion to the literature procedure (Scheme 4.1).[71] A slight change was made from the literature method used, due to the large amounts of water contained in crude **4.3** after addition to ice water. Upon dissolution of crude **4.3** in Et_2O, a separation was carried out to enable removal of most of the water from the product.

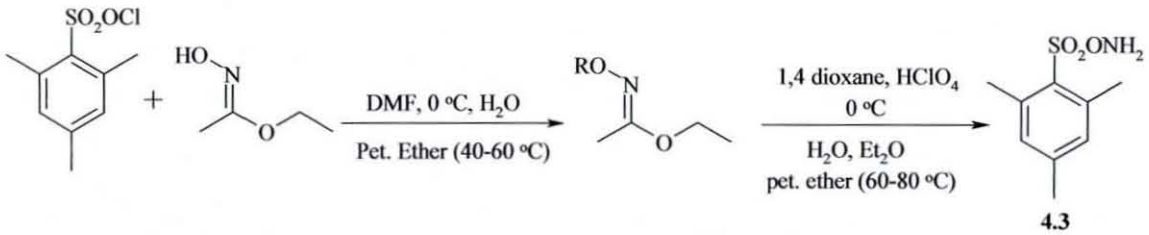

4.3

Scheme 4.1 - Preparation of o-mesitylenesulfonyl hydroxylamine, **4.3**

A number of reactions were then carried out using **4.3**, with varying results. Reaction of **4.3** with one equivalent of **2.1** over three days gave the monoaminated product, $[C_6H_4(P(NH_2)Ph_2)(SPh)][(CH_3)_3C_6H_2SO_2O]$ **4.4** (Scheme 4.2). The white solid was characterised using $^{31}P\{^1H\}$ NMR spectroscopy, the spectrum containing one peak at δ(P) 36.7 ppm. The infra-red spectrum also showed N-H stretches at 3054 cm^{-1}.

Reaction of two equivalents of **4.3** with **2.1** in CH_2Cl_2, followed by crystallisation with excess diethyl ether yielded the expected product, $\{C_6H_4(P(NH_2)Ph_2)(S(NH_2)Ph)\}\{(CH_3)_3C_6H_2SO_2O\}_2$ **4.5**, but in a mixture with the monoaminated product **4.4**. This was shown by $^{31}P\{^1H\}$ NMR spectroscopy, with chemical shifts of δ(P) 36 ppm and 34 ppm representing the mono- and dication respectively. It seems that from these and other reactions attempted the more basic phosphorus atom is aminated very quickly, with amination of the sulfide to form the sulfimide being completed much more slowly.

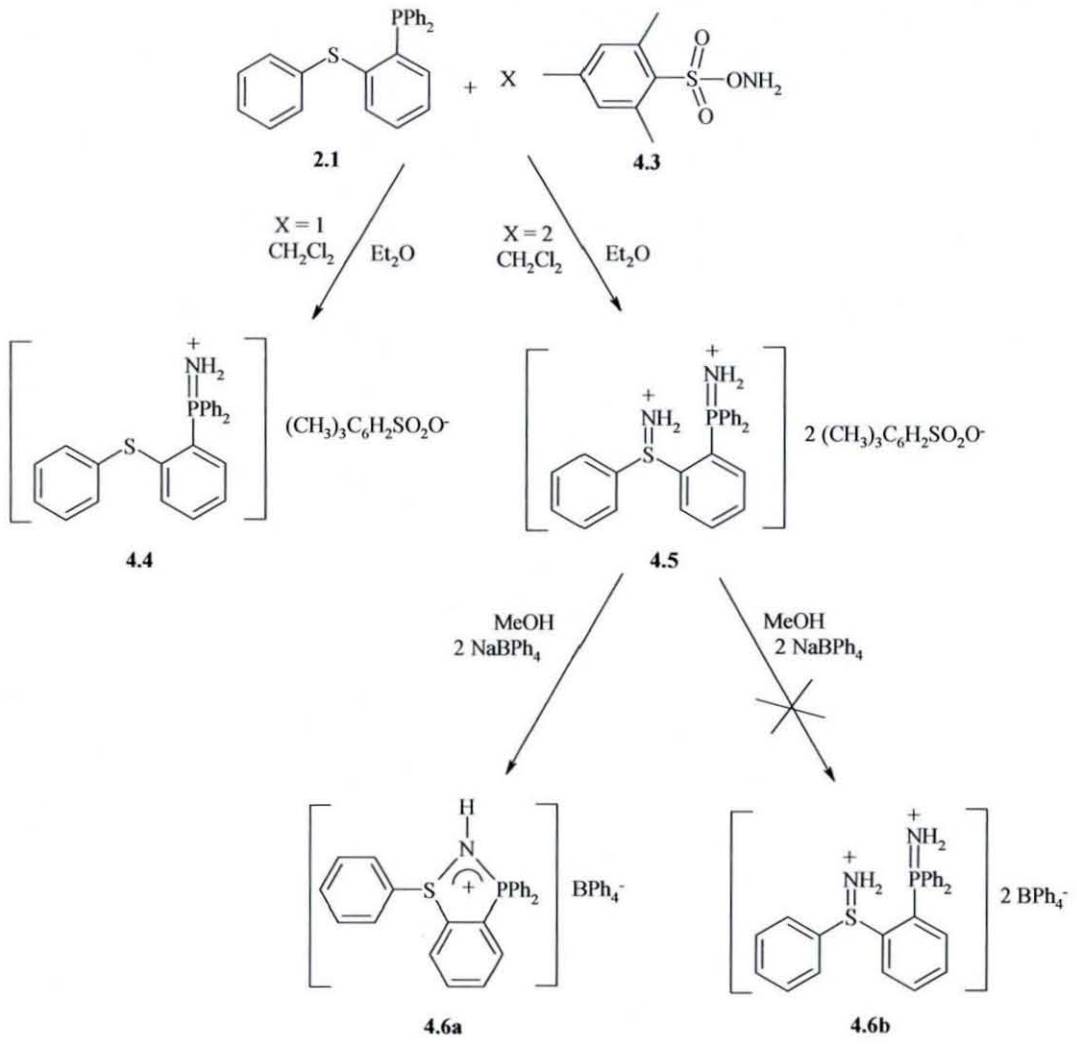

Scheme 4.2 – Preparation of **4.4b**, **4.5**, **4.6a** and **4.6b**

A simple anion exchange reaction using $NaBPh_4$ was carried out to replace the MSH anion. When the reaction was carried out as shown in Scheme 4.2, and the white solid product analysed using $^{31}P\{^1H\}$ NMR spectroscopy, an unexpected shift of δ(P) 73 ppm was observed. It was hypothesised that this might be due to cyclisation of the phosphazene and sulfimide groups, and loss of one NH_2 group, hence making this a singly charged species **4.6a**. Unfortunately, numerous crystallisation attempts to confirm this assumption failed, since no crystals suitable for X-ray analysis could be obtained. One such attempt yielded two kinds of crystals; one of which were needle-like, the others were found to be $NaBPh_4$. This point is of some significance, as if some $NaBPh_4$ is left in the reaction product and exactly two equivalents of $NaBPh_4$ were used initially, this must mean a maximum of only one equivalent has reacted, hence a singly charged species is present. This was followed up by reaction of exactly

one equivalent of $NaBPh_4$ with **4.5**, which still yielded the seemingly cyclised product. It can be assumed, therefore, that the close proximity of the two functionalities has a strong impact on the nature of the product when amine groups are added. Indeed, it has been documented that attempts to prepare compounds with multiple sulfimidium moieties in close proximity results in bridging of sulfimide groups.[143]

Attempts to crystallise both the mono- and diaminated phosphine sulfides have been unsuccessful, indicating a certain amount of instability or lack of crystallinity in this species. A product from one such crystallisation attempt was the phosphine oxide/sulfimide species $[C_6H_4(P(O)Ph_2)(S(NH_2)Ph)][(CH_3)_3C_6H_2SO_2O]$ **4.7**. Two main reasons could have resulted in the above product being formed; firstly the use of non-deoxygenated solvents, and secondly the presence of a small amount of $CHCl_3$ in the reaction, thus providing the opportunity for one NH_2 group to leave as $[NH_4]^+[(CH_3)_3C_6H_2SO_2O]^-$.[144] Despite attempts to rectify both of these problems and crystallise the dicationic species, attempts were unsuccessful.

The unit cell of **4.7** contains one main P=O/S=N cation, and one MSH anion (Figure 4.1a). The presence of sulfoxide and sulfimide functionalities allow intermolecular hydrogen bonding to occur, as shown in Figure 4.1a. Using both sulfimide protons, and both S=O sulfoxide groups on the anion, a 2-cation, 2-anion, 12-membered ring is formed. Due to the presence of more than one sulfoxide group on the MSH counter ion, H(1A) is shown to form two hydrogen bonds to O(3) and O(2) respectively. This is repeated for each sulfimide/anion interaction, but is omitted from Figure 4.1a for clarity. It could be proposed, therefore, that were the diaminated structure elucidated, it might form a similar hydrogen bonded ring system, possibly using just one hydrogen on each of the sulfimide groups. The packing diagram of **4.7** (Figure 4.1b) shows stacking of both S-Ph and P-Ph rings in an alternating fashion. This leaves a column through the centre of the molecules, into which the mesitylene methyl group *para*- to the SO_2O functionality is pointing.

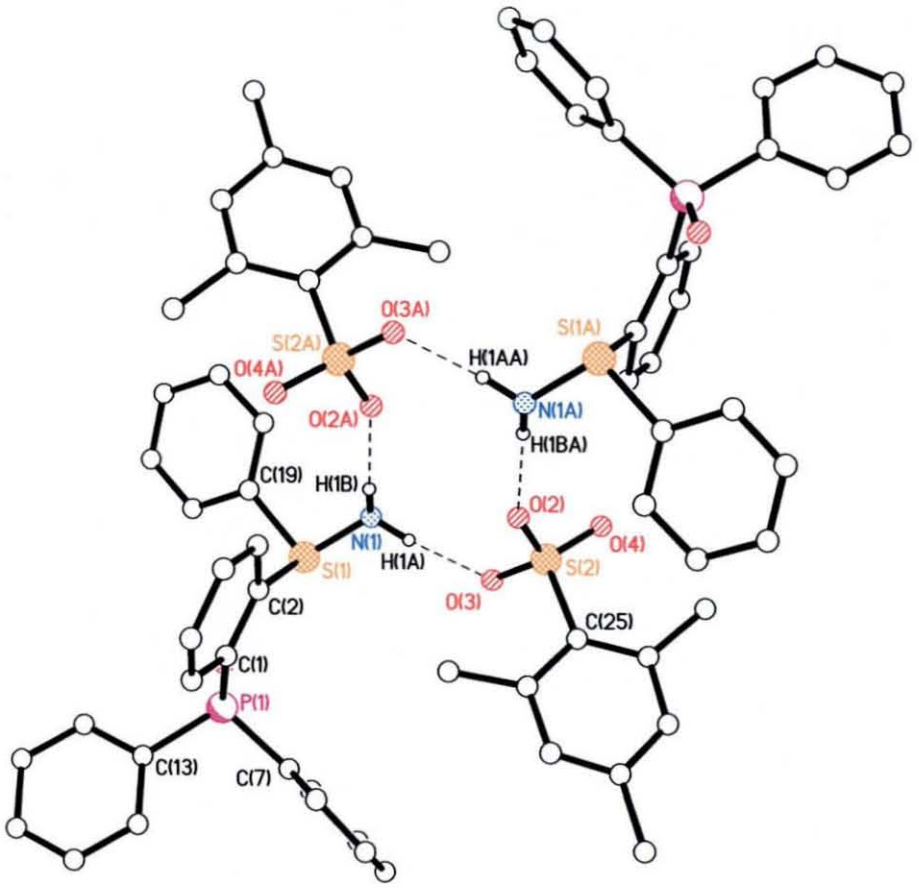

Figure 4.1a – Two cation-two anion hydrogen bonding in **4.7**

Bond Lengths (Å)		**Bond Angles (°)**	
S(1)-N(1)	1.616(3)	O(3)-S(2)-O(2)	111.17(15)
S(2)-O(2)	1.463(3)	O(4)-S(2)-O(3)	112.23(17)
S(2)-O(3)	1.462(3)	N(1)-S(1)-C(2)	107.01(18)
S(2)-O(4)	1.445(3)	O(1)-P(1)-C(1)	111.81(18)
Hydrogen bonds			
D-H…A	**(H…A) (Å)**	**(D…A) (Å)**	**<(DHA) (°)**
N(1)-H(1A)...O(3)	1.89(3)	2.787(4)	173(4)
N(1)-H(1BA)…O(2)	2.63(4)	3.148(4)	118(3)
N(1)-H(1B)…O(2A)	2.02(3)	2.901(4)	166(4)

Table 4.1 – Selected bond lengths and angles for **4.7**

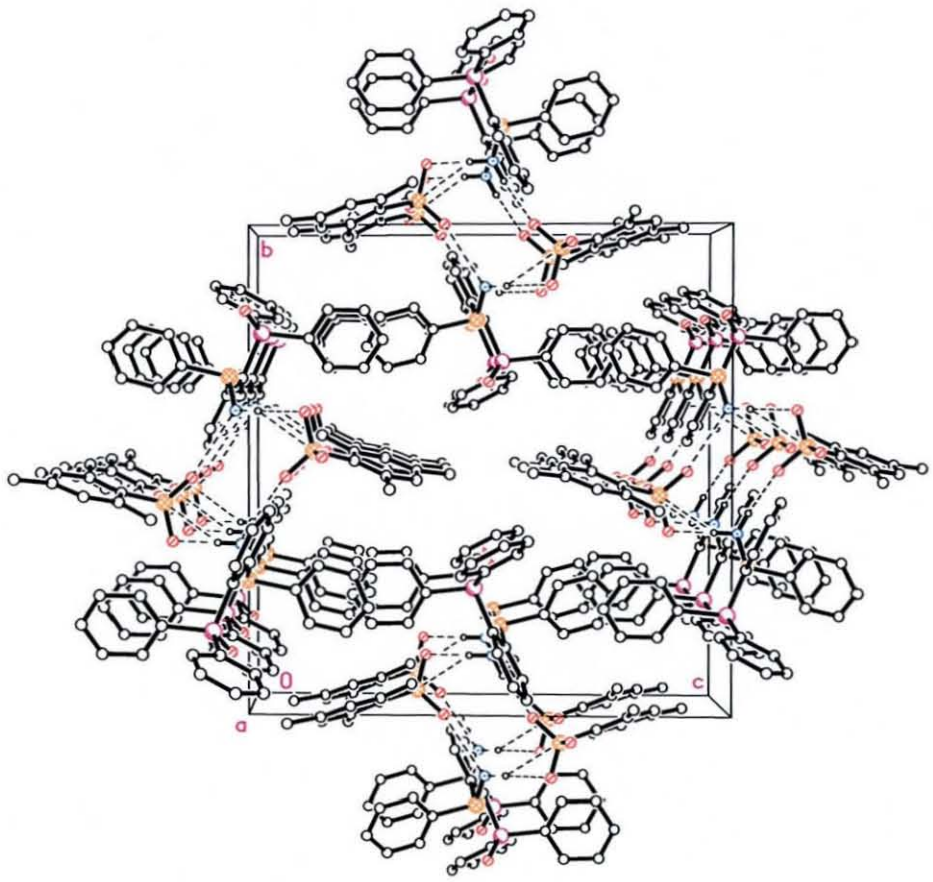

Figure 4.1b – Packing plot of **4.7**, showing alternate stacking of phosphorus and sulfide aromatic groups

Whilst the above product was unexpected, reaction of phosphine oxide **2.3**, prepared in Chapter Two, with MSH over 3 d gave a white solid product after purfication. The $^{31}P\{^{1}H\}$ NMR spectrum of this product shows one species at δ(P) 33 ppm; by comparison of this chemical shift with that of $C_6H_4(P(NH_2)Ph_2)(SPh)$ **4.4** (37 ppm) and **20** (29 ppm), it can be confidently assumed that the phosphine oxide/protonated sulfimide system **4.7** was synthesised stoichiometrically.

In a similar manner to that for preparing **4.5**, **2.32** was reacted with two equivalents of MSH in an attempt to aminate the two phosphorus atoms of **2.32** (Scheme 4.3). It was hoped that a similar reaction pattern would be observed as for **4.5** on reaction with $NaBPh_4$, but also that the $^{31}P\{^{1}H\}$ NMR spectrum would

indicate, via coupling patterns if the ring was formed, whether the structure postulated for **4.5** was correct. The product of the reaction with **4.3**, **4.8a**, contained two phosphazene moieties and two MSH anions, as shown in Scheme 4.3. The FAB^+ mass spectrum showed the required molecular ion peak at *m/z* 538 (relative abundance 50%), along with a peak at 228 (relative abundance 100%) due to loss of the alkyl-phosphine fragment. **4.8a** was reacted with two equivalents of $NaBPh_4$. The $^{31}P\{^1H\}$ NMR spectrum of product **4.8b** showed an extremely large shift in comparison to **4.8a**. The only peak apparent in the spectrum was a singlet at δ(P) 120 ppm. This is extremely unusual, due to the two inequivalent phosphorus environments in **2.32** and subsequently **4.8a**. Furthermore, the FAB^+ mass spectrum shows the same pattern as for **4.8a**, with a peak at *m/z* 539 corresponding to the bis-phosphazene dication. Peaks are again observed at *m/z* 228, and also at 310.

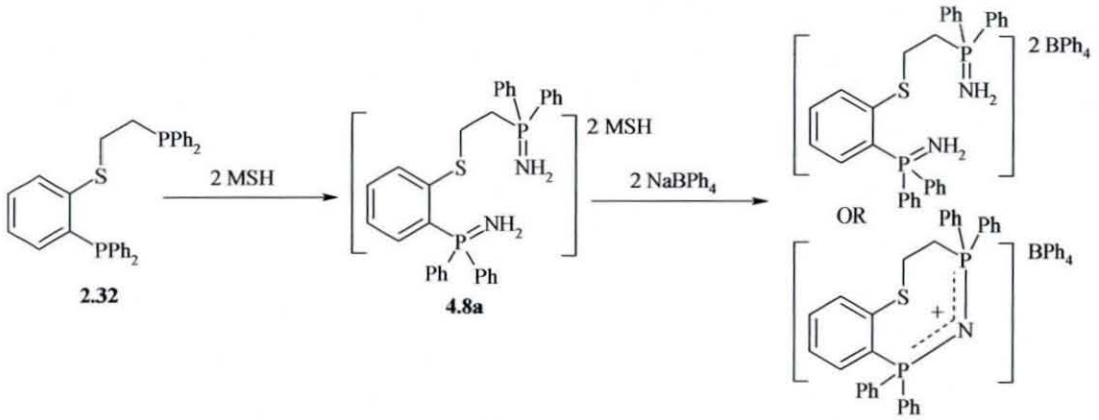

Scheme 4.3 – Preparation of **4.8a** and **4.8b**

In conclusion, the definitive identity of **4.6a** and **4.8b** is unknown. The cyclisation theory would be the most obvious answer due to trends previously observed when attempting multi-sulfimidation of trithiacrowns,[143] but the lack of coupling and different phosphorus signals in the $^{31}P\{^1H\}$ NMR spectrum for **4.8b** and mass spectrometry pattern discounts this. X-ray crystallography would give an answer as to the structures of the two products, however repeated attempts using a large range of solvent conditions and crystallisation methods were unsuccessful. A seemingly novel trend is observed nonetheless, however further tests would be needed to ascertain the definitive identity of the aminated products.

4.1.3 – Amination of Selenide-containing Ligands

Like the study of simple phosphine selenide systems, the chemistry of selenimides has only received limited attention. Some examples have been reported,[145] one of which concerning the water-free conversion of selenides into selenimides using TsI=Ph is of particular relevance.[146] **2.17** was reacted with two equivalents of **4.3** in CH_2Cl_2 to immediately form an off-white precipitate. After stirring the reaction for 24 h, both the solid and the filtrate were found to include phosphorus-containing species.

The filtrate was examined using $^{31}P\{^1H\}$ NMR spectroscopy. The spectrum contains a major peak at δ(P) 37.7 ppm, two minor peaks at δ(P) 32.3 ppm and 41 ppm, and an additional peak at δ(P) 73.5 ppm. The first two of these can be assigned by analogy with the sulfur species as $C_6H_4(P(NH_2)Ph_2)(SePh)$ **4.9a** (Figure 4.2) and $C_6H_4(P(NH_2)Ph_2)(Se(NH_2)Ph)$ **4.9b** respectively. Whilst the identity of the species giving a chemical shift of δ(P) 41 ppm is unknown, the peak at 73.5 ppm could be due to the cyclised product **4.9c** analogous to **4.9a**. Of course, this could either mean that the cyclisation of the sulfur species may not be due to the addition of $NaBPh_4$, or that the cyclisation of the selenium analogue may be more facile, even with only the MSH anion involved. The first of these ideas is made less possible by the knowledge that a test of simply allowing **4.5** to stand in a MeOH solution does not yield the ring system analogous to **4.9c**.

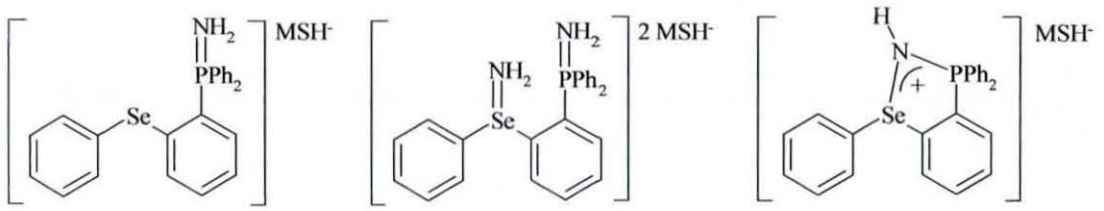

4.9a **4.9b** **4.9c**

Figure 4.2 – Preparation of selenimides **4.9a**, **4.9b** and **4.9c**

4.1.4 – Other routes to phosphazenes

A method similar to that employed by Chou *et al*[142] for the preparation of various triarylphosphazenes was used to prepare an analogous phosphazene-sulfide species. Reaction of **2.1** with one equivalent of bromine in toluene, followed by addition of a triethylamine and aniline mixture gave $C_6H_4\{P(NPh)Ph_2\}(SPh)$ **4.10**, shown in Scheme 4.4. This was characterised using $^{31}P\{^1H\}$ NMR spectroscopy, the only peak in both spectra being shifted around 33 ppm from δ(P) –12 ppm in the phosphine sulfide to 21 ppm for the phosphazene. The reaction probably proceeds via a dibromo phosphorus(V) species $C_6H_4\{P(Br_2)Ph_2\}(SPh)$, the bromide groups of which are easily displaced when attacked by the amine. The yield of this reaction, however, is quite poor (34%), but has not yet been optimised.

Attempts to coordinate a second equivalent of aniline to make $C_6H_4\{P(NPh)Ph_2\}\{S(NPh)Ph\}$ were unsuccessful. The reaction was only carried out at room temperature however; therefore stronger reaction conditions may be required. It may also be that the reaction is simply not sterically feasible, with so many aromatic groups in such close proximity. **2.1** was also reacted with one equivalent of 1,2 phenylenediamine to counteract the effects of having two phenyl groups (Scheme 4.4). It was hoped that an eight membered ring system may develop incorporating both the sulfimide and phosphazene functionalities. Such a reaction yielded a black side-product which was different from the aniline reaction, and an *in-situ* $^{31}P\{^1H\}$ NMR revealed two peaks, one at δ(P) –11 ppm (starting material) and another at 27 ppm, possibly **4.11a**. However, upon purification, the $^{31}P\{^1H\}$ NMR spectrum showed just one peak at δ(P) 29 ppm, corresponding to the phosphine oxide analogue, **2.3**. It is well known[147] that the phosphazene PNH_2 unit can readily hydrolyse, leaving the phosphine oxide as the main reaction product, and even numerous attempts gave a similar NMR pattern after the crude product was worked-up. Another possibility for the structure of the black side-product is the polymeric compound **4.11b** (Scheme 4.4). The insolubility of this side product also inferred this may be the case, though further tests would be needed to ascertain the definite structure of this material.

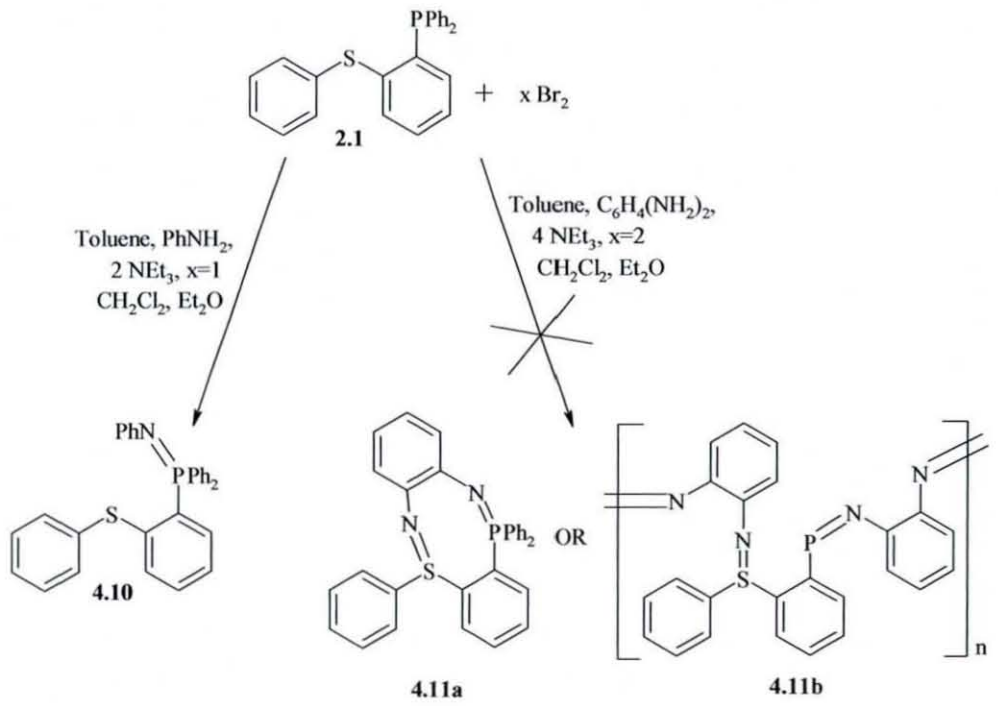

Scheme 4.4 - Reaction of **2.1** with amines to give compounds **4.10**, **4.11a** and **4.11b**

Reaction of sulfamic acid, H_2NSO_3H, with triphenylphosphine has been shown to produce the corresponding phosphazene when sodium methoxide was also added to the reaction (Equation 4.2).[148] This was attempted for the phosphine sulfide system **2.1**, however no reaction occurred after 24 h. A similar reaction to prove the method used ourselves was correct was carried out on triphenylphosphine; this gave some indication [peak at δ(P) 23 ppm in the $^{31}P\{^1H\}$ NMR spectrum] that the reaction works.

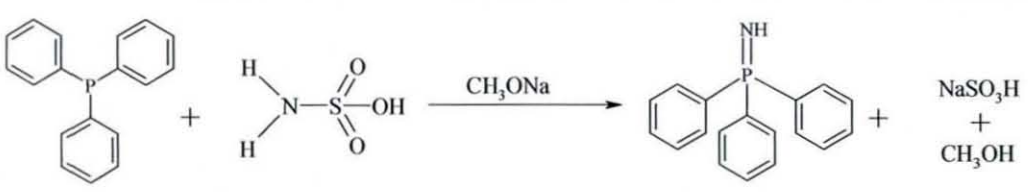

Equation 4.2 - Reaction of PPh_3 with sulfamic acid

4.1.5 - Amination of phospha-adamantane-based ligands

Reaction of MSH, **4.3** with ligands containing phospha-adamantane cages was attempted. It was hoped that the difference in the type of phosphine would contribute to a difference in reactivity. 1,2-C_6H_4(OMe)(PAd), **3.3**, was reacted with **4.3** in CH_2Cl_2 for 20 h (Scheme 4.5). Precipitation with Et_2O gave 1,2-C_6H_4(OMe)(PAdNH_2), **4.12** as a white crystalline solid in good yield (75 %). The $^{31}P\{^1H\}$ NMR spectrum showed a single species at δ(P) 20 ppm, which is slightly different when compared to phosphine-containing species such as **4.6a** and **4.8b**. The ^1H NMR spectrum also showed evidence of the aminated product. Peaks due to aromatic groups in **4.12** can be seen between δ(H) 7 and 8 ppm, whilst MSH peaks are evident along with a slightly broad NH_2 peak at 5.6 ppm. Infra-red analysis also gave good indication, with broad peaks around 3100 cm^{-1} corresponding to the added NH_2 functionality. An electrospray mass spectrum obtained clearly showed the cation (*m/z* 338) to be the molecular ion peak, with the anion (*m/z* 199) also clearly present.

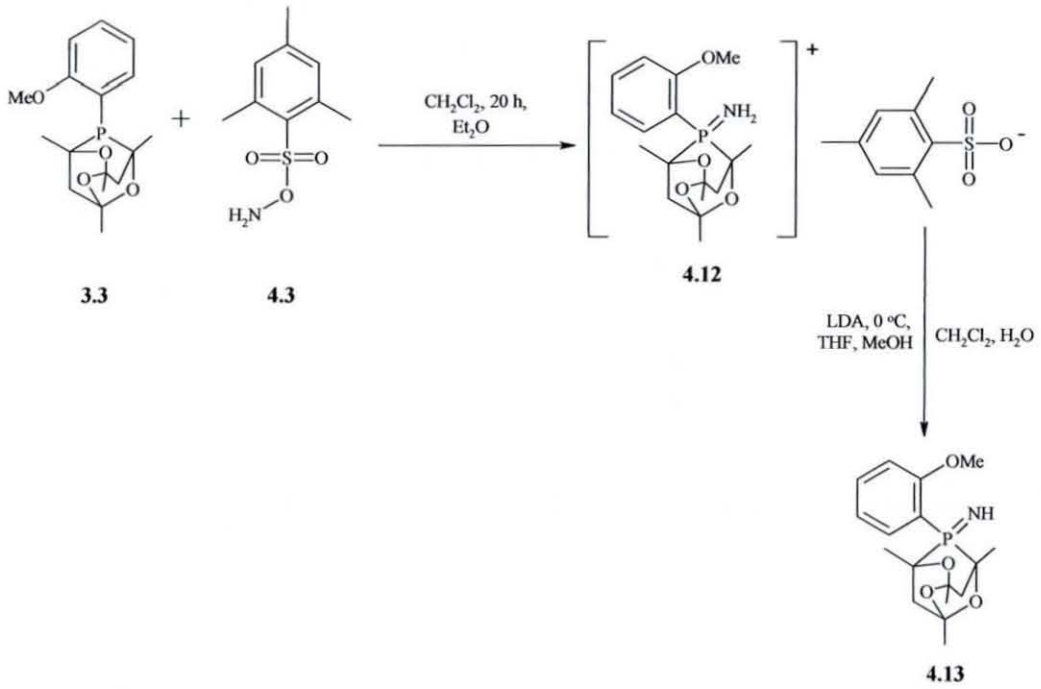

Scheme 4.5 – Preparation of compounds **4.12** and **4.13**

Crystals of **4.12** suitable for X-ray diffraction were grown by vapour diffusion of diethyl ether into a $CHCl_3$/MeOH solution. The crystal structure obtained (Figures 4.3a & 4.3b) confirms the structure of **4.12**. The phosphine of the phospha-adamantane cage is aminated, and as with products of reactions using MSH prepared

previously, the positive charge of the $P{=}NH_2$ group is balanced by one MSH anion. Hydrogen bonding exists between one NH_2 proton and one S=O group on the anion, as shown in Figure 4.3b and Table 4.2.

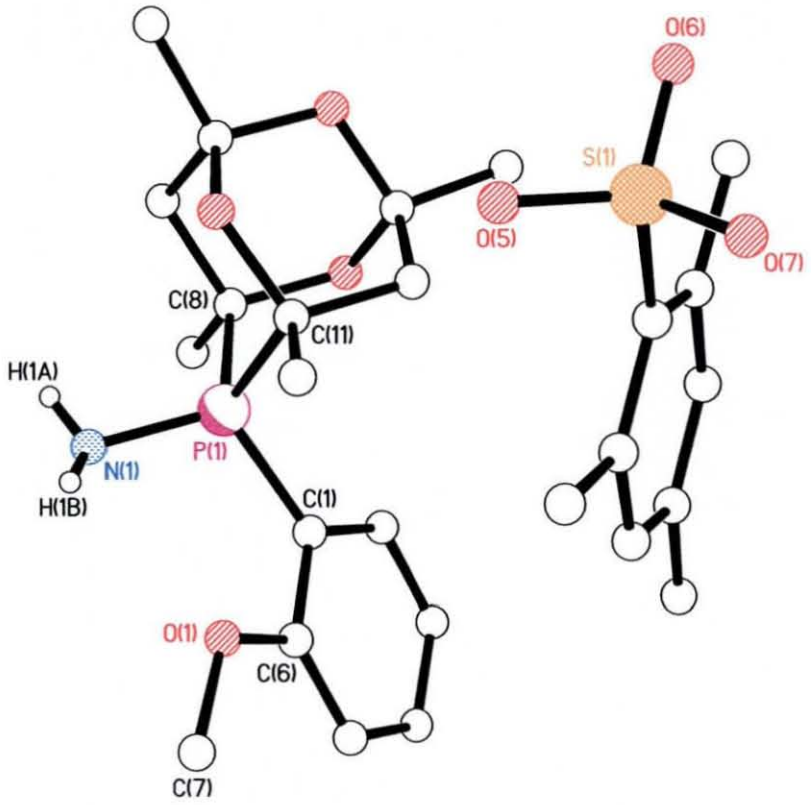

Figure 4.4a – X-ray structure of **4.12**

Bond Lengths (Å)		**Bond Angles (°)**	
P(1)–N(1)	1.624(18)	O(3)–S(2)–O(2)	111.17(15)
C(1)–P(1)	1.802(19)	O(4)–S(2)–O(3)	112.23(17)
O(1)–C(6)	1.353(4)	N(1)–S(1)–C(2)	107.01(18)
O(1)–C(7)	1.435(4)	O(1)–P(1)–C(1)	111.81(18)
		C(8)–P(1)–C(11)	97.77(14)
Hydrogen bonds			
D-H…A		**D(H…A) (Å)**	**D(D…A) (Å)**	**<(DHA) (°)**
N(1)–H(1A)...O(7A)		2.18(4)	2.914(3)	161.0(3)
N(1)–H(1B)..O(5AA)		2.21(5)	3.009(3)	162.8(3)

Table 4.2 – Selected bond lengths and angles for **4.12**

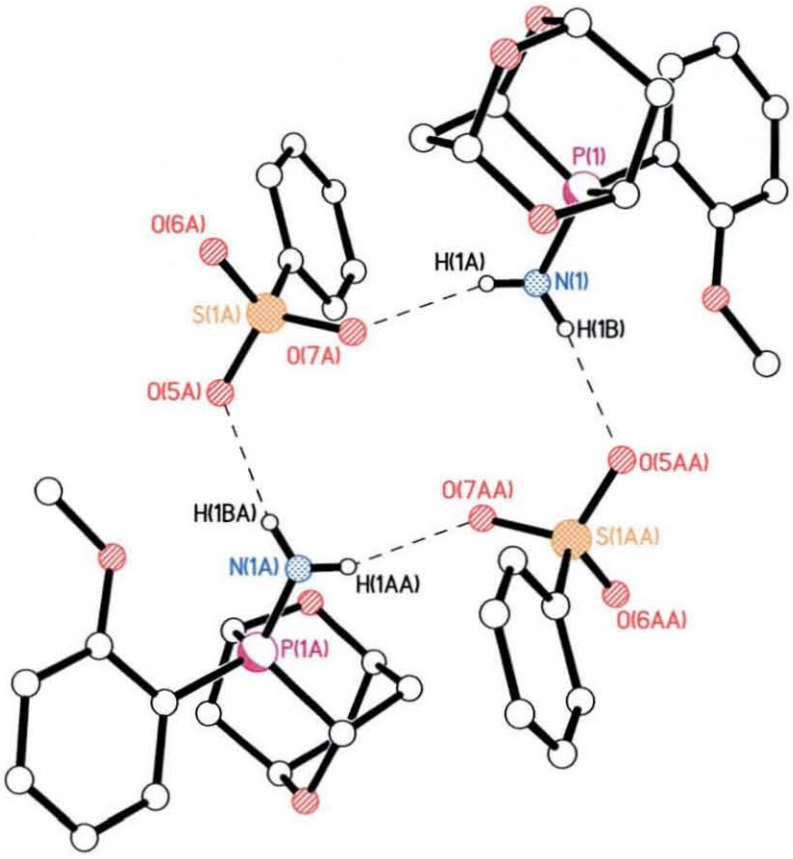

Figure 4.3b – Two cation-two anion hydrogen bonding in **4.12**

The lengths of the hydrogen bonds are slightly different to those reported for **4.7**; those for **4.12** are fairly consistent around 2 Å, whereas those for **4.7** are different [1.89(3) and 2.63(4) Å]. This may be attributed to the differences in the types of aminated product (phosphazene compared to sulfimide), and also probable fluxionality along the X=N (where X = S/P) bond. Comparison of the 'intracage angle' mentioned in Chapter Three should also be noted. **3.1** and **3.5**, both ligands containing phospha-adamantane fragments on aryl backbones, have fairly small intracage angles in comparison with subsequent complexes (*ca.* 92° compared to 94°). However the intracage angle for **4.12** is exceptionally large [97.7(14)°]. This is also reflected in the slightly shorter P-C distances within the phospha-adamantane cage for **4.12** [1.852(3) and 1.841(3) for **4.12**, compared to 1.886(3) and 1.888(3) for **3.5**]. The

presence of the phosphazene and hence the phosphorus(V) centre seems to be the reason for the notable increase in intracage angle.

Compound **4.12** was reacted with lithium diisopropylamide, LDA, prepared from diisopropylamine, to deprotonate the $P{=}NH_2$ group (Scheme 4.5). After a CH_2Cl_2/H_2O extraction to eliminate the Li-MSH side product, **4.13** was obtained as an off-white solid. The single peak in the $^{31}P\{^1H\}$ NMR spectrum exhibited a shift from δ(P) 20 to 14 ppm. N-H stretches in the infra-red spectrum also shifted to 3380 cm^{-1}, whilst another N-H peak appeared at 681 cm^{-1}.

Small-scale tests, reacting **4.13** with different metal centres, were carried out. **4.13** was firstly reacted with $CuCl_2$ in MeCN (Scheme 4.6). After stirring the yellow solution for 6 h, $^{31}P\{^1H\}$ NMR spectroscopy showed the single peak to have shifted from δ(P) 14 ppm to 22 ppm. The N-H stretches in the infra-red spectrum also shifted to 3442 and 691 cm^{-1}.

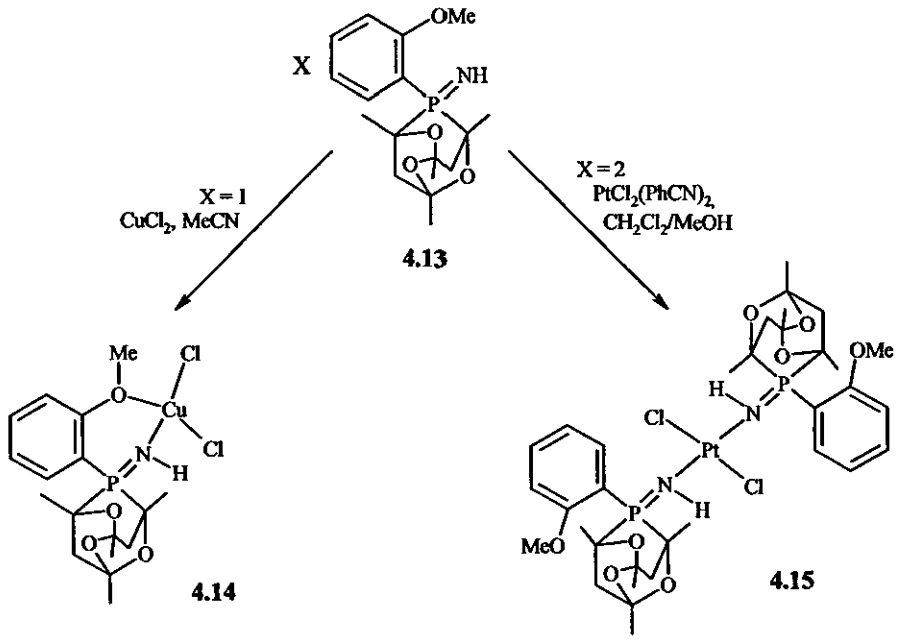

Scheme 4.6 - Complexation reactions of **4.13** to give **4.14** (Cu) and **4.15** (Pt)

Two equivalents of **4.13** were also added to $PtCl_2(PhCN)_2$ in a CH_2Cl_2/MeOH solvent mixture. A $^{31}P\{^1H\}$ NMR spectrum taken after 4 h showed two main regions of peaks. The first showed a major species at δ(P) 21 ppm, with a minor species at 24 ppm. A second region around –1 to –2 ppm exhibited the same peak pattern. A second equivalent of **4.13** was added, upon which the region of peaks around –2 ppm

almost completely disappeared. This left the two peaks between 20–23 ppm. Surprisingly, despite running high concentration samples of **4.13**, none of the expected ^{2}J(PtP) couplings were observed. Therefore, two theories are possible; that addition of the second equivalent of **4.13** cleaved a previously formed dimer complex similar to **3.6** to form the complex shown in Scheme 4.6, with the two peaks being due to *cis*– and *trans*–isomers of the product. The second, more likely theory is that, over time, the P=NH group is unstable, hydrolyses and forms the phosphine oxide; this is made more credible by the fact that adding H_2O_2 to a THF solution of **4.13b** gives a peak at δ(P) 20 ppm.

MSH **4.3** was added to the ruthenium complex **3.17** (Equation 4.3) to aminate the free phospha-adamantane group. As expected, the monocationic complex, $[RuCl_2(p\text{-cymene})\{Ph_2P(CH_2)_2(PAd{=}NH_2)\}]^{+}\{(CH_3)_3C_6H_2SO_2O\}^{-}$, **4.16** was formed. The uncoordinated phospha-adamantane group was readily aminated using the MSH. This is shown primarily by the large shift of the phospha-adamantane signal in the $^{31}P\{^{1}H\}$ NMR spectrum from δ(P) –26 ppm in **3.17** to 20 ppm in **4.16**. The electrospray mass spectrum shows the molecular ion peak of the cation at *m/z* = 750 (expected *m/z* = 750), and on a separate spectrum of the MSH anion at *m/z* 199. A further peak can be seen on the positive spectrum at 714, corresponding to loss of one chloride from the ruthenium centre. The loss of a chloride group is seen with a number of complexes containing chloride co-ligands prepared in previous Chapters. Infra-red spectroscopy showed the expected broad peak from the SO_2O group at 1165 cm^{-1} Unfortunately, despite numerous attempts to grow crystals suitable for X-ray crystallography, these proved unsuccessful.

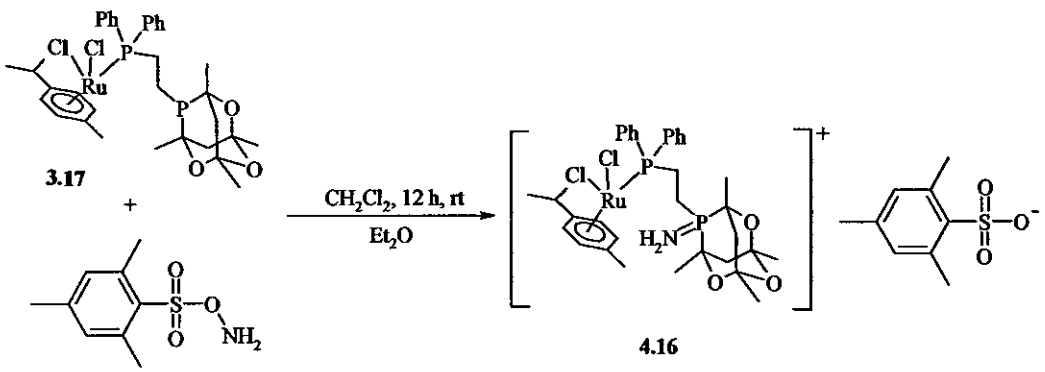

Equation 4.3 - Reaction of MSH, **4.3** with **3.17** to give compound **4.16**

4.2 – CONCLUSIONS

In summary, a number of aminated derivatives of ligands and complexes prepared in Chapters Two and Three have been prepared. When using ligands containing phosphine and chalcogenide groups, amination has occurred at the phosphorus centre, resulting in the formation of phosphazenes. Most of the reactions have been successful; however the hygroscopic nature of the P=N functionality has resulted in hydrolysis and the formation of phosphine oxides in some cases. Successful reactions have mainly used the aminating agent *o*-mesitylenesulfonyl hydroxylamine (MSH). The S=O groups on the MSH anion have resulted in a number of interesting cation-anion hydrogen-bonding patterns. Also very interestingly, reactions to exchange the MSH anion for a more organic anion such as BPh_4 has resulted in extreme shifts in the $^{31}P\{^1H\}$ NMR spectrum; it can be concluded that these could be due to cyclisation of the aminated groups as seen elsewhere, but further tests would need to be carried out to establish this for certain.

Chapter Five

~Catalytic Investigations ~

5.1 – AIMS OF THE CHAPTER

The main aim of the work in this Chapter was to establish the catalytic capabilities of the ligands and subsequent Pd(II) complexes prepared in previous Chapters. This would be carried out using Heck C-C bond formation as an initial catalysis reaction. It was envisaged that should the reactions prove successful at high catalyst loadings, the reaction conditions could be changed to maximise the TON's of the catalytic processes.

5.2 – HECK REACTIONS USING SOME Pd(II) CHAPTER TWO COMPLEXES

Having prepared a large number of potentially chelating phosphine-chalcogenide ligands and their subsequent Pd(II) dihalides, it was decided to test these complexes for their catalytic activity, initially in the Heck C-C bond formation reaction. The reaction was carried out using iodobenzene and styrene, using tributylamine as base (Equation 5.1). The reaction was carried out at 125 °C in dimethylformamide, and the product was isolated using one aqueous and one KCN (aq) washing, followed by crystallisation with cold HPLC grade methanol.

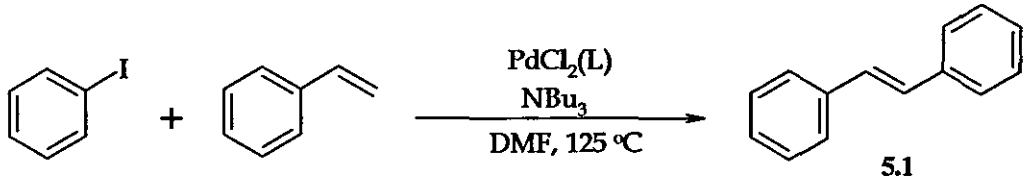

Equation 5.1 – Heck reaction used for catalysis experiments

It was decided that, should the reactions prove successful and, the complexes prepared prove to catalyse the transformation of iodobenzene, reaction conditions could then be optimised to obtain fastest rates and high turnover numbers (TON, defined as the number of moles of *t*-stilbene **5.1** formed divided by the number of moles of catalyst used). Table 5.1a shows results of the initial catalysis investigations. These results show that all of the Pd-L complexes prepared act as catalysts for the Heck reaction. The first two reactions attempted were performed in duplicate to check results and optimise yields. Other experiments were carried out as single reactions. Yields are of isolated *trans*-stilbene, hence *in-situ* yields may have been greater.

Table 5.1a – Results from Heck Reactions

Entry	Catalyst	Loading (x 10^{-5} mol)	Time (h)	Yield (%)	TON	TOF (g/h)
1	**2.8**	3.65	72	63	85	1.18
2	**2.9**	3.53	72	60	83	1.15
3	**2.25**	3.60	72	59	82	1.13
4	**2.31**	3.56	72	65	87	1.21
5	**2.26**	3.48	72	68	97	1.35
6	$PdCl_2\{Ph_2P(CH)_2PPh_2\}$ [109]	3.62	72	69	94	1.31
7	$PdCl_2\{Ph_2P(CH_2)_2PPh_2\}$ [109]	3.61	72	58	79	1.10
8	**2.41**	3.56	72	-	-	-
9	**2.42**	3.59	72	74	103	1.43
10	**2.42**	3.56	24	65	89	3.72
11	**2.42**	0.15	72	70	2015	27.99
12	**2.42**	0.017	72	65	19102	265.31
13	**2.43**	3.56	72	56	78	1.08
14	**2.48**	3.59	72	64	88	1.22
15	**2.48**	3.56	24	53	72	3.00
16	**2.48**	0.07	72	70	4949	68.74
17	**2.45**	3.49	72	49	79	1.10
18	**2.44**	3.60	72	71	98	1.36
19	**2.44**	3.56	24	59	81	3.38
20	**2.44**	0.13	72	66	2426	33.59
21	**2.47**	3.64	72	57	79	1.10

Table 5.1b – Chapter Two Complexes Used For Heck Reactions

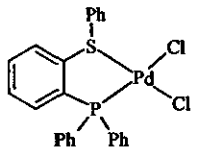

2.8

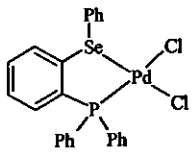

2.9

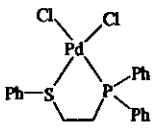

2.25

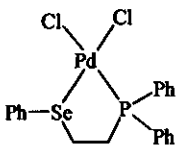

2.26

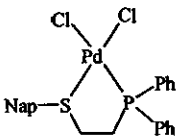

2.31

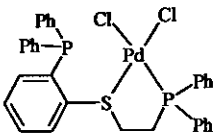

2.41

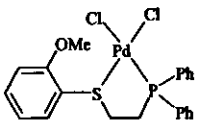

2.42

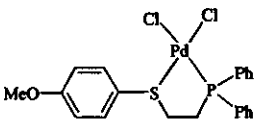

2.43

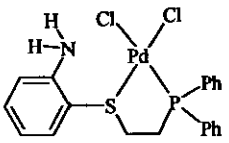

2.44

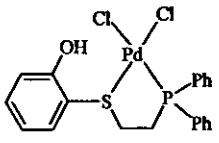

2.45

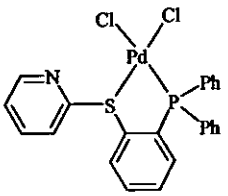

2.47

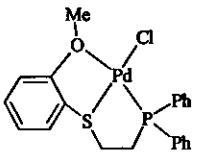

2.48

The results obtained also show that high yields can be obtained, even in some cases (entries 5, 9 and 18) better than those for the chelating diphosphine complexes (entries 6 & 7). These higher yields are made more interesting by the fact that some are obtained using the potentially tridentate P/S/*o*-OMe system **2.42**, and P/S/NH_2 system **2.44**, a trend which could be investigated further. Complex **2.43**, containing the *p*-OMe ligand, also gave a fairly good yield and hence TON. All of the products were pure as shown by ^{1}H NMR analysis, with some showing a small amount of $[HNBu_3^n]^+[I]^-$ side product. Signs of this impurity can be observed visually in the quality of the product formed, and the purity is generally a factor of how well the crude material, after reduction of the solvent, is washed with HPLC methanol.

The reactions involving the two bidentate phosphine/chalcogenide ligands (Entries 1-4) gave inconclusive results. Both phosphine sulfide complexes (**2.8** and **2.25**) gave fairly low isolated yields (63 and 59%). However, comparisons with the phosphine/selenide ligands are difficult, due to the fact that **2.9**, containing an aryl-based selenide, gave a lower yield (60%), whilst **2.26**, containing an alkyl-based selenide gave a slightly improved yield of 68%. However, encouragingly, both complexes containing the $X(CH_2)_2PPh_2$ (X = S/Se, **2.25** and **2.26**) group gave better results than the analogous diphosphine (Entry 7).[109]

The only reaction which gave poor results was that when using PdCl(**2.32**), **2.41**, as catalyst. Much of the crude material when reduced to dryness stayed as an oil at r.t., suggesting that the starting materials, all of which except the catalysts are liquids, were present. The lack of catalytic activity could be explained if all three donor atoms of the ligand (2 x P and S) were bound to the Pd centre. In contrast to a labile Pd-OMe bond, a second Pd-P bond would be relatively strong, and could adversely affect any potential catalytic activity.

Three reactions were also carried out using a reduced reaction time of 24 h. The complexes which gave some of the best yields in the initial 72 h experiments, **2.42** (Entry 9), **2.48** (Entry 14) and **2.44** (Entry 19) were used for these. As might be expected, these gave reduced yields and hence reduced TONs, however due to the reaction time result in better Turnover Frequencies (TOF). This may suggest that the

Heck reactions are quick to begin with, but then slow down due to consumption of reactants.

Catalyst concentrations play a major role in these experiments. A reaction containing around four times the previously used catalyst loadings was carried out using **2.8**. This reaction changed colour without the need for a higher temperature, and was carried out for 24 h. A combination of these conditions resulted in the yield obtained (46%) being the lowest of those that formed any product. Whilst being unsure of the deciding factor (*i.e.* time or concentration) as to the low yield, it can be assumed by the reasonable results obtained from other reactions carried out for 24 h that adding too much catalyst does adversely affect the reaction.

Due to the high catalyst loading used for initial experiments, *i.e.* 3.56×10^{-5} mol, TONs obtained were relatively low. Whilst this gave an indication that the complexes were acting as catalysts, it gave little indication of their efficiency. Therefore, experiments were carried out with catalyst loadings of 0.7×10^{-6} mol (for **2.48**), 1.3×10^{-6} mol (**2.44**) and 1.5×10^{-6} mol (**2.45**). These used the same reaction conditions of 3 d, at 125 °C in DMF. The yields obtained were not too dissimilar to those obtained using higher catalyst loading, only around 5% lower for both **2.48** and **2.44.** As a result of this, the TONs are shown to be much higher, between 2000-5000.

In order to investigate how much lower the catalyst loading could be taken, 1 cm^3 of a solution of **2.42** (0.003 g in 35 cm^3 DMF) was taken to obtain a catalyst loading of 1.7×10^{-7} mol. The reaction took on the familiar light brown colour after around 2 h, and upon completion gave a yield of *t*-stilbene of 65 %. Whilst this is slightly lower again than the previous experiment, for such a low catalyst loading, it is still a respectable yield. The TON and TOF obtained from this experiment (19102 and 265 respectively) show that **2.42** is a very efficient system for catalysis of the Heck reaction. Primary investigations into the catalytic suitability of these complexes for Heck coupling are promising, and experiments to ascertain the upper limit of TON and TOF for **2.42** and other complexes should show equally promising results.

5.3 – HECK REACTIONS USING SOME Pd(II) CHAPTER THREE COMPLEXES

Heck reactions were also carried out using complexes containing phospha-adamantane-based ligands. These were performed under the same conditions as in Chapter 5.1. The results are shown in Table 5.2a.

Table 5.2a – Results from Heck Reactions using Phospha-adamantane ligands

Entry	Catalyst	Loading (x 10^{-5} mol)	Time (h)	Yield (%)	TON	TOF (g/h)
22	**3.10**	3.60	72	70	95	1.32
23	**3.10**	0.15	72	65	2123	29.49
24	**3.10**	0.85	72	61	420	5.84
25	**3.10**	0.017	72	69	19888	276.22
26	**3.10**	0.0085	72	62	35963	499
27	**3.10**	0.000085	72	68	3,900000	54663
28	**3.10**	1.76	1	66	184	184
29	**3.8**	3.60	72	59	80	1.12
30	**3.8**	0.15	72	69	2254	31.31
31	**3.8**	0.85	72	73	420	5.84
32	**3.8**	0.017	72	63	18158	252.21
33	**3.8**	0.0085	72	52	30480	423
34	**3.8**	0.87	1	44	244	244
35	**3.13**	3.60	72	59	80	1.12
36	**3.13**	0.15	72	59	1927	26.77
37	**3.13**	0.85	72	68	392	5.44
38	**3.13**	0.017	72	64	18447	256.21
39	**3.13**	0.0085	72	32	18536	257
40	**3.13**	1.8	1	49	134	134
41	**3.9**	2.42	72	13	26	0.37
42	**3.7**	3.60	72	15	20	0.28
43	**3.19**	0.15	72	53	1731	24.05

Table 5.2b – Chapter Three Complexes Used For Heck Reactions

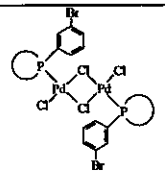

3.7

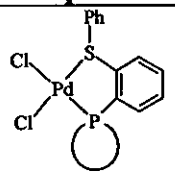

3.8

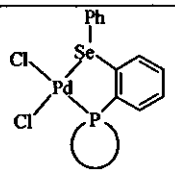

3.9

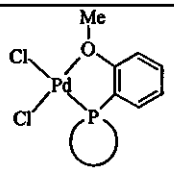

3.10

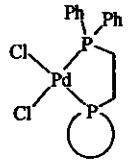

3.13

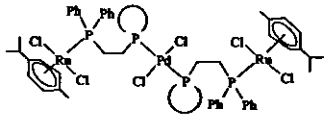

3.19

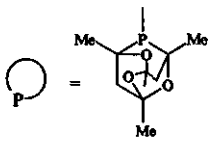

Catalytic activity was shown by all Pd(II) complexes used. As in Chapter 5.1, ^{1}H NMR spectra taken were compared with commercially available *t*-stilbene. Under the most widely used reaction conditions of reacting in DMF at 125 °C for 72 h, the poorest catalyst was the palladium dimer **3.7** (Entry 42). This produced a TON of 20 at a reasonably high loading. It had been seen in previous experiments that the dimer structure is unstable at high temperatures and the metal comes out of solution. It is probable that this occurred with the palladium dimer as the solution turned dark black when heated to 125 °C as the experimental parameters required.

Only a limited amount of catalytic behaviour was shown by compound **3.9** (entry 41). The yield obtained from the reaction (13%) is very uncharacteristic of almost all of this type of compound prepared. This is also rather surprising, as both compounds **2.9** and **2.26** (Entries 2 and 5, Table 5.1a) exhibited efficient catalytic behaviour, giving isolated yields of 60 and 68% respectively when using similar catalyst loadings of around 3.6×10^{-5} mol. It could be assumed that this was a problem with the specific compound, as the analogous sulfide-containing complex **3.8** gave no such problems.

Trinuclear compound **3.19** also catalysed the same Heck reaction. This gave a better yield than **3.9** and **3.7** of 53%, which, when using a catalyst loading of 0.15×10^{-5} mol meant that we obtained a respectable TON of 1731. Due mainly to other subsequent compounds exhibiting better catalytic activity, but also to a lack of **3.19**, we decided to concentrate on other compounds for optimisation.

Compounds **3.8**, **3.10** and **3.13** all produced good yields at high loadings. Catalyst **3.10** (Entry 22) produced the best isolated yield of 70% whilst **3.8** and **3.13** gave 59% yields (Entries 29 and 35). Once the nature of these products had been proved through comparison of the ^{1}H NMR spectra to commercially available *t*-stilbene, optimization of TON's was attempted for all three catalysts. Catalyst loadings of 0.15×10^{-5} mol and 0.017×10^{-5} mol were attempted, the latter requiring the preparation of stock solutions. Of the 0.15×10^{-5} mol loadings, catalyst **3.8** proved to be the optimum complex producing a yield of 69% and TON of 2254. Complexes **3.10** and **3.13** produced yields of 65% and 59% respectively; all of these yields being similar to those achieved using higher loadings. All three were therefore considered

for lower catalytic loadings. For the 0.017 x 10^{-5} mol loadings, compound **3.10** was the most efficient with a yield of 69% and TON 19888. Compounds **3.8** and **3.13** produced yields of 63% and 64% respectively.

Further experiments were carried out to see how low the catalyst loading could be taken. Experiments were carried out using catalyst loadings around 8 x 10^{-8}. These reactions gave yields generally slightly lower than those obtained when using 100-fold higher catalyst loadings. For example, when using 8.5 x 10^{-8} moles of $PdCl_2$(SPh/Cytop), the yield of *trans*-stilbene reduced to 52%, from 73% when 8.5 x 10^{-6} moles of the same complex was used.

The concentration of compound **3.10** was taken lower again. The 8.5 x 10^{-6} moles in the initial DMF solution of **3.10** were diluted by a further 10000th to give 8.5 x 10^{-10} moles of catalyst. Upon reaction, this still gave a highly respectable yield of *trans*-stilbene (68%); indeed this was slightly higher than some of the previous runs using higher loadings. This result showed **3.10** to be an extremely efficient catalyst, with a TON of almost 4000000. This is more than comparable to the excellent turnover numbers obtained using the diphosphine complexes show in Table 5.1a (Entries 6 and 7).[109]

The efficiency of the catalysts had been tested extensively resulting in impressive turnover numbers, especially for compounds **3.8** and **3.10**. However, the turnover frequencies obtained in both Chapters 5.1 and 5.2 were relatively low, due to the fairly long reaction times used for most Heck couplings (72 h). The same reactions were carried out over just 1 h, using catalysts **3.4**, **3.10**, **3.13**. Despite the much-shortened reaction times, during the reactions all the solutions became darker, a sign the couplings had worked. Indeed, the subsequent yields of *t*-stilbene (66, 44 and 49%, Entries 28, 34 and 40 respectively) indicate that the adamantane-containing complexes act efficiently as catalysts, not only in terms of amount of catalyst required, but also the amount of time needed for successful conversion. Compound **3.10** was once again shown to be the most effective, indeed the yield and hence turnover number obtained when reacting over just 1 h was only very slightly lower than that when using a very similar catalyst loading but an almost 3 d longer reaction time.

5.4 – POSSIBLE CATALYTIC CYCLES

With the suitability of the complexes for use in the Heck reaction established, and the limits of their efficiency primarily investigated, we began to think about the possible mechanisms by which these reactions may proceed. The most established, and until recently, most widely regarded catalytic cycle for the Heck reaction involved Pd(0) and Pd(II) species, the general form of which can be seen in Chapter One (Scheme 1.9). The initial oxidative addition reaction of the Pd(0) species is followed by addition of the alkene across the metal-carbon bond. The product is formed by β-hydrogen elimination.

Recent advances have resulted in two new theories being postulated. The first of these, an example of which was reported by Shaw *et al*,[149] is the formation of Pd(II) and Pd(IV) species during the course of the reaction. This is shown in Scheme

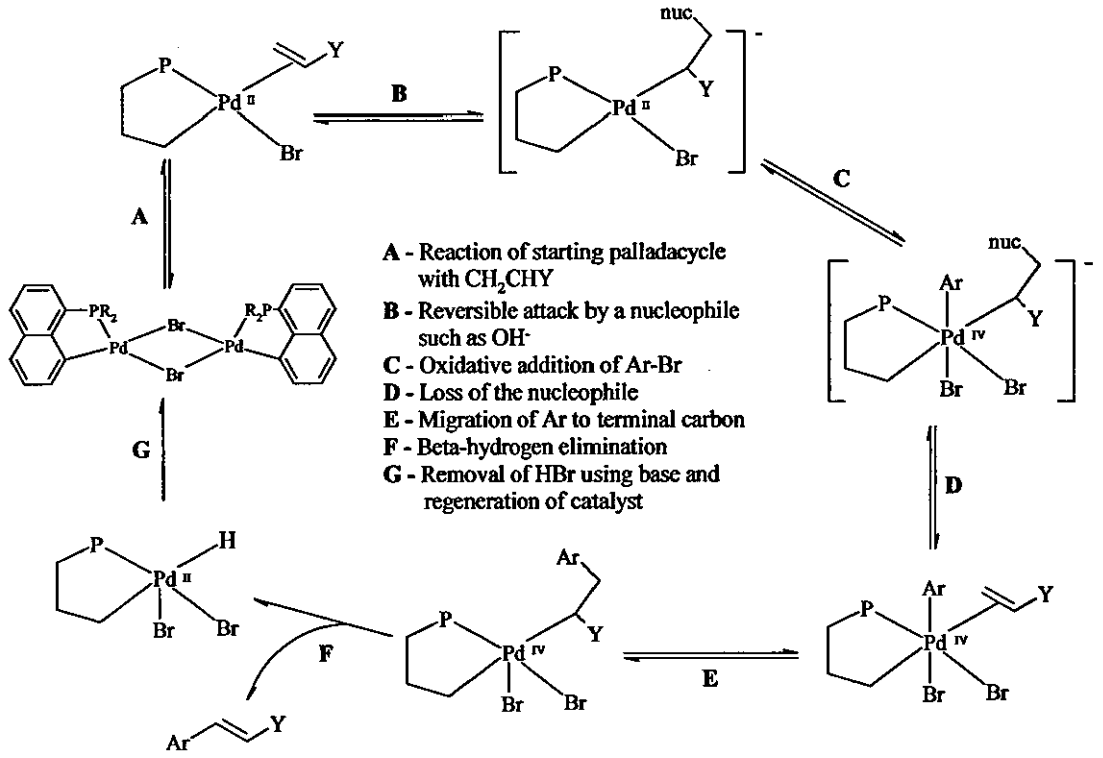

Scheme 5.1 - Heck Reaction mechanism proposed by Shaw

5.1. The main steps of the process can be seen within Scheme 5.1. The main difference between the Pd(0)/Pd(II) cycle and this is the nucleophilic attack on the Pd(II) coordinated alkene, which in turn promotes the oxidative addition of the aryl-

bromide starting material. Following migration of the aromatic group from the Pd(IV) centre to the terminal carbon of the alkyl chain, the *trans*- alkene is lost *via* β-hydrogen elimination, as in Scheme 1.9.

A further theory, postulated recently is that Pd(0) nanoparticles and colloidal systems prepared both intentionally and formed from degradation of higher oxidation state complexes are catalysts for the Heck reaction. de Vries and co-workers have put forward one such proposal recently.[150] This can be seen in Scheme 5.2.

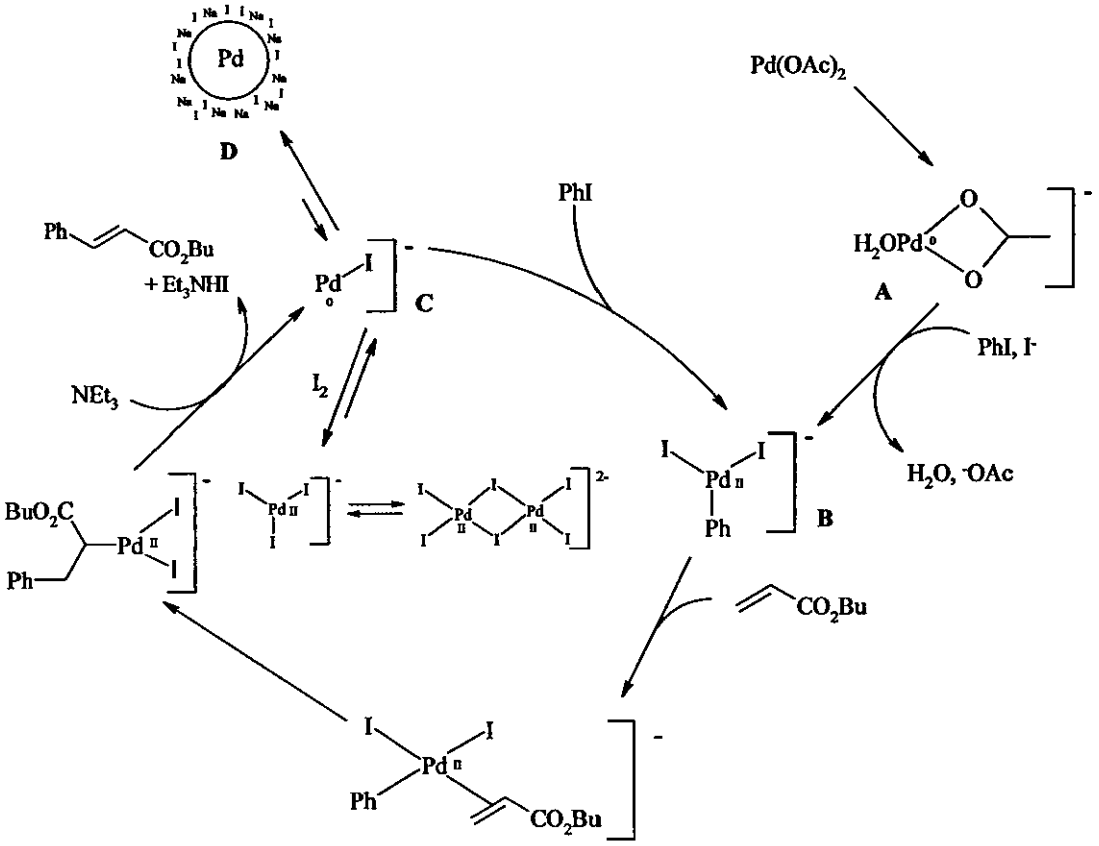

Scheme 5.2 - Heck Reaction mechanism proposed by de Vries

The reaction proceeds *via* similar reactions to those in the other two catalytic cycles mentioned previously. The Pd(0) species $H_2OPd(OAc)^-$, **A**, formed by reduction of $Pd(OAc)_2$, undergoes oxidative addition of the aryl-iodide. Insertion of an olefin across the metal after formation of the olefin complex is followed by β-hydrogen elimination of the product. The Pd(0) species $Pd\text{-}I^-$, **C** can then react with I_2, form soluble nanoparticles such as **D** or react with further aromatic halide to reform PdI_2Ph^-, **B**.

All three of the proposed mechanisms show plausible routes by which the complexes prepared in previous Chapters could react. Obviously the mechanisms shown are quite specific to the starting transition metal complexes prepared; the Shaw route, for example uses palladacycles whereas our complexes are of type $PdCl_2(L)_2$. It could be anticipated that catalytic cycles for compounds in this thesis would follow the route shown in Scheme 1.9; however a number of mechanistic studies would need to be carried out in order to ascertain this.

5.5 – CONCLUSIONS

The suitability of ligands and complexes synthesised in Chapters Two and Three has been analysed with respect to Heck C-C bond formation; these have given extremely interesting and promising results. Almost all complexes prepared showed some signs of catalytic activity, with some being as good as and better than established catalysts for the same reaction. The potential for optimisation of these catalytic values is large and could be a direction for further work to take.

Chapter Six

~Experimental ~

Unless otherwise stated, all preparations of phosphines were carried out under an inert atmosphere, using standard Schlenk-line techniques and freeze-thaw cycles where necessary. Solvents were purchased from Aldrich, Lancaster or Fisher, and deoxygenated before use where appropriate. Diethyl ether, toluene and tetrohydrofuran were distilled over sodium, whilst dichloromethane and acetonitrile were distilled over calcium hydride, both under an atmosphere of nitrogen.

The transition metal complexes Pd(Me)Cl(cod),[37] $PdCl_2$(cod),[151] $PtCl_2$(cod),[152] $PtMe_2$(cod),[153] $\{RuCl(\mu\text{-}Cl)(\eta^6\text{-}p\text{-cymene})\}_2$,[154] $\{RhCl(\mu\text{-}Cl)(\eta^5C_5(CH_3)_5)\}_2$, $\{IrCl(\mu\text{-}Cl)(\eta^5C_5(CH_3)_5)\}_2$ [155] and [AuCl(tht)][156] were all prepared according to the stated literature methods. $PdCl_2(MeCN)_2$ and $PdCl_2(PhCN)_2$ were purchased from Aldrich. Other starting materials were prepared using slightly changed known methods; these are shown throughout the experimental section.

^1H NMR spectra were recorded on a Bruker AC250 FT or FX400 FT spectrometer, with δ referenced to external tetramethylsilane. $^{31}P\{^1H\}$ NMR spectra were recorded on either a JEOL FX90Q, Bruker AC250 FT or FX400 FT spectrometer, with δ referenced to external H_3PO_4. Infra-red spectra were recorded as KBr pellets on a Perkin-Elmer System 2000 Fourier-transform spectrometer. Microanalyses were carried out by the Loughborough University Chemistry Department service. Fast atom bombardment (FAB), Electron Impact (EI) or Electrospray mass spectrometry were carried out by either the Swansea EPSRC Mass Spectrometry service or the Loughborough University Chemistry Department service. X-ray crystallography measurements were made on a Bruker AXS SMART 1000 CCD area-detector diffractometer using sealed-tube graphite-monochromated Mo–K_α radiation and narrow frame exposures (0.3°). Cell parameters were refined from the observed (ω) angles of all strong reflections in each data set. Intensities were corrected semiempirically for absorption, based on symmetry-equivalent and repeated reflections. All structures were refined on F^2 values for all unique data by full-matrix least-squares. Structural refinements were performed with full-matrix least-squares based on F2 by using the program SHELXTL.

6.1 - CHAPTER TWO EXPERIMENTAL

6.1.1 - Preparation of 2.1 – Method 1

Preparation of *o*-C_6H_4(SPh)Br

1,2 dibromobenzene (14.990 g, 63.5 mmol) and KOH (3.6 g, 64 mmol) were dissolved in dimethylacetamide (100 cm^3) by heating under reflux under N_2. Benzenethiol (7.0 g, 63.5 mmol) was added to the stirring solution, resulting in an orange/red solution and the formation of a white precipitate. This reaction mixture was heated to 160 °C for 24 h. After cooling to r.t., H_2O (100 cm^3) was added, and the contents transferred to a separating funnel. CH_2Cl_2 (100 cm^3) was added, after separation H_2O (6 x 100 cm^3) was added to wash. The organic layer was reduced to dryness, and the resulting oil purified by distillation, with the product being collected at 160 °C at 0.1 mmHg. Yield: 9.995 g (59%). ^{1}H NMR δ(H) ppm ($CDCl_3$): 6.9-7.5 (9H, m, 9 x Ph H). Product used for next stage without any further characterisation.

Preparation of $C_6H_4(PPh_2)$(SPh) 2.1

Degassed *o*-C_6H_4(SPh)Br (0.513 g, 19 mmol) was dissolved in Et_2O (25 cm^3). At 0 °C, *n*-butyl lithium (1.25 cm^3, 1.6 M in hexanes) was added dropwise to the flask over 10 min. After stirring at this temperature for 30 min, r.t. for 30 min. and again at 0 °C for 30 min, the solution turned yellow. Ph_2PCl (0.427 g in 20 cm^3 Et_2O) was added to the solution dropwise over a period of 20 min, resulting in the formation of a white precipitate. After stirring for 2-3 h, the solution was separated from the precipitate *via* canular, and degassed Et_2O (30 cm^3) added to wash. Removal of the solvent *in vacuo* gave a yellow oil, which after addition of absolute EtOH (5 cm^3) and placing in the freezer for 4 d resulted in formation of a white solid, which was filtered and dried *in vacuo*. Yield: 0.164 g (22%); $^{31}P\{^1H\}$ δ(P) ppm ($CDCl_3$): –12 ppm. ^{1}H δ(H) ppm ($CDCl_3$): 6.9-7.5 (9H, m, 9 x Ph H).

6.1.2 - Preparation of 2.1 – Method 2

Preparation of *o*-$C_6H_4(PPh_2)Br$ 2.2 - Prepared with slight changes from a known procedure.[126]

o-bromoiodobenzene (15.69 g, 55.6 mmol, K(OAc) (5.93 g, 70 mmol) and $Pd(OAc)_2$ (22.06 cm^3 of a $5x10^{-3}$ M solution) were dissolved DMA (78 cm^3). Ph_2PH (10.325 g, 55 mmol) was slowly added to the reaction mixture, and the mixture was heated to 160 °C for 5 d. After this time, H_2O (50 cm^3) was added, and CH_2Cl_2 (2 x 50 cm^3) was added to extract. The organic layers were combined, washed with an aqueous KCl solution (60 cm^3) and dried over $MgSO_4$. The remaining red solution was reduced to minimal volume, resulting in the formation of a white solid. Residual DMA was decanted, the white solid filtered then washed with cold absolute EtOH, and dried *in vacuo*. Yield: 5.871 g (31%); $^{31}P\{^1H\}$ δ(P) ppm ($CDCl_3$): –4.9 ppm. ^1H δ(H): 7.16- 7.29 (m, 14 H, arom. H). FAB MS, *m/z*: 341 [M^+].

Preparation of $C_6H_4(PPh_2)(SPh)$ 2.1

PhSH (0.97 g, 8.8 mmol) and ground KOH (0.98 g, 17.4 mmol) were added to DMA (80 cm^3) and stirred at r.t. for *ca.* 1 h. Separately, compound **2.2** (3 g, 8.8 mmol) was dissolved in DMA (20 cm^3), and added to the reaction mixture in two portions. The yellow DMA solution was then heated to *ca.* 160 °C for 5 d. After cooling to r.t., H_2O (100 cm^3) was added, then CH_2Cl_2 (2 x 60 cm^3) added to extract. The combined organic extracts were washed with H_2O (50 cm^3), dried over $MgSO_4$ and reduced to *ca.* 10 cm^3. Further H_2O (30 cm^3) was added to produce a white suspension, and this was allowed to stir for 24 h. The water was decanted from the resulting wax, and cold absolute EtOH (20 cm^3) added. The resulting white solid was filtered and dried *in vacuo*. Yield: 1.674 g, (51%). $^{31}P\{^1H\}$ δ(P) ppm ($CDCl_3$): –12 ppm ($CDCl_3$). ^1H δ(H) ppm ($CDCl_3$): 7.19-7.45 (m, 19 H, Ar-H). IR (cm^{-1}) (KBr): 1432 (med, P-Ph/C-H), 1085, 1022 (sh, C-P, C-S). C H N % Expected for $C_{24}H_{19}PS$ (370): C 77.81, H 5.17; Found: 77.29, H 4.98.

6.1.3 – Preparation of $C_6H_4(SPh)((P(O)Ph_2)$, 2.3

Compound **2.1** (0.25 g, 0.68 mmol) was dissolved in THF (10 cm^3), and H_2O_2 (0.844 mmol) was added as a THF solution (2 cm^3). After stirring for 26 h, the reaction mixture was reduced to dryness *in vacuo*, H_2O (20 cm^3) was added along with CH_2Cl_2 (3 x 20 cm^3) to extract. The combined organic extracts were dried over $MgSO_4$, reduced to dryness and dried overnight *in vacuo* to give a white solid. Yield: 0.163 g, 63%. $^{31}P\{^1H\}$ δ(P) ppm ($CDCl_3$): 30 ppm ($CDCl_3$). ^1H NMR δ(H) ppm ($CDCl_3$): 6.84-7.51 (19H, m, 19 x Ar-H). IR (cm^{-1}) (KBr): 1252 (P=O), C H N: Expected for $C_{24}H_{19}OPS$: C 72.60, H 4.96; Found: C 72.72, H 5.14 %.

Oxaziridene **2.7** (see **6.1.5**) was also used in a similar reaction to give the same oxidised product **2.3**.

6.1.4 – Reaction of 2.3 with $\{RuCl_2(p\text{-cymene})\}_2$, 2.4 / $\{RhCl_2Cp^*\}_2$, 2.5

$\{RuCl_2(p\text{-cymene})\}_2$ (0.061 g, 0.10 mmol) or $\{RhCl_2Cp^*\}_2$ (0.080 g, 0.13 mmol) were dissolved in CH_2Cl_2 (7.5 cm^3), and **2.3** (0.1 g, 0.26 mmol or 0.077 g, 0.20 mmol) was added. The mixture was allowed to stir for *ca.* 24 h, after which an aliquot was taken and an *in-situ* $^{31}P\{^1H\}$ NMR spectrum taken. This revealed little change, so the reaction was heated to 50 °C for 5 h. After this, the volume of both reactions was reduced to dryness, and the orange/red solid collected.

Yield (**2.4**): 0.063 g (91%). $^{31}P\{^1H\}$ δ(P) ppm ($CDCl_3$): 34.2. ^1H δ(H) ppm ($CDCl_3$): (all peaks extremely broad due to fluxionality: 1.24, (s, 3H, CH_3) 2.41 (sept, 1H, 6H), 2.92-2.99, d, 2 x CH_3), 7.39-7.98 (m, arom. H). IR (cm^{-1}) (KBr): 3048 (str, C-H deformations), 1440 (sh, P-Ph), 1261 (w, coordinated P=O), 292 (w, Ru-Cl). C H N Expected for $C_{34}H_{30}Cl_2OPSRu.0.5CH_2Cl_2$ (732): C 56.51, H 4.26; Found: C 57.08, H 5.11%.

Yield (**2.5**): 0.055 g (67%). $^{31}P\{^1H\}$ δ(P) ppm ($CDCl_3$) 34.1. IR (cm^{-1}) (KBr): 1447 (str, P-Ph), 1260 (v.weak, coordinated P=O), 1118, 1082, 1027 (med, C-P, C-S), 277 (sh, Rh-Cl). C H N: Expected for $C_{44}H_{34}SPClRh.3CH_2Cl_2$ (1015): C 55.60, H 3.98; Found: C 56.11, H 5.24%.

6.1.5 – Preparation of oxaziridene 2.7

Compound **2.6** (Aldrich) (0.750 g, 3.5 mmol) was dissolved in CH_2Cl_2 (50 cm^3), and *m*-CPBA (0.61 g, 3.5 mmol) was added. After stirring for 3 h, H_2O (3 x 50 cm^3) was added to remove any side-products, along with, separately, Na_2SO_3 (aq, 30 cm^3), $NaHCO_3$ (aq, 30 cm^3) and NaCl (aq, 30 cm^3). After separation, the organic layer was reduced to dryness, and the bright white solid collected. Yield: 0.73 g (90%). ^1H δ(H) ppm ($CDCl_3$): (see diagram below) 0.97, 1.14 (2 x s, 2 x 3H, C_A and C_C CH_3), 1.69-2.10 (m, 4H, C_I and C_J), 2.5-2.6 (2 broad, poorly resolved triplets, 1H, C_E), 3.02, 3.20 (2 x d, 2 x CH_2, C_D and C_F CH_2). $^{13}C\{^1H\}$ δ(C) ppm ($CDCl_3$): (see diagram below) 17.9, 18.3 (2 x s, 2 x CH_3, C_A and C_C), 25.6, 27.4 (2 x s, 2 x CH_2, C_D and C_I), 32.5 (s, CH_2, C_F), 44.7 (s, CH_3, C_E), 47.2 (s, CH_2, C_J), 52.9 (s, quat., C_B), 97.7 (s, quat., C_H), 160.8 (s, quat., C_G).

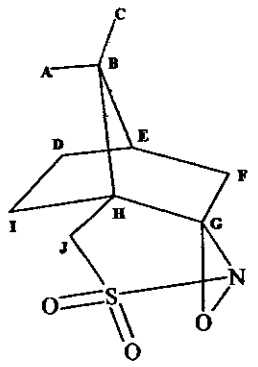

6.1.6 – Preparation of $PdCl_2$(2.1), 2.8

Compound **2.1** (0.150 g, 0.40 mmol) was dissolved in CH_2Cl_2 (10 cm^3) and added dropwise to a solution of $PdCl_2$(cod) (0.169 g, 0.40 mmol in 10 cm^3 CH_2Cl_2). After stirring for *ca.* 3 h, the volume of the yellow solution was reduced to 2-3 cm^3, and Et_2O (60 cm^3). The resulting bright yellow solid was filtered and dried *in vacuo*. Yield: 0.103 g (70 %). ^{31}P δ(P) ppm ($CDCl_3$): 58. ^1H δ(H) ppm ($CDCl_3$): 7.32-8.07 (m, 19H, PPh_2, C_6H_4 and SPh Ar-H). IR (cm^{-1}) (KBr): 3050 (P-Ar stretch), 1435 (Ar C=C), 744, 686 (Ar C-H), 335, 296 (med, 2 x Pd-Cl). C H N %: Calculated for $C_{24}H_{19}Cl_2PSPd.0.5CH_2Cl_2$ (590): C 49.86, H 3.33; Found: C 50.05, H 3.35.

6.1.7 - Preparation of Pd(Me)Cl(2.1), 2.9

Pd(Me)Cl(cod) (0.022 g, 0.084 mmol) was dissolved in $CDCl_3$ (2 cm^3), and **2.1** (0.028 g, 0.076 mmol) was added as a $CDCl_3$ solution (2 cm^3). After *ca.* 2 h stirring, a $^{31}P\{^1H\}$ NMR spectrum was taken of the sample. After this, Et_2O (50 cm^3) was added to yield a yellow/orange solid, which was filtered and dried *in vacuo*. Yield: 0.021 g (47%). $^{31}P\{^1H\}$ δ(P) ppm ($CDCl_3$): 51. C H N: Calculated for $C_{25}H_{22}ClPSPd$ (527): C 56.94, H 4.20; Found: C 56.42, H 3.91%.

6.1.8 – Preparation of $PtCl_2$(2.1), 2.10

$PtCl_2$(cod) (0.053 g, 0.142 mmol) was dissolved in CH_2Cl_2 (25 cm^3), and after stirring for *ca.* 5 min. Compound **2.1** (0.052 g, 0.142 mmol) was added, immediately turning the solution bright yellow. After stirring the reaction for *ca.* 2 h, the solution was reduced to 1-2 cm^3, and Et_2O (80 cm^3) was added. The resulting off-white precipitate **2.10** was filtered and dried *in vacuo*. Yield: 0.095 g, (53%). $^{31}P\{^1H\}$ δ(P) ppm ($CDCl_3$): 36 ppm (Pt–P product, ^1J(PtP) 3567 Hz). C H N: Calculated for $C_{24}H_{19}PSPtCl_2$ (636.4): C 50.95 H 4.81, Found: C 50.71, H 5.11%.

6.1.9 – Reaction of 2.1 with $\{RuCl_2(p\text{-cymene})\}_2$, 2.11

$\{RuCl_2(p\text{-cymene})\}_2$ (0.062g, 0.1 mmol) was dissolved in CH_2Cl_2 (10 cm^3). $C_6H_4(SPh)(PPh_2)$ (0.075 g, 0.2 mmol) was dissolved separately in CH_2Cl_2 (5 cm^3) and added to the stirring Ru-*p*-cymene solution. After stirring for 2 h, the volume was reduced to *ca.* 2-3 cm^3, and pet. ether (60-80 °C, 40 cm^3) was added to give a dark orange solid, which was filtered and collected. Yield: 0.10 g, 73%. $^{31}P\{^1H\}$ δ(P) ppm ($CDCl_3$): 57 ppm (Ru-P (chelated)). C H N: Calculated for $C_{34}H_{33}PSRuCl_2.0.75$ CH_2Cl_2 (740.3): 56.38, H 4.70; Found: C 56.30, H 4.74%.

$^{31}P\{^{1}H\}$ NMR spectroscopy tests using compound 2.10

6.1.10 – Preparation of $PtCl_2$(2.1)(PPh_3), 2.12

Excess PPh_3 was added to a $CDCl_3$ solution of **2.10**, and allowed to stir for *ca.* 2 h. The resulting solution was then analysed by $^{31}P\{^{1}H\}$ NMR spectroscopy. $^{31}P\{^{1}H\}$ δ(P) ppm ($CDCl_3$): –4.9 ppm (PPh_3 starting material), 17 (d, Pt-PPh_3, ^{1}J(Pt-P) 3281 Hz), 39 (d, Pt-P-S, P-monodentate, ^{1}J(Pt-P) 3510 Hz).

6.1.11 – Preparation of $PtCl_2$(2.1)(2.2), 2.13

o-$C_6H_4Br(PPh_2)$, **2.2** (0.011 g, 0.032 mmol) was dissolved in $CDCl_3$ and added to **2.10** (0.02 g, 0.031 mmol), and stirred for *ca.* 2 h. Initial analysis showed an incomplete reaction, therefore the mixture was left to stand for *ca.* 6 d. $^{31}P\{^{1}H\}$ δ(P) ppm ($CDCl_3$): -4.92 ppm ($BrPPh_2$ starting material), 18 (d, Pt-P(Br), ^{1}J(Pt-P) 3391 Hz, 37 (d, Pt-P-S (P-monodentate, ^{1}J(Pt-P) 3550 Hz).

6.1.12 – Preparation of $PtCl_2$(2.1)$_2$, 2.14

Compound **2.1** (0.011 g, 0.030 mmol) was dissolved in $CDCl_3$ (2 cm^3), added to **2.10** (0.019 g, 0.030 mmol in $CDCl_3$ (2 cm^3)) and stirred for 2 h. The resulting solution was analysed by $^{31}P\{^{1}H\}$ NMR spectroscopy. $^{31}P\{^{1}H\}$ δ(P) ppm ($CDCl_3$): 36 (**2.10** starting material), 25 (s, $PtCl_2$(P-S)$_2$ **2.14**, ^{1}J(Pt-P) 3508 Hz).

6.1.13 – Preparation of $C_6H_4(SPh)((P(S)Ph_2)$ 2.15

$C_6H_4(SPh)(PPh_2)$ **2.1** (0.15 g, 0.4 mmol) was dissolved in THF, and S_8 (0.025g, 0.01 mmol) was added as a solid. After heating to reflux for 1 h, the volume of solution was reduced to dryness to yield a white solid, which was collected. Yield: 0.078 g, (48%). $^{31}P\{^1H\}$ δ(P) ppm ($CDCl_3$): 42 (P=S). IR (cm^{-1}) (KBr): 2961 (C-H stretch), 689 (Ar deformation), 637 (s, P=S).

6.1.14 – Preparation of $C_6H_4(SPh)\{P(Se)Ph_2\}$ 2.16

$C_6H_4(SPh)(PPh_2)$ **2.1** (0.15 g, 0.405 mmol) was dissolved in toluene (25 cm^3) and selenium powder (0.032 g, 0.405 mmol) was added as a solid. This reaction mixture was heated to reflux for *ca.* 4 h, after which the clear solution was filtered to remove any remaining selenium. Reduction to dryness yielded an oil containing a small amount of selenium. The oil was redissolved in CH_2Cl_2 (5 cm^3), refiltered, and the volume reduced to dryness, yielding an off-white solid which was collected. Yield: 0.063 g, (35%). $^{31}P\{^1H\}$ δ(P) ppm ($CDCl_3$): 32.9 (product, ^1J(P-Se) 1159 Hz). C H N: Calc. for $C_{24}H_{19}PSSe$ (482): C, 64.14; H, 4.26%; Found: C, 64.64; H, 4.46%.

6.1.15 – Preparation of $C_6H_4(SePh)(PPh_2)$, 2.17

Ground KOH (0.284 g, 5.05 mmol) was dissolved in DMA (50 cm^3), PhSeH (0.579 g, 2.53 mmol) was added, and the resulting orange solution was degassed. **2.2** (0.784 g, 2.30 mmol) was dissolved separately in DMA (30 cm^3) and added to the stirring PhSeH solution over 5 min. After 3 d heating at 170 °C, H_2O (80 cm^3) was added, along with CH_2Cl_2 (2 x 50 cm^3). The organic extracts were combined, H_2O (50 cm^3) added to wash, dried over $MgSO_4$ and the volume reduced to *ca.* 5-10 cm^3. H_2O was added to form a white suspension; this was allowed to stir overnight to solidify, after which the clear water layer was decanted. Cold absolute EtOH (40 cm^3) was added to wash the resulting of-white solid **2.17**, and this was filtered and dried *in vacuo*. Yield: 0.504g, (53 %). $^{31}P\{^1H\}$ δ(P) ppm ($CDCl_3$): –9 ppm (product, ^3J(P-Se) 209 Hz). ^{77}Se δ(Se) ppm ($CDCl_3$): 205. ^1H δ(H) ppm ($CDCl_3$): 7.12-7.46 (m, 19H, Ph-H). IR (cm^{-1}) (KBr): 1435 (str, P-Ph), 1090, 1019 (sh, C-P, C-Se). C H N: Calc. for $C_{24}H_{19}PSe$ (417): C, 69.07; H, 4.59%; Found: C, 68.28; H, 4.40%.

6.1.16 – Small scale reactions of $PtCl_2$(cod) and Pd(Me)Cl(cod) with 2.17 - 2.18/2.19

$PtCl_2$(cod) (0.018 g, 0.048 mmol/Pd(Me)Cl(cod) (0.013 g, 0.048 mmol) were dissolved in a minimal amount of $CDCl_3$, and *o*-$C_6H_4(PPh_2)(SePh)$ (0.02 g, 0.048 mmol) was added to both stirring solutions. The reactions were left to stir for *ca.* 2 h, after which the solutions were analysed using $^{31}P\{^1H\}$ NMR spectroscopy.

No yields obtained due to nature of reactions.

$PtCl_2$: $^{31}P\{^1H\}$ δ(P) ppm ($CDCl_3$): 37 (Pt-P complex, ^1J(Pt-P) 3548 Hz).

Pd(Me)Cl: $^{31}P\{^1H\}$ δ(P) ($CDCl_3$): 54. ^1H δ(H) ppm: 1.65 (s, 3H, Pd-CH_3), 7.09-7.92 (m, 19 H, arom. H).

6.1.17 – Reaction of 2.17 with $\{RhCl_2Cp^*\}_2$, 2.20

$\{RhCl_2Cp^*\}_2$ (0.022 g, 0.036 mmol) was dissolved in MeOH (7.5 cm^3), and *o*-$C_6H_4(PPh_2)(SePh)$ (0.03 g, 0.072 mmol) was added. After allowing the reaction to stir for *ca.* 24 h, the red solution was analysed by $^{31}P\{^1H\}$ NMR spectroscopy (1 doublet at 50 ppm, 1 doublet at 63 ppm). The reaction was redissolved in MeOH (20 cm^3) and heated to reflux for 24 h. The sample was analysed by $^{31}P\{^1H\}$ NMR spectroscopy. $^{31}P\{^1H\}$ δ(P) ppm ($CDCl_3$): 50.1 & 51.4 (d, 55% of P-containing material, Rh-P-Se complex – chelated ligand), 63.4 & 64.8 ppm (d, 40% of P-containing material, Rh-P-Se complex – monodentate P-bound ligand).

6.1.18 - Preparation of $Ph_2P(CH_2)_2SPh$, 2.21.

Vinyldiphenylphosphine (0.5 g, 1.73 mmol) was placed in a Schlenk tube and heated to 110 °C. Thiophenol (0.191 g, 1.74 mmol) was then added and the reaction mixture was stirred for 5 min. AIBN (0.09 g) was added, visibly producing a gaseous side product. The mixture was stirred at 110 °C for 14 h, after which the temperature was turned to 80 °C, and the contents placed under vacuum for 6 h to eliminate volatile side products. The solid product was collected upon cooling. Yield: 0.49 g (88%). $^{31}P\{^1H\}$ δ(P) ppm ($CDCl_3$): –15 ($CH_2CH_2PPh_2$). ^1H δ(H) ppm : 2.41-2.48 & 2.89-2.99 (2 x dd, 4 H, 2 x CH_2), 7.22-7.31 (m, 18 H, Ar-H). FAB MS, *m/z*: 322 [M^+].

6.1.19 - Preparation of $Ph_2P(CH_2)_2SePh$, 2.22.

Compound **2.22** was prepared as above for **2.21**, using vinyldiphenylphosphine (0.3 g, 1.41 mmol), PhSeH (0.220 g, 1.4 mmol) and AIBN (0.053g). $^{31}P\{^1H\}$ δ(P) ppm ($CDCl_3$): –15 ($CH_2CH_2PPh_2$). ^1H δ(H) ppm ($CDCl_3$): 2.35-2.41 & 2.91-2.98 (2 x dd, 4 H, 2 x CH_2), 7.24-7.33 (m, 18 H, Ar-H). FAB MS, *m/z*: 369 [M^+].

6.1.20 – Preparation of $\{Ph_2P(CH_2)_2S(C_6H_4)p\text{-}Me\}$, 2.23.

Vinyldiphenylphosphine (0.518 g, 2.44 mmol) was heated to 110 °C, after which *p*-thiocresol (0.303 g, 2.44 mmol) and AIBN (0.02 g) were added. The mixture was stirred overnight, after which the temperature was reduced to 80 °C and the volatile components removed *in vacuo*. Yield: 0.602 g (73%). $^{31}P\{^1H\}$ δ(P) ppm ($CDCl_3$): –17 ($CH_2CH_2PPh_2$). ^1H δ(H) ppm ($CDCl_3$): 1.85 (s, 3 H, CH_3), 3.56 (m, 4 H, 2 x CH_2), 7.04-7.78 (m, 14 H, arom. H). FAB MS, *m/z*: 336 [M^+]. C H N; Calculated for $C_{21}H_{21}PS$ (336): C 75.06, H 8.39%; Found: C 74.37, H 8.78%.

6.1.21 – Preparation of $\{Ph_2P(CH_2)_2S(Naphthyl)\}$, 2.24.

Vinyldiphenylphosphine (0.943 g, 4.44 mmol) was heated to 110 °C, and 2-thionaphthol (0.712 g, 4.45 mmol) and AIBN (0.025 g) were added. The mixture was stirred for 16 h, the volatile components removed under vacuum as for **2.21-2.23**, and the solid product collected. Yield: 1.243 g (75%). $^{31}P\{^1H\}$ δ(P) ppm ($CDCl_3$): –17 ($CH_2CH_2PPh_2$). ^1H δ(H) ppm ($CDCl_3$): 3.75 (m, 4 H, 2 x CH_2), 7.12-7.82 (m, 18 H, Naphthyl and PPh_2 arom. H). FAB MS, *m/z*: 345 [M^+]. IR (cm^{-1}) (KBr): 3052 (med, Ar C-H), 1624 (med, naphthyl Ar), 1433 (sh, P-Ar), 812, 473 (vs, naphthyl). C H N: Calculated for $C_{24}H_{22}PS$ (345): C 83.55, H 6.38%; Found: C 84.10, H 6.79%.

6.1.22 – Preparation of $PdCl_2\{Ph_2P(CH_2)_2XPh\}$ (X = S/Se)

$Ph_2P(CH_2)_2XPh$ (0.1 g, 0.31 mmol (X = S) / 0.27 mmol (X = Se)) was dissolved in CH_2Cl_2 (5 cm^3) and added to $PdCl_2(cod)$ (0.089 g, 0.31 mmol where X = S, 0.077 g, 0.27 mmol where X = Se) in CH_2Cl_2 (10 cm^3). The mixtures were stirred for 4 h, after which the solutions were reduced to *ca.* 2 cm^3 in volume. Et_2O (70 cm^3) was then added to give bright yellow solids, which were filtered and dried *in vacuo*.

6.1.23 – Preparation of $PdCl_2$(2.21), 2.25

Yield: 0.109 g (70%). $^{31}P\{^1H\}$ δ(P) ppm (DMSO): 66 ($CH_2CH_2PPh_2$). ^1H δ(H) ppm ($CDCl_3$): 3.14 (v broad peak, 4H 2 x CH_2), 7.53-7.99 (m, 15H, PPh_2 and SPH Ar-H). IR (cm^{-1}) (KBr): 3074 (P-Ar C-H) 743, 685 (Ar C-H), 532 (P-Ar), 289 & 321 (sh, 2 x Pd-Cl). C H N; Calculated for $C_{20}H_{19}PSCl_2Pd$ (500): C 48.07, H 3.83%; Found: C 47.72, H 3.29%.

6.1.24 – Preparation of $PdCl_2$(2.22), 2.26

Yield: 0.081 g (55%). $^{31}P\{^1H\}$ δ(P) ppm (DMSO): 63 ($CH_2CH_2PPh_2$). ^1H δ(H) ppm ($CDCl_3$): 3.02 and 3.36 (2 x m, 4H, 2 x CH_2), 7.41-7.98 (m, 15H, PPh_2 and SPH Ar-H). IR (cm^{-1}) (KBr): 748, 688 (Ar C-H), 557 (C-Se-C), 525 (P-Ar), 291 & 320 (sh, 2 x Pd-Cl). C H N; Calculated for $C_{20}H_{19}PSeCl_2Pd$ (546): C 43.95, H 3.50%; Found: C 43.62, H 3.16%.

6.1.25 – Preparation of Pd(Me)Cl(2.21), 2.27

Compound **2.27** was prepared in the same way as **2.25** and **2.26**, using PdMeCl(cod) (0.081 g, 0.305 mmol), and $PPh_2(CH_2CH_2)SPh$ **2.21** (0.098 g, 0.305 mmol) in CH_2Cl_2 (2 x 2.5 cm^3). Yield: 0.13 g (66%). $^{31}P\{^1H\}$ δ(P) ppm (DMSO): 55. ^1H δ(H) ppm (DMSO): 1.00 (s, 3 H, Pd-CH_3), 2.79 (broad s, 4 H, 2 x CH_2), 7.37-7.97 (m, 18 H, PPh_2 & Se-Ph Ar-H). IR (cm^{-1}) (KBr): 1437 (P-Ar), 741, 691 (Ar C-H), 529 (C-Se-C stretch) 280 (1 x PdCl). C H N; Calculated for $C_{21}H_{22}PSClPd$ (480): C 52.5, H 4.61%; Found: C 53.2, H 5.01%.

6.1.26 – Preparation of Pd(Me)Cl(2.22), 2.28

Compound **2.28** was prepared in the same way as **2.25** and **2.26**, using PdMeCl(cod) (0.1 g, 0.37 mmol), and $PPh_2(CH_2CH_2)SePh$ **2.22** (0.139 g, 0.377 mmol) in CH_2Cl_2 (2 x 2.5 cm^3). Yield: 0.13 g (66%). $^{31}P\{^1H\}$ δ(P) ppm (DMSO): 55. ^1H δ(H) ppm (DMSO): 1.00 (s, 3H, Pd-CH_3), 2.79 (broad s, 4H, 2 x CH_2), 7.37-7.97 (m, 18H, PPh_2 & Se-Ph Ar-H). IR (cm^{-1}) (KBr): 1437 (P-Ar), 741, 691 (Ar C-H), 529 (C-Se-C stretch) 280 (1 x PdCl). C H N; Calculated for $C_{21}H_{22}PSeClPd$ (526): C 47.93, H 4.21%; Found: C 47.48 H 3.99%.

6.1.27 – Preparation of RuCl(*p*-cymene)(2.22), 2.29

$\{RuCl_2(p\text{-cymene})\}_2$ (0.05 g, 0.081 mmol) was dissolved in CH_2Cl_2 (5 cm^3), and $\{Ph_2P(CH_2)_2SePh\}$ **2.22** was added as a CH_2Cl_2 (5 cm^3) solution. The deep red solution was stirred for 3 h, and then reduced to *ca.* 2-3 cm^3. Et_2O (60 cm^3) was added to give a, orange precipitate, which was filtered and dried *in vacuo*. Yield: 0.245 g (71%). $^{31}P\{^1H\}$ δ(P) ppm ($CDCl_3$): 23. ^1H δ(H) ppm ($CDCl_3$): 0.84, (d, 6H, 2 x CH_3) 1.86, (s, 3H, CH_3) 2.5 (sept, 1H, 6H), 7.39-7.98 (m, 15 H, arom. H). C H N: Calc. for $C_{30}H_{33}PSeCl_2Ru$ (676): C 53.30, H 4.92%; Found: C 53.16, H 4.82%.

6.1.28 – $PtCl_2$(2.22), 2.30 was prepared in a similar way as **2.25-2.27**, starting with $PtCl_2(PhCN)_2$. Yield: 0.04 g (30%). $^{31}P\{^1H\}$ δ(P) ppm ($CDCl_3$): 40 (**2.30** product, ^1J(PtP) 3596. No Se coupling seen). ^1H δ(H) ppm ($CDCl_3$): 7.17-7.98 (m, 19H, PPh_2/SPh/C_6H_4 Ar-H). IR (cm^{-1}) (KBr): 1437 (P-Ar), 743, 689 (Ar C-H), 531 (C-Se-C stretch), 280, 325 (2 x Pt-Cl). C H N; Calculated for $C_{20}H_{19}PSeCl_2Pt$ (635): C 37.81, H 3.01%; Found: C 37.05, H 2.77%.

6.1.29 – Preparation of $PdCl_2$(2.24), 2.31

Compound **2.31** was prepared in much the same way as for **2.25-2.28**, starting with $PdCl_2$(cod), compound **2.24** (0.313 g, 0.840 mmol), and using Et_2O (50cm^3) and pet. ether (60-80 °C, 20 cm^3) for work-up. Yield: 0.374 g (81%). $^{31}P\{^1H\}$ δ(P) ppm ($CDCl_3$): 58. ^1H δ(H) ppm ($CDCl_3$): 2.65-3.10 (m, 4H, 2 x CH_2), 7.21-7.78 (Naphth/PPh_2 Ar-H). IR (cm^{-1}) (KBr): 3052 (P-Ar C-H stretch), 1433 (P-Ar), 822, 808, 745, 688 (Naphthyl Ar deform.) 329, 287 (2 x Pd-Cl).

6.1.30 - Preparation of $C_6H_4(SH)(PPh_2)$, 2.33 – Prepared with slight changes from a known procedure.[132]

^{n}BuLi (23.23 cm^3 of a 2.5 M solution in hexane) was added to a mixture of thiophenol (3 g, 27.2 mmol) and TMEDA (6.75 g, 58.1 mmol) in cyclohexane (30 cm^3) at 0 °C. The solution was stirred at r.t. overnight, upon which an off-white precipitate formed. The precipitate was filtered on a Schlenk frit, washed with hexanes (2 x 25 cm^3) and redissolved in THF (60 cm^3). Ph_2PCl (4.14 g, 18.8 mmol based on 70% conversion to *o*-$C_6H_4(SLi)(Li)$) was added via pressure equalising dropping funnel to the solution at –78 °C. After further stirring overnight at r.t., the solution was acidified with dilute cold sulphuric acid, and concentrated *in vacuo*. The residue was dissolved in Et_2O (50 cm^3), washed with H_2O (50 cm^3), dried over $MgSO_4$ and reduced to dryness to afford a grey solid, which was dried overnight *in vacuo*. Yield: 3.8 g (48%). $^{31}P\{^1H\}$ δ(P) ppm ($CDCl_3$): –12. ^1H δ(H) ppm ($CDCl_3$): 4.1 (s, 1H, SH), 7.2-7.45 (m, 14 H, 12 x PPh_2 Ar-H & 4 x C_6H_4). FAB^+ MS *m/z:* 293 [M^+].

6.1.31 – Preparation of $Ph_2P(CH_2)_2S(C_6H_4)o$-PPh_2, 2.32

Vinyldipenylphosphine (0.615 g, 2.90 mmol) was heated to 110 °C, and $C_6H_4(SH)(PPh_2)$ (0.853 g, 2.90 mmol) was added in several portions. After addition was complete, and after stirring for 5 min, AIBN (0.020 g) was added. The mixture was stirred for *ca.* 12 h, after which the temperature was reduced to 80 °C and the volatile components removed *in vacuo* to leave a yellow oil. Yield: 1.372 g (93%); $^{31}P\{^1H\}$ δ(P) ppm ($CDCl_3$): –16 ($CH_2CH_2PPh_2$), –13 ($C_6H_4PPh_2$). ^1H δ(H) ppm ($CDCl_3$): 2.25-2.43 & 2.75-2.97 (2 x dd, 4H, 2 x CH_2), 6.68-7.23 (m, 20H, 20 x PPh_2 Ar-H). FAB MS *m/z*: 507 [M^+], 321 ($Ph_2P(CH_2)_2S(C_6H_4)^+$); 293 ($C_6H_4(SH)(PPh_2)$); 133 (PPh_2^+).

6.1.32 – Preparation of *o*- and *p*- $Ph_2P(CH_2)_2S(C_6H_4)OMe$, 2.34 (*o*-) / 2.35 (*p*-)

The reaction was carried out in much the same way as for **2.32** above, using vinyldiphenylphosphine (0.593 g (*o*-) / 0.526 g (*p*-)), 2/4-methoxythiophenol (0.392 g / 0.347 g) and AIBN (0.014 g / 0.012 g). The reactions were stirred at 110 °C for 18 h, and then placed under vacuum for 6 h at 80 °C. The products were collected as a light brown solid (**2.34**) and a white waxy solid (**2.35**).

6.1.33 – Preparation of $Ph_2P(CH_2)_2S(C_6H_4)o$-OMe, 2.34

Yield: 0.82 g (83%). $^{31}P\{^1H\}$ δ(P) ppm ($CDCl_3$): –17 ($CH_2CH_2PPh_2$). ^1H δ(H) ppm ($CDCl_3$): 2.31-2.38 & 2.90-2.99 (2 x dd, 4H, 2 x CH_2), 3.82 (t, 3H, OCH_3, 7.11-7.22 (m, 12H, 12 x PPh_2 Ar-H). FAB MS *m/z*: 353 [M^+], 247 ($PPh_2CH_2CH_2S^+$); 185 (PPh_2^+); 139 ($C_6H_4(OMe)S^+$). IR (cm^{-1}) (neat on CsI plate): 3068 (P-Ar CH stretch), 1433 (O-Me stretch), 743, 696 (Ar C-H), 505 (P-Ar).

6.1.34 – Preparation of $Ph_2P(CH_2)_2S(C_6H_4)p$-OMe, 2.35

Yield: 0.57 g (65%). $^{31}P\{^1H\}$ δ(P) ($CDCl_3$): –17 ppm ($CH_2CH_2PPh_2$). ^1H δ(P) ppm ($CDCl_3$): 2.28-2.35 & 2.82-2.88 (2 x dd, 4H, 2 x CH_2), 3.80 (s, 3H, OMe CH_3), 6.82-6.85 (dd, 4H, 2 x Ar-H), 7.27-7.36 (m, 12H, PPh_2 Ar-H). FAB MS *m/z*: 353 [M^+], 247 ($PPh_2CH_2CH_2S^+$), 215 ($PPh_2CH_2CH_2^+$), 185 (PPh_2^+), 138 ($C_6H_4(OMe)S^+$). IR (cm^{-1}) (neat on CsI plate): 3053 (P-Ar CH stretch), 1492 (O-Me stretch), 1245 (Ar-O-Me), 1179 (Ar C-H stretch), 1029 (OMe), 740, 696 (Ar C-H), 510 (P-Ar).

6.1.35 - Preparation of {$Ph_2P(CH_2)_2S(C_6H_4)o$-OH}, 2.36

Vinyldiphenylphosphine (0.528 g, 2.5 mmol) was heated to 110 °C, and 2-hydroxythiophenol (0.31 g, 2.5 mmol) and AIBN (0.015 g) added. The mixture was stirred for 16 h, and the volatile components removed by placing under vacuum at 80 °C. The product was stored as a clear oil in the Schlenk tube used for the reaction. Yield: 0.501 g (60 %). $^{31}P\{^1H\}$ δ(P) ppm ($CDCl_3$): –17 ppm ($CH_2CH_2PPh_2$). ^1H δ(H) ppm ($CDCl_3$): 2.25-2.29 & 2.70-2.81 (2 x dd, 4H, 2 x CH_2), 7.00-7.86 (m, Ar-H). IR (cm^{-1}) (neat on CsI plate): 3394 (OH), 3069 (P-Ar C-H stretch), 1573 (Ar C=C), 748, 696 (Ar C-H), 507 (P-Ar).

6.1.36 – $Ph_2P(CH_2)_2S(C_6H_4)o$-NH_2, 2.37 was prepared in much the same way as **2.36**, starting with 2-aminothiophenol (0.655 g, 5.2 mmol). The product was also a yellow oil, which solidified to a waxy material upon cooling. Yield: 1.103 g (62%). $^{31}P\{^1H\}$ δ(P) ppm ($CDCl_3$) –17 ($CH_2CH_2PPh_2$). ^1H δ(H) ppm ($CDCl_3$): 2.29, 2.78 (2 x m, 2 x 2H, 2 x CH_2), 4.30 (s, 2H, NH_2), 6.68, 7.15 (2 x m, 4H, C_6H_4 Ar-H), 7.28-7.83 (m, 14H, PPh_2 Ar-H). FAB MS *m/z*: 337 [M^+]. IR (cm^{-1}) (neat on CsI plate): 3455, 3355 (NH_2), 3067 (P-Ar C-H stretch), 1605 (NH_2), 743, 696 (Ar C-H), 507 (P-Ar).

NMR experiments using 2.37 and Ph_2PCH_2OH

6.1.37 – Preparation of $PPh_2(CH_2)_2S(C_6H_4)o$-$NH(CH_2)PPh_2$, 2.38

Ph_2PCH_2OH (0.087 g, 0.41 mmol) was dissolved in MeOH (5 cm^3), and added to **2.37** (0.137 g, 0.41 mmol), also in MeOH (5 cm^3). The reaction was stirred for 6 h at r.t., after which the solvent was reduced to dryness and the product dried *in vacuo* for 24 h. Yield: 0.147 g (68%). $^{31}P\{^1H\}$ δ(P) ppm: –13 (NCH_2PPh_2), –17 ($SCH_2CH_2PPh_2$).

6.1.38 – Preparation of $[PPh_2(CH_2)_2S(C_6H_4)o$-$N\{(CH_2)PPh_2\}_2]$, 2.39

The reaction was carried out in much the same way as for **2.38**, using Ph_2PCH_2OH (0.204 g, 0.95 mmol) and **2.37** (0.16 g, 0.47 mmol) in a total of 10 cm^3 MeOH. Yield: 0.198 g (57%) $^{31}P\{^1H\}$ δ(P) ppm ($CDCl_3$): –13 (NCH_2PPh_2), –17 ($SCH_2CH_2PPh_2$).

6.1.39 – Preparation of $Ph_2P(C_6H_4)S(C_5H_5N)$, 2.40

Compound **2.33** (0.505 g, 1.72 mmol) and KOH (0.217 g, 3.86 mmol) were dissolved in DMA (40 cm^3), and bromopyridine (0.271 g, 1.71 mmol) in DMA (20 cm^3) was added dropwise. The reaction was stirred at 160 °C for 60 h, after which water (60 cm^3) was added. CH_2Cl_2 (2 x 50 cm^3) was added, the combined organic extracts dried over $MgSO_4$, and the volume of solution reduced to *ca.* 10 cm^3. H_2O (40 cm^3) was added, and the white suspension was stirred overnight. The remaining water was decanted from the waxy solid, and cold absolute EtOH added to yield the grey solid product, which was filtered and dried *in vacuo*. Yield: 0.213 g (33%). $^{31}P\{^1H\}$ δ(P) ppm ($CDCl_3$): –10 ($C_6H_4PPh_2$). ^1H δ(H) ppm ($CDCl_3$): 6.76, 6.97, 7.65 (3 poorly resolved doublets, 4H, C_6H_4(P/S) H), 7.27-7.41 (m, 14H, aromatic Pyridyl and PPh_2 H). FAB MS: *m/z* 359 [M^+].

6.1.40 – Preparation of $PdCl_2$(2.32), 2.41

Compound **2.32** (0.141 g, 0.278 mmol) was dissolved in CH_2Cl_2 (7.5 cm^3), and added dropwise to a solution of $PdCl_2$(cod) (0.072 g, 0.253 mmol) in CH_2Cl_2 (7.5 cm^3). The yellow solution was stirred for *ca.* 4 h, after which the volume was reduced to *ca.* 2-3 cm^3. Et_2O (60 cm^3) was added to crystallise a yellow solid, which was filtered and dried *in vacuo*. Yield 0.112 g (59%). $^{31}P\{^1H\}$ δ(P) ppm ($CDCl_3$): 40 ($CH_2CH_2PPh_2$) and 47 ($C_6H_4PPh_2$, ^2J(PP) 1554 Hz). FAB MS *m/z*: 649 [M^+ - Cl], 507 ($PPh_2(CH_2)_2S(C_6H_4)PPh_2^+$); 185 ($PPh_2^+$, due to loss of $PdCl_2$ ($PPh_2(CH_2)_2S(C_6H_4)$); 399 ($PPh_2(CH_2)_2^+$ + PPh_2^+). IR (cm^{-1}) (KBr): 3049 (Ar C-H), 741, 690 (Ar C-H stretches), 512 (Ar-P), 324, 280 (2 x Pd-Cl). C H N: Calc. for $C_{32}H_{28}P_2SCl_2Pd$ (683): C, 56.20; H, 4.05%; Found: C, 56.94; H, 4.05%.

6.1.41 – Preparation of $PdCl_2$(2.34), 2.42

{$Ph_2P(CH_2)_2S(C_6H_4)$*o*-OMe} **2.34** (0.239 g, 0.66 mmol) was dissolved in CH_2Cl_2 (15 cm^3) and added dropwise to a solution of $PdCl_2$(cod) in CH_2Cl_2 (15 cm^3). The solution was stirred for 2 h, after which the volume was reduced to 2-3 cm^3. Et_2O (75 cm^3) was added to yield the yellow product, which was dried *in vacuo* and collected. Yield: 0.302 g (85%). $^{31}P\{^1H\}$ δ(P) ppm (DMSO): 71 ($CH_2CH_2PPh_2$). ^1H δ(H) ppm (DMSO): 2.94-2.96 (br s, 4H, 2 x CH_2), 3.60 (s, 3H, OCH_3), 7.03-8.01 (m, 14H, PPh_2 and S-Ar Ar H). IR (cm^{-1}) (KBr): 1434 (Ar-OMe), 1105 (sh, C-OMe), 710, 689 (Ar CH), 528 (P-Ar), 281 & 315 (m, sh, 2 x Pd-Cl). C H N: Calc. for $C_{21}H_{21}OPSCl_2Pd$ (530): C, 47.61; H, 4.05%; Found: C, 47.05; H, 3.87%.

The following complexes were all prepared in the same way as **2.41/2.42**:

6.1.42 – Preparation of $PdCl_2$(2.35), 2.43 Yield: 0.302 g (85%). $^{31}P\{^1H\}$ δ(P) ppm (DMSO): 65 ($CH_2CH_2PPh_2$). ^1H δ(H) ppm (DMSO): 2.75 (broad m, 4H, 2 x CH_2), 3.80 (s, 3H, OCH_3), 6.91-7.92 (m, 14H, PPh_2 and C_6H_4 Ar-H). IR (cm^{-1}) (KBr): 1493 (str, Ar-OMe), 1435 (str, Ar-OMe), 1104 (Ar C-H stretch), 1026 (OMe), 710, 689 (Ar CH), 533 (P-Ar), 325, 283 (med, 2 x Pd-Cl). C H N: Calc. for $C_{21}H_{21}OPSCl_2Pd$ (530): C, 47.61; H, 4.05%; Found: C, 47.08; H, 3.76%.

6.1.43 – Preparation of $PdCl_2$(2.37), 2.44. Yield: 0.141 g (78%). ^{31}P $\{^1H\}$ δ(P) ppm (DMSO): 71. ^1H δ(H) ppm (DMSO): 2.94 (br s, 4H, 2 x CH_2), 6.62, 7.23 (2 t, 2H, 2 C_6H_4S/N Ar-H), 6.76 (d, 2H, 2 C_6H_4S/N Ar-H), 7.56-7.65 (m, 10H, PPh_2 Ar-H). IR (cm^{-1}) (KBr): 3393 (str, br, NH_2), 1615 (str, sh, NH_2), 1250 (w, sh, NH_2), 286 & 314 (m, sh, 2 x Pd-Cl). C H N: Calc. for $C_{21}H_{26}NPSCl_2Pd.0.25CH_2Cl_2$ (515): C 45.34, H 3.81, N 3.26%; Found: C 45.08, H 3.83, N 2.73%.

6.1.44 – Preparation of $PdCl_2$(2.36), 2.45. Yield: 0.157 g (80%). $^{31}P\{^1H\}$ δ(P) ppm: 70 ($CH_2CH_2PPh_2$). ^1H δ(H) ppm (DMSO): 2.96 (broad m, 4H, 2 x CH_2), 5.52 (s, 1H, OH), 6.73-7.96 (m, 14H, PPh_2 and C_6H_4 Ar-H). IR (cm^{-1}) (KBr): 3196 (br, OH), 746, 690 (Ar C-H), 532 (P-Ar), 326, 280 (med, 2 x Pd-Cl). C H N: Calc. for $C_{20}H_{19}OPSCl_2Pd.0.5CH_2Cl_2$ (557): C 44.21, H 3.53%; Found: C 44.21, H 3.32%.

6.1.45 – Preparation of $PtMe_2$(2.37), 2.46. Prepared in the same way as **2.41/2.42**, using $PtMe_2$(cod) as starting material. Yield: 0.075 g (70 %). $^{31}P\{^1H\}$ δ(P) ppm (DMSO): 46. ^1H δ(H) ppm (DMSO): 2.94, 2.32 (2 x m, 4H, 2 x CH_2), 4.96 (s, 2H, NH_2), 6.65, 7.16 (2 x m, 4H, 4 x C_6H_4S/N Ar-H), 6.76 (d, 2H, 2 C_6H_4S/N Ar-H), 7.41-7.71 (m, 10H, PPh_2 Ar-H). IR (cm^{-1}) (KBr): 3387 (br, NH_2), 1616 (str, sh, NH_2), 1253 (sh, NH_2). C H N: Calc. for $C_{22}H_{26}NPSPt$ (562): C 46.97, H 4.66, N 2.49%; Found: C 47.03, H 4.73, N 2.44%.

6.1.46 – Preparation of $PdCl_2$(2.40), 2.47. Yield: 0.075 g (68%). $^{31}P\{^1H\}$ δ(P) ppm (DMSO): 59. ^1H δ(H) ppm: 7.16-7.81 (m, PPh_2 Ar-H's, C_6H_4, & C_5H_5N). IR (cm^{-1}) (KBr): 3050 (med, Pyr C-H stretch), 1558, 1571, 1435, 1419 (sh, Pyr C=C, C=N), 1101 (sh, C-H deform.), 689 (Ar C-H), 545 (str, sh, P-Ar), 328, 290 (med, 2 x Pd-Cl). C H N: Calc. for $C_{23}H_{18}NPSCl_2Pd.0.25CH_2Cl_2$ (570): C 48.99, H 3.27, N 2.45%; Found: C 49.32, H 2.60, N 1.67%.

6.1.47 – Test reaction of 2.42 with $AgBF_4$, 2.48.

$AgBF_4$ (0.019 g, 0.100 mmol) was dissolved in CH_3NO_2 (5 cm^3), and added dropwise to a solution of compound **2.42** (0.053 g, 0.100 mmol) in CH_3NO_2 (20 cm^3) using slight warming. The clear yellow solution was allowed to stir overnight, after which the volume was reduced to 2 cm^3. Et_2O (50 cm^3) and pet. ether (60-80 °C, 40 cm^3) was added, to yield a bright yellow solid which was filtered and dried *in vacuo*. Yield: 0.045 g (81%). $^{31}P\{^1H\}$ δ(P) ppm: 69. IR (cm^{-1}) (KBr): 1586, 1479 (coordinated OMe), 1056 (v br., BF_4), 726, 690 (Ar C-H), 529 (P-Ar), 298 (w, 1 x Pd-Cl).

6.1.48 – Test reaction of 2.43 and $PdCl_2$(cod) with $AgBF_4$, 2.49.

$\{Ph_2P(CH_2)_2S(C_6H_4)p\text{-}OMe\}$ **2.35** (0.116 g, 0.33 mmol) in CH_2Cl_2 (5 cm^3) was added to $PdCl_2$(cod) (0.094 g, 0.33 mmol) in CH_2Cl_2 (10 cm^3), and the reaction mixture stirred for 1.5 h. $AgBF_4$ (0.064 g, 0.33 mmol) was added, causing a orange red precipitate to form, and this mixture was stirred overnight. The resulting red/brown mixture was reduced to *ca.* 3 cm^3 in volume, and Et_2O (60 cm^3) was added to form an orange precipitate, which was filtered and dried *in vacuo*. Yield: 0.125 g (72%). $^{31}P\{^1H\}$ δ(P) ppm: 44 ($PdCl_2$(**2.35**)$_2$, 62 (**2.43**), 69 (**2.49**).

6.2 – CHAPTER THREE EXPERIMENTAL

6.2.1 - Preparation of *o*-C_6H_4(Br)(PAd), 3.1

1,2-bromoiodobenzene (7.5 g, 26.5 mmol) was added to a solution of $Pd(OAc)_2$ (10.6 cm^3 of a 5 x 10^{-3} mol solution, 0.05 mmol) and K(OAc) (2.07 g, 29.2 mmol) in DMA (70 cm^3), and the whole mixture degassed. **1.113** (4.9 g, 26.5 mmol) was added dropwise over 20 min, and the mixture heated to reflux for 2 d. The solution was cooled, H_2O (50 cm^3) added and the product extracted into CH_2Cl_2 (2 x 50 cm^3). The organic extracts were combined and washed with a saturated KCl solution (50 cm^3), and dried over $MgSO_4$. The volume of the remaining solution was reduced to *ca.* 20 cm^3, and placed in the fridge. The resulting solid was filtered, washed with cold absolute ethanol (2 x 10 cm^3) and dried *in vacuo*. Yield: 5.3 g (55%). $^{31}P\{^1H\}$ δ(P) ppm ($CDCl_3$): –29.6. ^1H δ(H) ppm ($CDCl_3$): 1.22-2.10 (m, 16H, PAd CH_3/CH_2), 7.14, 7.26 (2 x t, 2H, 2 x Ar-H), 7.56, 8.19 (d, 2H, 2 x Ar-H). FAB MS, *m/z*: 371 [M^+].

6.2.2 - Preparation of *m*-C_6H_4(Br)(PAd), 3.2

Compound **3.2** was synthesised using a similar method to that for preparing **3.1**, using 1,3-bromoiodobenzene. Yield: 5.3 g, (55%). $^{31}P\{^1H\}$ δ(P) ppm ($CDCl_3$): –24.5. ^1H δ(H) ppm ($CDCl_3$): 1.24-2.07 (m, 16H, PAd CH_3/CH_2), 7.26 (q, 1H, Ar-H *m*- to PAd), 7.52 (q, 1H, Ar-H *o*- to PAd), 7.98 (q, 1H, Ar-H *p*- to PAd), 8.00 (t, 1H, Ar-H *o*- to both Br and PAd). FAB MS, *m/z*: 372 [$M^+ + 1$]. C H N: Calc. for $C_{16}H_{20}O_3PBr$ (371): C 51.79, H 5.43; Found: C 51.14, H 5.38 %.

6.2.3 - Preparation of *o*-(C_6H_4)(OMe)(PAd), 3.3

3.3 was prepared using a similar method to that for **3.1**, using *o*-iodoanisole and phospha-adamantane **1.113**. Yield: 0.430 g (67%). $^{31}P\{^1H\}$ δ(P) ppm ($CDCl_3$): –41.61. ^1H δ(H) ppm: 1.41-2.13 (m, 16H, adamantane CH_3/CH_2), 3.85 (s, 3H, OMe), 6.87-7.00 (2 x q, 2H, 2 x Ar-H), 7.35 (q, 1H, Ar-H), 8.09 (q, 1H, Ar-H). FAB MS *m/z*: 323 ($M^+ + 1$). C H N: Calc. for $C_{17}H_{23}PO_4$ (322): C 63.34, H 7.19; Found: C 62.72, H 7.28 %.

6.2.4 - Preparation of *o*-C_6H_4(SPh)(PAd), 3.4

3.1 (1 g, 2.694 mmol) was dissolved in DMA (30 cm^3). This was added to a separate solution of PhSH (0.297 g, 2.694 mmol) and KOH (0.34 g, 6.061 mmol) in DMA (40 cm^3). The reaction mixture was stirred at 160 °C for 5 d, after which water (70 cm^3) was added, giving a light brown suspension. CH_2Cl_2 (2 x 70 cm^3) was added, the combined organic extracts washed with H_2O (60 cm^3) and dried over $MgSO_4$. Reduction of the volume of solvent to *ca.* 10 cm^3, followed by addition of further H_2O (30 cm^3) gave a cloudy suspension. This was stirred for 16 h, and the resulting brown solid isolated by decanting the water. Cold absolute ethanol (25 cm^3) was added, and the resulting solid filtered and dried *in vacuo*. Yield: 0.609 g (56%). $^{31}P\{^1H\}$ δ(P) ppm ($CDCl_3$): –37.72. ^1C δ(C) ppm ($CDCl_3$): 26.6, 26.7 (s, 2 x PAd CH_3), 27.8 and 28.1, 28.3 and 28.5 (2 x d, 2 x PAd CH_3), 36.5 (s, PAd CH_2), 45.9 (d, PAd CH_2), 73.6 and 73.9, 74.3 and 74.4 (2 x d, 2 x quat. PAd C *ipso*- to P), 96.1, 96.9 (2 x s, 2 x quat. PAd C), 126.5, 127.5, 129.4, 130.1, 130.9, 131.0, 132.0, 133.9, 134.0 (9 x s, 9 x Ar-H), 134.4 and 134.7, 135.2 and 135.3, 145.5 and 145.8 (3 x d, 3 x quat. Ar-C). ^1H δ(H) ppm ($CDCl_3$): 1.35-2.35 (m, 16H, PAd, CH_2/CH_3), 7.27-7.50 (m, 9H, 9 x C_6H_4 and SPh Ar-H). C H N: Calc. for $C_{22}H_{25}SPO_3.CH_3CH_2OH$ (446): C 64.62, H 7.00; Found: C 65.98, H 6.60%.

6.2.5 – Preparation of *o*-C_6H_4(SePh)(PAd), 3.5

3.1 (0.373 g, 1.005 mmol) was dissolved in DMA (30 cm^3), and added dropwise to a separate solution of PhSeH (0.158 g, 1.005 mmol) and KOH (0.085 g, 1.110 mmol) in DMA (30 cm^3). The reaction mixture was stirred at 160 °C for 7 d under nitr, after which H_2O (60 cm^3) was added, turning the dark brown solution to a light brown suspension. CH_2Cl_2 (2 x 60 cm^3) was added to extract the product, the combined organic extracts were washed with H_2O (60 cm^3) and dried over $MgSO_4$. Reduction of the volume of solvent to *ca.* 15 cm^3, followed by addition of further H_2O (30 cm^3) gave a cloudy suspension. This was stirred for 12 h, resulting in the formation of a brown solid. The water was decanted, cold absolute ethanol (20 cm^3) added, and the resulting solid filtered and dried *in vacuo*. Yield: 0.178 g (40%). $^{31}P\{^1H\}$ δ(P) ppm ($CDCl_3$): –34.69 [^3J(P-Se) 198 Hz]. ^1H δ(H) ppm ($CDCl_3$): 1.35-2.10 (m, 16H, PAd,

CH_2/CH_3), 6.95-7.30 (m, 9H, 9 x C_6H_4 and SPh Ar-H). IR (cm^{-1}) (KBr): 2987 (Ar C-H), 1446 (Ar C=C), 1377 (Ar C-P), 1263 (C-Se), 445 (med, C-Se-C). C H N: Calc. for $C_{22}H_{25}SePO_3$ (447): C 59.07, H 5.63; Found: C 58.52, H 5.65%.

General procedure for the preparation of $[PdCl_2\{X\}]$ / $RuCl_2$(p-cymene){X} / $RhCl_2$(Cp){X} / Ir Cl_2(Cp){X} (X = phospha-adamantane based ligand)

The required amount of transition metal complex was dissolved in CH_2Cl_2 (10 cm^3). The corresponding amount of phosphine ligand {X} was weighed out and dissolved in CH_2Cl_2 (10 cm^3) in a conical flask. Whilst stirring the transition metal complex, the phosphine ligand was added dropwise. The mixture was left to stir for 3-4 h. The volume of solvent was then reduced to 2-3 cm^3. Excess Et_2O and pet ether 60-80 °C were added to give the solid product, which was filtered and dried *in vacuo*. The following complexes were all prepared using this general procedure:

6.2.6 - Preparation of $PdCl_2(3.1)_2$, 3.6

Yield 0.013 g (10%). $^{31}P\{^1H\}$ δ(P) ppm (d_6 DMSO): 1.25, 2.77 (s, $PdP(C_6H_4)Br$). ^1H δ(H) ppm (d_6 DMSO): 1.40, 1.41 (s, 3H), 1.51, 1.57 (s, 3H) 1.97-2.07 (m, 4H), 7.25-7.41 (m, 2H Ar-H), 7.62-7.70 (dd, 1H Ar-H), 8.35-8.43 (dd, 1H Ar-H). IR (cm^{-1}) (KBr): 2928 (Ar C-H), 1654 (Ar C=C), 1382 (C-P), 755 (C-Br), 248, 265 (2 x Pd-Cl). C H N: Calc. for $C_{32}H_{40}Pd_2Cl_4P_2O_6Br_2$ (1097): C 35.0, H 3.7; Found: C 40.0, H 4.2%.

6.2.7 - Preparation of $PdCl_2(3.2)_2$, 3.7

Yield 0.084 g (42%). $^{31}P\{^1H\}$ δ(P) ppm (d_6 DMSO): 7.27, 7.34 (s, $PdP(C_6H_4)Br$). ^1H δ(H) ppm (d_6 DMSO): 1.32, 1.37 (s, 3H), 1.48-1.58 (m, 6H) 1.70-1.81 (m, 4H), 7.18-7.23 (m, 1H Ar-H), 7.47-7.48 (m, 1H Ar-H) 7.86-7.95 (dd, 1H Ar-H), 8.12-8.16 (dd, 1H Ar-H). IR (cm^{-1}) (KBr): 2988 (Ar C-H), 1559 (Ar C=C), 1379 (C-P), 786 (C-Br), 220, 255 (2 x Pd-Cl). C H N: Calc. for $C_{32}H_{40}Pd_2Cl_4P_2O_6Br_2$ (1097): C 35.0, H 3.7; Found: C 39.4, H 4.2%.

6.2.8 - Preparation of $PdCl_2$(3.4), 3.8

Compound **3.4** (0.075 g, 0.187 mmol) was dissolved in CH_2Cl_2 (10 cm^3), and added dropwise to a separate solution of $PdCl_2(PhCN)_2$ (0.072 g, 0.187 mmol) in CH_2Cl_2 (10 cm^3). The bright yellow solution was allowed to stir for 4 h, after which the volume was reduced in volume to *ca.* 3 cm^3. Et_2O (50 cm^3) was added to give a yellow precipitate which was filtered and dried *in vacuo*. Yield: 0.089 g (82%). $^{31}P\{^1H\}$ δ(P) ppm (d_6 DMSO): 47.60 (s, $PdP(C_6H_4)SPh$). ^1H δ(H) ppm (d_6 DMSO): 1.25, 1.33 (s, 3H), 1.45, 1.49 (s, 3H) 1.81-1.98 (m, 4H), 7.30-7.41 (m, 3H Ar-H), 7.49-7.59 (m, 5H Ar-H) 8.35-8.38 (dd, 1H Ar-H). IR (cm^{-1}) (KBr): 2922 (Ar C-H), 1577 (Ar C=C), 1379 (C-P), 1211 (C-S), 334, 290 (2 x Pd-Cl). ES MS, *m/z*: 543 (M^+ -Cl), 506 (M^+ -2 x Cl); C H N: Calc. for $C_{22}H_{25}PdCl_2SPO_3$ (578): C 45.7, H 4.4; Found: C 45.3, H 4.3%.

6.2.9 - Preparation of $PdCl_2$(3.5), 3.9

In a very similar manner to that for the preparation of **3.8**, **3.9** was prepared using ligand **3.5.** Yield 0.031 g (61%). $^{31}P\{^1H\}$ δ(P) ppm (d_6 DMSO): 45.80, 46.56 (s, $PdP(C_6H_4)SePh$). ^1H δ(H) ppm (d_6 DMSO): 1.49-1.66 (m, 6H), 1.77-199 (m, 6H) 2.15-2.25 (m, 4H), 7.34-7.50 (m, 5H Ar-H), 7.74-7.91 (m 2H), 7.95-7.97 (dd, 1H Ar-H), 8.50-8.59 (dd, 1H Ar-H). IR (cm^{-1}) (KBr): 2988 (Ar C-H), 1572 (Ar C=C), 1380 (C-P), 1212 (C-Se), 327, 293 (2 x Pd-Cl). C H N: Calc. for $C_{22}H_{25}PdCl_2SePO_3$ (625): C 42.3, H 4.0; Found: C 40.2, H 3.8%.

6.2.10 - Preparation of $PdCl_2$(3.3), 3.10

Yield 0.089 g (68%). $^{31}P\{^1H\}$ δ(P) ppm (d_6 DMSO): 13.72, 14.20 (s, $PdP(C_6H_4)OMe$). ^1H δ(H) ppm (d_6 DMSO): 1.29, 1.38 (s, 3H), 1.44, 1.49 (s, 3H) 1.84-2.02 (m, 4H), 6.88-6.96 (m, 2H Ar-H), 7.40-7.44 (dd, 1H Ar-H), 7.96 (s, 1H Ar-H). IR (cm^{-1}) (KBr): 2959 (Ar C-H), 1587 (Ar C=C), 1379 (C-P), 1202 (C-O), 263 (Pd-Cl). C H N: Calc. for $C_{17}H_{23}PdCl_2PO_4$ (500): C 41.0, H 4.7; Found: C 40.3, H 4.8%.

6.2.11 - Preparation of $PdCl_2(3.3)_2$, 3.11

Yield 0.085 g (75%). $^{31}P\{^1H\}$ δ(P) ppm (d_6 DMSO): –4.23, –3.98 (s, $PdP(C_6H_4)OMe$). ^1H δ(H) ppm (d_6 DMSO): 1.35-1.99 (m, 32H, PAd CH_2/CH_3), 3.98 (s, 3H, OMe), 6.8-8.2 (m, 8H, Ar-H). C H N: Calc. for $C_{34}H_{46}PdCl_2P_2O_8.0.75CH_2Cl_2$ (886): C 47.12, H 5.32; Found: C 47.19, H 5.20%.

Chemistry of alkyl-based phospha-adamantanes

6.2.12 - Preparation of $PPh_2(CH_2)_2$(PAd), 3.12

Vinyldiphenylphosphine (0.752 g, 3.54 mmol) was heated to 110 °C and **1.113** (0.68 g, 3.54 mmol) added in several portions with stirring. AIBN (0.02 g) was then added, and the reaction mixture allowed to stir for 6 h. The temperature was reduced to 80 °C, and the system placed under vacuum to remove the volatile components, giving the product as a yellow waxy material. Yield: 0.812 g (57%). $^{31}P\{^1H\}$ δ(P) ppm ($CDCl_3$): –25.25, –25.02 (d, Cytop P), –12.86, –12.58 (d, PPh_2); ^1H NMR δ(P) ppm ($CDCl_3$): 1.14, 1.18 (s, 6H, 2 x CH_3), 1.20, 1.27 (s, 6H, 2 x CH_3), 1.71 (m, 4H, 2 x CH_2), 1.70 (dd, 2H, CH_2), 1.85 (dd, 2H, CH_2), 7.19-7.37 (m, 10H, Ar-H); ES MS, *m/z*: 428 [M^+], 285 ($PAd(CH_2)_2P^+$), 213 ($PPh_2CH_2CH_2^+$), 185 (PPh_2^+). IR (cm^{-1}) (neat on CsI plate): 2936 (CH_2 C-H stretch), 1340 (s, C-H deformation), 1088 (s, C-O-C), 978 (s, C-O stretch), 853 (sh, Ar out of plane vibrations), 794 (s, P-C stretching vibration) 741, 697 (s, Ar ring deformation) 508 (s, P-Ar). C H N: Calc. for $C_{24}H_{30}P_2O_3$ (428): C 67.28, H 7.06; Found: C 66.74, H 7.12.

6.2.13 - Preparation of $PdCl_2${3.12}, 3.13

Compound **3.12** (0.06 g, 0.14 mmol) was dissolved in CH_2Cl_2 (10 cm^3), and added dropwise to a solution of $PdCl_2(PhCN)_2$ (0.055 g, 0.14 mmol) dissolved separately in CH_2Cl_2 (10 cm^3). After stirring for 3 h, the volume of the solution was reduced to 2-3 cm^3, and Et_2O (60 cm^3) added. The resulting yellow precipitate was filtered and dried *in vacuo*. Yield 0.112 g (76%) yellow solid. $^{31}P\{^1H\}$ δ(P) ppm ($CDCl_3$): 60.92, 60.97 (d, ^2J(PP) 8 Hz, 1 x P, PAd) 65.79, 65.84 (d, ^2J(PP) 8 Hz, 1 x P, PPh_2). ^1H δ(H) ppm ($CDCl_3$): 1.30, 1.31 (s, 3H), 1.43, 1.47 (s, 3H), 1.50-1.53 (m, 4H), 1.71-1.83 (m, 4H, $2CH_2$), 7.35-7.57 (m, 6H Ar-H), 7.96-8.01 (dd, 4H Ar-H). IR (cm^{-1}) (KBr): 2915 (Ar C-H), 1636 (Ar C=C), 1377, 1435 (2 x C-P), 320, 283 (2 x Pd-Cl). FAB MS, *m/z*: 604 [M^+], 569 (M^+ – Cl). C H N: Calc. for $C_{24}H_{30}PdCl_2P_2O_3$ (625): C 47.6, H 5.0; Found: C 47.8, H 4.9%.

6.2.14 - Preparation of $PtMe_2$(3.12), 3.14

Compound **3.12** (0.095 g, 0.234 mmol) was dissolved in CH_2Cl_2 (5 cm^3), and added dropwise to a separate solution of $PtMe_2$(cod) (0.078 g, 0.234 mmol) in CH_2Cl_2 (10 cm^3) with stirring. The colourless solution was stirred for 3 h, after which the volume of solution was reduced to *ca.* 2-3 cm^3. Addition of petroleum ether (60-80 °C, 40 cm^3) gave a bright white solid, which was filtered and dried *in vacuo*. Yield: 0.051 g (32%). $^{31}P\{^1H\}$ δ(P) ppm ($CDCl_3$): 49.50 (d, ^1J(PtP) 1795 Hz, ^2J(PP) 10 Hz, 1 x P, PPh_2), 38.1 (d, ^1J(PtP) 1697 Hz, ^2J(PP) 10 Hz, 1 x P, PAd). ^1H δ(H) ppm: 0.5-2.6 (m, 20H, PAd H and PCH_2CH_2P), 1.36 and 1.40 (2 x s, 6H, 2 x Pt-CH_3), 7.19-7.69 (m, 10H, Ar-H). IR (cm^{-1}) (KBr): 2871, 2919 (PAd CH_3), 1636 (Ar C=C), 1378, 1435 (2 x C-P), 1089 (PAd C-O-C), 699, 746 (Ar C-H). FAB MS *m/z*: 653 [M^+]. C H N: Calc. for $C_{26}H_{36}PtP_2O_3.Et_2O$ (727): C 49.5, H 6.3; Found: C 49.6, H 5.7%.

6.2.15 – Preparation of $RuCl_2$(p-cymene){3.12}, 3.17

{RuCl(μ-Cl)(η^6-*p*-cymene)}$_2$ (0.131 g, 0.021 mmol) was dissolved in CH_2Cl_2 (10 cm^3). Separately, **3.12** (0.184 g, 0.043 mmol) was dissolved in CH_2Cl_2 (15 cm^3), and added dropwise to the stirring Ru dimer solution. The mixture was allowed to stir for *ca.* 3 h, after which the solution was concentrated to 2-3 cm^3, and Et_2O (50cm^3) was added to yield a bright orange solid, which was filtered and dried *in vacuo*. Yield 0.104 g (66%). $^{31}P\{^1H\}$ δ(P) ppm ($CDCl_3$): –26.38, –26.60 (d, PAd), 25.21, 25.43 (d, ^3J(PP) 31 Hz, Ru-PPh_2). ^1H δ(H) ppm ($CDCl_3$): 0.81-2.56 (m, 29H, PAd H, *p*-cymene CH_3 and PCH_2CH_2P), 2.58 (hept, 1H, *p*-cymene CH), 4.92-5.32 (m, 4H, *p*-cymene Ar-H), 7.26-7.93 (m, 10H, 10 x PPh_2 Ar-H). IR (cm^{-1}) (KBr): 2960 (Ar C-H), 2921 (sp^3 C-H), 1637 (Ar C=C), 1378, 1437 (2 x C-P), 1215 (C-O) 294 (w, Ru-Cl). FAB MS, *m/z*: 735 [M^+], 699 (M^+ - Cl^-), 664 (M^+ - 2 x Cl^-), 529 (Ru(**3.12**)$^+$), 428 (PAd$(CH_2)_2PPh_2^+$) CHN: Calc. for $C_{34}H_{44}RuCl_2P_2O_3.CH_2Cl_2$ (820): C 51.3, H 5.7; Found: C 52.7, H 5.6%.

6.2.16 – Preparation of AuCl[$RuCl_2$(p-cymene){$PPh_2(CH_2)_2$Cytop}], 3.18

AuCl(THT) (0.035 g, 0.1 mmol) was dissolved in CH_2Cl_2 (5 cm^3), and a separate solution of **3.12** (0.81 g, 0.1 mmol) in CH_2Cl_2 (10 cm^3) was added dropwise. After, 3 h stirring, the volume of the solution was reduced to *ca.* 3 cm^3, Et_2O (50 cm^3) added, and the resulting orange solid filtered and dried *in vacuo*. Yield 0.053 g (50%). $^{31}P\{^1H\}$ δ(P) ppm ($CDCl_3$): 22.06, 22.45 (2 x s, 1 x P, Ru-PPh_2 from different species), 30.56, 30.85 (2 x s, 1 x P, PAd from different species). ^1H δ(H) ppm ($CDCl_3$): 0.78-2.19 (m, 29 H, 16 x PAd H, 3 x *p*-cymene CH_3), 2.48 (hept, 1H, *p*-cymene CH), 4.69-5.29 (m, 4H, *p*-cymene Ar-CH), 7.43-7.82 (m, 10H, PPh_2 Ar-H). IR (cm^{-1}) (KBr): 3040 (Ar C-H), 2917 (sp^3 C-H), 1629 (Ar C=C), 1381, 1438 (2 x C-P), 1212 (C-O), 322, 292 (Ru-Cl/Au-Cl). C H N: Calc. for $C_{34}H_{44}RuAuCl_3P_2O_3$ (967): C 42.2, H 4.6; Found: C 41.6, H 4.4%.

6.2.17 – Preparation of $PdCl_2[RuCl_2(p\text{-cymene})\{3.12\}]_2$, 3.19

Compound **3.17** (0.060 g, 0.008 mmol) was dissolved in CH_2Cl_2 (5 cm^3). The solution was added to $PdCl_2(PhCN)_2$ (0.016 g, 0.004 mmol) in CH_2Cl_2 (5 cm^3), and stirred for 22 h. The dark orange solution was reduced in volume to *ca.* 2-3 cm^3 and Et_2O (40 cm^3) was added to yield an orange solid which was filtered and dried *in vacuo*. Yield 0.035 g (51%). $^{31}P\{^1H\}$ δ(P) ppm ($CDCl_3$): 9.5 and 10.0 (2 x dd, 2 x Pd-PAd due to 2 different species in equal quantities), 23.9 and 24.3 (2 x dd, 2 x Ru-PPh_2 due to 2 different species in equal quantities). ^1H δ(H) ppm ($CDCl_3$): (most peaks are duplicate due to diastereomeric nature of product): 0.84-1.92 (m, 58H, PAd H, PCH_2CH_2P and 3 x *p*-cymene CH_3), 2.9 (hept, 1H, *p*-cymene CH), 4.90-5.29 (m, 8H, *p*-cymene Ar-H), 7.44-7.92 (m, PPh_2 Ar-H). IR (cm^{-1}) (KBr): 3053 (Ar C-H), 2925 (sp^3 C-H), 1628 (Ar C=C), 1378, 1437 (2 x C-P), 1215 (C-O). ES MS, *m/z*: 1645 [M^+] and 1610 (M^+ - Cl), 876 ($PdCl(\mathbf{3.12})^+$), 699 ($ClRu(p\text{-cymene})(\mathbf{3.12})^+$). C H N: Calc. for $C_{66}H_{88}Ru_2PdCl_2P_4O_6.CH_2Cl_2$ (1730): C 46.5, H 5.2; Found: C 47.1, H 5.1%.

6.2.18 – Preparation of $PtCl_2[RuCl_2(p\text{-cymene})\{3.12\}]_2$, 3.20

In a similar manner to that for making **3.19**, **3.20** was prepared using $PtCl_2(PhCN)_2$. Yield 0.060 g (72%). $^{31}P\{^1H\}$ δ(P) ppm ($CDCl_3$) (^2J(PP) coupling indistinguishable): 23.6 and 24.0 (2 x dd, 2 x Ru-PPh_2 due to 2 different species), 2.46 and 3.11 (2 x dd, ^1J(PtP) 2585 Hz, 2 x Pt-PAd due to 2 different species). ^1H δ(H) ppm ($CDCl_3$) (most peaks are duplicate due to diastereomeric nature of product): 0.72-2.56 (m, 58H, PAd H, PCH_2CH_2P and 3 x *p*-cymene CH_3), 2.9 (hept, 1H, *p*-cymene CH), 4.77-5.25 (m, 8H, *p*-cymene Ar-H), 7.37-7.86 (m, PPh_2 Ar-H). ES MS, *m/z*: 1735 [M^+] and 1700 (M^+ -Cl). IR (cm^{-1}) (KBr): 3053 (Ar C-H), 2925, 2964 (sp^3 C-H), 1628 (Ar C=C), 1378, 1437 (2 x C-P), 1215 (C-O), 300 (*trans*-Pt-Cl). C H N: Calc. for $C_{66}H_{88}Ru_2PdCl_2P_4O_6.CH_2Cl_2$ (1743): C 49.6, H 5.4; Found: C 47.1, H 5.1%

6.2.19 – Preparation of $RhCl_2(Cp^*)${3.12}, 3.21a

Using a similar procedure as for **3.17**, **3.21a** was prepared using $\{RhCl(\mu\text{-}Cl)(\eta^5\text{-}C_5Me_5)\}_2$. Yield 0.022 g (29%), orange crystals. $^{31}P\{^1H\}$ δ(P) ppm ($CDCl_3$): –25.7 (d, 1 x P, PAd), 30.0 and 30.8 (2 x d, 2 x P, different stereoisomers). ^1H δ(H) ppm ($CDCl_3$): IR $\nu(cm^{-1})$ (KBr): 2988 (Ar C-H), 2919 (sp^3 C-H), 1638 (Ar C=C), 1379, 1437 (2 x C-P), 1216 (C-O). FAB MS, *m/z*: 667 [M^+], 632 (M^+ - Cl^-). C H N: Calc. for $C_{29}H_{35}RuCl_2P_2O_3$ (667): C 52.2, H 5.3; Found: C 52.4, H 6.0%.

Two drops of MeOH were added to the $CDCl_3$ solution of **3.21a**, and the $^{31}P\{^1H\}$ NMR spectrum rerun after 10 m and 6 h. When [RhCl(Cp^*){**3.12**}]Cl **3.21b** was fully formed after 6 h, the data observed was as follows: δ(P) ppm ($CDCl_3$): Minor species: 47.5 and 48.3 (2 x d, ^2J(PP) 24 Hz, 1 x P, Rh-PAd), 61.8 and 62.6 (2 x d, ^2J(PP) 24 Hz, 1 x P, Rh-PPh_2). Major species: 56.0 and 56.8 (2 x d, ^2J(PP) 15 Hz, 1 x P, Rh-PAd), 63.1 and 63.9 (2 x d, ^2J(PP) 15 Hz, 1 x P, Rh-PPh_2).

6.2.20 – Preparation of $IrCl_2(Cp^*)\{PPh_2(CH_2)_2Cytop\}$, 3.22

Using a similar procedure as for **3.17**, **3.22** was prepared using $\{IrCl(\mu\text{-}Cl)(\eta^5\text{-}C_5Me_5)\}_2$. Yield 0.049 g (23%) yellow solid. $^{31}P\{^1H\}$ δ(P) ppm ($CDCl_3$): –25.46, –25.26 (d, PAd), –1.70, –1.45 (d, PPh_2). ^1H δ(H) ppm ($CDCl_3$): 0.54-1.93 (m, 35H, Cp^* CH_3, PAd H and PCH_2CH_2P, 7.33-7.57 (m, 10H, PPh_2 Ar-H). IR (cm^{-1}) (KBr): 2991 (Ar C-H), 2921 (sp^3 C-H), 1637 (Ar C=C), 1379, 1437 (2 x C-P), 1216 (C-O). FAB MS *m/z*: M^+ = 826.79, Found: 791 (M^+ - Cl). C H N: Calc. for $C_{34}H_{45}IrCl_2P_2O_3.CHCl_3$ (946): C 44.4, H 4.9; Found: C 45.0, H 5.1%.

6.3 - CHAPTER FOUR EXPERIMENTAL

6.3.1 - Reaction of 2.1 with Chloramine T and Acetic acid

Compound **2.1** (0.15 g, 0.405 mmol) was dissolved in MeOH (10 cm^3). Glacial acetic acid (0.041 g) in MeOH (5 cm^3) was then added over 5 min via syringe. Separately, Chloramine T (0.113 g) was also dissolved in MeOH (5 cm^3) and added to the previous solution. After stirring for 15 min at r.t. and 2.5 h at 50 °C, extra chloramine T (0.011 g) was added as a MeOH solution (2 cm^3). After heating for a further 1 h at 50 °C, the reaction mixture was cannulated onto a NaOH solution (40 cm^3), causing a suspension to form. The light brown solid contained in the suspension was filtered and dried *in vacuo*. Yield: 0.072 g. $^{31}P\{^1H\}$ δ(P) ppm ($CDCl_3$): 29 ppm (**2.3**). IR (KBr) (cm^{-1}): 1439 (str, C-H/P-Ph) 1252 (med, P=O).

6.3.2 - Preparation of *o*-(mesitylenesulfonyl)acetohydroxamate – Prepared using a slightly changed known procedure.[71]

Triethylamine (15.90 g, 157 mmol) and ethylacetohydroxamate (16.419 g, 159 mmol) were dissolved in DMF (50 cm^3), and mesitylenesulfonyl chloride was added in several portions with stirring at 0 °C. After stirring for 20 min at 0 °C, the mixture was poured onto ice water. The resulting white precipitate was then filtered, dried and recrystallised from pet. ether (60-80 °C). Yield: 28.018 g, (64%). The product was used in the next stage (6.3.3) without any analysis.

6.3.3 - Preparation of *o*-mesitylenesulfonylhydroxylamine, 4.3

o-(mesitylenesulfonyl)acetohydroxamate (3.51 g, 12.8 mmol) was dissolved in dioxane (10 cm^3), and, with stirring at 0 °C. Enough perchloric acid was added to make the clear solution turn to a thick suspension. Ice water was added to the mixture to give a white precipitate, which was filtered *in vacuo*. Et_2O was added to dissolve the solid, and, after separation from residual water in a separating funnel, enough petroleum ether (60-80 °C) was added to yield a white solid. An ice bath was required to fully achieve this, after which the white solid was filtered and dried. More product was retrieved from the filtrate after reduction of the solvent volume. Yield: 1.949 g (71%). Partly due to the explosive nature of **4.3**, the product was used without further analysis.

CAUTION *o*-mesitylenesulfonylhydroxylamine is highly toxic and can spontaneously detonate, especially when dry and if placed under vacuum pressure. Care must be taken when handling; all measurements and use must be carried out wearing protective clothing and in a suitable fume cupboard.

6.3.4 – Preparation of $[C_6H_4(P(NH_2)Ph_2)(SPh)]^+[MSH]^-$, 4.4

$C_6H_4(PPh_2)(SPh)$ (0.95 g, 2.57 mmol) was dissolved in CH_2Cl_2 (10 cm^3), and MSH (0.664 g, 3.08 mmol) was added to the reaction in several portions. The reaction mixture was stirred for *ca.* 3 d, after which the yellow suspension was filtered. The filtrate was reduced to dryness to yield a sticky off-white solid. Et_2O (5 cm^3) was added to wash away any residual MSH, decanted, and the product placed under high power vacuum to yield a white solid. Yield: 1.417 g, (92%). $^{31}P\{^1H\}$ δ(P) ppm (DMSO): 37.0. ^1H δ(H) ppm (DMSO): 2.20 (s, 3H, MSH CH_3), 2.56 (s, 6H, 2 x CH_3), 6.29 (br s, 2H, NH_2), 6.74 (s, 2H, 2 x MSH Ar-H), 7.03-7.82 (m, 19H, PPh_2/SPh/C_6H_4). IR (cm^{-1}) (KBr): 3055 (v br, N-H stretch) 1439 (s, Ar-P C-H), 1180 (SO_2 S=O stretch) 1117, 1085, 1015 (s, C-P, C-S), 728 (s, Ar C-H). C H N: Calc. for $C_{32}H_{32}O_3S_2N_2P$ (588): C 67.67, H 5.51, N 2.39; Found: C 67.66, H 5.69, N 2.48%.

6.3.5 – Preparation of $[C_6H_4(P(NH_2)Ph_2)(SNH_2)Ph)]^{2+}$ 2[MSH]$^-$, 4.5

$C_6H_4(PPh_2)(SPh)$ (1.14 g, 3.07 mmol) was dissolved in CH_2Cl_2, and, with stirring, *o*-mesitylenesulfonylhydroxylamine (1.386 g, 6.44 mmol) was added in several portions. After stirring for 3 d at r.t., the white precipitate formed was filtered and washed with ether. The waxy material resulting from this was then dried under high power vacuum to yield a light brown solid. Yield: 0.915 g, (41%). $^{31}P\{^1H\}$ δ(P) ppm (DMSO): 36 ($P{=}NH_2$ only), 34 ($P{=}NH_2$ and $S{=}NH_2$). ^1H δ(H) ppm (DMSO): 2.29 (s, 6H, 4 x MSH CH_3), 2.60 (s, 12H, 2 x CH_3), 6.25 (br s, 4H, 2 x NH_2), 6.81 (s, 4H, 4 x MSH Ar-H), 7.12-7.94 (m, 19H, PPh_2/SPh/C_6H_4). FAB MS, *m/z*: 800 $[cation]^+$.

6.3.6 – Reaction of 4.5 with $NaBPh_4$ - 4.6a/4.6b

Compound **4.5** (0.5 g, 0.624 mmol) was dissolved in MeOH (10 cm^3), and with stirring, $NaBPh_4$ (0.45 g, 1.25 mmol) in MeOH (5 cm^3) was added dropwise. The reaction was allowed to stir for 2 h, during which time a white precipitate formed. This precipitate was filtered and dried *in vacuo*. Yield: 0.343 g, (74%). $^{31}P\{^1H\}$ δ(P) ppm (DMSO): 73. ^1H δ(H) ppm (DMSO): 7.07-7.97 (m, 59H, BPh_4 PPh_2/SPh/C_6H_4). C H N: IR (cm^{-1}) (KBr): 3055 (v br, N-H), 1437 (str, P-Ph/C-H), 1114, 1065, 1047 (str, C-P, C-S). Calc. for $C_{32}H_{32}O_3S_2N_2P$ (588): C 80.86, H 5.59, N 1.99; Found: C 80.64, H 5.53, N 1.70%.

6.3.7 – Reaction of phosphine oxide 2.3 with 4.3 - 4.7

$C_6H_4(P(O)Ph_2)(SPh)$ **2.3** (0.165 g, 0.43 mmol) was dissolved in CH_2Cl_2 (7.5 cm^3), and **4.3** (0.110 g, 5.12 mmol) was added as a solid in three portions. The reaction mixture was allowed to stir for *ca.* 3 d, after which the white suspension was filtered, and the solid dried under high power vacuum to yield a white solid, **4.7** which was collected. Yield: 0.229 g (83%). $^{31}P\{^1H\}$ δ(P) ppm ($CDCl_3$): 33. $\{^1H\}$ δ(H) ppm ($CDCl_3$): 2.29 (s, 3H, 1 x MSH CH_3), 2.49 (s, 6H, 2 x MSH CH_3), 6.73 (s, 2H, MSH 2 x Ar-H), 7.20-8.30 (m, 19H, SPh/PPh_2) Ar-H). IR (cm^{-1}) (KBr): 3150 (br, N-H), 2971 (br C-H), 1437 (sh, P-Ph), 1603 (med, C=C), 1180 (br, P=O), 1118, 1085, 1013 (sh, C-P, C-

S), 851 (sh, S=N). Calc. for $C_{33}H_{32}O_4S_2NP.0.5CH_2Cl_2$ (643): C 63.44, H 5.17, N 2.18; Found: C 63.18, H 5.20, N 1.81%

6.3.8 - Reaction of $\{Ph_2P(CH_2)_2S(C_6H_4)o\text{-}PPh_2\}$, 2.32 with 2 x 4.3 - 4.8a

Compound **2.32** (1.372 g, 2.71 mmol) was dissolved in CH_2Cl_2 (20 cm^3) and **4.3** (1.22 g, 5.69 mmol) was added in several portions as a solid. The solution turned orange with a small amount of white solid present. The mixture was stirred for 24 h, after which the solution was reduced to dryness. Et_2O (10 cm^3) was added, decanted off, and the waxy material dried *in vacuo*. Yield 1.755 g (69%). $^{31}P\{^1H\}$ δ(P) ppm (DMSO): 38.9 ($(CH_2)_2P{=}NPh_2$), 35.7 ($C_6H_4P{=}NPh_2$). ^1H δ(H) ppm (DMSO): 2.05 (s, 6 H, 2 x MSH CH_3), 2.32 (s, 12 H, 4 x MSH CH_3) 3.43-3.78 (m, 4 H, 2 x CH_2), 7.15-7.78 (m, 46 H, MSH, PPh_2 Ar-H). FAB^+ MS: *m/z*: 538 [$cation^+$], 228 ($(C_6H_4(PNH_2)Ph_2)S^+$). IR (cm^{-1}) (KBr): 849 ($S{=}NH_2$), 1187 (SO_2^-), 3059 (br, N-H). C H N: Calc. for $C_{50}H_{54}P_2S_3O_6N_2$ (937): C 64.09, H 5.81, N 2.99%; Found: C 63.88, H 6.45, N 3.27%.

6.3.9 - Reaction of $[Ph_2P(NH_2)(CH_2)_2S(C_6H_4)o\text{-}PPh_2(NH_2)]^{2+}[MSH]^{2-}$ 4.8a with $NaBPh_4$ - 4.8b

Compound **4.8a** (0.5 g, 0.53 mmol) was dissolved in MeOH (10 cm^3). Separately, (0.41 g, 1.2 mmol) was dissolved in MeOH (5 cm^3). The solution was stirred for 12 h, during which time a white solid appeared, with a yellow/orange solution above. The mixture was reduced in volume to *ca.* 7-8 cm^3, and the white solid filtered and dried *in vacuo*. Yield 0.512 g (82%). $^{31}P\{^1H\}$ δ(P) ppm ($CDCl_3$): 120.7. ^1H TO ADD. FAB^+ MS, *m/z*: 539 [$cation^+$], 228 ($(C_6H_4(PNH_2)Ph_2)S^+$). IR (cm^{-1}) (KBr): 3053 1560, 1438, 853, 700, 684. C H N: Calc. for $C_{80}H_{72}P_2B_2N_2S.CHCl_3$ (1176): C, 81.63, H 6.17, N 2.38; Found: C 74.93, H 6.27, N 2.14%. Structure of **4.8b** currently remains unknown.

6.3.10 – Reaction of 2.17 with 4.3 – 4.9

Compound **2.17** (0.2 g, 0.48 mmol) was dissolved in CH_2Cl_2 (7.5 cm^3) and MSH (0.229 g, 1.06 mmol) was added as a solid in several portions. This immediately resulted in formation of an off-white precipitate. The reaction was stirred for *ca.* 24 h, after which the now brown solid was filtered and collected. The filtrate was also reduced to dryness and the brown solid collected and dried *in vacuo*.

Yield (Solid): 0.075 g, (25 %). $^{31}P\{^1H\}$ δ(P) ppm (DMSO): 76 (**4.9c**), 38 ($P=NH_2$), 35 ppm ($P=NH_2$ + $S=NH_2$).

Yield (Filtrate): 0.224 g, (74%). $^{31}P\{^1H\}$ δ(P) ppm (DMSO): 38 (66% of P-containing product, $P=NH_2$ only), 32 (P=O product). IR (cm^{-1}) (KBr): 3054 (str, N-H), 2960, 1437 (str, C-H/P-Ph), 1603 (med, C=C), 1110, 1085, 1014 (str, C-P, C-S), 850 (med, small amount of Se=N).

6.3.11 - Preparation of $C_6H_4(SPh)\{P(NPh)Ph_2\}$ using aniline – 4.10

Compound **2.1** (0.25 g, 0.675 mmol) was dissolved in toluene (5 cm^3). A separate solution of Br_2 (0.108 g, 0.675 mmol) in toluene (1 cm^3) was then added to the phosphine solution at 6-8 °C *via* syringe over 5 min. Separately, aniline (0.0628 g, 0.675 mmol) and triethylamine (0.137 g, 1.35 mmol) were placed in toluene (2 cm^3) and added to the reaction mixture. After stirring for 4 h, during which time a suspension began to form, the mixture was filtered, and the volume of solution reduced to dryness to yield a yellow oil, which upon recrystallisation from CH_2Cl_2/Et_2O gave a light yellow solid. Yield: 0.103 g, (34%). $^{31}P\{^1H\}$ δ(P) ppm ($CDCl_3$): 21 (P=N-Ph). ^1H δ(H) ppm ($CDCl_3$): 6.70-7.31 (m, 24xH, P=NPh **H** and PPh **H**. IR (KBr) (cm^{-1}): 1493 (sh, P=N), 1430 (med, C-H/P-Ph), 1112, 1090, 1031 (sh, C-P, C-S).

6.3.12 - Reaction of 2.1 with 1,2-phenylenediamine – 4.11

Compound **2.1** (0.25 g, 0.67 mmol) was dissolved in toluene (2 cm^3). Separately, bromine (0.216 g, 1.37 mmol) was placed in toluene (1 cm^3), and this was added to the phosphine sulfide with stirring at 8-10 °C. After 30 min further stirring at r.t., triethylamine (0.173 g) and 1,2-phenylenediamine (0.073 g, 0.68 mmol) were dissolved in toluene/methanol (3:1, 4 cm^3) and added to the reaction. Stirring of the reaction lead to the formation of a green/dark brown suspension, which was filtered off and the filtrate reduced to dryness. Petroleum ether (60-80 °C, 30 cm^3) was added to the resulting oil and the suspension cooled to *ca.* 0 °C for 2 h. After this, the resulting brown solid was filtered and dried *in vacuo*.

In-situ $^{31}P\{^1H\}$ δ(P) 27 ppm ($CDCl_3$).
Product $^{31}P\{^1H\}$ δ(P) 29 ppm (P=O) **2.3** ($CDCl_3$).

6.3.13 – Reaction of *o*-C_4H_4(OMe)(PAd), 3.3 with MSH, 4.3 - 4.12

Compound **3.3** (0.25 g, 0.78 mmol) was dissolved in CH_2Cl_2 (10 cm^3). Separately, compound **4.3** (0.209 g, 0.97 mmol) was dissolved in CH_2Cl_2 (10 cm^3) and added dropwise to the stirring **3.3** solution. After *ca.* 2 h stirring, the volume of the solution was reduced to 5 cm^3, and Et_2O (80 cm^3) added. The resulting bright white solid was filtered and dried *in vacuo*. Yield: 0.26 g (62%). $^{31}P\{^1H\}$ δ(P) ppm ($CDCl_3$): 21. δ(H) ppm ($CDCl_3$): 1.20, 1.37, 1.58, 2.07 (4 x d, 12, PAd CH_3), 1.80-2.00 (m, 4H, 2 x PAd CH_2), 3.9 (s, 3H, OCH_3), 5.62 (s, 2H, 2 x MSH Ar C-H)), 6.71 (s, 2H, 2 x MSH Ar C-H), 7.08-8.04 (m, 4H, 4 x C_6H_4 Ar-H). ES MS, *m/z*: 338 $[cation]^+$, 199 $[MSH]^-$. C H N: Calc. for $C_{26}H_{36}PO_2S.0.75CH_2Cl_2$ (600): C, 53.54, H 6.30, N 2.33; Found: C 53.68, H 6.27, N 2.14%.

6.3.14 – Preparation of LDA

Diisopropylamine (0.25 g, 2.47 mmol) was cooled to 0 °C and 2.0 M ^{n}BuLi (1.24 cm^3, 2.48 mmol) was added dropwise over 5 min. The yellow mixture was stirred in ice for a further 25 min, then added to **4.13** accordingly.

6.3.15 – Reaction of $[C_6H_4(OMe)(PAd{=}NH_2)]^+[MSH]^-$, 4.12 with LDA – 4.13

Compound **4.12** (0.15 g, 0.28 mmol) was dissolved in THF (15 cm^3), and LDA (0.037 g, 0.34 mmol) was added dropwise at 0 °C. The solution was allowed to stir for 12 h, after which an *in-situ* $^{31}P\{^1H\}$ NMR spectrum was taken. The solution was then taken to dryness, and CH_2Cl_2 (3 x 5 cm^3) added along with H_2O (10 cm^3) to extract the product into the organic layer. The organic extracts were dried over $MgSO_4$, the volume taken to *ca.* 2-3 cm^3, and Et_2O added to give an off-white solid which was filtered and dried *in vacuo*. Yield: 0.065 g (43%). $^{31}P\{^1H\}$ δ(P) ppm ($CDCl_3$): 14. ^1H δ(H) ppm ($CDCl_3$): 1.21-2.14 (m, 16H, PAd CH_2/CH_3), 4.8 (br s, 1H, NH), 6.93-7.35 (m, 4H, C_6H_4 Ar C-H). ES MS, *m/z*: 338 $[Cation]^+$, 100%. IR (cm^{-1}) (KBr): 3380 (sh, N-H), 1455 (med, P-C), 1257 (str, Ar-OMe), 1020 (str, C-O-C), 766 (med, Ar C=C), 681 (med, N-H).

6.3.16 – Small scale preparation of $CuCl_2$(4.13) – 4.14

Compound **4.13** (0.025 g, 0.05 mmol) was dissolved in MeCN (10 cm^3) at 0 °C, and, with stirring, $CuCl_2$ (0.007 g, 0.05 mmol) was added as a solid. After 6 h stirring, a $^{31}P\{^1H\}$ NMR spectrum was taken. Using the same sample, the volume of the solution taken to *ca.* 2-3 cm^3. Addition of Et_2O (40 cm^3) yielded a yellow solid which was filtered and dried *in vacuo*. Yield 0.019 g (47%). $^{31}P\{^1H\}$ δ(P) ppm (C_6D_6): 22. δ(H) ppm ($CDCl_3$ post isolation): 1.43-2.01 (m, 32H, PAd CH_2/CH_3), 6.99-7.62 (m, 8H, C_6H_4 Ar C-H). IR (cm^{-1}) (KBr): 691 (med, N-H), 764 (w, Ar C=C), 1029 (w, C-O-C), 1242 (str, Ar-OMe), 1452 (med, P-C), 3442 (br, N-H).

6.3.17 – Small scale preparation of $PtCl_2$(4.13)$_2$ – 4.15

One equivalent of **4.13** (0.015 g, 0.04 mmol in 5 cm^3 DCM/MeOH) was added to $PtCl_2(PhCN)_2$ (0.021 g, 0.04 mmol) in CH_2Cl_2 (5 cm^3). After 2 h stirring, a $^{31}P\{^1H\}$ NMR spectrum was taken. Using the same sample, a second equivalent of **4.13** was added and stirred for a further 1 h, after which a second NMR spectrum was taken. NMR (1): $^{31}P\{^1H\}$ δ(P) ppm (C_6D_6): –2.3, –2.5 (d, {$PtCl_2$(μ-Cl)(**4.13**)}$_2$), 21.2 and 23.5.

NMR (2): $^{31}P\{^1H\}$ δ(P) ppm (C_6D_6): 22.2 and 26.5 ($PtCl_2$(**4.13**)$_2$ or phosphine oxide).

6.1.18 – Reaction of {$RuCl_2$(*p*-cymene)($PPh_2(CH_2)_2$PAd)}, 3.17 with 4.3 – 4.16

Compound **3.17** (0.054 g, 0.074 mmol) was dissolved in CH_2Cl_2 (5cm^3), after which **4.3** (0.016 g, 0.074 mmol) was added as a solid in several portions. The red solution was stirred for 10 h, after which the solution was reduced to dryness. After adding $CDCl_3$ to carry out an *in-situ* $^{31}P\{^1H\}$ NMR spectroscopy experiment, Et_2O (40 cm^3) was added to yield a red/brown solid, which was filtered and dried *in vacuo*. Yield: 0.056 g (80%). Yield: 0.065 g (43%). $^{31}P\{^1H\}$ δ(P) ppm ($CDCl_3$): 23.2, 22.9 (d, Ru-PPh_2, ^3J(PP) 44 Hz), 32.6, 32.4 (d, PAd=NH_2, ^3J(PP) 44 Hz). ^1H δ(H) ppm ($CDCl_3$): 0.87-2.50 (m, 38H, *p*-cym/PAd/$(CH_2)_2$/MSH CH_2/CH_3 peaks, differentiation not possible), 5.24-5.43 (*p*-cym, 4H, Ar-CH), 6.73 (s, 2H, MSH Ar C-H), 7.27-7.87 (m, 10H, PPh_2 Ar C-H). ES$^+$ MS: *m/z*: 750 [cation]$^+$, 199 [MSH]$^-$. IR (cm^{-1}) (KBr): 681 (med, N-H), 766 (med, Ar C=C), 1020 (str, C-O-C), 1257 (str, Ar-OMe), 1455 (med, P-C), 3380 (sh, N-H). Calc. for $C_{43}H_{59}P_2NSO_6RuCl_2.0.5CH_2Cl_2$ (993): C, 52.62, H 6.09, N 1.41; Found: C 52.43, H 6.08, N 1.85%.

6.4 – CATALYTIC INVESTIGATIONS

6.4.1 - General - Preparation of *t*-stilbene

Iodobenzene (1 g, 4.90 mmol), styrene (0.766 g, 7.35 mmol) and tributylamine (0.1.104 g, 6.00 mmol) were placed in DMF (2cm^3). The appropriate amount of catalyst was added, and the mixture heated to 125 °C for 1 or 3 d (both catalyst loadings and times shown in Tables 5.1a and 5.2a). The reaction mixture was taken up in CH_2Cl_2 (10 cm^3) and washed with H_2O (10 cm^3). After a further washing with KCN (5 cm^3 of a 6 x 10^{-2} M solution), the solvent was reduced to dryness *in vacuo*. The remaining solid was washed with HPLC MeOH, and the product filtered and dried *in vacuo*. % Yields are shown in Tables 5.1a and 5.2a.

General: ^1H δ(H) ppm ($CDCl_3$): 7.12-7.40 (m, 12 H, 2 x C_6H_5 & 2 x CH)

~*Conclusions*~

The work undertaken has encompassed a number of new areas, and left a number of directions open for investigation. A new, reliable method for the preparation of phosphine/chalcogenide ligands, based on aromatic backbones has been established. Various transition metal complexes of these ligands have also been prepared and characterised. Indeed, the complexes containing selenide functionalities are the first of their type to be characterised by X-ray crystallography. The bidentate ligands $Ph_2P(CH_2)_2XPh$ (X=S/Se) have been prepared using vinyldiphenylphosphine, thiophenol or phenylselenol and AIBN as the radical source in a solvent free, reliable radical reaction. This approach was also used to synthesise a number of potentially tridentate ligands. Various substituted thiols were used to give ligands containing combinations of phosphine, sulfide, ether and amine functionalities. Subsequently, Pd(II)/Pt(II) complexes have been synthesised, exhibiting varying modes of coordination, mainly through chelation of the phosphine and chalcogenide groups. This Chapter has exhibited the potential for synthesis of new multifunctional ligands containing various combinations of P/S/O and N-containing functionalities. Whilst the initial complexes prepared appear to coordinate only through the phosphine and sulfide groups, further experiments performed show the ability of the 'pendant' functionalities to also coordinate to the metal centres.

The chemistry of compounds containing phospha-adamantane (PAd) moieties has received relatively little attention in comparison to that of compounds containing other bulky phosphine groups. A large number of novel ligands containing a phospha-adamantane group have been prepared *via* methods established for phosphine/chalcogenide ligands mentioned above, and their coordination chemistry investigated. Ligands based on the phospha-adamantane fragment, aromatic backbone and sulfide, selenide, ether and bromide functionalities are reported. Ligands containing the chalcogenide functionalities formed κ^2-*P,P`*-chelated complexes with metal centres such as Pd(II) and Pt(II) and have been characterised both spectroscopically and crystallographically. Using various stoichiometries of ligands containing bromide and ether groups, Pd(II) chloro-bridged dimers and *trans*-bis-phosphines respectively were prepared.

A new unsymmetrical diphosphine, $Ph_2P(CH_2)_2PAd$ has also been prepared using the radical initiation method, and used to coordinate to various transition metal centres; whilst κ^2-*P,P`*-chelation occurs when using Pd(II) and Pt(II) precursors, it was found that complexes formed using ruthenium chloro-bridged dimers can also act as κ^1-*P*-monodentate tertiary phosphines. Complicated $^{31}P\{^1H\}$ NMR spectroscopy patterns are observed when the latter is used to form *trans*-Pd(II) and Pt(II) complexes. The versatility of the diphosphine has been shown by the coordination to a number of other metal centres, including Au(I), Rh(I) and Ir(I). The work in this Chapter shows how combinations of the bulkiness of the phosphine group, and choice of metal can be used to impart different modes of coordination within transition metal complexes. The discovery of novel heterobimetallic complexes is an interesting area into which further research could be taken.

Novel derivatives of the phosphine-based ligands have also been prepared. This has been carried out using using hydrogen peroxide and *o*-mesitylenesulfonyl hydroxylamine (MSH) to oxidise and aminate the phosphine and sulfide functionalities. The ionic products of the amination reactions contained an SO_2O^- unit, leading to hydrogen bonding motifs in the extended structure of the compounds. Subsequent metathesis reactions of the MSH salts using $NaBPh_4$ gave mixed results. Most gave the tetraphenylborate salts of the protonated iminophosphines or sulfimides. However, reaction of $NaBPh_4$ with bis-aminated phosphines such as *o*-{$(S(NH_2)Ph)C_6H_4(P(NH_2Ph_2)$}2{MSH} resulted in an extremely large downfield shift in the $^{31}P\{^1H\}$ NMR spectrum. Reasons for this trend have been postulated using previous observations for bis-sulfide ligands.

The complexes prepared from PPh_2 and phospha-adamantane-based ligands in previous Chapters have been analysed for their efficiency to catalyse Heck C-C bond formation reactions between iodobenzene and styrene. Almost all complexes prepared exhibit catalytic activity at relatively high catalyst loadings. A number of the complexes investigated further by lowering catalyst loadings still give excellent yields, even at extremely low loading levels. When the reaction times were reduced, yields of *trans*-stilbene remained high. It can be concluded therefore, that the efficiency of a number of these catalysts is extremely good, and the potential for this

to be further analysed is ostensibly also great. The mechanism by which these catalysts may act has been researched, but additional mechanistic studies would be required to ascertain any definitive conclusions on this area.

A number of other areas could be looked into further from this work. Possibly the most interesting of these would be to establish the limits to which the catalyst loadings could be lowered, and hence the TON's increased for the Heck reaction. The suitability of these catalysts for use in other organic reactions could also be analysed. The cause of the trends in structural change of aminated phosphine/sulfides, noticed in the $^{31}P\{^{1}H\}$ NMR spectra is still unresolved, and is a point of interest. Also, the further potential for the complexes containing tridentate ligands is evident. The coordination studies at the end of Chapter Two show that the 'free' functionality could be used to form extended structures and give different modes of ligation.

~*References*~

1 A. G. Orpen, N. G. Connelly, *J. Chem. Soc., Chem. Commun.*, 1985, 1310.

2. a) G. Dyer, M. O. Workman, D. W. Meek, *Inorg. Chem.*, 1967, **6**, 1404. b) L. M. Venanzi, *Angew. Chem., Int. Ed.*, 1964, **3**, 453.

3. E. Hauptman, P. Fagan, W. Marshall, *Organometallics*, 1999, **18**, 2061.

4. D. Morales, R. Poli, P. Richard, J. Andrieu, *J. Chem. Soc., Dalton Trans.*, 1999, 867.

5. N. Brugat, A. Polo, A. Alvarez-Larena, J. F. Piniella, J. Real, *Inorg. Chem.*, 1999, **38**, 4829.

6. P.Rigo, M. Bressan, *Inorg. Chem.*, 1975, **14**, 1491.

7. G. K. Anderson, R. Kumar, *Inorg. Chem.*, 1984, **23**, 4064.

8. A. R. Sanger, *Can. J. Chem.*, 1983, **61**, 2214.

9. K. Matsuzaki, H. Kawaguchi, P. Voth, K. Noda, S. Itoh, H. D. Takagi, K. Kashiwabara, K. Tatsumi, *Inorg. Chem.*, 2003, **42**, 5320.

10. S. Iwatsuki, T. Suzuki, A. Hasegawa, S. Funahashi, K. Kashiwabara, H. D. Takagi, *J. Chem. Soc., Dalton Trans.*, 2002, 3593.

11. N. Taguchi, K. Kashiwabara, K. Nakajima, H. Kawaguchi, K. Tatsumi, *J. Organomet. Chem.*, 1999, **587**, 290.

12. V. C. Gibson, N. J. Long, A. J. P. White, C. K. Williams, D. J. Williams, *Organometallics*, 2002, **21**, 770.

13. V. C. Gibson, N. J. Long, A. J. P. White, C. K. Williams, D. J. Williams, *J. Chem. Soc., Chem. Commun.*, 2000, 2359.

14. P.Pellon, G. Gachot, J. Le Bris, S. Marchin, R. Carlier, D. Lorcy, *Inorg. Chem.*, 2003, **42**, 2056.

15. D. Canseco-Gonzalez, V. Gomez-Benitez, O. Baldovino-Pantaleon, S. Hernandez-Ortega, D. Morales-Morales, *J. Organomet. Chem.*, 2004, **689**, 174.

16. J. Duran, N. Brugat, A. Polo, C. Segura, J. Real, X. Fontrodona, J. Benet-Buchholz, *Organometallics*, 2003, **22**, 3432.

17. C. A. Grapperhaus, S. Poturovic, M. S. Mashuta, *Inorg. Chem.*, 2005, **44**, 8185.

18. R. Malacea, J-C. Daran, S. B. Duckett, J. P. Dunne, C. Godard, E. Manoury, R. Poli, A. C. Whitwood, *J. Chem. Soc., Dalton Trans.*, 2006, 3350.

19. J. Spencer, V. Gramlich, R. Hausel, A. Togni, *Tetrohedron: Asymmetry*, 1996, 7, 41.

20. D. Enders, R. Peters, R. Lochtman, G. Raabe, *Angew. Chem., Int. Ed.*, 1999, **38**, 2421.

21. O. G. Mancheno, J. Priego, S. Cabrera, R. G. Arrayas, T. Llamas, J. C. Carretero, *J. Org. Chem.*, 2003, **68**, 3679.

22. P. Pérez-Lourida, J. Romero, J. A. García-Vázquez, A. Sousa, Y. Zheng, J. R. Dilworth, J. Zubieta, *J. Chem. Soc., Dalton Trans.*, 2000, 769.

23. G. Dyer, D. W. Meek, *J. Am. Chem. Soc.*, 1967, **89**, 3983.

24. E. G. Hope, T. Kemmitt, W. Levason, *J. Chem. Soc., Perkin Trans.*, 1987, 487.

25. S. K. Harbron, S. J. Higgins, E. G. Hope, T. Kemmitt, W. Levason, *Inorg. Chim. Acta,* 1987, **130**, 43.

26. D. Cauzzi, C. Graiff, M. Lanfranchi, G. Predieri, A. Tiripicchio, *Inorg. Chim. Acta,* 1998, **273**, 320.

27. J. C. Fitzmaurice, D. J. Williams, P. T. Wood, J. D. Woollins, *J. Chem. Soc., Chem. Commun.*, 1988, 741.

28. P. Bhattacharyya, A. M. Z. Slawin, J. D. Woollins, *J. Chem. Soc., Dalton Trans.*, 2001, 301.

29. J. E. Aguado, S. Canales, M. Concepción Gimeno, P. G. Jones, A. Laguna, M. Dolores Villacampa, *J. Chem. Soc., Dalton. Trans.*, 2005, 3005.

30. J. A. Adeleke, Y. W. Chen, L. K. Liu, *Organometallics,* 1992, **11**, 2453.

31. S. Narayan, V. K. Jain, B. Varghese, *J. Chem. Soc., Dalton Trans.*, 1998, 2359.

32. V. K. Jain, S. Kannan, R. J. Butcher, J. P. Jasinski, *J. Chem. Soc., Dalton Trans.*, 1993, 1509.

33. W. L. Steffen, G. J. Palenik, *Inorg. Chem.*, 1976, **15**, 2432.

34. S. E Durran, M. R. J. Elsegood, M. B. Smith, *New J. Chem.*, 2002, **26**, 1402.

35. H. A. Ankersmit, N. Veldman, A. L. Spek, K. Vrieze, G. van Koten, *Inorg. Chim. Acta,* 1996, **252**, 339.

36. H. A. Ankersmit, P. T. Witte, H. Kooijinan, M. T. Lakin, A. L. Spek, K. Goubitz, K. Vrieze, G. van Koten, *Inorg. Chem.*, 1996, **35**, 6053.

37. R. Rulke, J. M. Ernsting, A. L. Spek, C. J. Elsevier, P. W. N. M. van Leeuwen, K. Vrieze, *Inorg. Chem.*, 1993, **32**, 5769.

38. C. A. McAuliffe, D. W. Meek, *Inorg. Chim. Acta,* 1971, **5**, 270.
39. D. L. DuBois, D.W. Meek, *Inorg. Chem.,* 1976, **15**, 3076.
40. L. Sacconi, *J. Chem. Soc A*, 1970, 248.
41. R. D. Waid, D. W. Meek, *Inorg. Chem.,* 1984, **23**, 778.
42. M. H. P. Rietveld, D. M. Grove, G. van Koten, *New J. Chem.,* 1997, **21**, 751.
43. M. E. Vanderboom, C. L. Higgitt, D. Milstein, *Organometallics*, 1999, **18**, 2413.
44. E. Cerrada, L. R. Falvello, M. B. Hursthouse, M. Laguna, A. Luquin, C. Pozo-Gonzalo, *Eur. J. Inorg. Chem.,* 2002, 826.
45. A. R. Genge, A. M. Gibson, N. Guymer, G. Reid, *J. Chem. Soc., Dalton Trans.,* 1996, 4099.
46. C. Grazia Arena, D. Drommi, F. Faraone, C. Graiff, A. Tiripicchio, *Eur. J. Inorg. Chem.,* 2001, 247.
47. L. V. Andreasen, O. Simonsen, O. Wernberg, *Inorg. Chim. Acta,* 1999, **295**, 153.
48. E. Kyba, C. N. Clubb, S. B. Larson, V. J. Scheuler, R. E. Davis, *J. Am. Chem. Soc.,* 1985, **107**, 2141.
49. E. Kyba, R. E. Davis, C. W. Hudson, A. M. John, S. B. Brown, M. J. McPhaul, L-K. Liu, A. C. Glover, *J. Am. Chem. Soc.,* 1981, **103**, 3868.
50. E. Kyba, S-S. P. Chou, *J. Org. Chem.*, 1981, **46**, 860.
51. D. Drommi, F. Nicoló, C. G. Arena, G. Bruno, F. Faraone, R. Gobetto, *Inorg. Chim. Acta,* 1994, **221**, 109.
52. E. Drent, P. Arnoldy, P. H. M. Budzelaar, *J. Organomet. Chem.,* 1993, **455**, 247.
53. M. J. Green, K. J. Cavell, P. G. Edwards, *J. Chem. Soc., Dalton Trans.,* 2000, 853.
54. M. J. Green, K. J. Cavell, P.G. Edwards, R. P. Tooze, B. W. Skelton, A. H. White, *J. Chem. Soc, Dalton Trans.,* 2004, 3251.
55. P. Wehman, R. E. Rülke, V. E. Kaasjager, P. C. J. Kamer, H. Kooijman, A. L. Spek, C. J. Elsevier, K. Vrieze, P. W. N. M. van Leeuwen, *J. Chem. Soc., Chem. Commun.,* 1995, 331.
56. S. E. Durran, M. B. Smith, A. M. Z. Slawin, J. W. Steed, *J. Chem. Soc.,* Dalton Trans., 2000, 2771.

57. S. E. Durran, M. R. J. Elsegood, N. Hawkins, M. B. Smith, S. Talib, *Tet. Lett.*, 2003, **44**, 5255.

58. M. R. J. Elsegood, M. B. Smith, P. M. Staniland, *Inorg. Chem.*, 2006, **45**, 6761.

59. K. G. Gaw, A. M. Z. Slawin, M. B. Smith, *Organometallics*, 1999, **18**, 3255.

60. S. Oae, N. Furukawa, *Sulfilimines and Related Derivatives,* 1983, American Chemical Society, Washington.

61. A. D. M Curtis, R. McCague, C. A. Ramsden, M. R. Raza, *J. Chem. Soc., Chem. Commun.*, 1999, 189.

62. A. Kucsman, F. Ruff, I. Kapovits, *Tetrahedron*, 1966, **22**, 1575.

63. G. Schulz, G. Kresze, *Angew. Chem., Int. Ed.*, 1963, **2**, 736.

64. H. S. Raper, *Report of the British Chemical Warfare Department*, May 1917.

65. F. G. Mann, W. J. Pope, *J. Chem. Soc.*, 1922, **121**, 1052.

66. T. L. Gilchrist, C. J. Moody, *Chemical Reviews*, 1977, **77**, 409.

67. A. K. Sharma, T. Ku, A. D. Dawson, D. Swern, *J. Org. Chem.*, 1975, **40**, 2758.

68. J. A. Franz, J. C. Martin, *J. Am. Chem. Soc.*, 1975, **97**, 583.

69. F. G. Yamagishi, D. R. Rayner, E. T. Zwicker, D. J. Cram, *J. Am. Chem. Soc.*, 1973, **95**, 1916.

70. Y. Hayashi, D. Swern, *J. Am. Chem. Soc.*, 1973, **95**, 5205.

71. Y. Tamura, K. Sumoto, H. Matsushima, H. Taniguchi, M. Ikeda, *J. Org. Chem.*, 1973, **38**, 4324.

72. Y. Tamura, H. Matsushima, J. Minamikawa, M. Ikeda, K. Sumoto, *Tetrahedron,* 1975, **31**, 3035.

73. A. L. Marzinzik, K. B. Sharpless, *J. Org. Chem.*, 2001, **66**, 594.

74. J. L. Davidson, P. N. Preston, S. A. R. Spankie, G. Douglas, K. W. Muir, *J. Chem. Soc., Dalton Trans.*, 1989, 497.

75. P. F. Kelly, A. M. Z. Slawin, *Eur. J. Inorg. Chem.*, 2001, 263.

76. M. R. J. Elsegood, K. E. Holmes, P. F. Kelly, J. Parr, J. M. Stonehouse, *New J. Chem.*, 2002, **26**, 202.

77. M. R. J. Elsegood, K. E. Holmes, P. F. Kelly, E. J. MacLean, J. Parr, J. M. Stonehouse, *Eur. J. Inorg. Chem.*, 2003, 120.

78. S. H. Dale, M. R. J. Elsegood, K. E. Holmes, P. F. Kelly, *Acta Crystallogr.*, 2005, **61**, m34.

79. K. E. Holmes, P. F. Kelly, M. R. J. Elsegood, *CrystEngComm*, 2002, **4**, 545.

80. K. E. Holmes, P. F. Kelly, S. H. Dale, M. R. J. Elsegood, *CrystEngComm*, 2006, **8**, 391.

81. W. Clegg, S. H. Dale, D. Drennan, P. F. Kelly, *J. Chem. Soc., Dalton Trans*, 2005, 3140.

82. S. M. Aucott, M. R. Bailey, M. R. J. Elsegood, L. M. Gilby, K. E. Holmes, P. F. Kelly, M. J. Papageorgiou, S. Pedron-Haba, *New. J. Chem.*, 2004, **28**, 959.

83. *IUPAC Compendium of Chemical Terminology*, 2nd Ed. 1997, **67**, 1357.

84. H. Staudinger, J. Meyer, *Helv. Chim. Acta,* 1919, 635.

85. A. W. Johnson , *Ylides and Imines of Phosphorus.*, J. Wiley & Sons, New York, Chichester, Brisbane, Toronto, Singapore, 1993, ch. 13.

86. P. Imhoff, C. J. Elsevier, C. H. Stam, *Inorg. Chim. Acta,* 1990, **175**, 209.

87. S. A. Bell, S. J. Geib, T. Y. Meyer, *J. Chem. Soc, Chem. Commun.*, 2000, 1375.

88. B. L. Shaw, *J. Organomet. Chem.*, 1980, **200**, 307.

89. M. Ohff, A. Ohff, M. E. van der Boom, D. Milstein, *J. Am. Chem. Soc.*, 1997, **119**, 687.

90. J. P. Stambuli, M. Buhl, J. F. Hartwig, *J. Am. Chem. Soc.*, 2002, **124**, 9346.

91. F. Paul, J. Patt, J. F. Hartwig, *Organometallics*, 1995, **14**, 3030.

92. R. A. Widehoefer, H. A. Zhong, S. L. Buchwald, *Organometallics,* 1996, **15**, 2745.

93. M. Epstein, S. A. Buckler, *J. Am. Chem. Soc.*, 1961, **83**, 3279.

94. V. Gee, A. G. Orpen, H. Phetmung, P. G. Pringle, R. I. Pugh, *J. Chem. Soc., Chem. Commun.*, 1999, 901.

95. C. A. Tolman, *Chem. Rev.*, 1977, **77**, 313.

96. P. H. M. Budzelaar, E. Drent, P. G. Pringle, *Eur. Pat.*, 97 302 079, 1996.

97. C-A. Carraz, D. W. Stephan, *Organometallics*, 2000, **19**, 3791.

98. I. R. Butler, U. Griesbach, P. Zanello, M. Fontani, D. Hibbs, M. B. Hursthouse, K. L. M. Abdul Malik, *J. Organomet. Chem.*, 1995, **565**, 243.

99. G. A. Molander, C-S Yun, M. Ribagorda, B. Biolatto, *J. Org. Chem.*, 2003, **68**, 5534.

100. I. R. Butler, P. K. Baker, G. R. Eastham, K. M. Fortune, P. N. Horton, M. B. Hursthouse, *Inorg. Chem. Commun.*, 2004, **7**, 1049.

101. H. A. Dieck, R. F. Heck, *J. Am. Chem. Soc.*, 1974, **96**, 1113.

102. A. de Meijere, F. E. Meyer, *Angew. Chem., Int. Ed.,* 1995, **33**, 2379.

103. N. Miyaura, A. Suzuki, *Chem. Rev.,* 1995, **95**, 2457

104. M. Kranenburg, Y. E. M. van der Burgt, P. C. J. Kamer, P. W. N. M. van Leeuwen, K. Goubitz, J. Fraanje, *Organometallics;* 1995, **14**, 3081.

105. E. Drent, P. H. M. Budzelaar, *Chem. Rev.*, 1996, **96**, 663.

106. A. Sommazzi, F. Garbassi, *Prog. Polym. Sci.*, 1997, **22**, 1547.

107. N Brugat, A. Polo, A. Alvarez-Larena, J. Francesc Piniella, J. Real, *Inorg. Chem.*, 1999, **38**, 4829.

108. R. F. Heck, J. P. Nolley, Jr., *J. Org. Chem.,* 1972, **37**, 2320.

109. B. L. Shaw, S. D. Perera, *J. Chem. Soc., Chem. Commun.,* 1998, 1863.

110. R. F. Heck, *Vinyl Substitution with Organopalladium Intermediates,* in *Comprehensive Organic Synthesis*, ed. B M. Trost, I. Fleming, Pergamon, Oxford, 1991, vol. 4, p. 833.

111. W. Cabri, I. Candiani. A. Bedeschi, *J. Org. Chem.,* 1992, **57**, 3558.

112. A. F. Littke, G. C. Fu, *J. Am. Chem. Soc.,* 2000, **122**, 4020.

113. J. Yin, M. P. Rainka, X. Zhang, S. L. Buchwald, *J. Am. Chem. Soc.,* 2002, **124**, 1162.

114. R. B. Bedford, S. L. Hazelwood, P. N. Horton, M. B. Hursthouse, *J. Chem. Soc., Dalton Trans.,* 2003, 4164.

115. J. R. Dilworth, J. R. Miller, N. Wheatley, M. J. Baker, J. G. Sunley, *J. Chem. Soc., Chem. Commun.,* 1995, 1579.

116. S. Gladiali, F. Grepioni, S. Medici, A. Zucca, Z. Berente, L. Kollár, *Eur. J. Inorg. Chem.,* 2003, 556.

117. C. Abu-Gnim, I. Amer, *J. Organomet. Chem.*, 1996, **516**, 235.

118. P. Dani, T. Karlen, R. A. Gossage, S. Gladiali, G. van Koten, *Angew. Chem., Int. Ed.,* 2000, **39**, 743.

119. M. Kranenburg, P. C. J. Kamer, P. W. N. M. van Leeuwen, *Eur. J. Inorg. Chem.,* 1998, 25.

120. B. M. Trost, B. Breit, S. Peukert, J. Zambrano, J. W. Ziller, *Angew. Chem., Int. Ed.,* 1995, **34**, 2386.

121. R. I. Pugh, E. Drent, P. G. Pringle, *J. Chem. Soc., Chem. Commun.,* 2001, 1476.

122. S. J. Dosset, A. Gillon, A. G. Orpen, J. S. Fleming, P. G. Pringle, D. Wass, M. Jones, *J. Chem. Soc., Chem. Commun.,* 2001, 699.

123. D. Gerristma, T. Brenstrum, J. McNulty, A. Capretta, *Tet. Lett.*, 2004, **45**, 8319.

124. G. Adjabeng, T. Brenstrum, J. Wilson, C. Frampton, A. Robertson, J. Hillhouse, J. McNulty, A. Capretta, *Org. Letters*, 2003, **5**, 953.

125. T. Brenstrum, D. A. Gerristma, G. M. Adjabeng, C. S. Frampton, J. Britten, A. J. Robertson, J. McNulty, A. Capretta, *J. Org. Chem.*, 2004, **69**, 7635.

126. P. Machnitzki, T. Nickel, O. Stelzer, C. Landgrafe, *Eur. J. Inorg. Chem.*, 1998, 1029.

127. F. A Davis, B-C Chen, *Chem. Rev.*, 1992, **92**, 919.

128. F.A. Davis, J.C. Towson, M.C. Weismiller, S. Lal, P.J. Carroll, *J. Am. Chem. Soc.*, 1998, **110**, 8477.

129. C.P. Brock, W.B. Schweizer, J.D. Dunitz, *J. Am. Chem. Soc.*, 1985, **107**, 6964.

130. S.K. Harbron, S.J. Higgins, E.G. Hope, T. Kemmitt, W. Levason, *Inorg. Chim. Acta*, 1987, **130**, 43.

131. D. L. Dubois, W. H. Myers, D. W. Meek, *J. Chem. Soc., Dalton Trans.*, 1975, 1011.

132. E. Block, G. Ofori-Okai, J. Zubieta, *J. Am. Chem. Soc.*, 1989, **111**, 2327.

133. O. Grossman, C. Azzeraf, D. Gelman, *Organometallics*, 2006, **25**, 375.

134. G. M. Brown, M. R. J. Elsegood, A. J. Lake, N. M. Sanchez-Ballester, M. B. Smith, T. S. Varley, K. Blann, *Eur. J. Inorg. Chem.*, 2007, 1405.

135. S. J. Coles, P. G. Edwards, M. B. Hursthouse, K. M. Abdul Malik, J. L. Thick and R. P. Tooze, *J. Chem. Soc., Dalton Trans.*, 1997, 1821.

136. Q. Zhang, S. M. Aucott, A. M. Z. Slawin, J. D. Woollins, *Eur. J. Inorg. Chem*, 2002, 1635.

137. D. C. Smith Jr., C. M. Haar, E. D. Stevens, S. P. Nolan, *Organometallics*, 2000, **19**, 1427.

138. R. Baldwin, M. A. Bennett, D. C. R. Hockless, P. Pertici, A. Verrazzani, G. Barretta, F. Marchetti, P. Salvadori, *J. Chem. Soc., Dalton Trans.*, 2002, 4488.

139. M. R. J. Elsegood, M. B. Smith, N. M. Sanchez-Ballester, *Acta Cryst.*, 2006, **E62**, m2838.

140. A. B. Chaplin, C. Fellay, G. Laurenczy, P. J. Dyson, *Organometallics*, 2007, **26**, 586.

141. G. Celentano, S. Colonna, N. Gaggero, C Richelmi *Chem. Commun.*, 1998, 701.

142. W-N. Chou, M. Pomerantz, *J. Org. Chem.*, 1991, **56**, 2762.

143. M. R. J. Elesegood, L. M. Gilby, K. E. Holmes, P. F. Kelly, *Can. J. Chem.*, 2002, **80**, 1410.

144. S. M. Aucott, S. H. Dale, M. R. J. Elsegood, K. E. Holmes, L. M. Gilby, P. F. Kelly, *Acta Cryst.*, 2005, C**61**, 134.

145. N. Kurose, T. Takahashi, T. Koizumi, *J. Org. Chem.*, 1996, **61**, 2932.

146. H. Takada, M. Oda, Y. Miyake, K. Ohe, S. Uemura, *Chem. Commun.*, 1998, 1557.

147. F. Palacios, C. Alonso, J. Pagalday, A. M. Ochoa de Retana, G. Rubiales, *Org. Biomol. Chem.*, 2003, **1**, 1112.

148. R. Appel, W. Buchner, E. Guth, *Liebings Ann. Chem.*, 1958, **53**, 618.

149. B. L. Shaw, S. D. Perera, E. A. Staley, *Chem. Commun.*, 1998, 1361.

150. J. G. de Vries, *J. Chem. Soc., Dalton Trans.*, 2006, 421.

151. D. Drew, J. R. Doyle, *Inorg. Synth.*, 1972, **13**, 47.

152. J. X. McDermott, J. F. White, G. M. Whitesides, *J. Am. Chem. Soc.*, 1976, **98**, 6521.

153. E. Costa, P. G. Pringle, M. Ravetz, *Inorg. Synth.* 1997, **31**, 284.

154. M. A. Bennett, A. K. Smith, *J. Chem. Soc., Dalton Trans.*, 1974, 233.

155. C. White, A. Yates, P. M. Maitlis, *Inorg. Synth.*, 1992, **29**, 228.

156. P. Uson, A. Laguna, M. Laguna, *Inorg. Synth.*, 1989, **26**, 85.